AD-A068 389 ENVIRONMENTAL RESEARCH INST OF MICHIGAN ANN ARBOR IN--ETC F/G 17/5
STATISTICAL ANALYSES OF TERRAIN DATA.(U)
FEB 79 A J LAROCCA, J R MAXWELL N60530-78-C-0009
UNCLASSIFIED ERIM-132300-2-F NL

1 OF 3
AD
A068389

LEVEL II

12

132300-2-F

AD A068389

DDC FILE COPY

Final Report

STATISTICAL ANALYSIS OF TERRAIN DATA

ANTHONY J. LAROCCA, J. ROBERT MAXWELL
Infrared and Optics Division

FEBRUARY 1979

Approved for Public Release
Distribution Unlimited

Optical Signatures Program
Naval Weapons Center
China Lake, California

ENVIRONMENTAL
RESEARCH INSTITUTE OF MICHIGAN
FORMERLY WILLOW RUN LABORATORIES THE UNIVERSITY OF MICHIGAN
BOX 8618 • ANN ARBOR • MICHIGAN 48107

79 05 07 021

NOTICES

Sponsorship. The work reported herein was conducted by the Environmental Research Institute of Michigan (formerly the Willow Run Laboratory of the University of Michigan) for the Naval Weapons Center, China Lake, California, under Contract Number N60530-78-C-009. The Project Managers were Dr. Jon Wunderlich and Dr. Lowell Wilkins.

Unclassified

SECURITY CLASSIFICATION OF THIS PAGE (When Data Entered)

REPORT DOCUMENTATION PAGE		READ INSTRUCTIONS BEFORE COMPLETING FORM
1. REPORT NUMBER 132300-2-F	2. GOVT ACCESSION NO	3. RECIPIENT'S CATALOG NUMBER
4. TITLE (and Subtitle) Statistical Analyses of Terrain Data.		5. TYPE OF REPORT & PERIOD COVERED Final Report
		6. PERFORMING ORG REPORT NUMBER ERIM 132300-2-F
7. AUTHOR(s) A. J. LaRocca and J. R. Maxwell		8. CONTRACT OR GRANT NUMBER(s) N60530-78-C-0089
9. PERFORMING ORGANIZATION NAME AND ADDRESS Infrared and Optics Division, Environmental Research Institute of Michigan, Ann Arbor, Michigan 48107		10. PROGRAM ELEMENT PROJECT TASK AREA & WORK UNIT NUMBERS Feb 79
11. CONTROLLING OFFICE NAME AND ADDRESS Dr. Jon Wunderlich, Code 39403, Naval Weapons Center, China Lake, CA 93555		12. REPORT DATE December 1978
		13. NUMBER OF PAGES 247
14. MONITORING AGENCY NAME AND ADDRESS (if different from Controlling Office) Receiving Officer, Naval Weapons Center, China Lake, CA 93555	249p	15. SECURITY CLASS (of this report) Unclassified
		15a. DECLASSIFICATION/DOWNGRADING SCHEDULE N/A

16. DISTRIBUTION STATEMENT (of this Report)

Approved for Public Release; Distribution Unlimited

Anthony J./Larocca J. Robert/Maxwell

17. DISTRIBUTION STATEMENT (of the abstract entered in B

18. SUPPLEMENTARY NOTES

19. KEY WORDS (Continue on reverse side if necessary and identify by block number)

Terrain backgrounds, IR imagery, Statistical analyses, Multispectral data

20. ABSTRACT (Continue on reverse side if necessary and identify by block number)

As part of a continuing effort by the Naval Weapons Center, and in support of the Navy Optical Signatures Program, data on various terrain backgrounds were ~~have been~~ collected ~~by the Environmental Research Institute of Michigan~~ and ~~have been~~ analyzed to present their statistical features. ~~This report describes~~ some of those characteristics are described in the form of histograms, ellipse "pictures," and power spectra for the following infrared spectral

DD FORM 1473, 1 JAN 73 EDITION OF 1 NOV 65 IS OBSOLETE

Unclassified

SECURITY CLASSIFICATION OF THIS PAGE (When Data Entered)

408 259

Unclassified
SECURITY CLASSIFICATION OF THIS PAGE (When Data Entered)

20. ABSTRACT (Cont'd)

micrometers

bands: 2.0 - 2.6, 3.0 - 4.2, 3.5 - 3.9, 3.9 - 4.7, 4.5 - 5.5, 5.1 - 5.7, and 9.0 - 11.4 μm. An attempt is made to demonstrate various meteorological and other influences on the statistics by comparing the data in different spectral regions taken at different times and under differing conditions. Using these results and those from future analyses of other scenery, one would hope eventually to be able to categorize terrain backgrounds according to a few easily recognizable parameters.

Unclassified
SECURITY CLASSIFICATION OF THIS PAGE (When Data Entered)

TABLE OF CONTENTS

LIST OF FIGURES

LIST OF FIGURES (CONTINUED)

LIST OF TABLES

1.0
INTRODUCTION AND SUMMARY

A backgrounds measurement and analysis program is being conducted for the Navy Optical Signatures Program for the purpose of generating calibrated digital imagery over various terrain backgrounds, generating statistics for these scenes useful for classifying various background types, and for developing statistical measures that can be related to various system performance characteristics.

Previous efforts on this program have included a literature search and bibliography of available backgrounds data [Reference 1]. In addition, selected terrain backgrounds data collected with the ERIM airborne multispectral scanner were analyzed and the results reported [References 2 and 3]. ERIM airborne multispectral scanner data are especially suitable for terrain backgrounds analysis because the data are multispectral, registered, calibrated, in digital format, available with a ground spatial resolution of two to three feet, and provide a large coverage of the terrain. The data that were available for the early analysis efforts reported in References 2 and 3 were primarily data in spectral bands positioned between 1.0 and 2.5 μm and in the 8.0 - 13.5 μm spectral region.

The current report extends the work reported in Reference 2, using airborne data collected over a desert and mountainous terrain at Nellis Air Force Base in February 1978. Data were collected with the ERIM M-7 multispectral scanner in the mid-IR in spectral bands from 2.0 - 2.6, 3.0 - 4.2, 3.5 - 3.9, 3.9 - 4.7, 4.5 - 5.5, and 5.1 - 5.7 μm, as well as in the spectral band from 9.0 - 11.4 μm.

An extensive series of flights at Nellis AFB was made in order to assess and compare the statistical characteristics of the desert and mountainous terrain under a variety of conditions. A subset of the data

was selected in order to analyze the desert and mountainous terrain and to determine the effects of various parameters on the statistics. The analysis has included measurement of means, standard deviations, spectral correlation coefficients, ellipse statistics, histograms, and power spectra.

Several observations were reported in Reference 2 on the data, among which were: effects of spectral band changes; differences in terrain clutter; effect of depression angle changes; effect of solar radiation. Many of the same observations were made in the analysis for this report and various comparisons were made to determine consistencies or trends. These are discussed in the following paragraphs.

(1) One might expect differences in the results in accordance with flight direction. Some results were borrowed from Reference 2 to increase the sample size. Even with these, the differences are not dramatic, although we do note, for example, that the clutter appears to be smallest for flights heading northerly, compared to flights headed southward. On the basis of these data, we would not consider flight direction an important controlling parameter. However, we have so far only been able to test for depression angles of 35° or greater. Perhaps a more dramatic tendency, both in average temperature and clutter differences, will be found for shallower depression angles, particularly over mountains.

(2) As regards clear vs overcast conditions, the data confirm the predictable: that the mean temperatures and the clutter are less for overcast conditions than for clear, sunny conditions.

(3) An attempt to compare the morning desert with the afternoon desert was compromised by the reduction in afternoon sun radiation through an overcast layer of clouds. The afternoon values are, therefore, less than the morning values through a loss of radiative input. An interesting observation is made, however, due to the presence of a dry lake bed situated in the desert which appears generally cooler in

the thermal region than the desert under both clear- and cloudy-sky conditions. Conversely, because of an apparently high short-wavelength reflectance at the lake floor, the spectral regions influenced by sunlight show a positive contrast in lake radiance compared to desert radiance.

(4) Comparing the thermal regions at 4.5 - 5.5 μm and 9.0 - 11.4 μm yields the anticipated outcome that the apparent temperatures agreed within a factor which could easily account for the higher absorption in the 4.5 - 5.5 μm region than in the 9.0 - 11.4 μm region.

The remainder of the report is devoted to (Section 2) a brief description of the ERIM multispectral scanner used to collect the data analyzed in this report; (Section 3) a discussion of the results of the analysis, showing the statistics, and making comparisons among the results. Conclusions are derived in Section 4, based on observations made in Section 3. Appendices A and B are included to collect the numerous histograms of the various sub-areas into which the scenery was divided and to demonstrate one-dimensional Wiener spectra of the scenery.

2.0
MULTISPECTRAL SCANNER

Figure 1 is a schematic of the M-7 multispectral scanner. Radiation in the visible portion of the spectrum is collected in detector position number 3, dispersed, and sensed with 12 photomultipliers. By use of a dichroic beam splitter, energy beyond 0.9 μm is directed to detector position number 2. For the flights at Nellis AFB and Pt. Mugu, a two- or three-element InSb detector array was placed in detector position 2 with each detector element appropriately filtered. The two-element InSb array was filtered to 3.5 - 3.9 and 3.9 - 4.7 μm. The three-element InSb array used for some flights was filtered to 2.0 - 2.6, 3.0 - 4.2, and 4.5 - 5.5 μm. A filtered HgCdTe detector was used in detector position 1A. On some flights, a 5.1 - 5.7 μm filter was used, on others a 9.0 - 11.4 μm filter was used. It is important to note that the data in all 12 visible bands, the 2 (or 3) InSb mid-IR bands, and the filtered HgCdTe band are collected simultaneously and can be spatially registered by accounting for the delay between the two InSb detectors.

The InSb detectors are 2.5 mrad detectors and the HgCdTe detector is 2.9 mrad. The scanning motor scans 60 lines/sec. The detectors scan across up to six calibration sources located inside the scanner housing with each rotation of the scan mirror. The various IR channels are calibrated with two controlled blackbody sources located in the scanner housing. The scanner is mounted in a C-47 aircraft that flys with a typical ground speed of 202 ft/sec. Hence, a scan line is recorded for every 3.4 ft of aircraft motion at a scan rate of 60 lines/sec. At an aircraft altitude of 1300 ft, with a detector resolution of 2.5 mrad, the imagery produced is contiguous with a ground resolution of 3.4 ft. At lower altitudes, the data are somewhat undersampled, and at higher altitudes, the data are oversampled. As part of the calibration procedure, an appropriate number of lines are averaged so that in the resulting image,

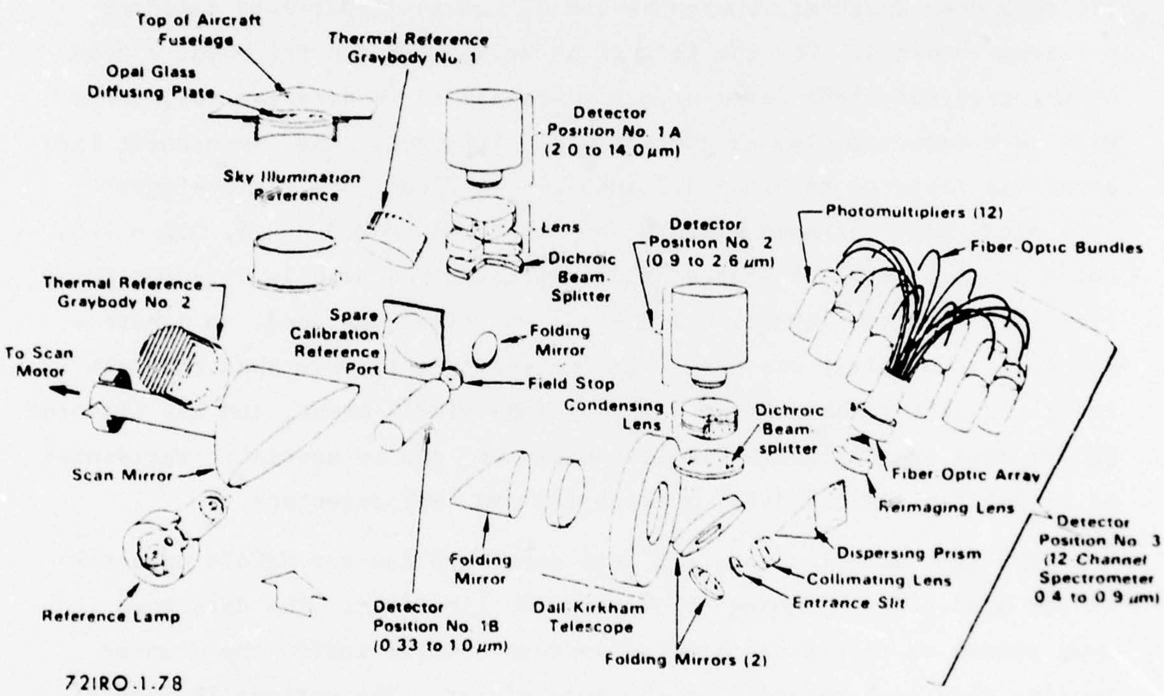

FIGURE 1. OPTICAL SCHEMATIC OF ERIM EXPERIMENTAL MULTISPECTRAL SCANNER, M-7

there is only one digital value for each resolution size (2.5 mrad) ground spot in the image. Calibrated data tapes are maintained for further analysis as necessary.

3.0
DISCUSSION OF RESULTS

The results presented in this report are an extension of those presented in Reference 2, obtained from images collected around Nellis Air Force Base, Nevada, in mountainous and in desert regions. To the extent that suitable examples could be obtained from various flights, the sets presented in Table 1 were chosen to show how parameters external to the sensor affect the quality and distribution of data obtained by the sensor. One would hope, then, on the basis of a few external parameters, to be able to predict with reasonable accuracy results from any given situation.

Variability in the data collection was introduced in several ways. One of these was by utilizing a variety of spectral regions among which were: 2.0 - 2.6, 3.0 - 4.2, 3.5 - 3.9, 3.9 - 4.7, 4.5 - 5.5, 5.1 - 5.7, and 9.0 - 11.4 μm. Times of flight for the chosen data were midmorning and midafternoon. Meteorological conditions were fortuitous. The choice of meteorological parameters was determined by availability. They enter into the analysis only in some generalized way as indicated mainly by cloud conditions as shown at the bottom of Table 1. Other variables given in Table 1 are: altitude of aircraft, which was 1000 ft for all runs in this report except one; depression angle, which was always 35° for the runs in this report except in the single higher-altitude case; direction of flight, to account for sun angle effects.

3.1 HISTOGRAMS

Figure 2 presents pictorial analogies of the IR imagery obtained over mountains with the scanner in many of the spectral regions from which the data were statistically analyzed. One should be able to recognize in the photos of Figure 2 some of the statistical features derived from the histograms which follow. In Reference 2, the various spectral

TABLE 1

NELLIS AFB DATA ANALYSIS

(Spectral Bands, Altitude, Depression Angle, Time, Flight Direction, Approximate Ground Coverage)

NEVI	2.0-2.6, 3.0-4.2, 4.5-5.5, 5.1-5.7 μm
(2-25-78)	1000 Ft. Altitude
	35° Depression Angle
	1510 Hrs., East, Mountains
	1750 x 6750 Ft^2
NEVJ	2.0-2.6, 3.5-3.9, 3.9-4.7 μm
(2-25-78)	1000 Ft. Altitude
	35° Depression Angle
	1528 Hrs., South, Mountains
	1750 x 6750 Ft^2
NEVK	2.0-2.6, 3.5-3.9, 3.9-4.7 μm
(2-25-78)	1000 Ft. Altitude
	35° Depression Angle
	1543 Hrs., North, Mountains
	1750 x 6750 Ft^2
NEVL	3.5-3.9, 3.9-4.7, 5.1-5.7 μm
Desert 1	1000 Ft. Altitude
Dry Lake	35° Depression Angle
Desert 2	1554 Hrs., East, Desert
(2-25-78)	1750 x 6750 Ft^2 Total
	1750 x 2700, Desert 1
	1750 x 2700, Desert 2
	1750 x 1350, Dry Lake

TABLE 1 (Continued)

NEVM	2.0-2.6, 3.5-3.9, 3.9-4.7 μm
(2-26-78)	1000 Ft. Altitude
	35° Depression Angle
	1022 Hrs., East, Mountains
	1750×6750 Ft^2
NEVN	2.0-2.6, 3.0-4.2, 4.5-5.5, 9.0-11.4 μm
(2-26-78)	1000 Ft. Altitude
	35° Depression Angle
	1044 Hrs., East, Mountains
	1750×6750 Ft^2
NVG1	2.0-2.6, 3.0-4.2, 4.5-5.5, 9.0-11.4 μm
(2-25-78)	1750 Ft. Altitude
	90° Depression Angle
	0926 Hrs., West, Mountains
	1850×6750 Ft^2
NVH1	2.0-2.6, 3.0-4.2, 4.5-5.5, 9.0-11.4 μm
Desert 1	1000 Ft. Altitude
Dry Lake	35° Depression Angle
Desert 2	1051 Hrs., East, Desert
(2-25-78)	1750×6750 Ft^2 Total
	1750 x 2700, Desert 1
	1750 x 2700, Desert 2
	1750 x 1350, Dry Lake

Meteorology:

2-25-78, AM - High, thin, scattered clouds, visibility = 15 miles

2-25-78, PM - Scattered clouds, light haze in target area; visibility = 35 miles, complete cloud cover for NEVL;

2-26-78, AM - High overcast, light haze in target area; visibility = 15 miles.

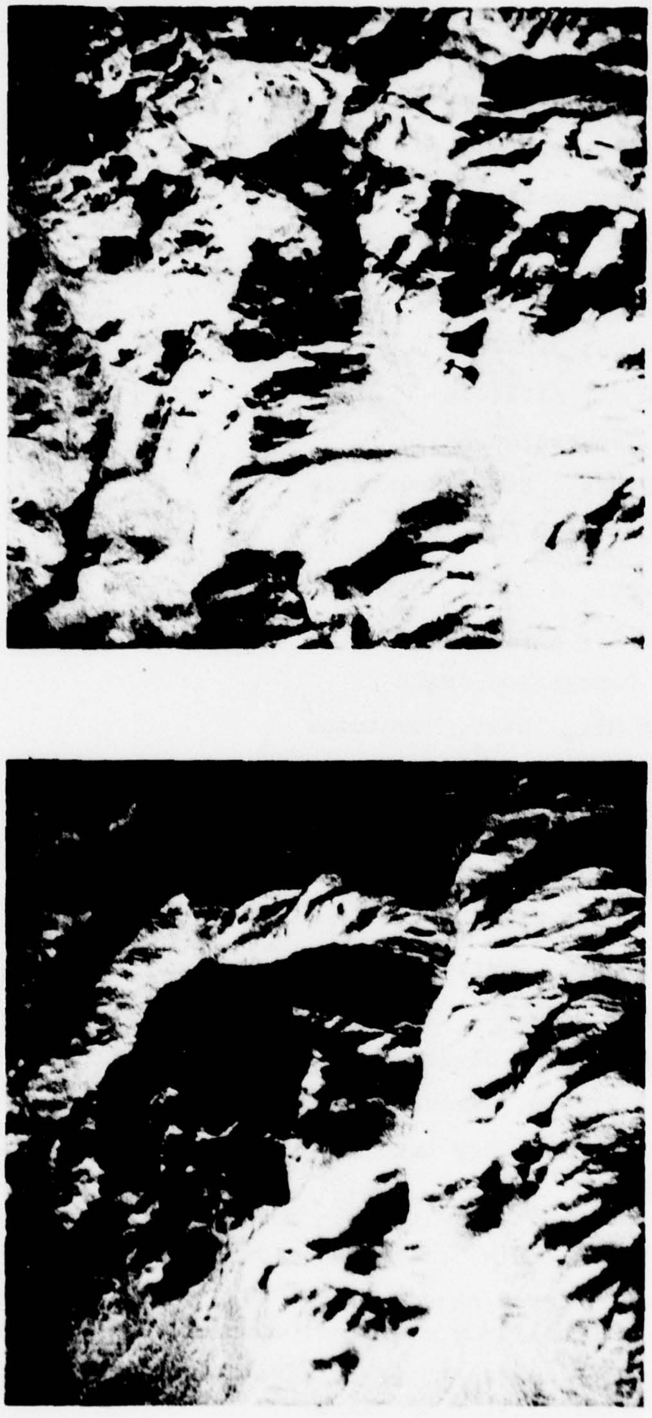

FIGURE 2a. AERIAL PHOTOS, NELLIS AFB MOUNTAINS

Clear, 3.9-4.7, 0914, 90° Depression

Clear, 3.9-4.7, 1034, 35° Depression

O'Cast, 3.9-4.7, 1022, 35° Depression

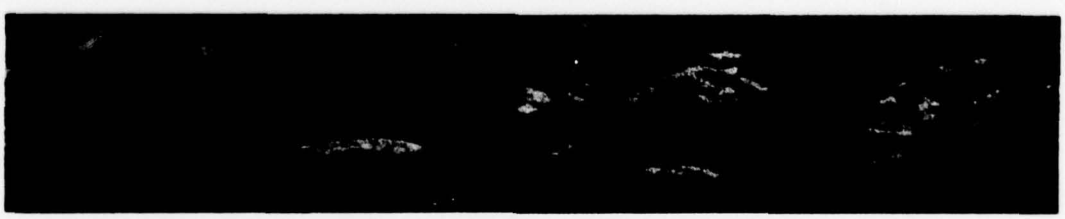

Clear, 3.9-4.7, 1511, 35° Depression

FIGURE 2b. IMAGERY, NELLIS AFB MOUNTAINS

regions were compared. In Figure 2 of this report, we present the same spectral region for different times of day and/or meteorological conditions. Figure 3 shows similar imagery for the desert regions around Nellis AFB in different spectral regions than those presented in Reference 2. Except in the few cases in which the data were faulty, there is a histogram for each condition indicated in Table 1. The channel containing the 5.1 - 5.7 μm filter provided the worst data, i.e., noisy, because of the narrowness of the filter and the effect of H_2O vapor absorption, although some data in this band are presentable.

One set of histograms is presented in Figures 4 through 11 in the same order as shown in Table 1 with:

Figure 4:	NEVI	Figure 8:	NEVN
Figure 5:	NEVJ	Figure 9:	NEG1
Figure 6:	NEVK	Figure 10:	NEVL
Figure 7:	NEVM	Figure 11:	NVH1

The statistics in these histograms represent data from the total area analyzed from the scene, as indicated for each run in Table 1; for example, 1570 x 6750 ft^2 for NEVI. This area is represented by about one-third of the central portions in Figure 2. Since the desert regions were divided into three separate areas — an east and west desert region and a dry lake — NEVL and NVH1 as shown in Figure 3 are composed of three regions in which the total-area statistics are analyzed. Consult Table 1 for the appropriate sizes of the regions analyzed.

The circles in these figures represent a normal distribution with the same average and standard deviation as the experimental curve. They are separated in intervals of 1/2-σ.

In addition to total-area statistics, the regions were subdivided into subareas for which the statistics are presented in Appendix A to demonstrate homogeneity or lack thereof. Those are presented on a linear graph as opposed to the semilog plot of the data presented in this section. The mountain scenes were divided into 4 equal subareas; the three desert

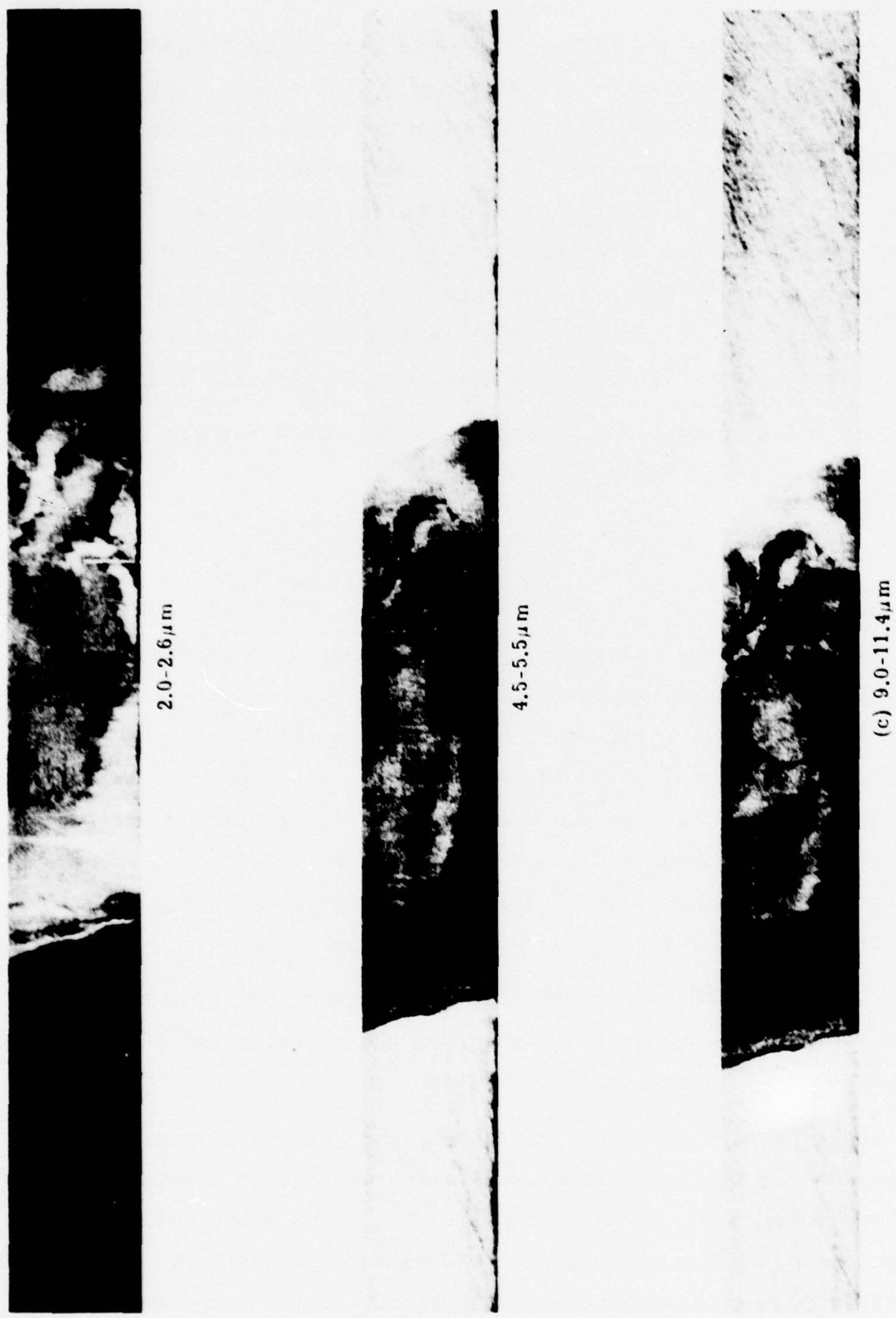

FIGURE 3. DESERT AND DRY LAKE NELLIS AFB IMAGERY

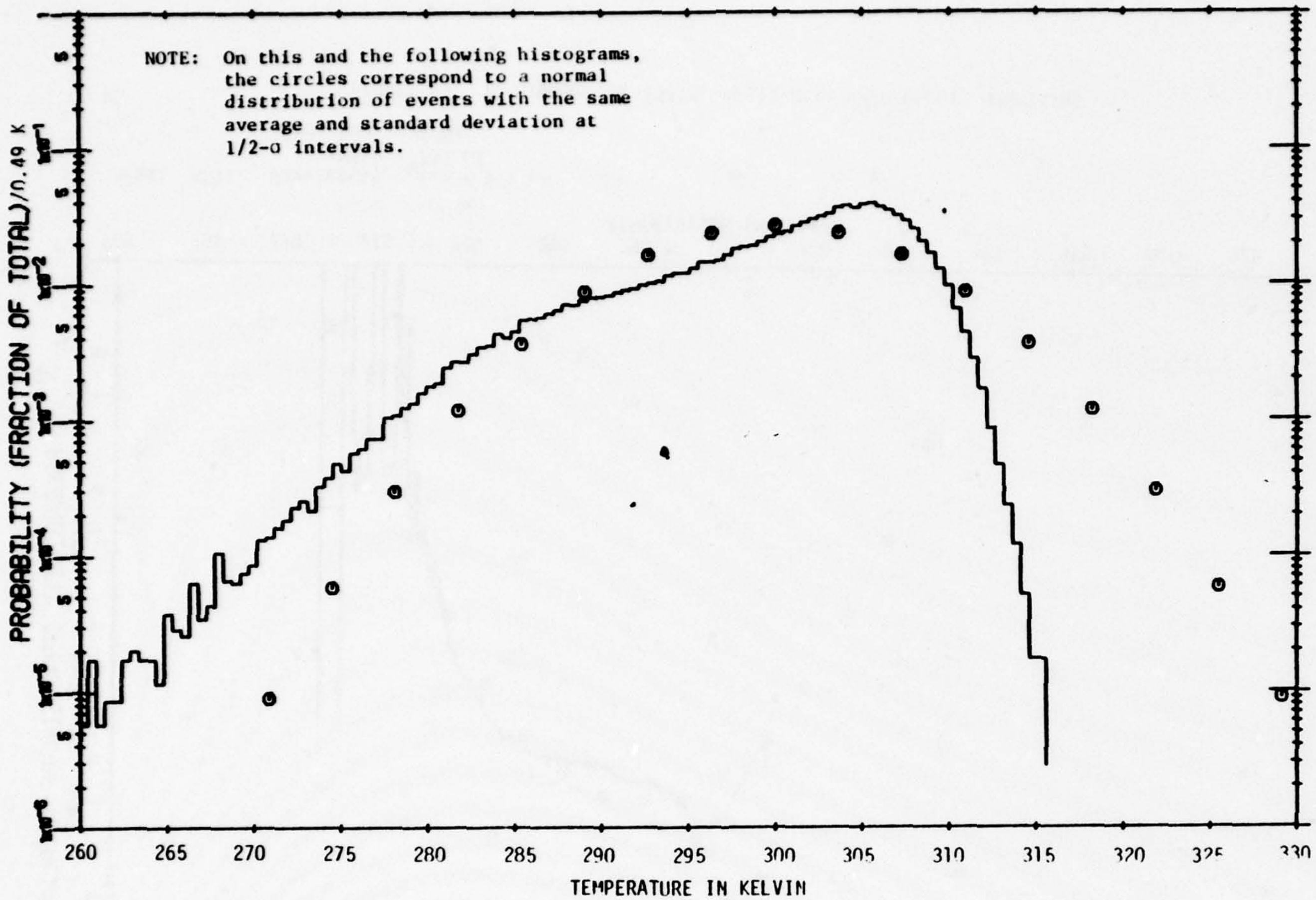

Area: NEVI Wavelength = 3.0-4.2 μm
Mean = 300.00
Std. Dev. = 7.28

FIGURE 4a. HISTOGRAM OF (TOTAL-AREA) DATA OVER NELLIS MOUNTAINS

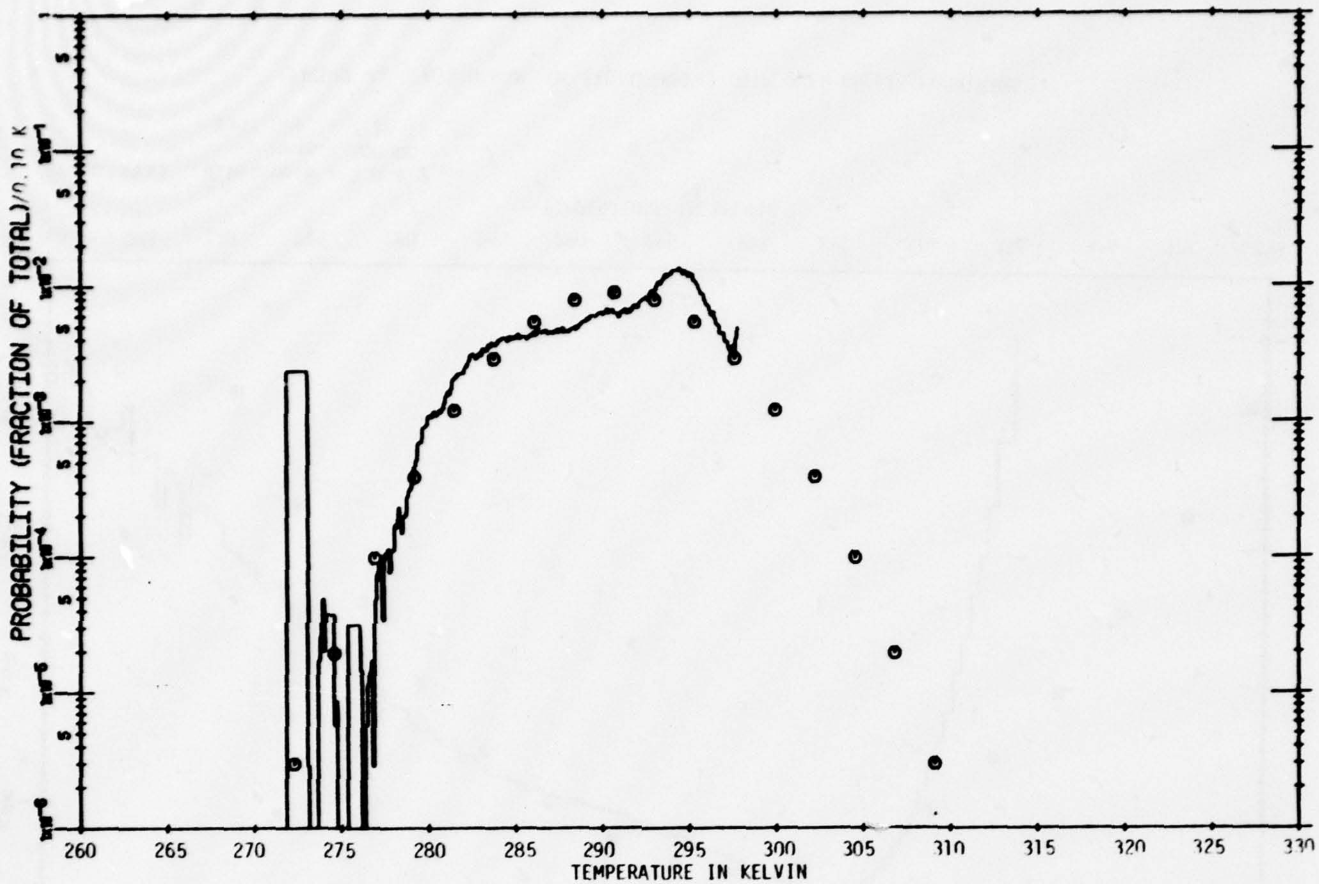

Area: NEVI Wavelength = 4.5 - 5.5 μm
Mean = 290.68
Std. Dev. = 4.60

FIGURE 4b. HISTOGRAM OF (TOTAL-AREA) DATA OVER NELLIS MOUNTAINS

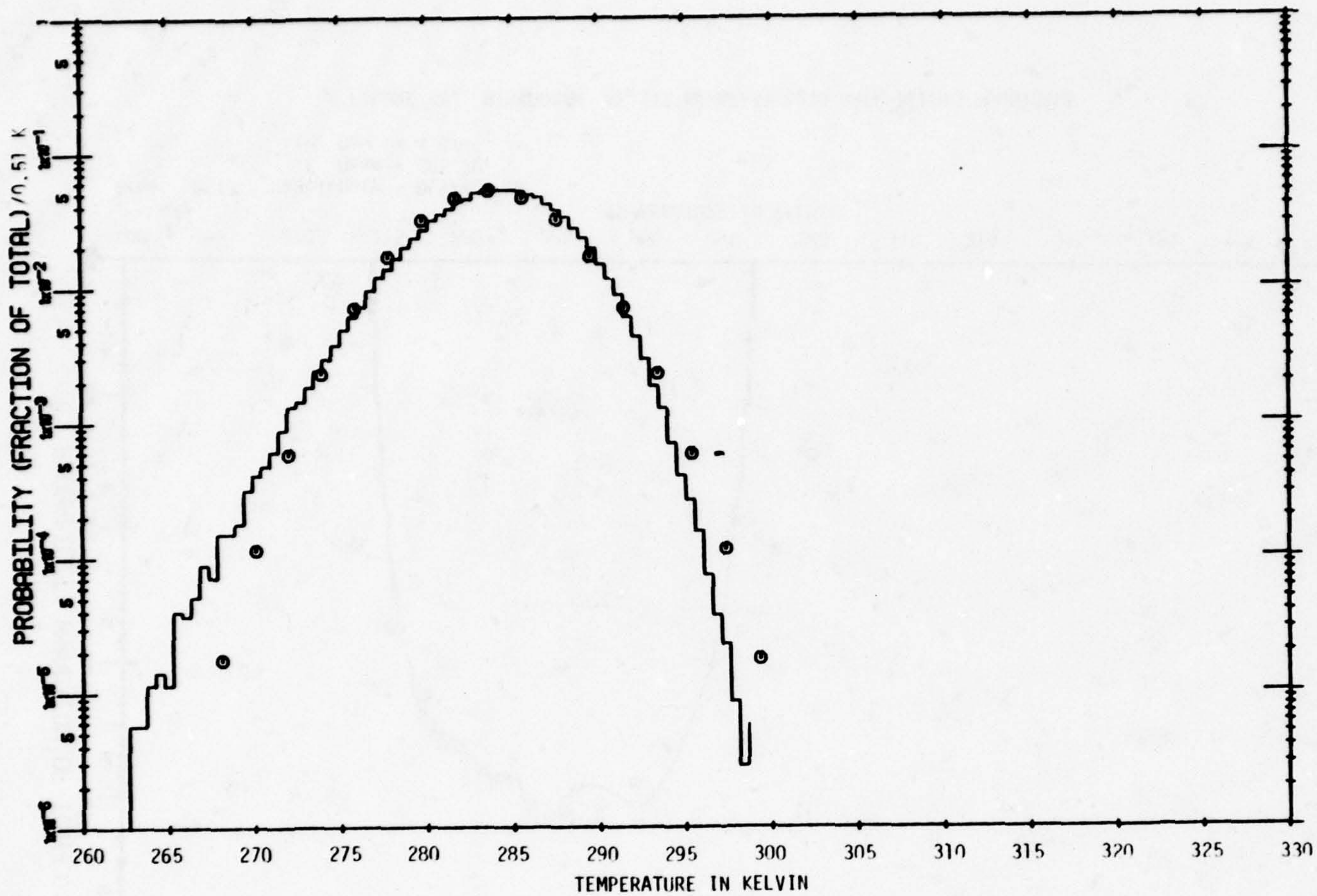

Area: NEVI Wavelength = 5.1-5.7 μm
Mean = 283.71
Std. Dev. = 3.90

FIGURE 4c. HISTOGRAM OF (TOTAL-AREA) DATA OVER NELLIS MOUNTAINS

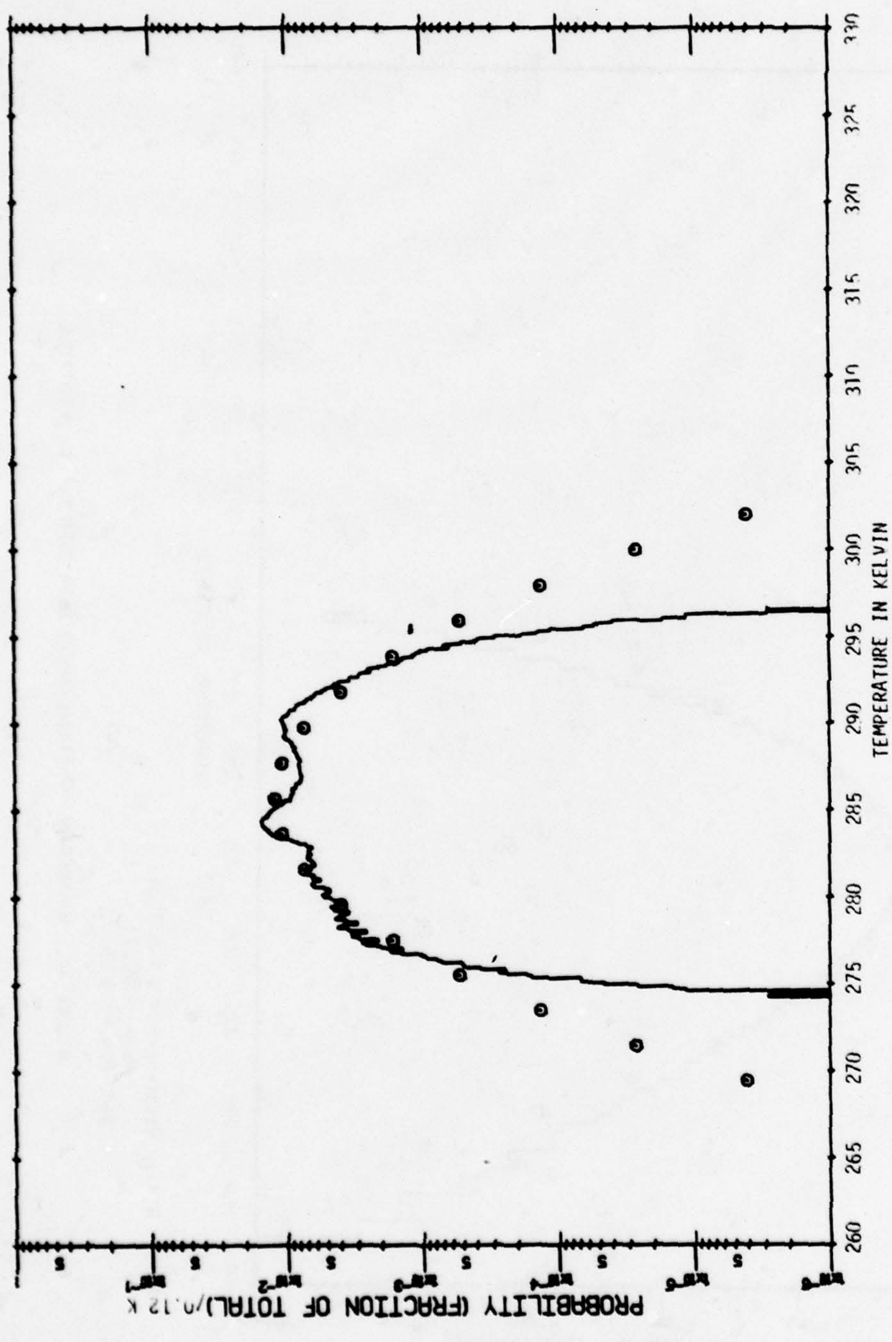

Area: NEVJ Wavelength = 3.9-4.7 μm
Mean = 285.70
Std. Dev. = 4.07

FIGURE 5a. HISTOGRAM OF (TOTAL-AREA) DATA OVER NELLIS MOUNTAINS

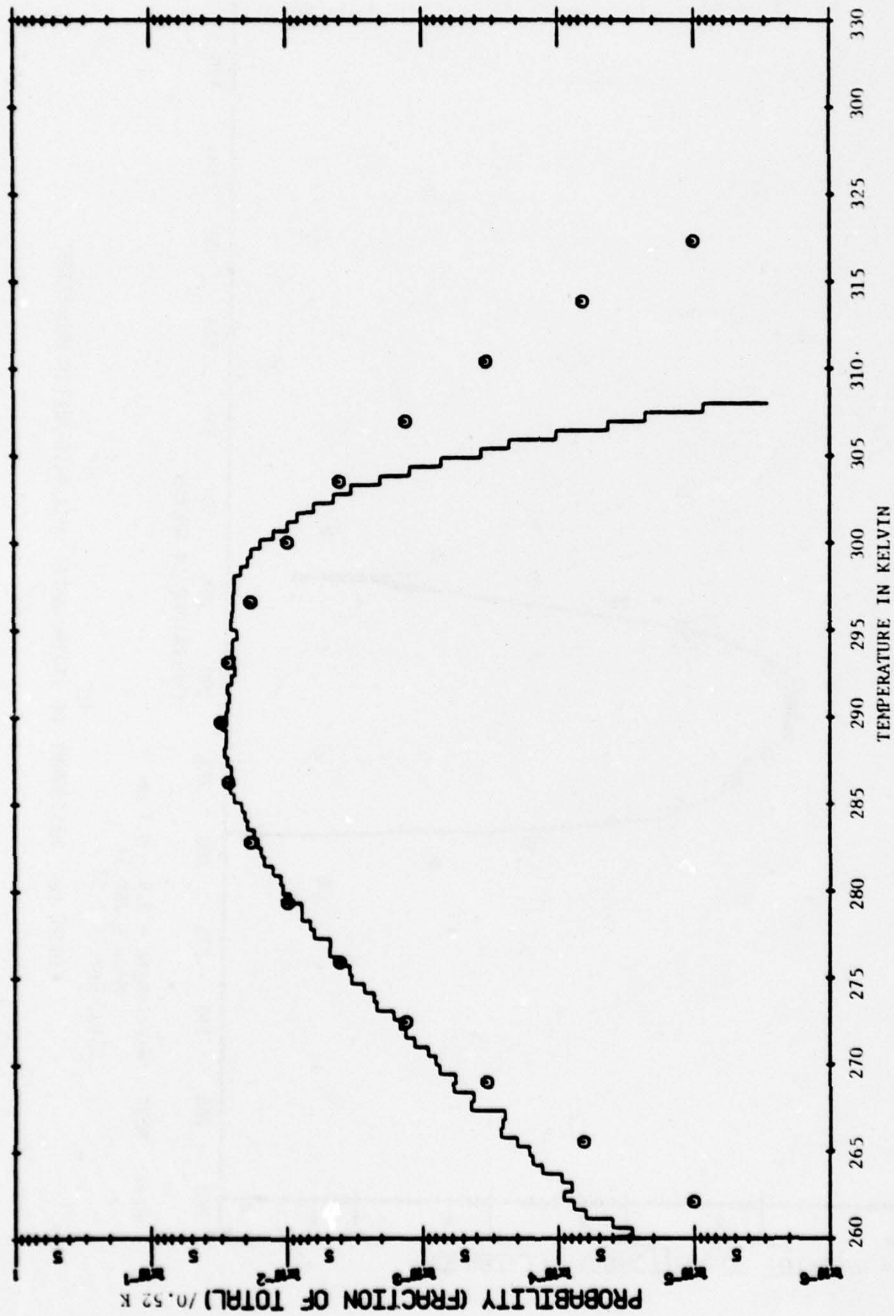

Area: NEVJ Wavelength = 3.5 - 3.9 µm
Mean = 289.71
Std. Dev. = 6.90

FIGURE 5b. HISTOGRAM OF (TOTAL, AREA) DATA OVER NELLIS MOUNTAINS

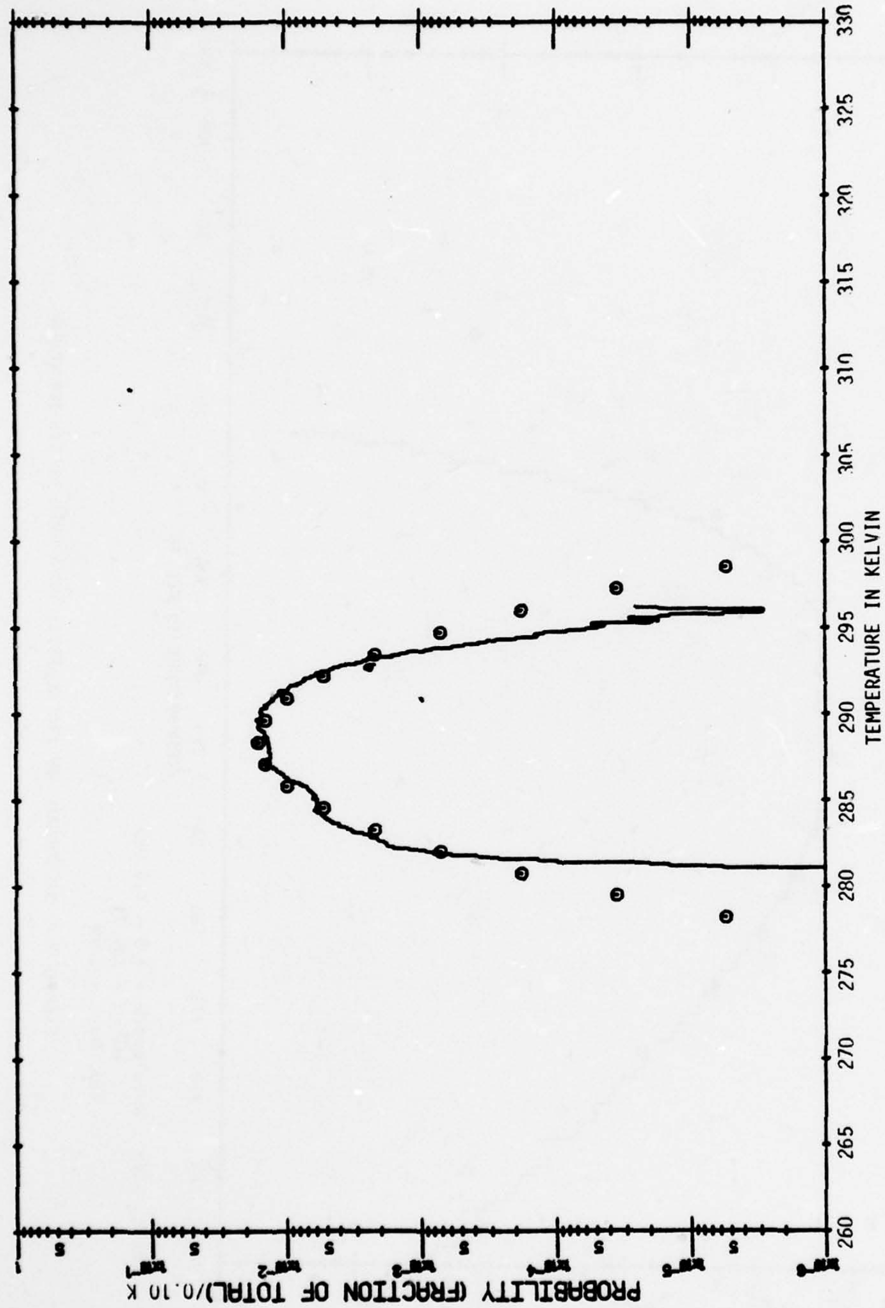

Area: NEVK Wavelength = 3.9 - 4.7 µm
Mean = 288.34
Std. Dev. = 2.53

FIGURE 6a. HISTOGRAM OF (TOTAL-AREA) DATA OVER NELLIS MOUNTAINS

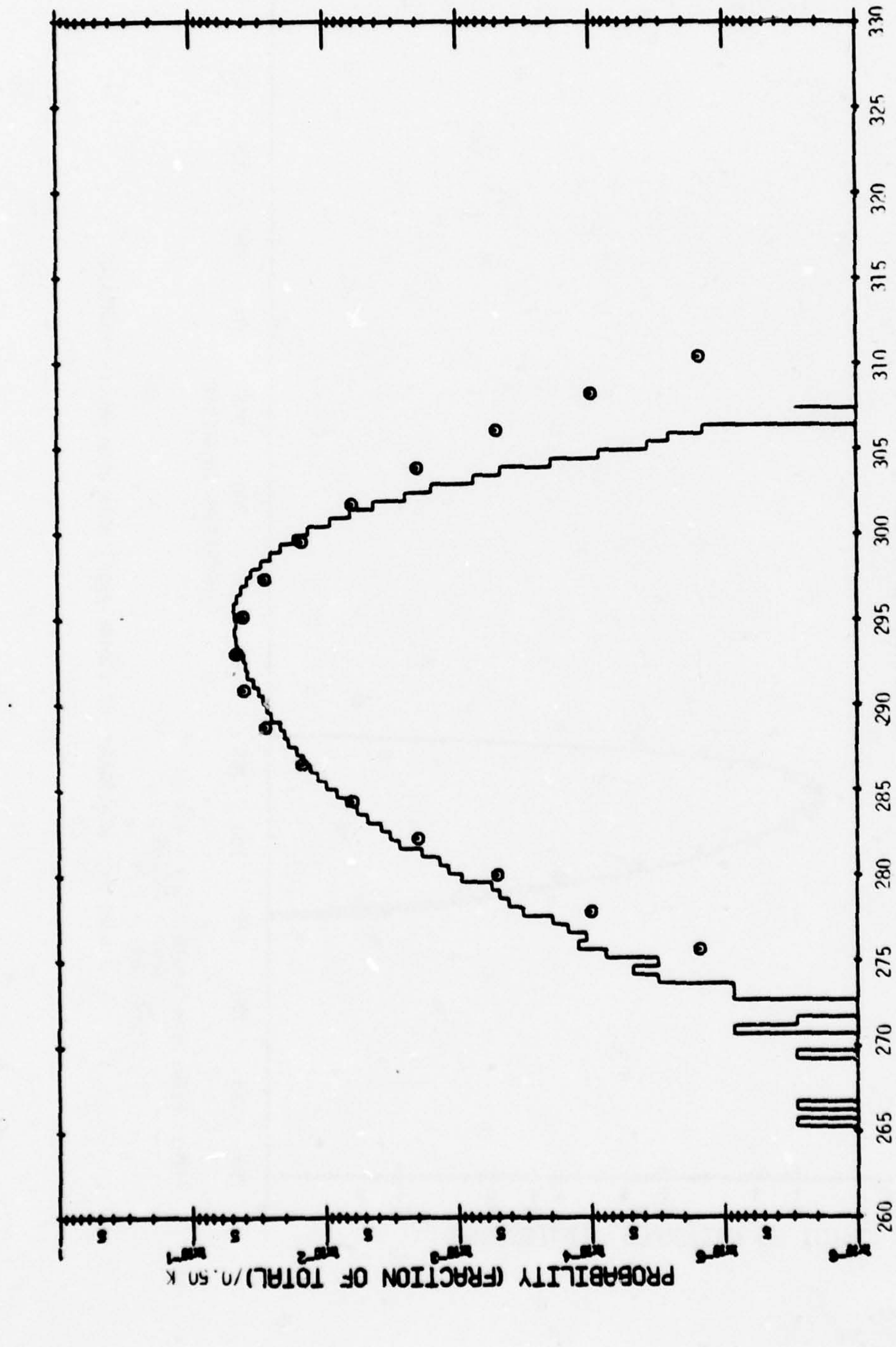

Area: NEVK Wavelength = 3.5 - 3.9 μm
Mean = 293.06
Std. Dev. = 4.34

FIGURE 6b. HISTOGRAM OF (TOTAL-AREA) DATA OVER NELLIS MOUNTAINS

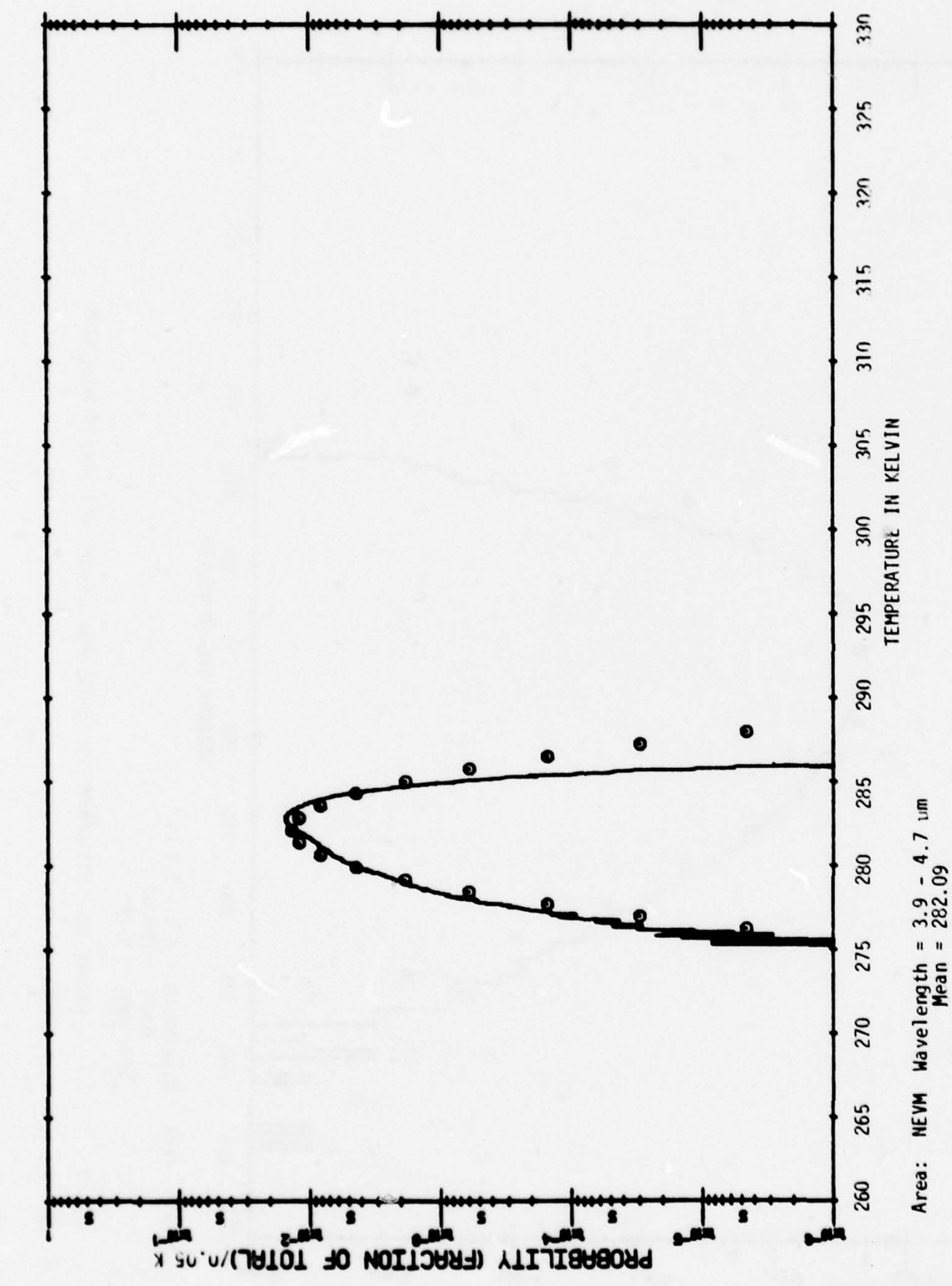

FIGURE 7a. HISTOGRAM OF (TOTAL-AREA) DATA OVER NELLIS MOUNTAINS

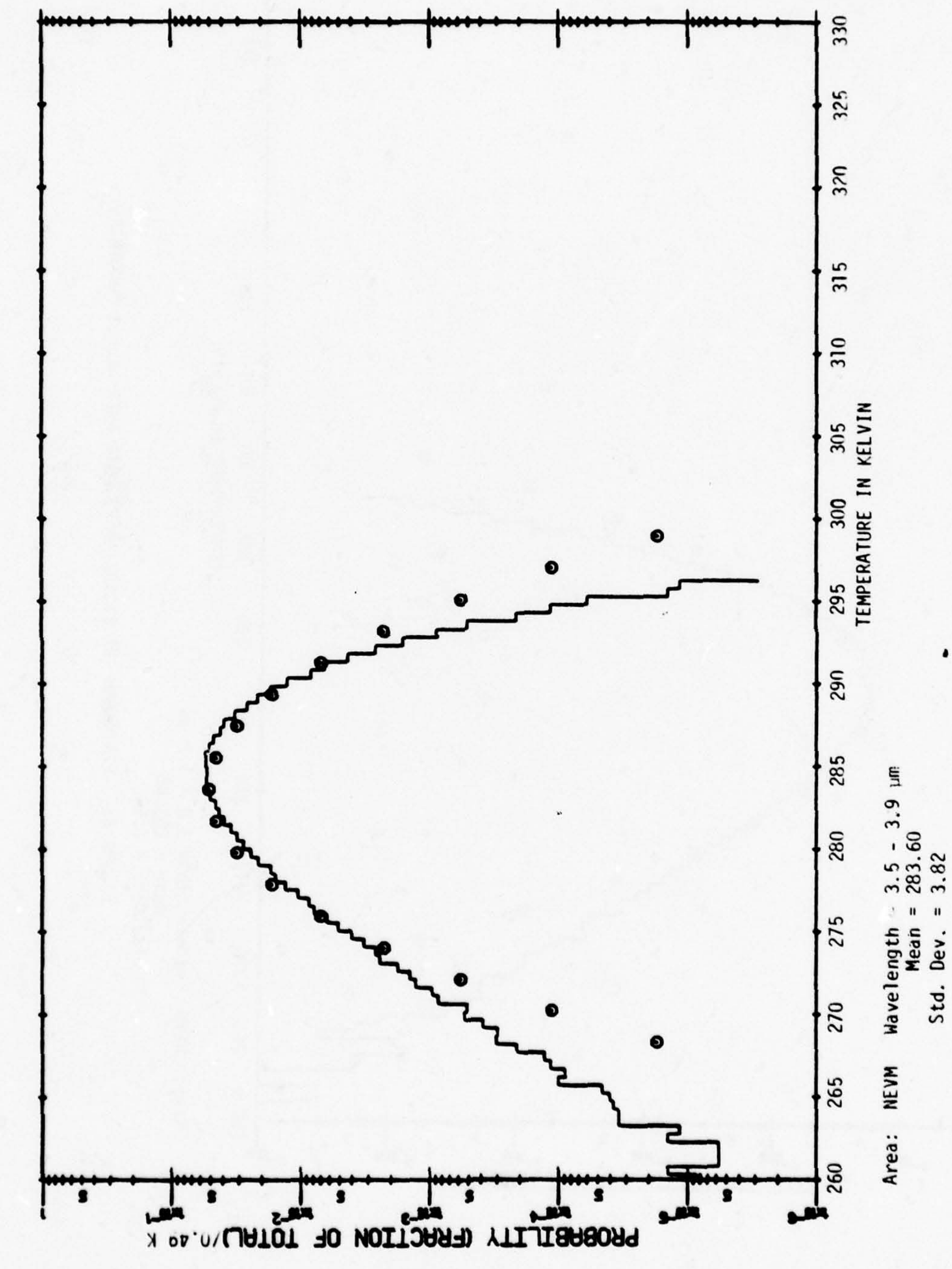

FIGURE 7b. HISTOGRAM OF (TOTAL-AREA) DATA OVER NELLIS MOUNTAINS

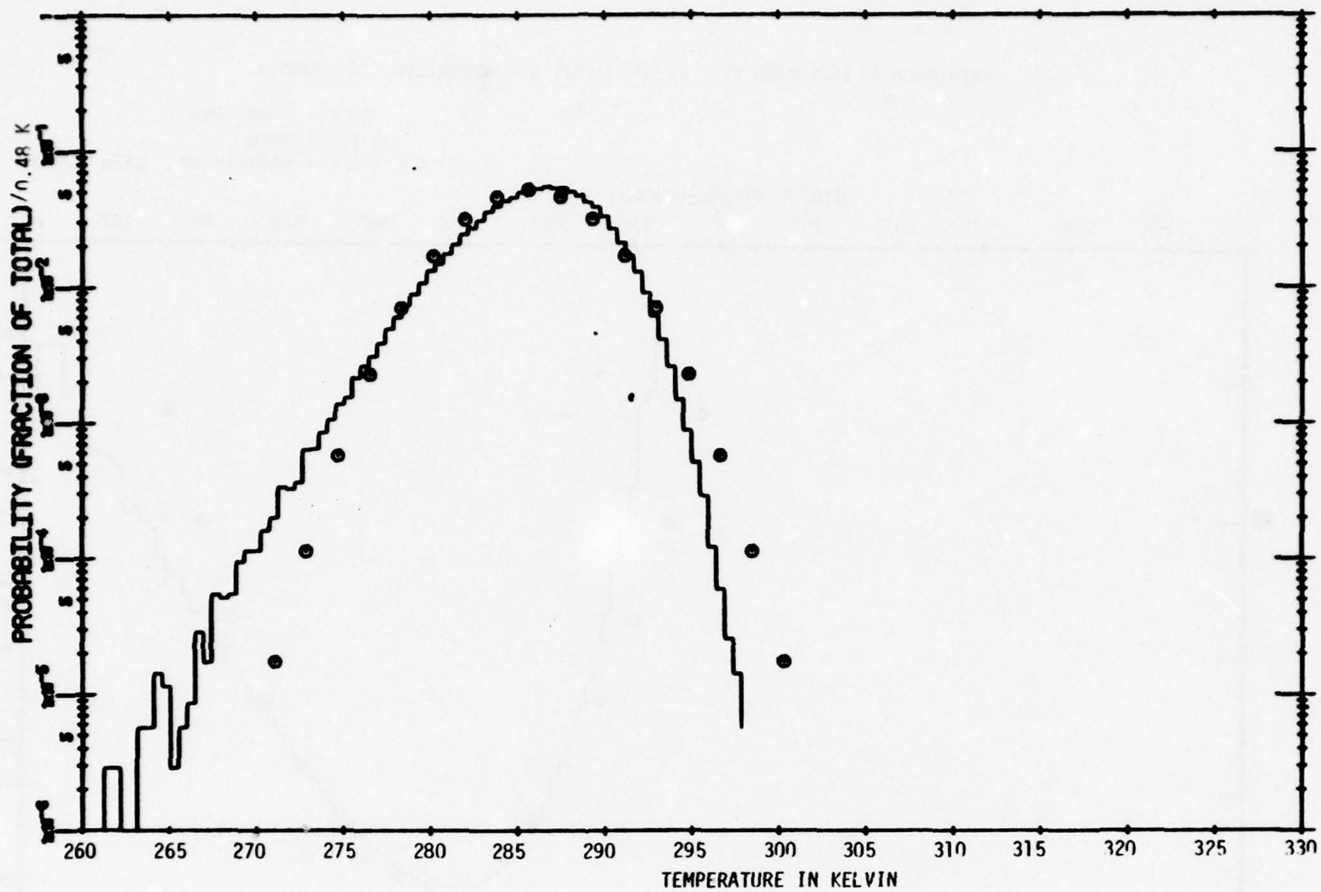

Area: NEVN Wavelength = 3.0 - 4.2 μm
Mean = 285.68
Std. Dev. = 3.65

FIGURE 8a. HISTOGRAM OF (TOTAL-AREA) DATA OVER NELLIS MOUNTAINS

Area: NEVN Wavelength = 4.5 - 5.5 μm
Mean = 283.12
Std. Dev. = 1.50

FIGURE 8b. HISTOGRAM OF (TOTAL-AREA) DATA OVER NELLIS MOUNTAINS

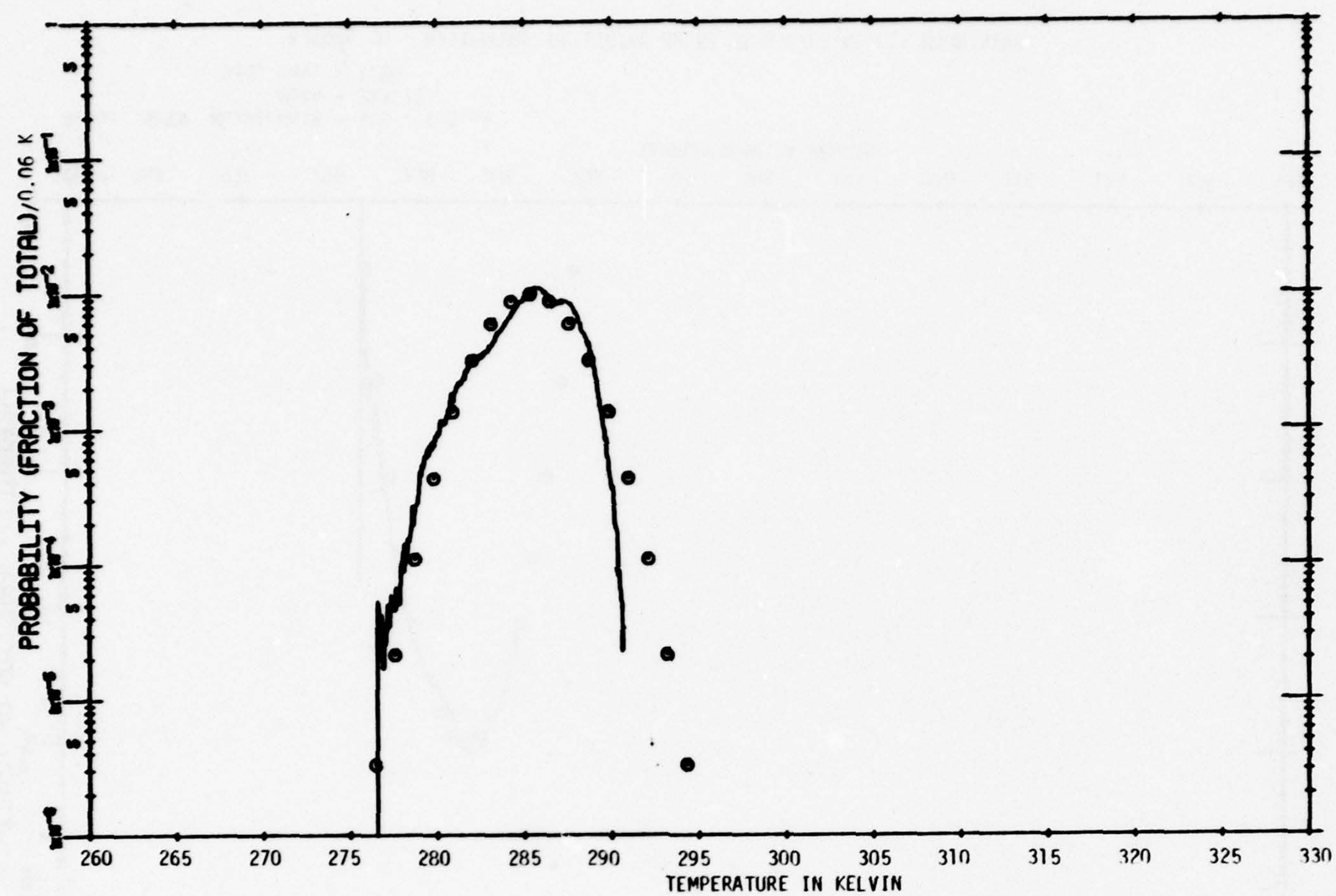

Area: NEVN Wavelength = 9.0 - 11.4 μm
Mean = 285.37
Std. Dev. = 2.23

FIGURE 8c. HISTOGRAM OF (TOTAL-AREA) DATA OVER NELLIS MOUNTAINS

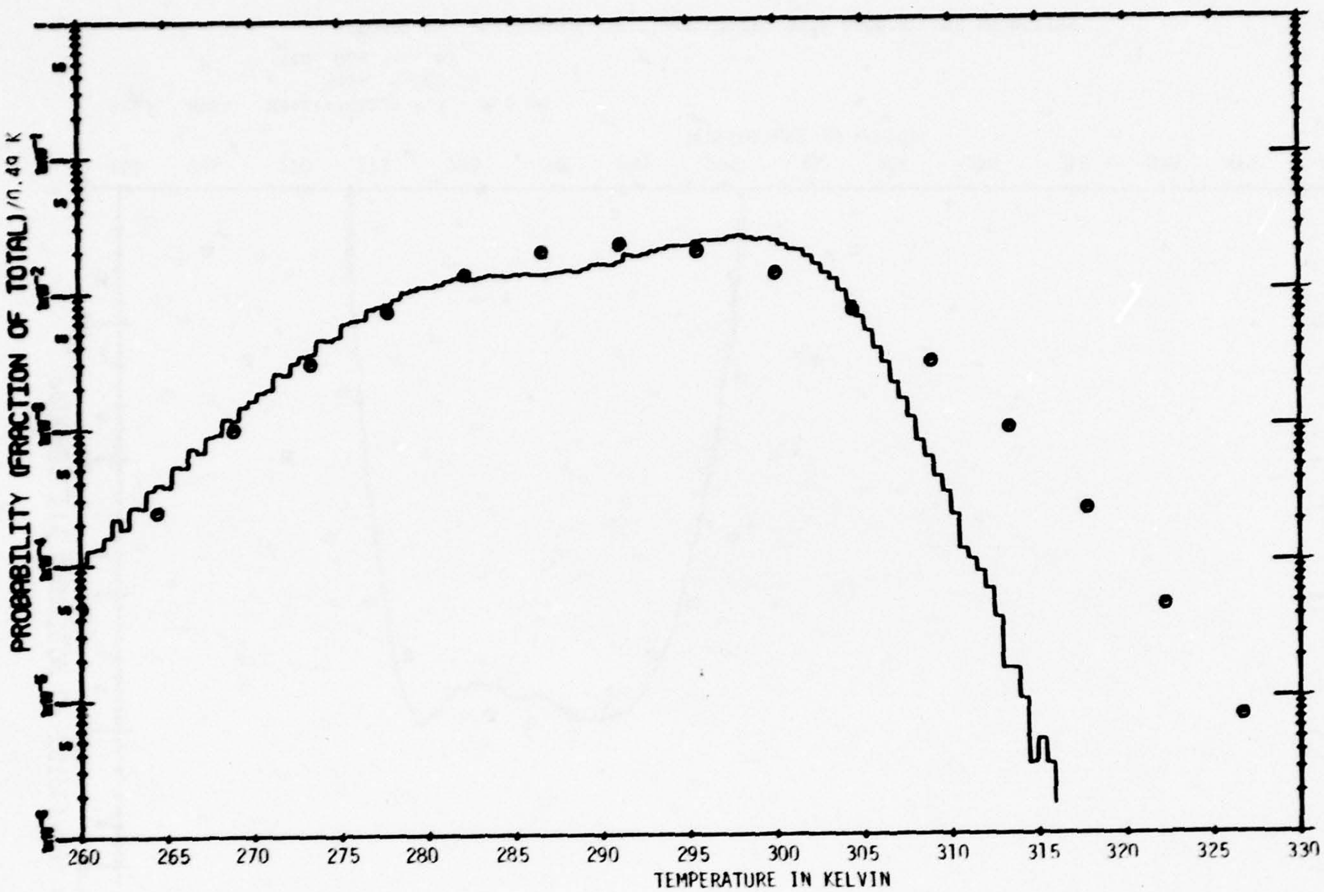

Area: NVG1 Wavelength = 3.0 - 4.2 μm
Mean = 291.12
Std. Dev. = 8.39

FIGURE 9a. HISTOGRAM OF (TOTAL-AREA) DATA OVER NELLIS MOUNTAINS

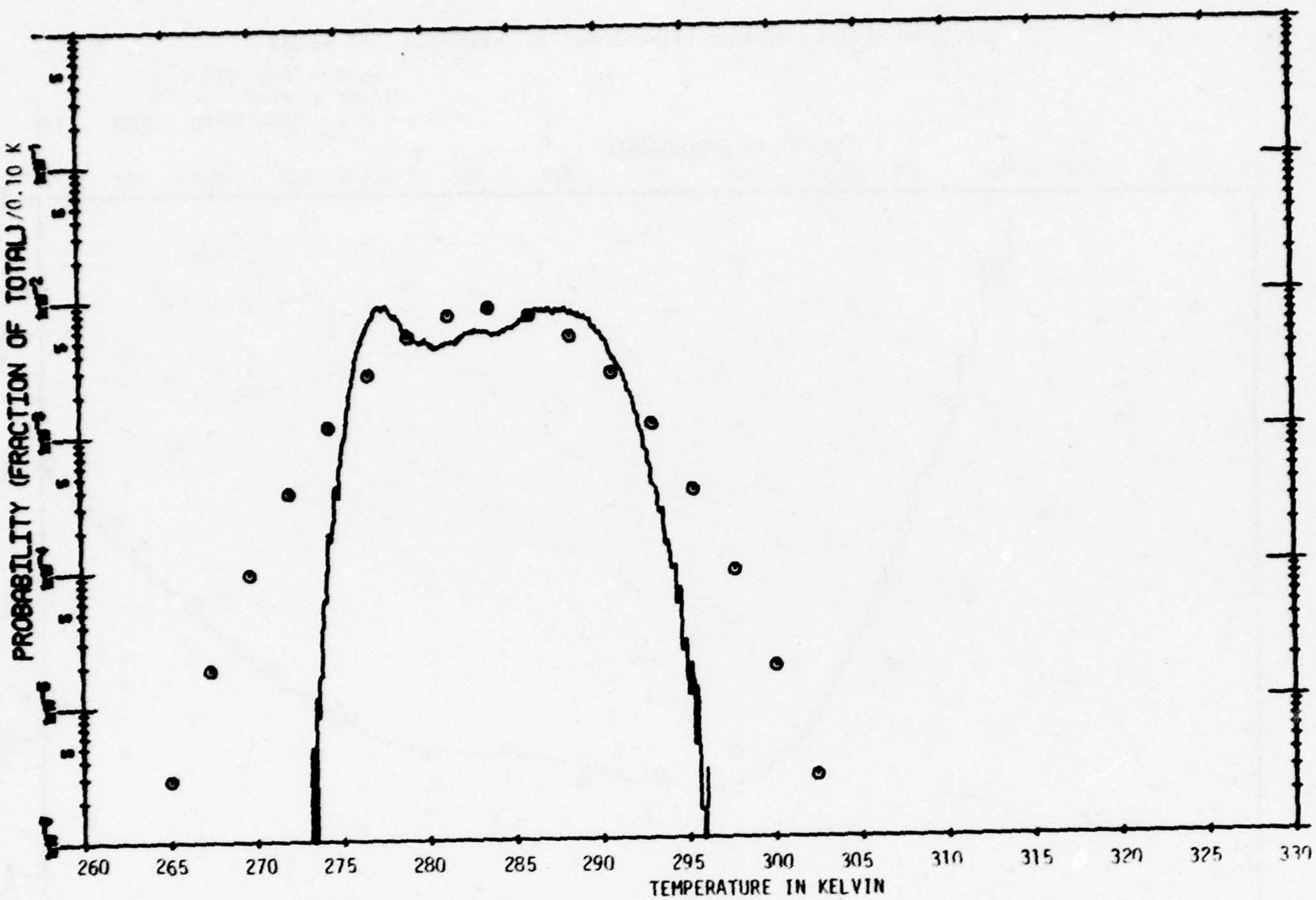

Area: NVG1 Wavelength = 4.5 - 5.5 μm
Mean = 283.73
Std. Dev. = 4.67

FIGURE 9b. HISTOGRAM OF (TOTAL-AREA) DATA OVER NELLIS MOUNTAINS

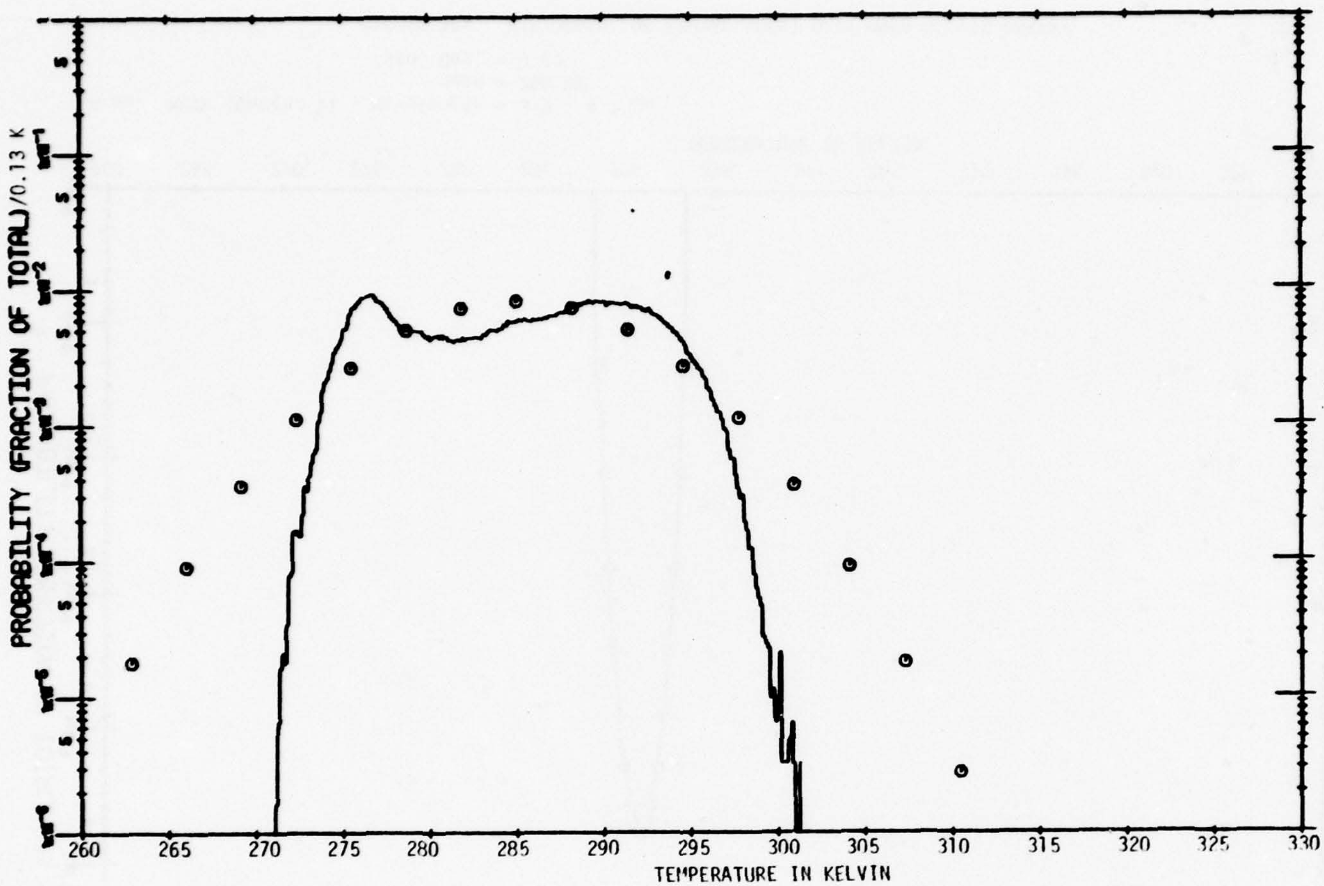

Area: NVG1 Wavelength = 9.0 - 11.4 μm
Mean = 285.06
Std. Dev. = 6.35

FIGURE 9c. HISTOGRAM OF (TOTAL-AREA) DATA OVER NELLIS MOUNTAINS

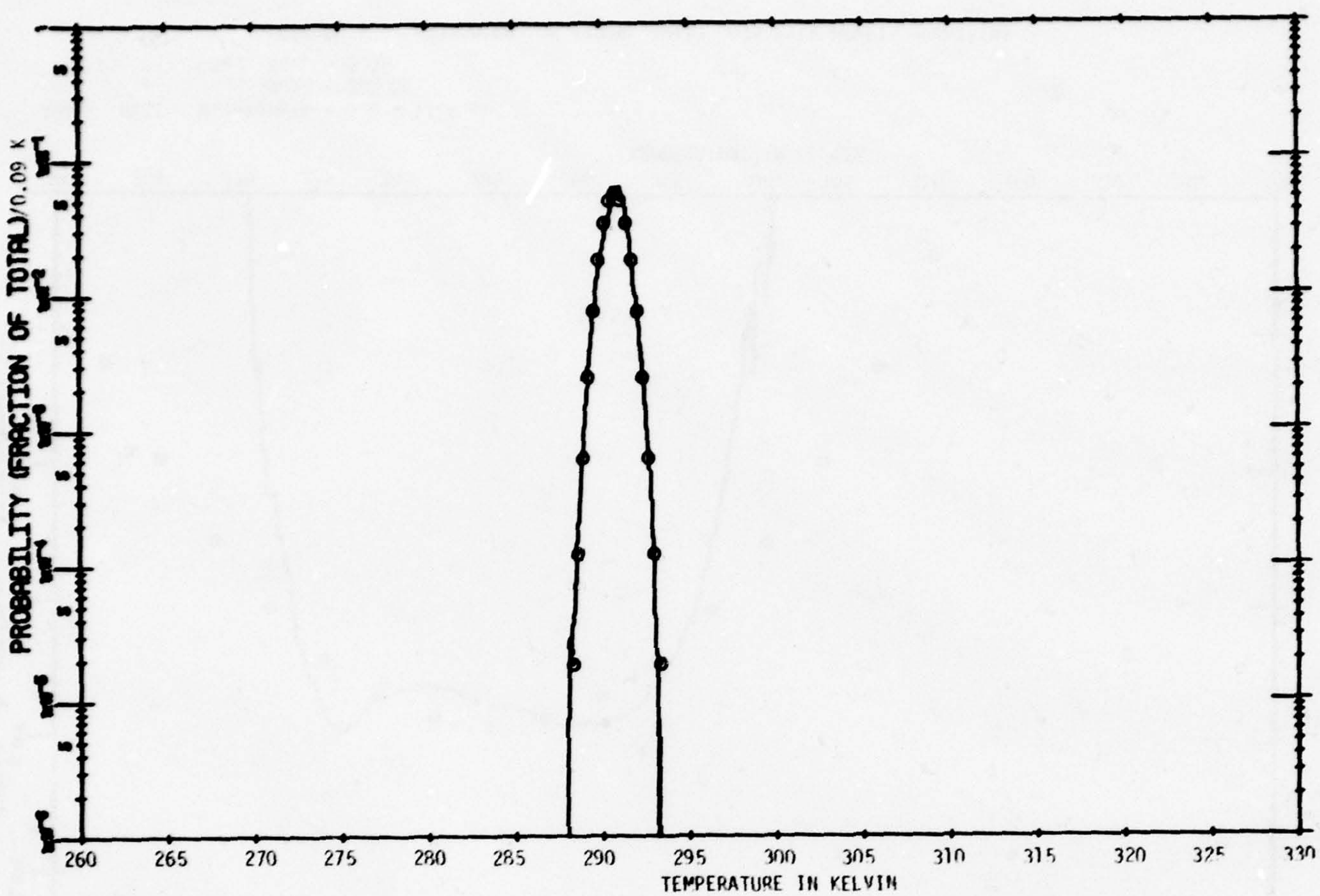

Area: NEVL (Desert 1) Wavelength = 3.9 - 4.7 μm
Mean = 290.84
Std. Dev. = 0.63

FIGURE 10a. HISTOGRAM OF (TOTAL-AREA) DATA OVER NELLIS DESERT

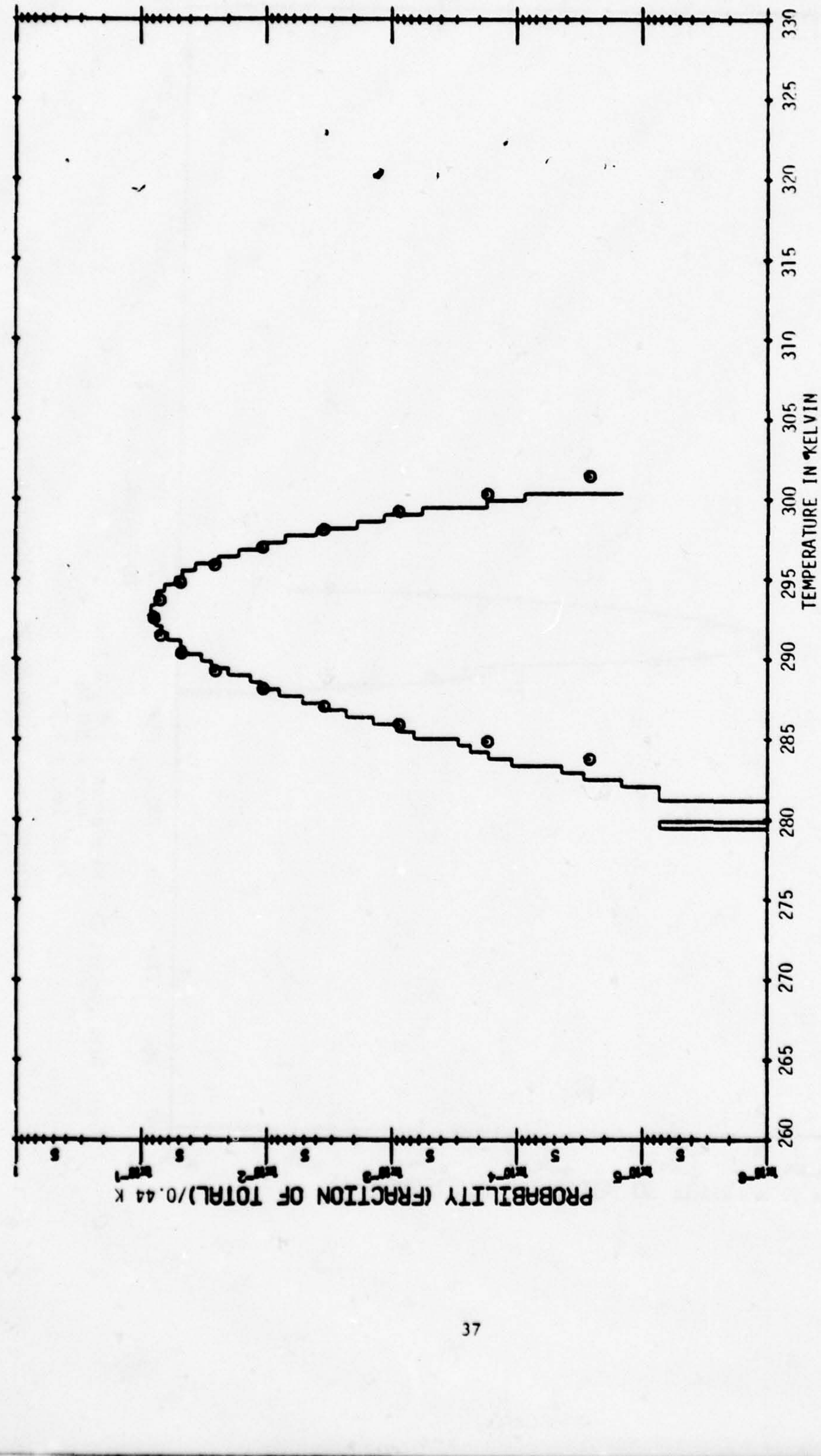

Area: NEVL (Desert 1) Wavelength = 3.5 - 3.9 μm
Mean = 292.60
Std. Dev. = 2.21

FIGURE 10b. HISTOGRAM OF (TOTAL-AREA) DATA OVER NELLIS DESERT

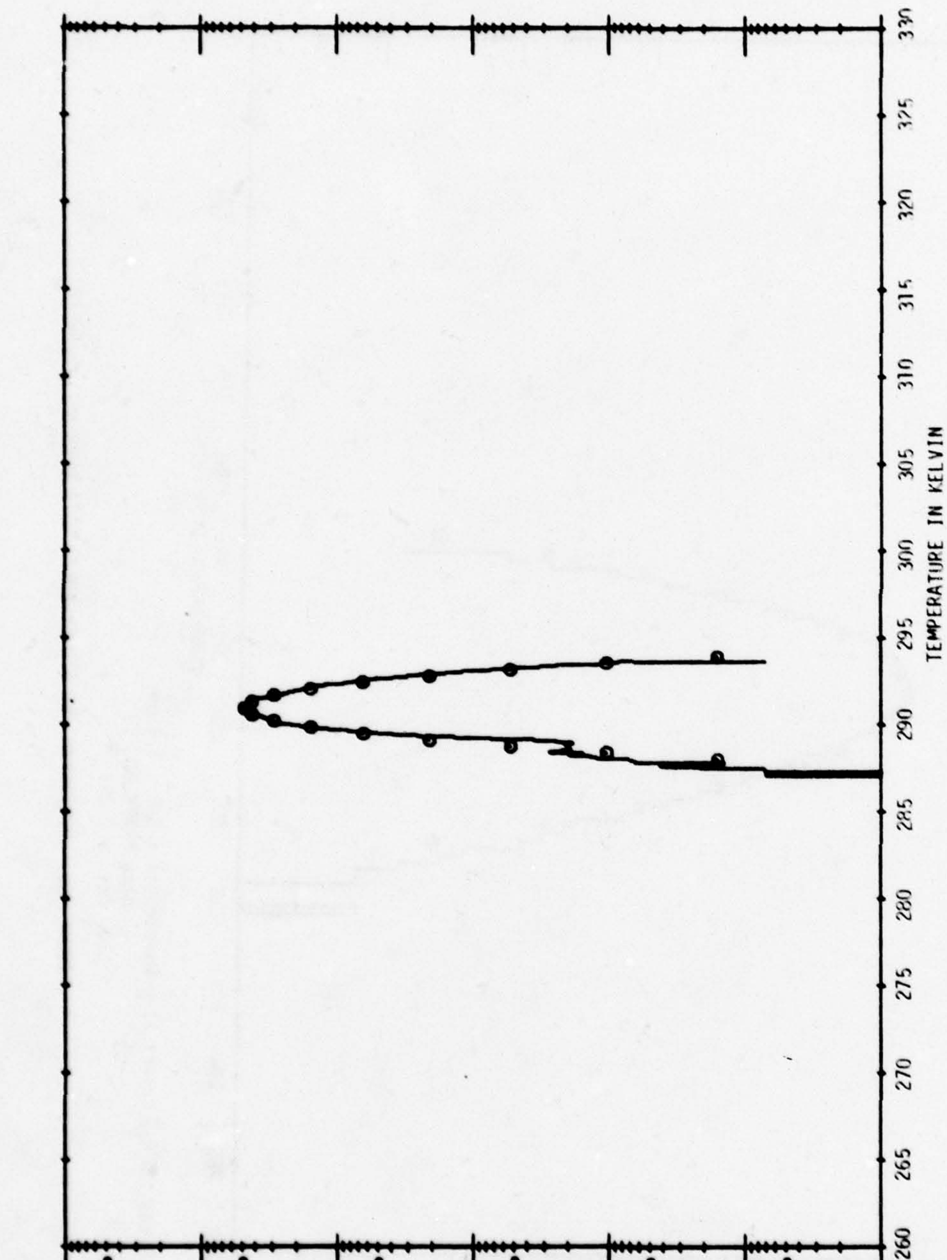

Area: NEVL (Desert 2) Wavelength = 3.9 - 4.7 μm
Mean = 290.95
Std. Dev. = 0.74

FIGURE 10c. HISTOGRAM OF (TOTAL-AREA) DATA OVER NELLIS DESERT

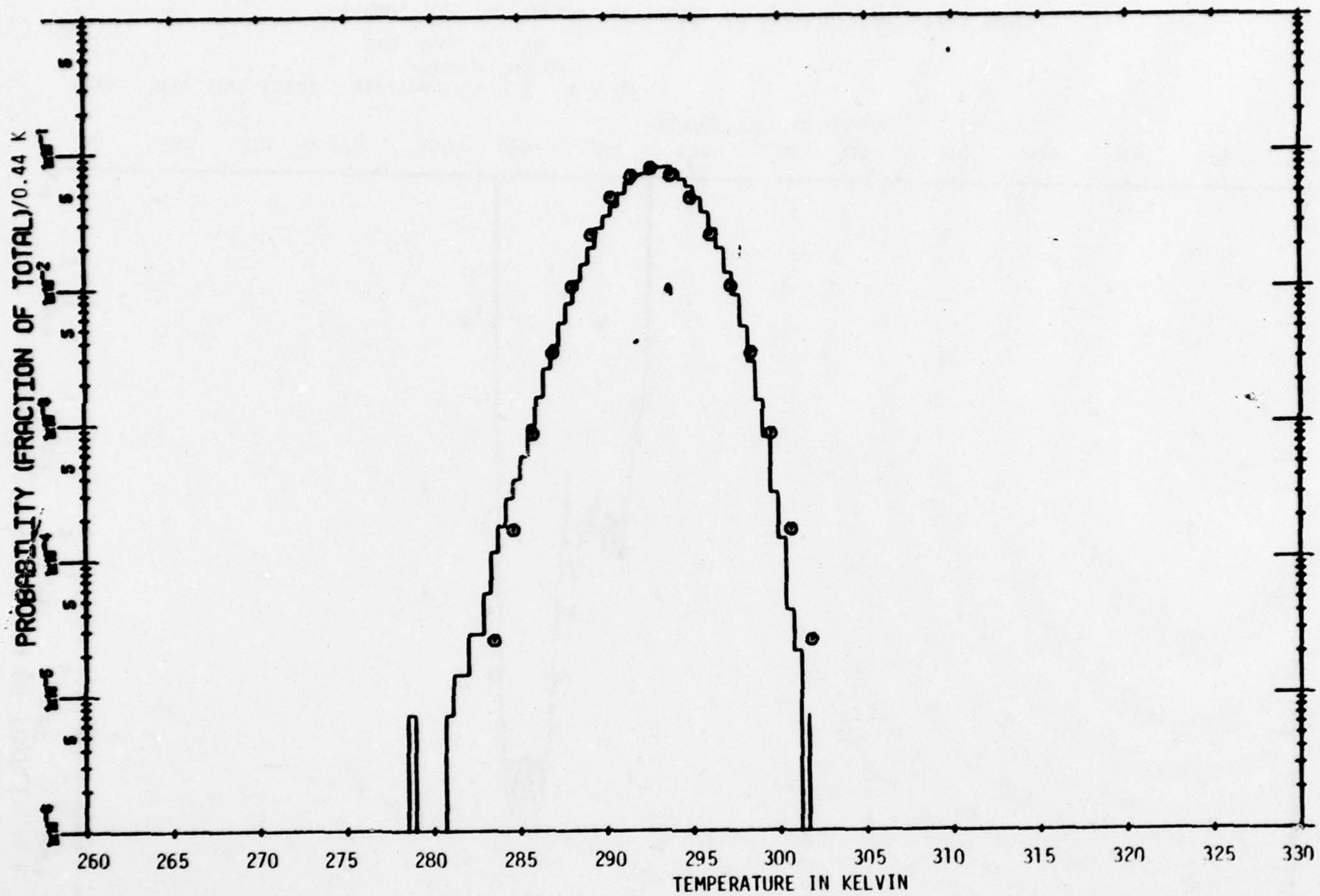

Area: NEVL (Desert 2) Wavelength = 3.5 - 3.9 μm
Mean = 292.66
Std. Dev. = 2.28

FIGURE 10d. HISTOGRAM OF (TOTAL-AREA) DATA OVER NELLIS DESERT

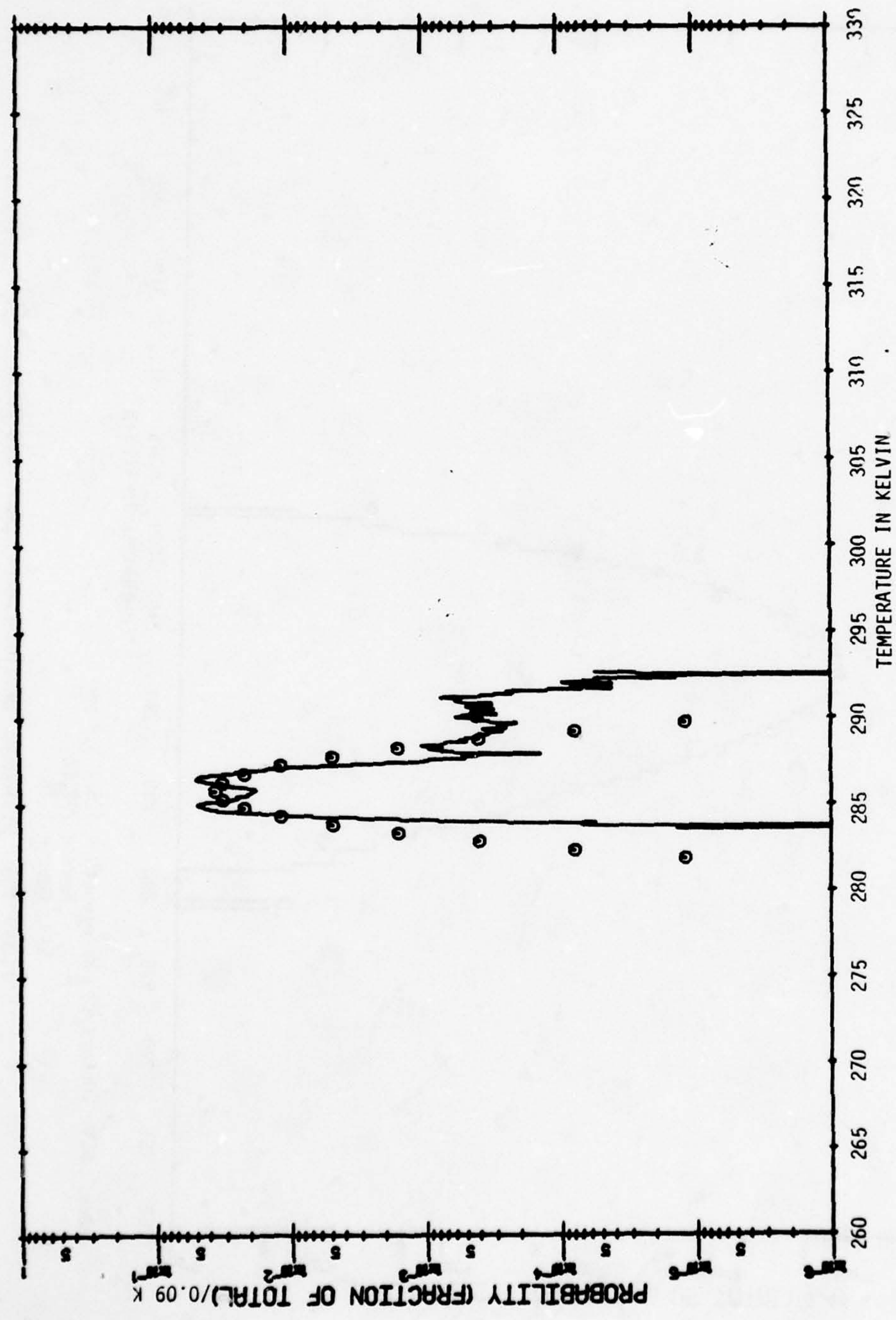

Area: NEVL (Dry Lake) Wavelength = 3.9 - 4.7 µm
Mean = 285.83
Std. Dev. = 0.98

FIGURE 10e. HISTOGRAM OF (TOTAL-AREA) DATA OVER NELLIS DESERT

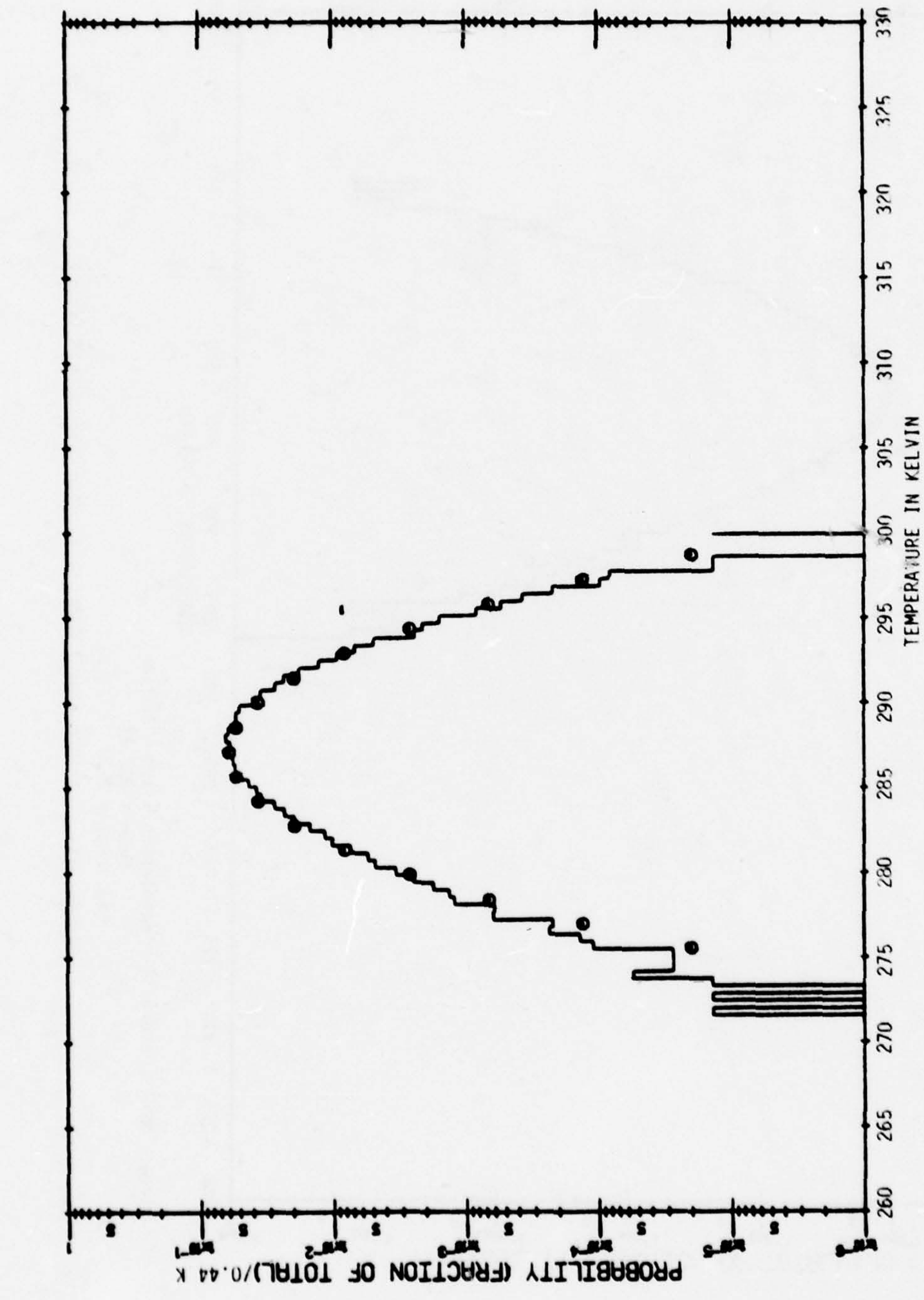

Area: NEVL (Dry Lake) Wavelength = 3.5 - 3.9 μm
Mean = 287.11
Std. Dev. = 2.89

FIGURE 10f. HISTOGRAM OF (TOTAL-AREA) DATA OVER NELLIS DESERT

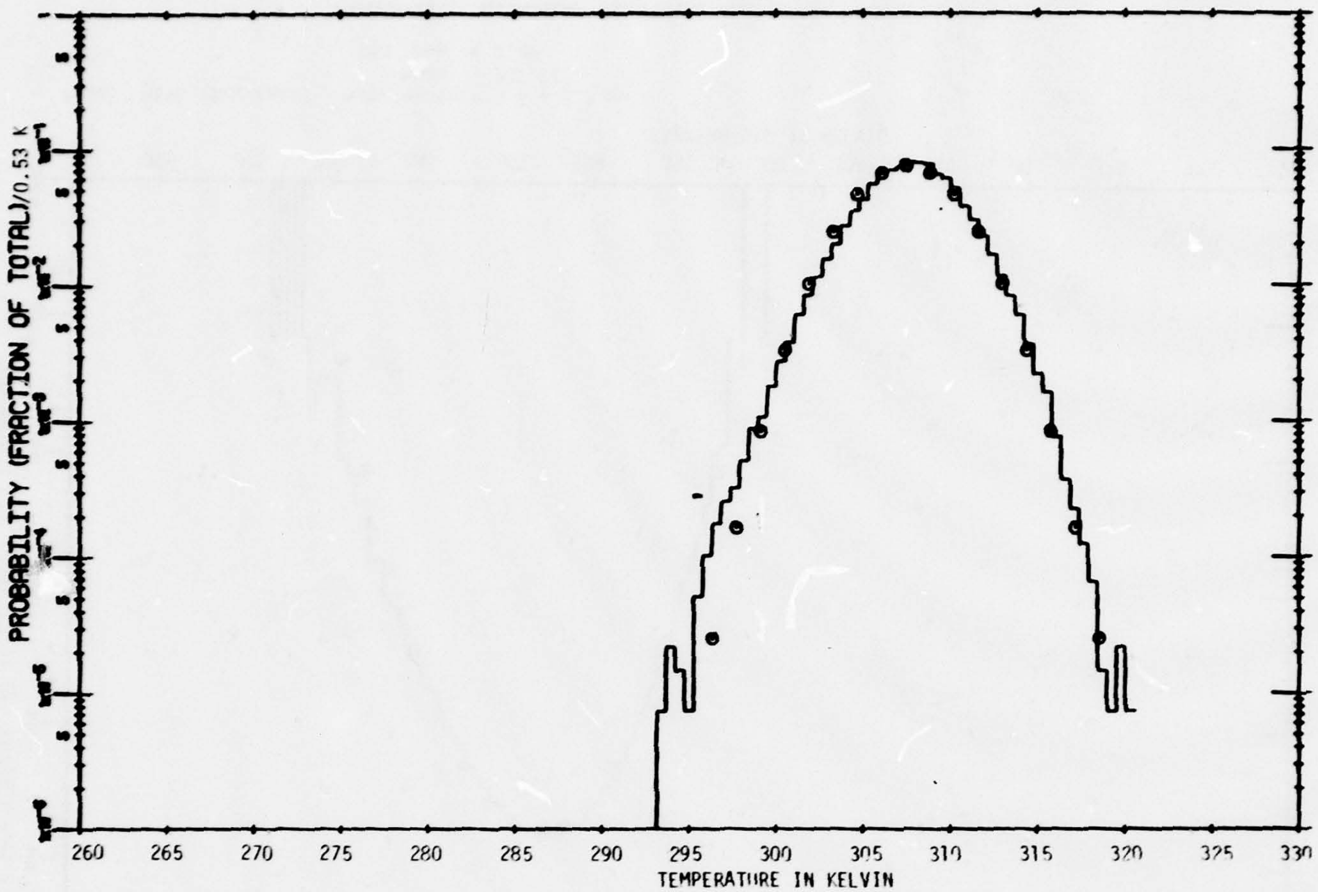

Area: NVH1 (Desert 1) Wavelength = 3.0 - 4.2 μm
Mean = 307.45
Std. Dev. = 2.77

FIGURE 11a. HISTOGRAM OF (TOTAL-AREA) DATA OVER NELLIS DESERT

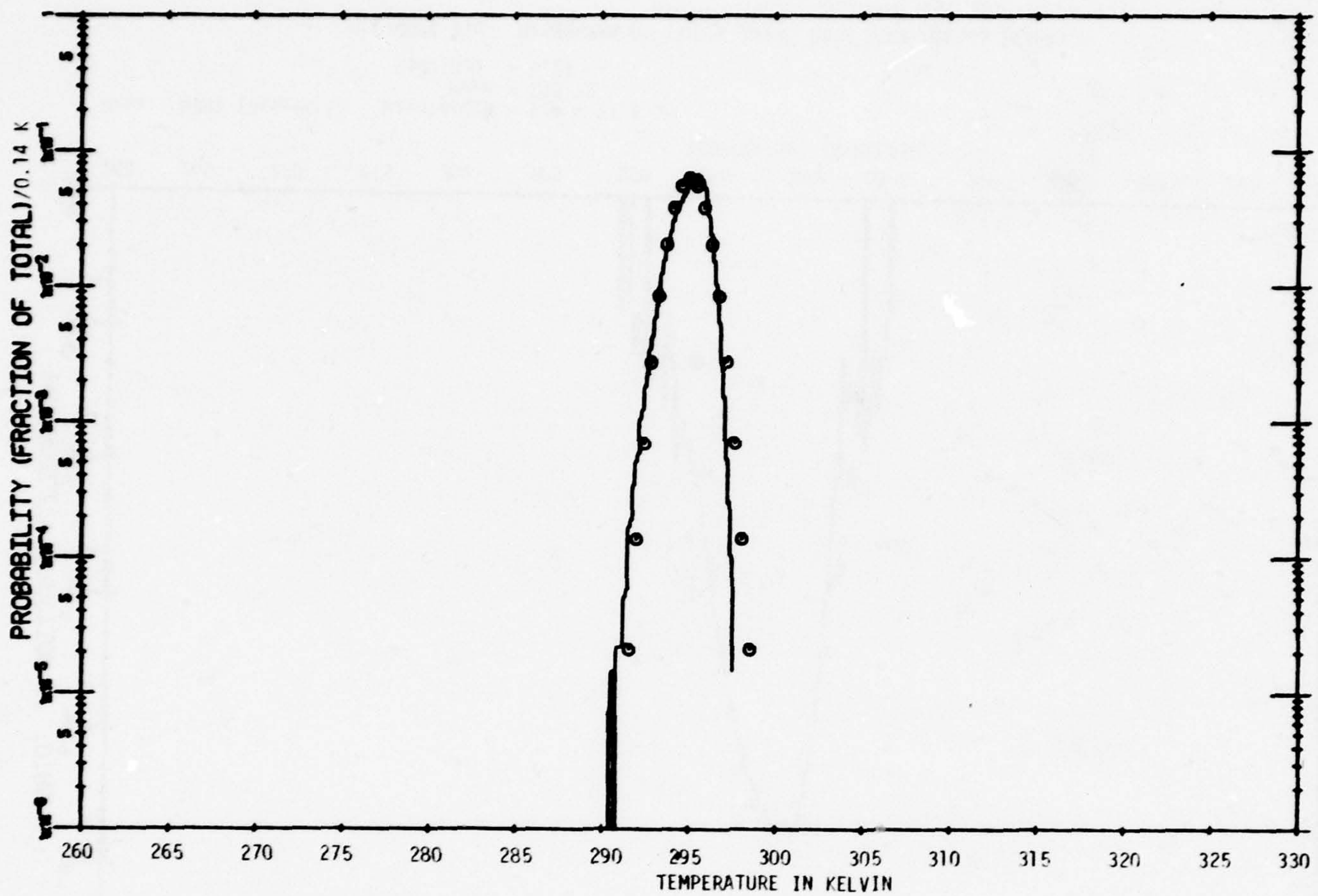

Area: NVH1 (Desert 1) Wavelength = 4.5 - 5.5 μm
Mean = 295.02
Std. Dev. = 0.87

FIGURE 11b. HISTOGRAM OF (TOTAL-AREA) DATA OVER NELLIS DESERT

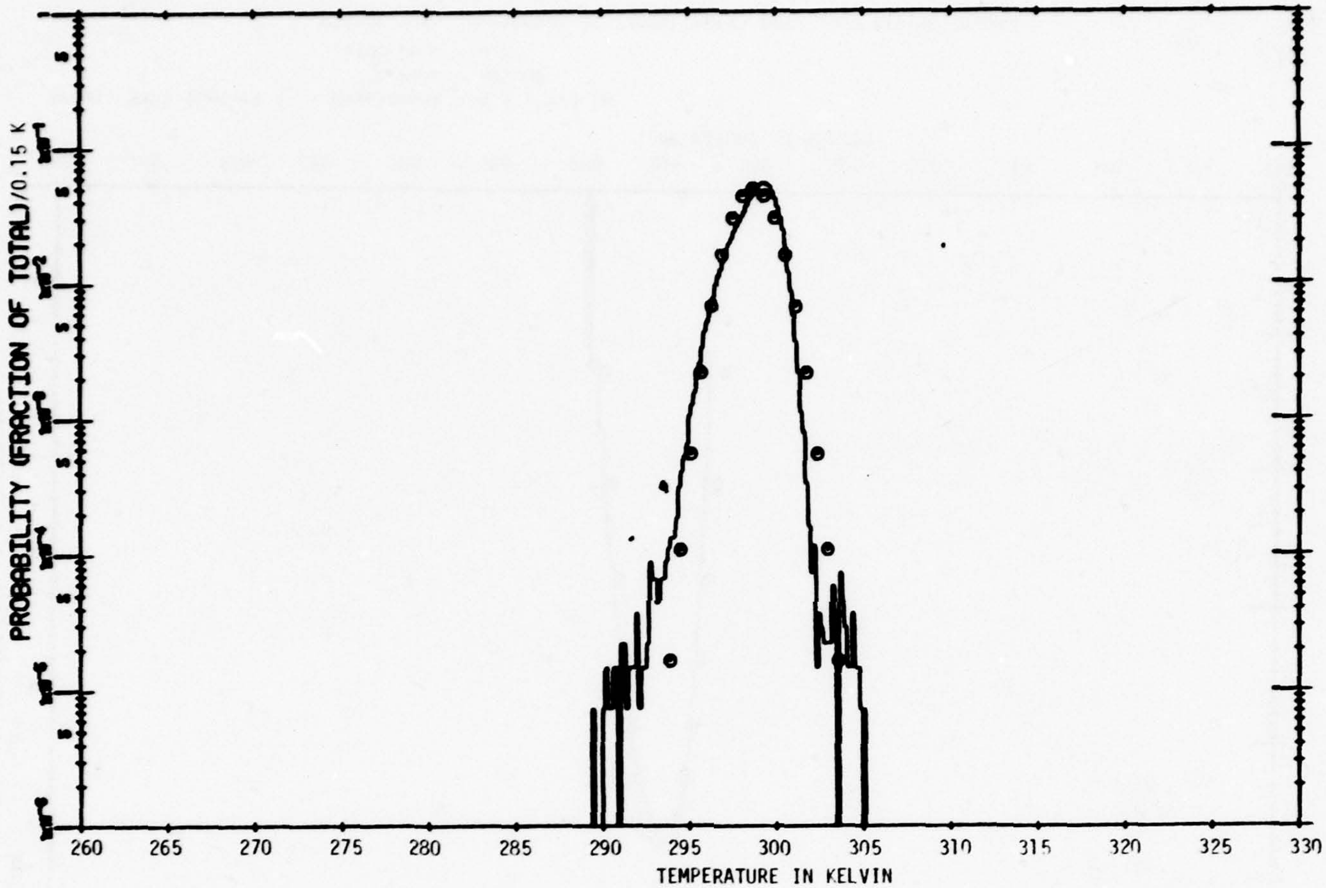

Area: NVH1 (Desert 1) Wavelength = 9.0 - 11.4 μm
Mean = 298.72
Std. Dev. = 1.21

FIGURE 11c. HISTOGRAM OF (TOTAL-AREA) DATA OVER NELLIS DESERT

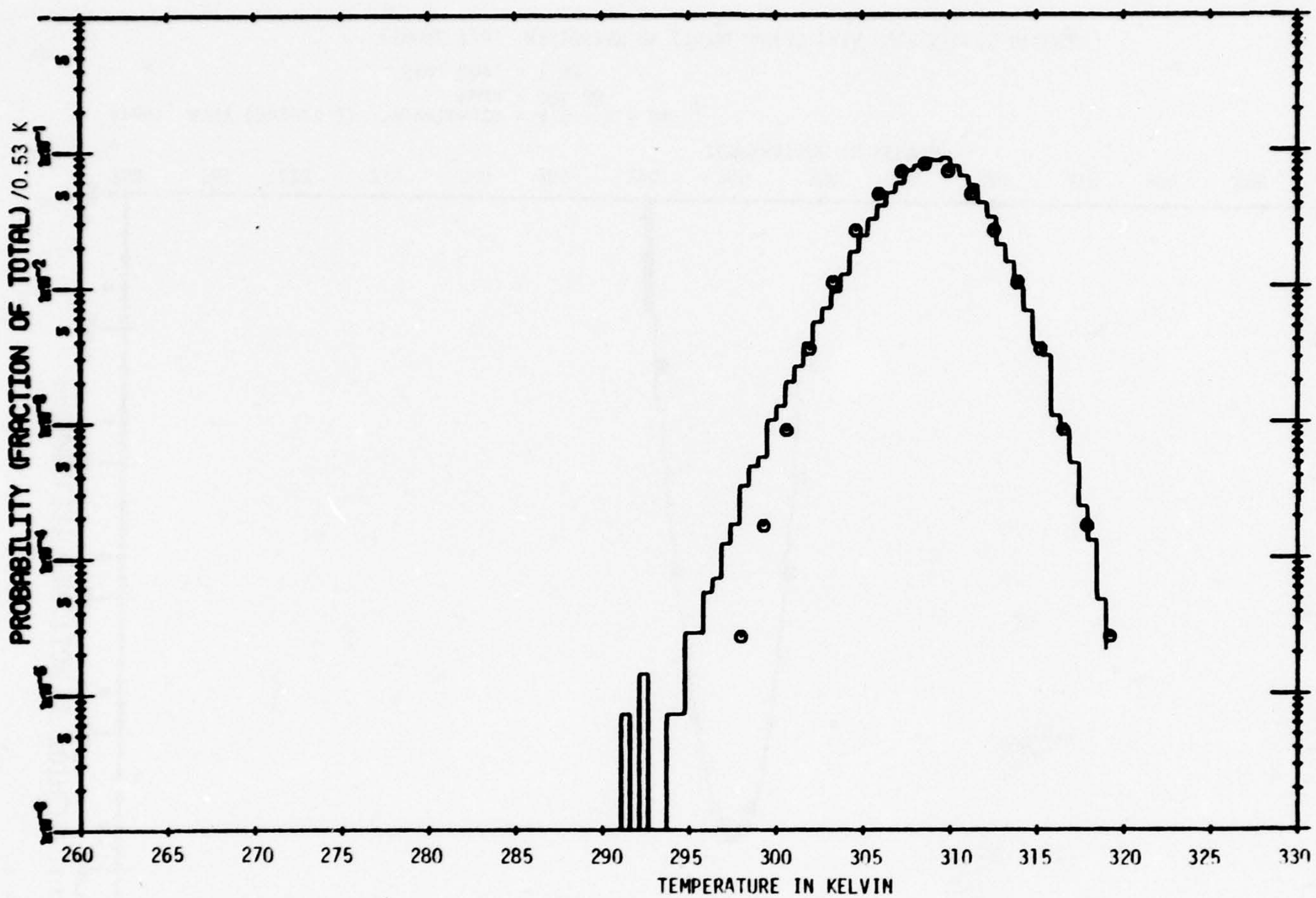

Area: NVH1 (Desert 2) Wavelength = 3.0 - 4.2 μm
Mean = 308.60
Std. Dev. = 2.65

FIGURE 11d. HISTOGRAM OF (TOTAL-AREA) DATA OVER NELLIS DESERT

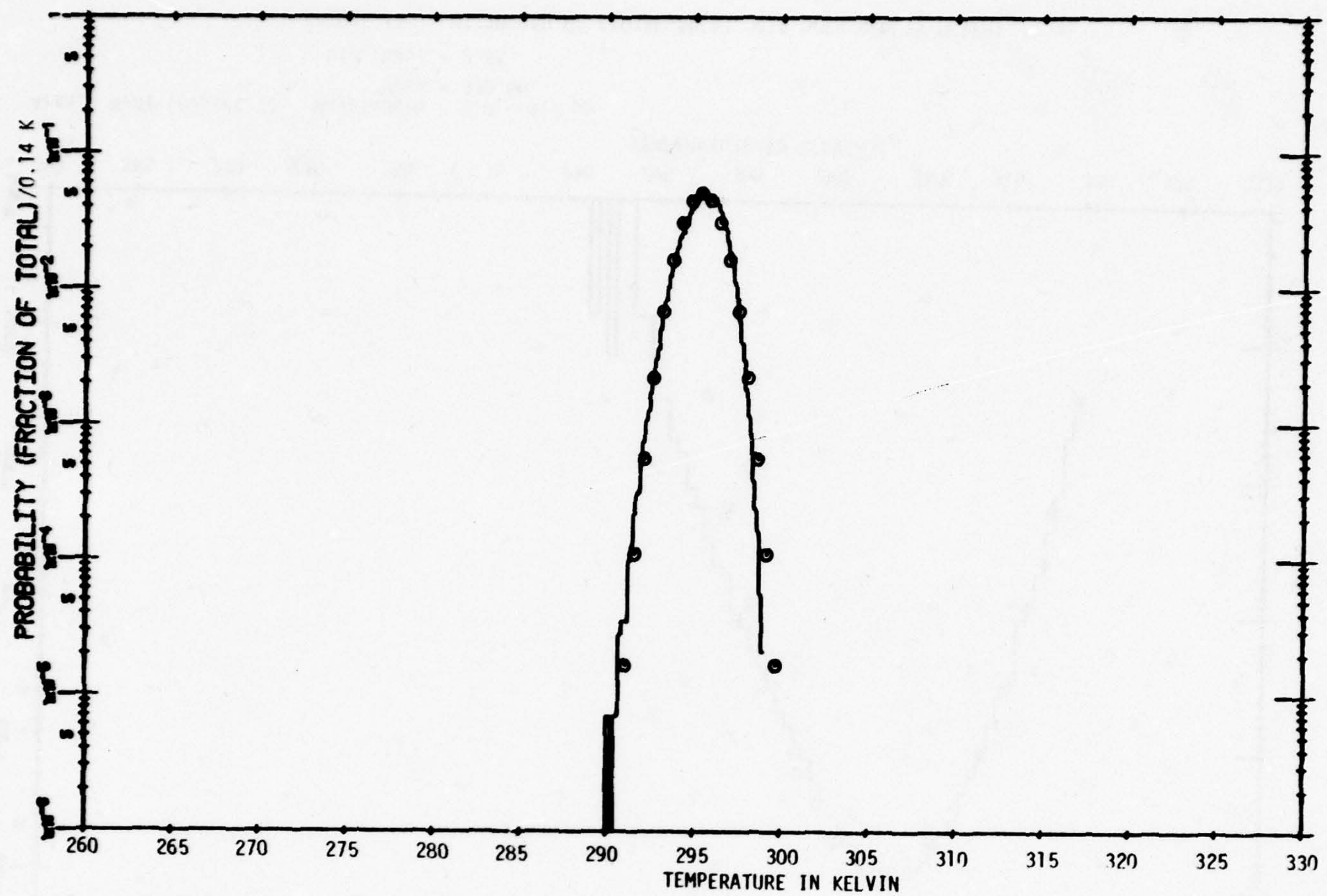

Area: NVH1 (Desert 2) Wavelength = 4.5 - 5.5 μm
Mean = 295.38
Std. Dev. = 1.08

FIGURE 11e. HISTOGRAM OF (TOTAL-AREA) DATA OVER NELLIS DESERT

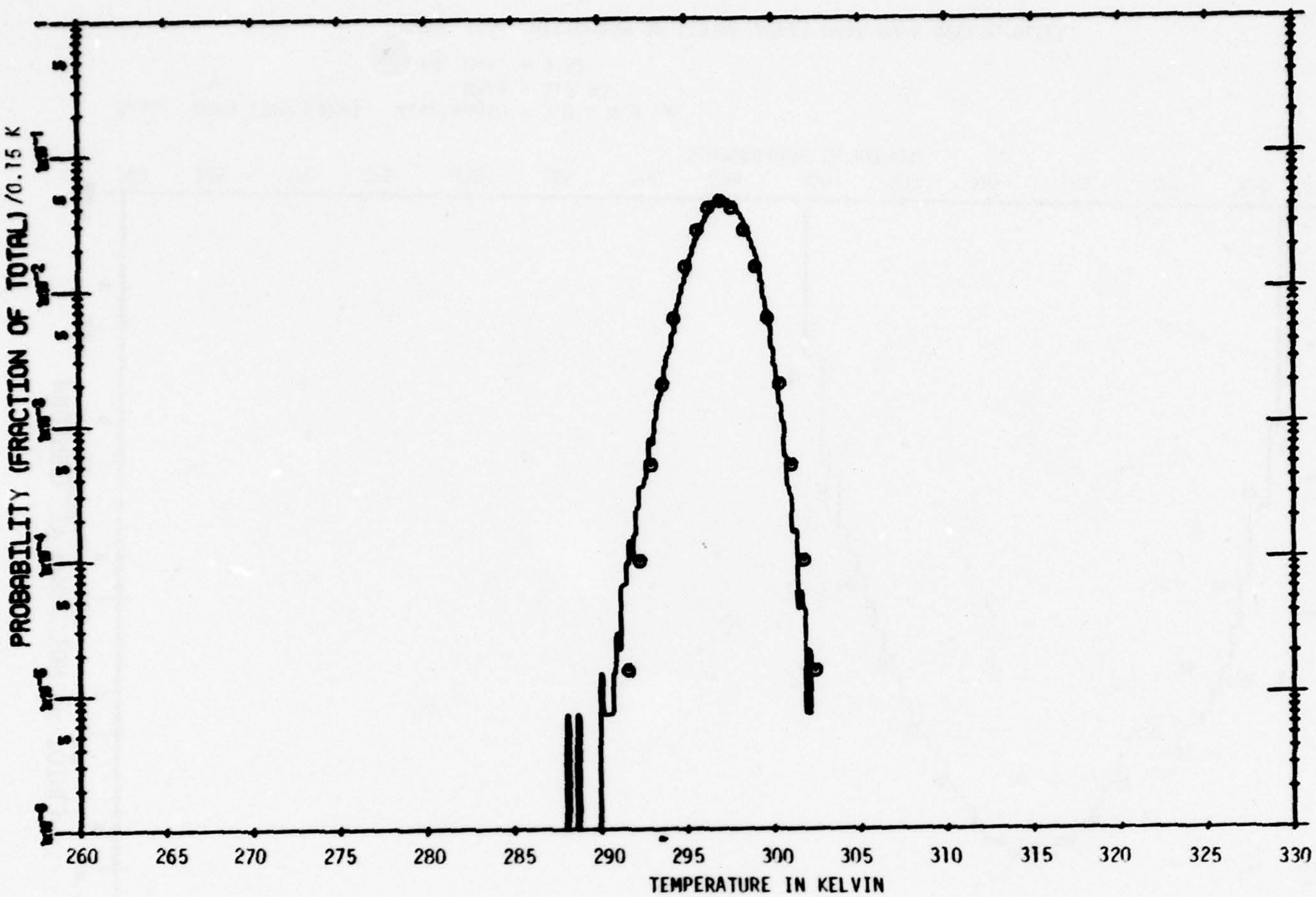

Area: NVH1 (Desert 2) Wavelength ≈ 9.0 - 11.4 μm
Mean ≈ 297.01
Std. Dev. ≈ 1.35

FIGURE 11f. HISTOGRAM OF (TOTAL-AREA) DATA OVER NELLIS DESERT

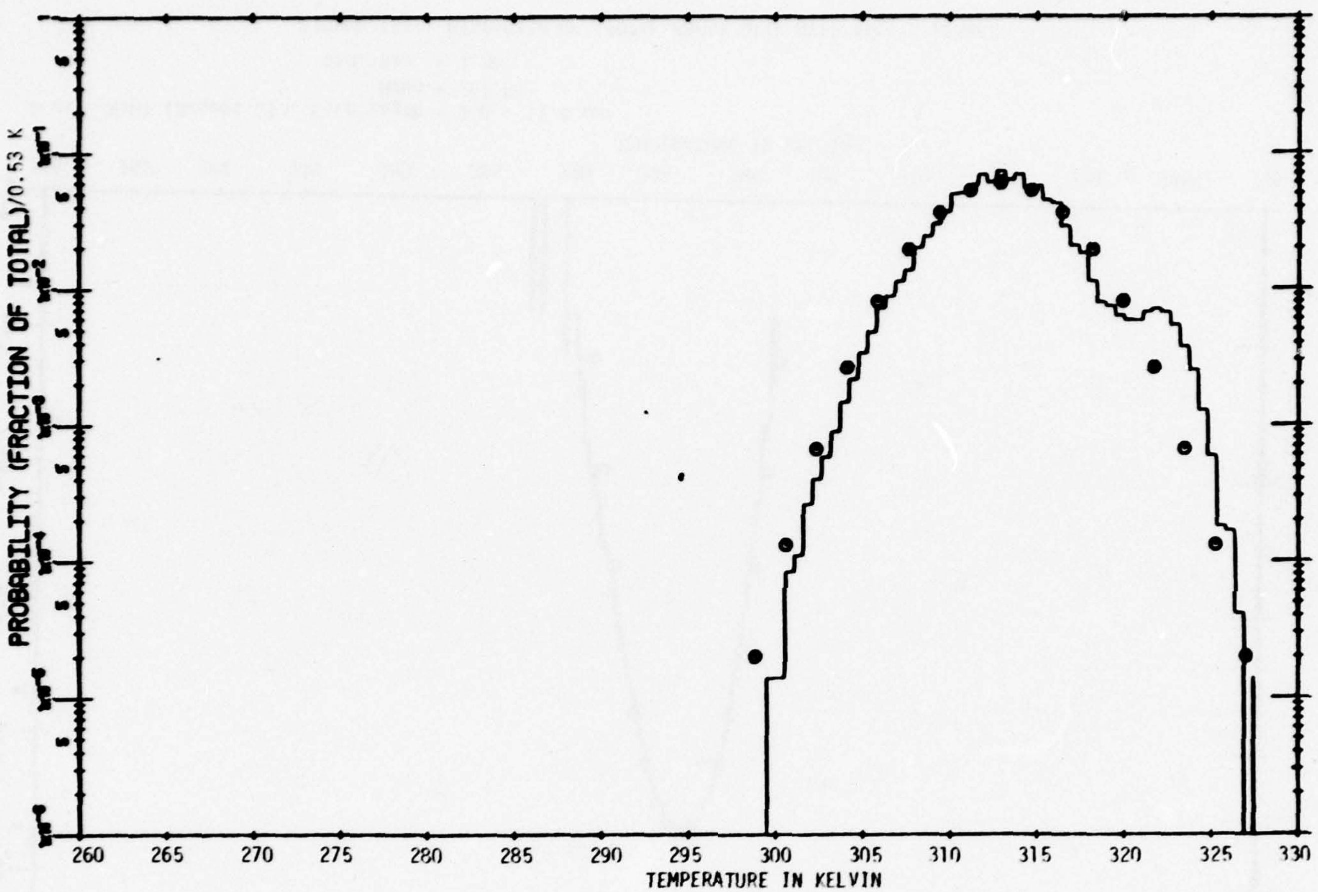

Area: NVH1 (Dry Lake) Wavelength = 3.0 - 4.2 μm
Mean = 312.90
Std. Dev. = 3.52

FIGURE 11g. HISTOGRAM OF (TOTAL-AREA) DATA OVER NELLIS DESERT

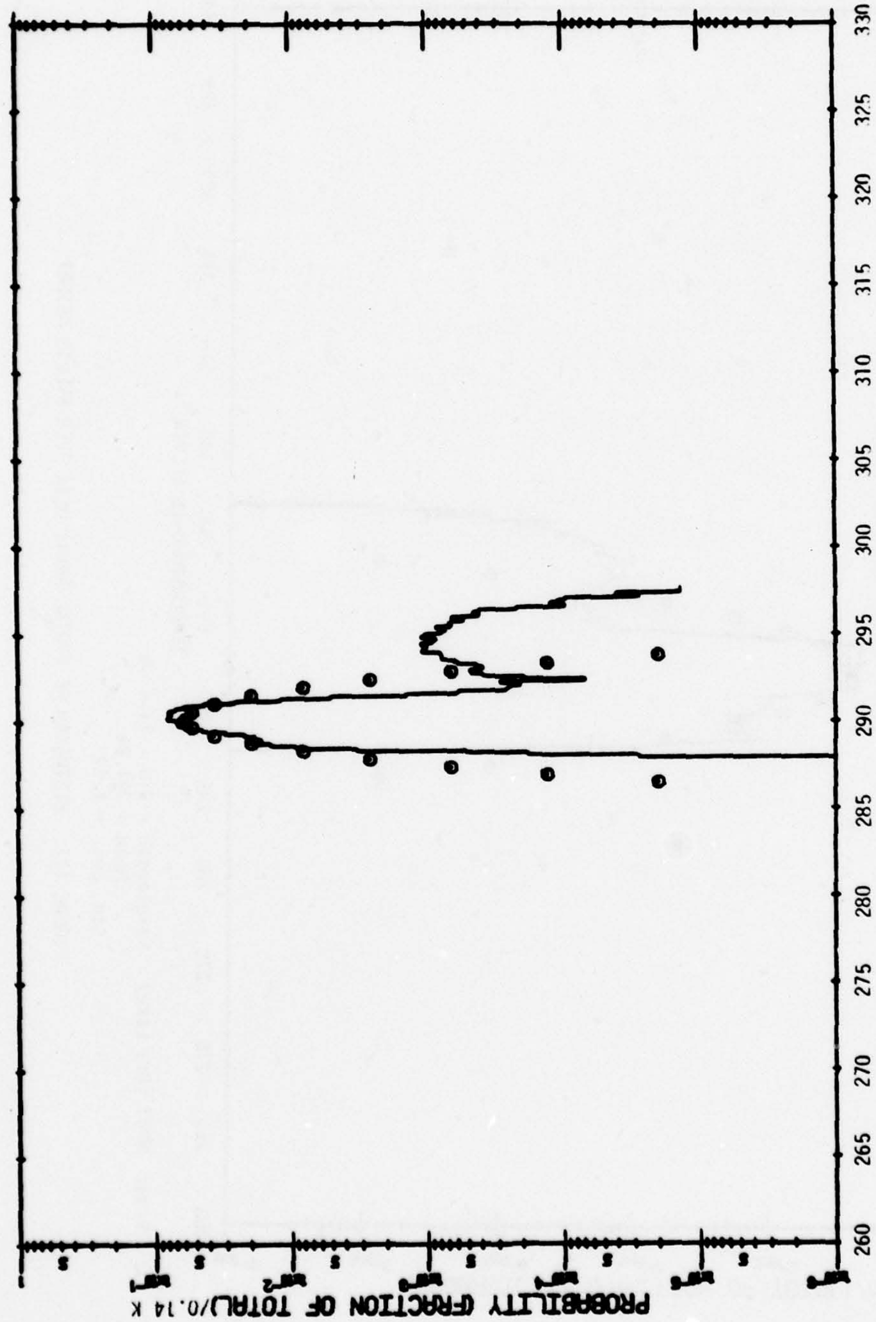

Area: NVH1 (Dry Lake) Wavelength = 4.5 - 5.5 μm
Mean = 290.16
Std. Dev. = 0.91

FIGURE 11h. HISTOGRAM OF (TOTAL-AREA) DATA OVER NELLIS DESERT

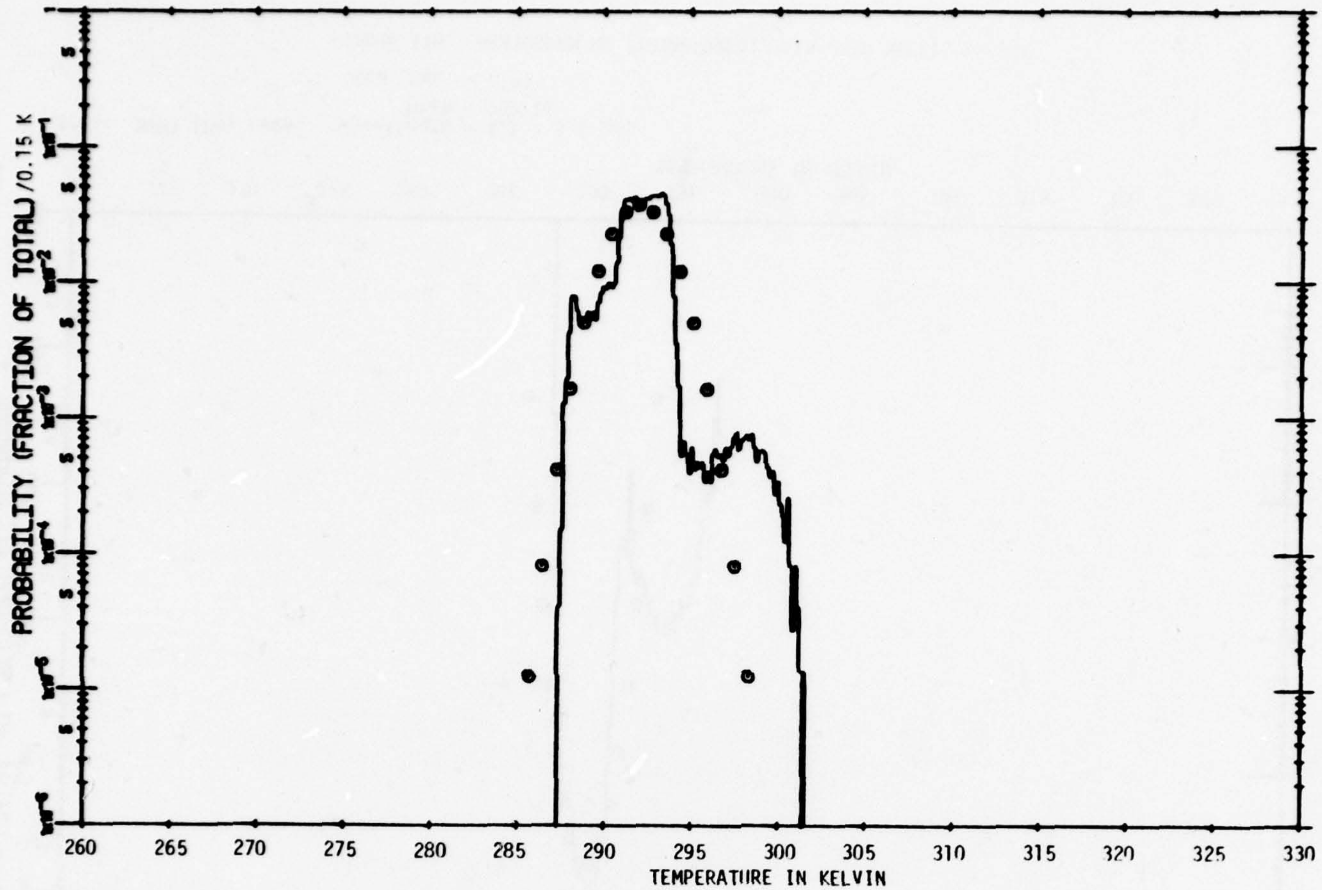

Area: NVH1 (Dry Lake) Wavelength = 9.0 - 11.4 μm
Mean = 291.94
Std. Dev. = 1.57

FIGURE 11i. HISTOGRAM OF (TOTAL-AREA) DATA OVER NELLIS DESERT

areas were each divided into 2. The total-area statistics are also presented in Appendix A to show comparisons with the subarea statistics. The graphs showing total-area statistics must be completely consistent with the data presented in this section. Table 2 summarizes the means and standard deviations of the subareas and total areas for the curves presented in Appendix A. Two sets of statistics are presented, one for scene temperature distributions, and one for scene radiance distribution. The histograms corresponding to the radiance statistics are shown as follows:

Figure 12: NEVI
Figure 13: NEVJ
Figure 14: NEVK
Figure 15: NEVM
Figure 16: NEVN
Figure 17: NVG1
Figure 18: NEVL
Figure 19: NVH1

The two-fold reason for presenting both is that the original set, i.e., temperature distributions, agrees with the format of Reference 2, and the radiance distributions will perhaps satisfy different users.

Table 3 and Figure 20 are included here to help the reader understand how the energy is distributed among the various bands. One may discern from them how the signals in different regions relate to each other. Precise correlations cannot be obtained from them, however, because of the host of meteorological and physical factors which come into play. They might be used, though, to infer some generalized qualitative behavior in the histograms. Table 3, for instance, shows the radiance from a diffuse terrain element caused solely by sunlight and from its thermal emission in the various bands indicated. From the calculated ratios, it is seen that reflected sunlight predominates in the 2.0 - 2.6 μm band, can be equally as effective as thermal radiation at 3.5 - 3.9 μm, and diminishes in effectiveness beyond. One important factor which is not included in Table 3 is the possible strong spectral

TABLE 2

MEANS AND STANDARD DEVIATIONS FOR SUBAREAS AND TOTAL AREAS IN TEMPERATURES (K)

	2.0-2.6 μm	3.0-4.2 μm	3.5-3.9 μm	3.9-4.7 μm	4.5-5.5 μm	5.1- 5.7 μm	9.0-11.4 μm
NEVI							
Sub 1		296.70±7.56			287.73±4.39	282.48±4.09	
2		303.81±4.25			293.63±3.37	285.39±3.59	
3		301.92±6.25			291.67±3.90	283.94±3.53	
4		297.55±7.91			289.67±4.41	283.05±3.71	
Total		300.00±7.28			290.68±4.60	283.71±3.90	
NEVJ							
Sub 1			286.16±8.04	283.28±4.77			
2			287.01±5.35	283.81±2.77			
3			295.69±4.47	289.64±2.39			
4			290.02±4.61	286.08±2.24			
Total			289.71±6.90	285.70±4.07			
NEVK							
Sub 1			295.64±3.01	290.17±1.58			
2			292.87±3.74	287.98±1.89			
3			294.19±4.03	289.27±2.40			
4			289.53±3.91	285.92±1.90			
Total			293.06±4.33	288.34±2.53			

TABLE 2 (Continued)

MEANS AND STANDARD DEVIATIONS FOR SUBAREAS AND TOTAL AREAS IN TEMPERATURES (K)

	2.0-2.6 μm	3.0-4.2 μm	3.5-3.9 μm	3.9-4.7 μm	4.5-5.5 μm	5.1- 5.7 μm	9.0-11.4 μm
			NEVL (Desert #1)				
Sub 1			292.49±2.20	290.70±0.59			
2			292.71±2.20	290.98±0.63		N.G.	
Total			292.60±2.21	290.84±0.63			
			NEVL (Desert #2)				
Sub 1			292.74±2.27	291.00±0.73			
2			292.58±2.28	290.90±0.73		N.G.	
Total			292.66±2.28	290.95±0.74			
			NEVL (Dry Lake)				
Sub 1			287.84±2.68	286.38±0.69			
2			286.39±2.91	285.28±0.92		N.G.	
Total			287.11±2.89	285.83±0.98			
			NEVM				
Sub 1			283.14±3.69	281.69±1.22			
2			284.26±3.69	282.64±1.32			
3			282.94±3.96	281.61±1.58			
4			284.07±3.76	282.42±1.44			
Total			283.60±3.82	282.09±1.46			

TABLE 2 (Continued)

MEANS AND STANDARD DEVIATIONS FOR SUBAREAS AND TOTAL AREAS IN TEMPERATURES (K)

	2.0-2.6 μm	3.0-4.2 μm	3.5-3.9 μm	3.9-4.7 μm	4.5-5.5 μm	5.1- 5.7 μm	9.0-11.4 μm
NEVN							
Sub 1		284.49±3.57			282.40±1.25		284.13±1.76
2		287.51±2.98			284.39±0.94		287.05±1.36
3		284.66±3.90			282.40±1.62		284.39±2.59
4		286.05±3.24			283.30±1.09		285.91±1.64
Total		285.68±3.65			283.12±1.50		285.37±2.23
NVG1							
Sub 1		294.77±7.69			285.73±4.06		287.87±5.67
2		288.66±10.55			282.05±5.18		283.03±7.11
3		292.27±8.06			284.92±4.42		286.37±5.97
4		288.77±7.37			282.23±3.72		282.96±4.98
Total		291.12±8.89			283.73±4.67		285.06±6.35
NVH1 (Desert #1)							
Sub 1		308.40±2.53			295.20±0.78		298.92±1.12
2		306.51±2.67			294.83±0.91		298.51±1.25
Total		307.45±2.77			295.02±0.87		298.72±1.21

TABLE 2 (Concluded)

MEANS AND STANDARD DEVIATIONS FOR SUBAREAS AND TOTAL AREAS IN TEMPERATURES (K)

	2.0-2.6 μm	3.0-4.2 μm	3.5-3.9 μm	3.9-4.7 μm	4.5-5.5 μm	5.1- 5.7 μm	9.0-11.4 μm
NVH1 (Desert #2)							
Sub 1		308.88±2.57			295.44±1.11		297.01±1.41
2		308.31±2.69			295.31±1.05		297.00±1.28
Total		308.60±2.65			295.38±1.08		297.01±1.35
NVH1 (Dry Lake)							
Sub 1		311.66±2.64			290.41±0.88		292.41±1.42
2		314.14±3.82			289.90±0.87		291.46±1.57
Total		312.90±3.52			290.16±0.91		291.94±1.57

TABLE 2a

MEANS AND STANDARD DEVIATIONS FOR SUBAREAS AND TOTAL AREAS IN RADIANCE VALUES ($\mu w\text{-}cm^{-2}\text{-}ster^{-1}$)

	2.0-2.6 μm*	3.0-4.2 μm	3.5-3.9 μm	3.9-4.7 μm	4.5-5.5 μm	5.1- 5.7 μm	9.0-11.4 μm
NEVI							
Sub 1	55.01±25.40	42.66±12.47			177.08±26.43	125.92±16.89	
2	62.01±17.79	55.78±8.92			215.36±21.19	138.34±15.92	
3	59.92±21.92	52.36±12.18			202.15±25.17	131.93±15.14	
4	45.24±23.43	44.37±13.28			188.99±27.36	128.09±15.61	
Total	55.75±23.28	48.79±13.02			195.89±28.94	131.07±16.61	
NEVJ							
Sub 1			9.37±3.48	50.75±10.21			
2			9.44±2.33	51.31±5.87			
3			13.86±2.57	64.62±5.98			
4			10.77±2.28	56.07±5.12			
Total			10.86±3.26	55.68±9.00			
NEVK							
Sub 1			13.72±1.79	66.01±4.07			
2			12.17±2.03	60.44±4.56			
3			12.93±2.18	63.70±5.90			
4			10.48±1.85	55.80±4.19			
Total			12.33±2.31	61.49±6.09			

*Note: The units for the 2.0 - 2.6 μm band are $\mu w\text{-}cm^{-2}\cdot ster^{-1}\text{-}\mu m^{-1}$.

TABLE 2a (Continued)

MEANS AND STANDARD DEVIATIONS FOR SUBAREAS AND TOTAL AREAS IN RADIANCE VALUES ($\mu w\text{-}cm^{-2}\text{-}ster^{-1}$)

	2.0-2.6 μm*	3.0-4.2 μm	3.5-3.9 μm	3.9-4.7 μm	4.5-5.5 μm	5.1- 5.7 μm	9.0-11.4 μm
			NEVL (Desert #1)				
Sub 1			11.88±1.17	67.28±1.52			
2			12.00±1.18	67.99±1.66		N. G.	
Total			11.94±1.18	67.64±1.63			
			NEVL (Desert #2)				
Sub 1			12.02±1.22	68.07±1.96			
2			11.93±1.22	67.79±1.94		N. G.	
Total			11.97±1.22	67.93±1.95			
			NEVL (Dry Lake)				
Sub 1			9.62±1.19	56.67±1.63			
2			9.00±1.23	54.20±2.10		N. G.	
Total			9.31±1.25	55.44±2.25			
			NEVM				
Sub 1			7.75±1.33	46.77±2.33			
2			8.18±1.39	48.86±2.59			
3			7.69±1.40	46.71±3.04			
4			8.11±1.39	48.35±2.75			
Total			7.93±1.40	47.67±2.85			

*Note: The units for the 2.0 - 2.6 μm band are $\mu w\text{-}cm^{-2}\cdot ster^{-1}\text{-}\mu m^{-1}$.

TABLE 2a (Continued)

MEANS AND STANDARD DEVIATIONS FOR SUBAREAS AND TOTAL AREAS IN RADIANCE VALUES (μw-cm^{-2}-ster^{-1})

	2.0-2.6 μm*	3.0-4.2 μm	3.5-3.9 μm	3.9-4.7 μm	4.5-5.5 μm	5.1- 5.7 μm	9.0-11.4 μm
				NEVN			
Sub 1	15.96±5.25	24.02±3.89			146.16±6.69		1800.8±56.42
2	19.92±4.67	27.49±3.66			156.55±5.09		1894.5±44.80
3	15.98±5.54	24.25±4.21			146.25±8.30		1809.8±81.98
4	17.33±4.59	25.76±3.76			150.68±5.79		1857.3±53.29
Total	17.30±5.28	25.38±4.13			149.91±7.83		1840.6±71.53
				NVG1			
Sub 1	53.18±23.30	39.27±10.96			164.96±22.47		1925.1±184.30
2	38.64±29.05	31.51±14.14			146.31±27.38		1774.8±226.02
3	40.84±19.87	35.50±11.58			160.34±24.54		1875.2±193.42
4	35.77±16.19	30.20±9.39			146.42±19.84		1768.9±157.93
Total	42.12±23.58	34.13±12.18			154.51±25.14		1836.1±203.25
				NVH1 (Desert #1)			
Sub 1	81.66±10.15	66.59±6.71			225.70±5.72		2308.3±41.26
2	66.26±7.39	61.79±6.62			222.87±6.62		2292.8±46.11
Total	73.96±11.75	64.19±7.09			224.29±6.34		2300.6±44.44

Note: The units for the 2.0 - 2.6 μm band are μw-cm$^{-2}\cdot$ster^{-1}-μm^{-1}.

TABLE 2a (Concluded)

MEANS AND STANDARD DEVIATIONS FOR SUBAREAS AND TOTAL AREAS IN RADIANCE VALUES ($\mu w\text{-}cm^{-2}\text{-}ster^{-1}$)

	2.0-2.6 μm*	3.0-4.2 μm	3.5-3.9 μm	3.9-4.7 μm	4.5-5.5 μm	5.1- 5.7 μm	9.0-11.4 μm
NVH1 (Desert #2)							
Sub 1	67.69±7.68	67.89±6.88			227.57±8.16		2238.4±51.02
2	61.70±7.43	66.39±6.99			226.38±7.75		2238.1±46.29
Total	64.70±8.13	67.14±6.97			226.97±7.98		2238.2±48.71
NVH1 (Dry Lake)							
Sub 1	135.82±16.53	75.74±7.74			192.71±5.82		2076.2±48.89
2	150.66±24.33	83.75±12.45			189.04±5.82		2040.9±54.88
Total	143.24±22.09	79.74±11.11			190.87±6.10		2058.6±54.89

Note: The units for the 2.0 - 2.6 μm band are $\mu w\text{-}cm^{-2}\cdot ster^{-1}\text{-}\mu m^{-1}$.

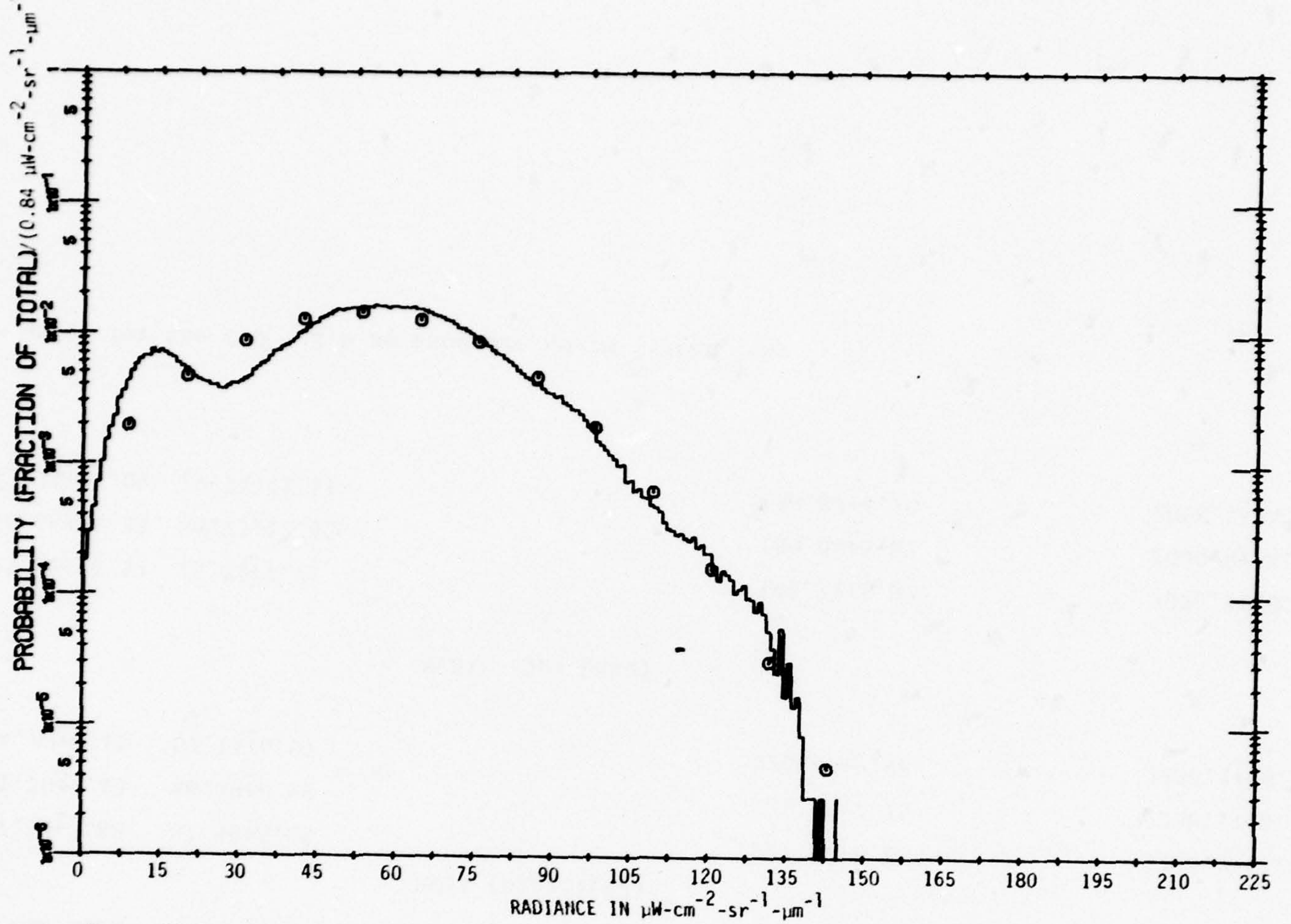

Area: NEVI Wavelength = 2.0-2.6 μm
Mean = 55.75
Std. Dev. = 23.28

FIGURE 12a. HISTOGRAM OF (TOTAL-AREA) DATA OVER NELLIS MOUNTAINS

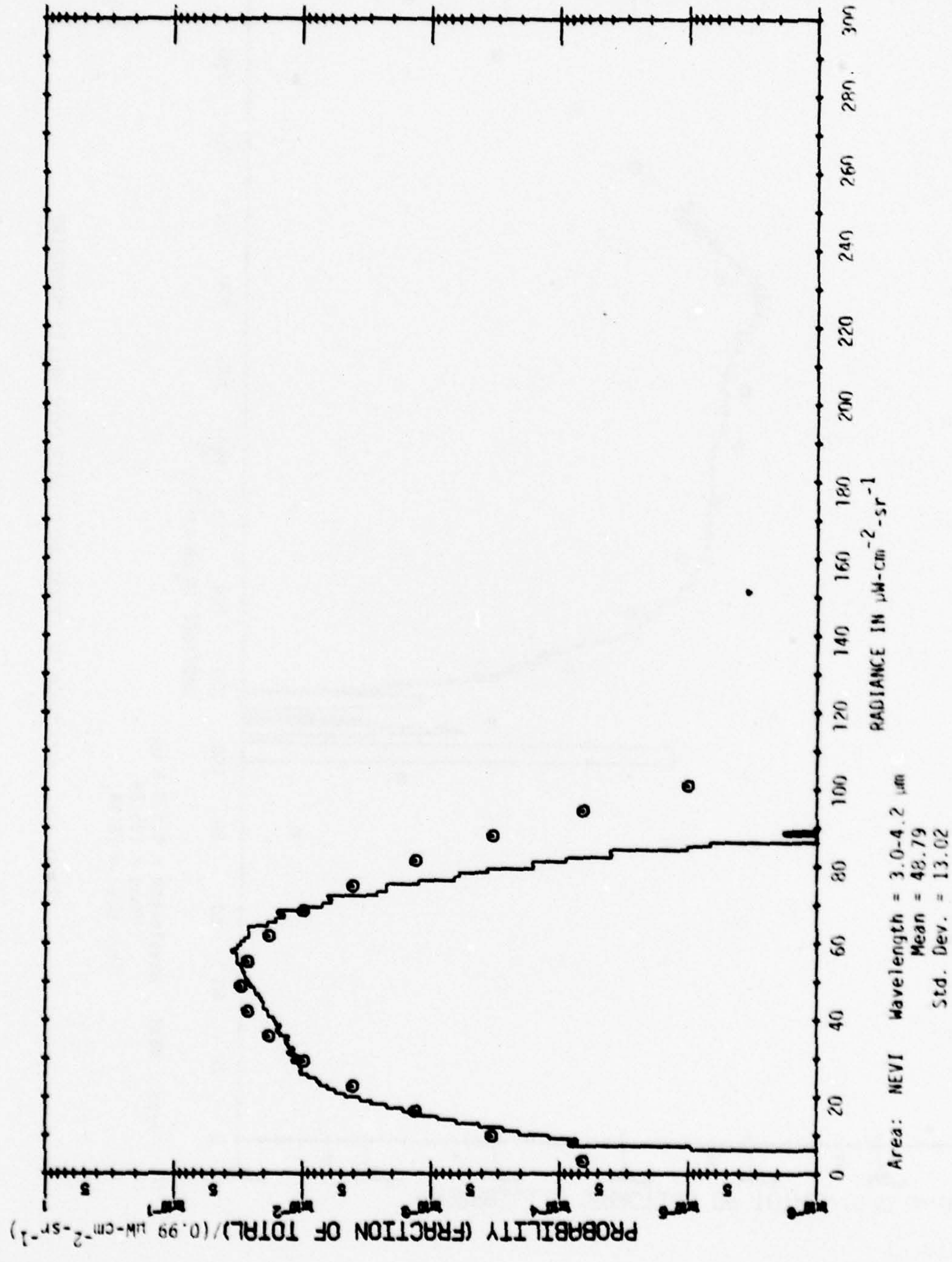

FIGURE 12b. HISTOGRAM OF (TOTAL-AREA) DATA OVER NELLIS MOUNTAINS

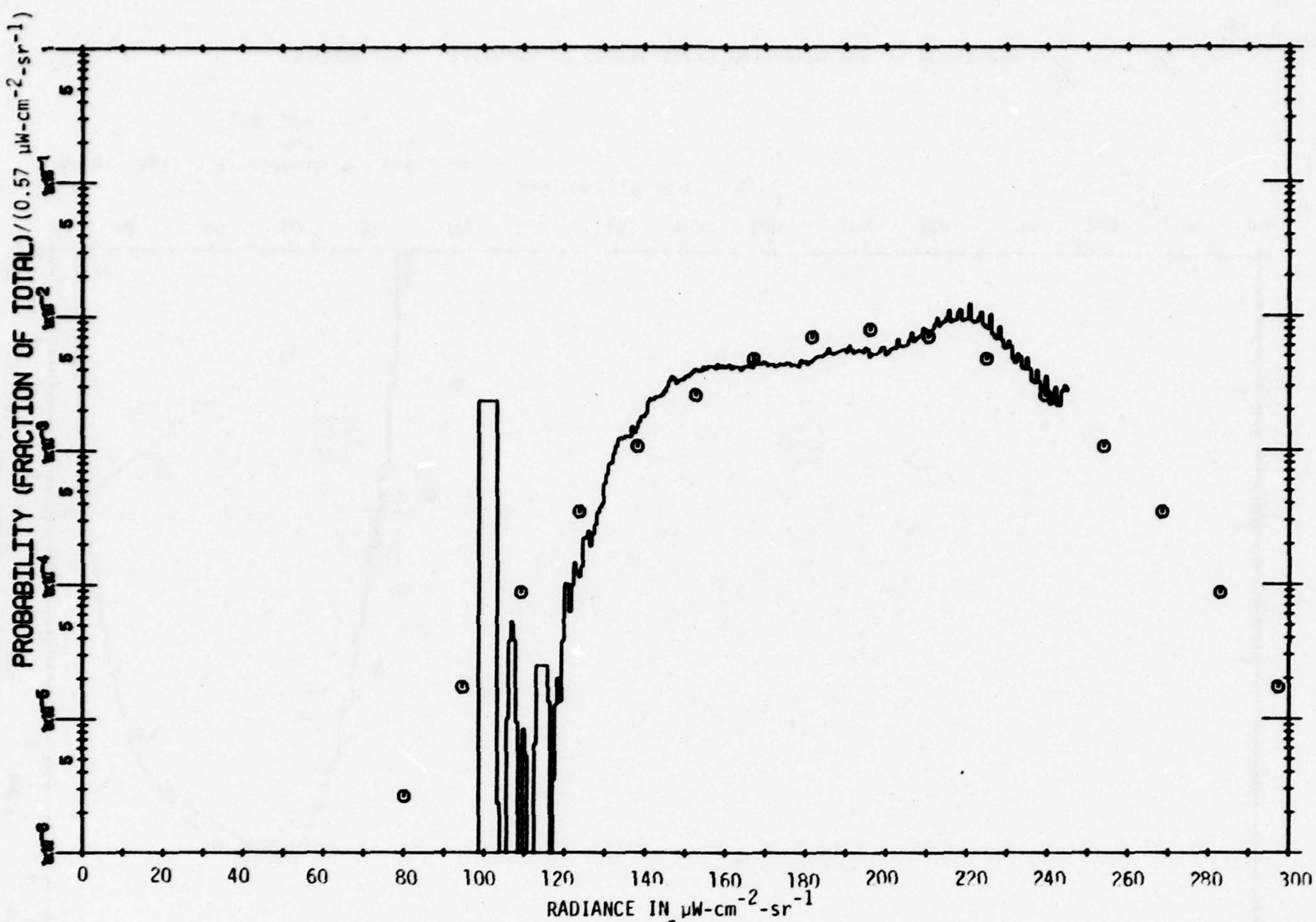

Area: NEVI Wavelength = 4.5-5.5 µm
Mean = 195.89
Std. Dev. = 28.94

FIGURE 12c. HISTOGRAM OF (TOTAL-AREA) DATA OVER NELLIS MOUNTAINS

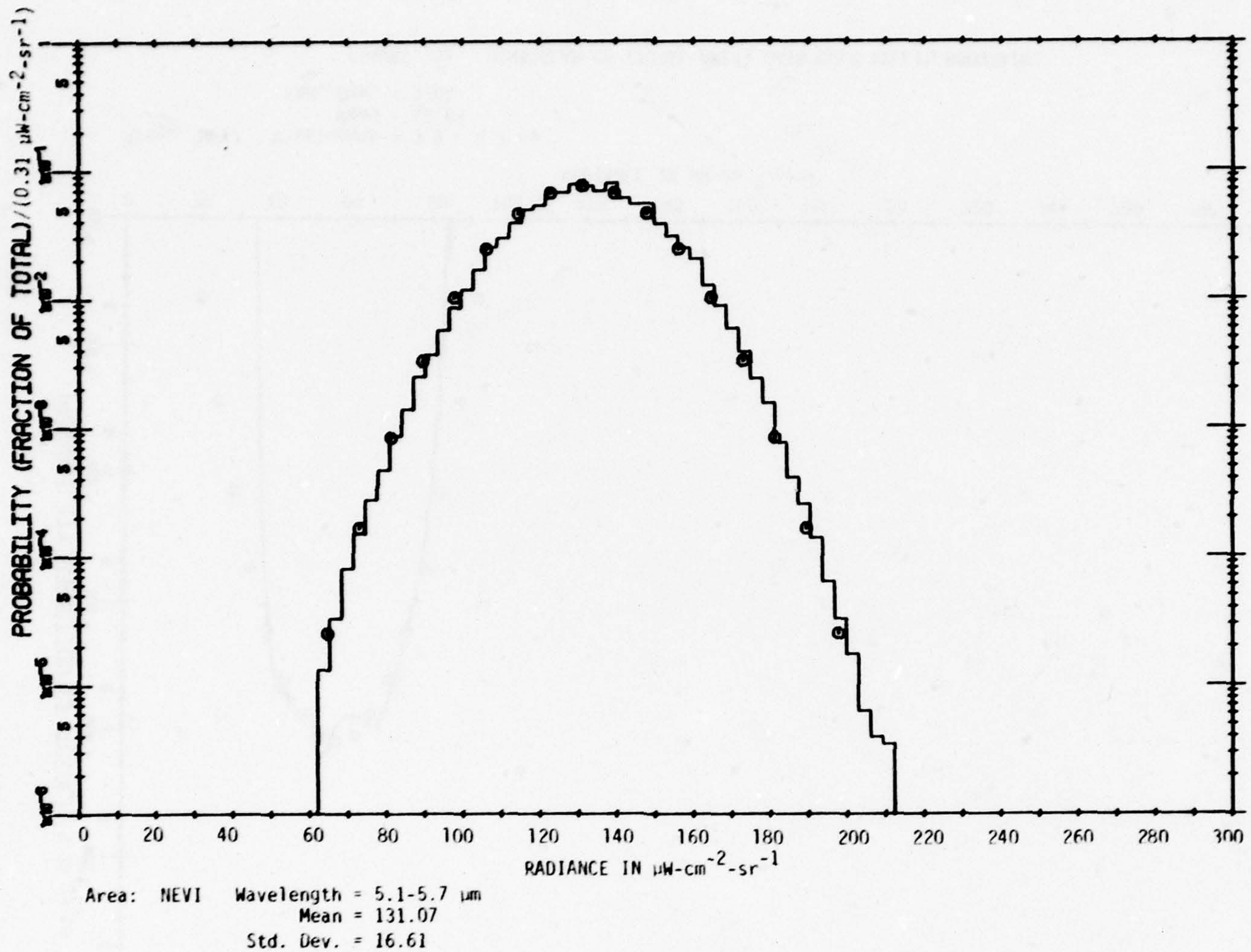

FIGURE 12d. HISTOGRAM OF (TOTAL-AREA) DATA OVER NELLIS MOUNTAINS

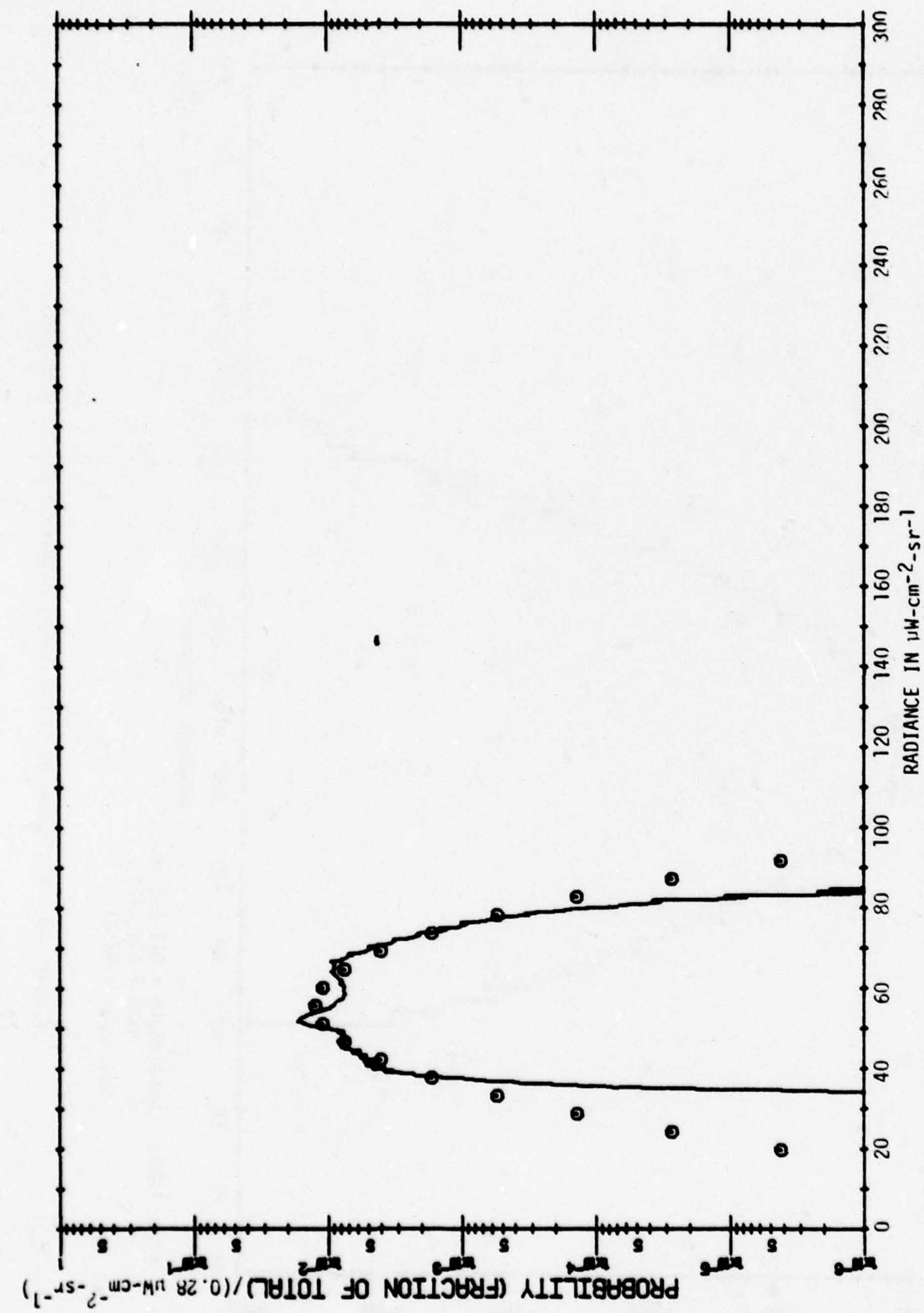

Area: NEVJ   Wavelength = 3.9 - 4.7 μm
Mean = 55.68
Std. Dev. = 9.00

FIGURE 13a. HISTOGRAM OF (TOTAL-AREA) DATA OVER NELLIS MOUNTAINS

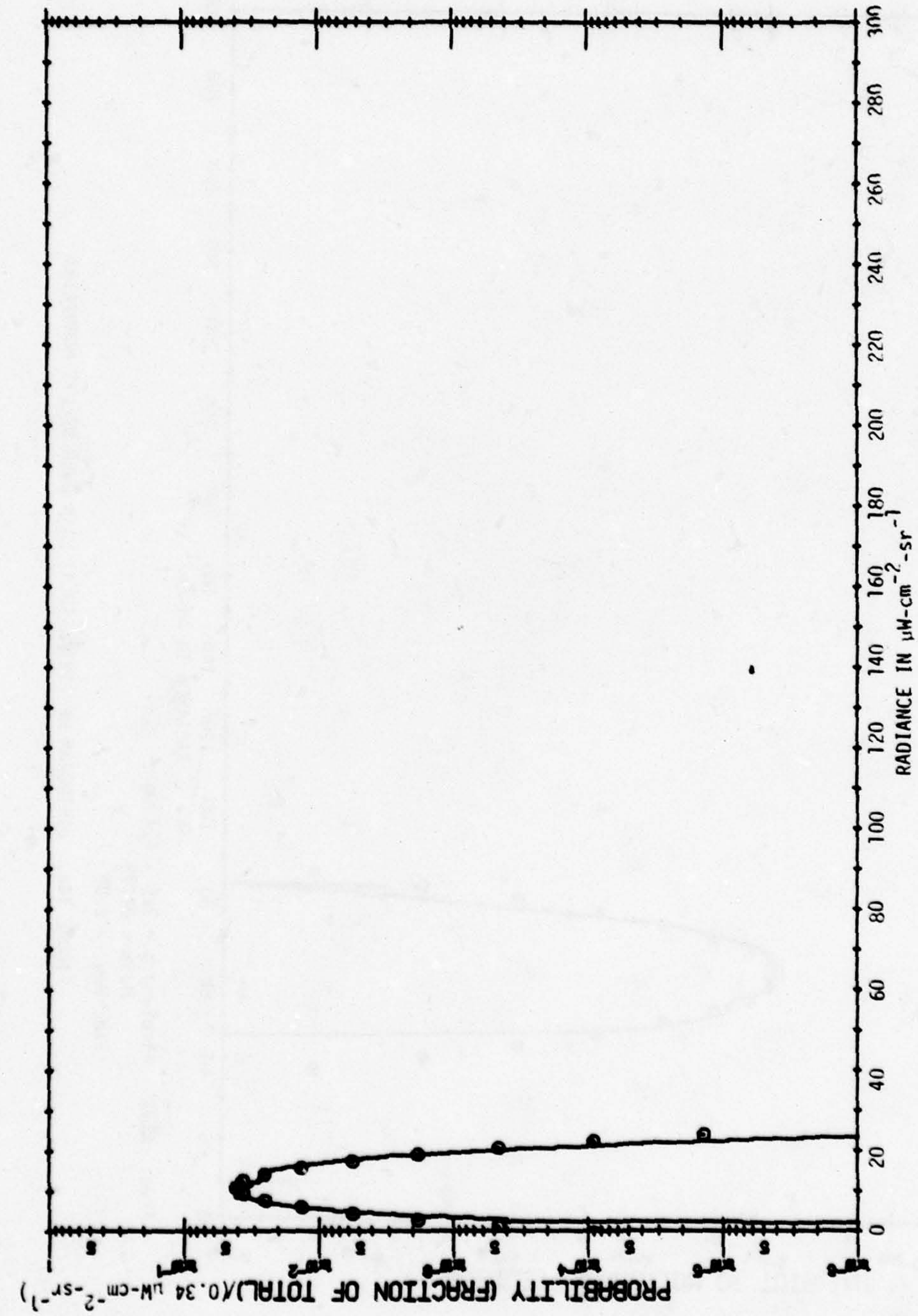

Area: NEVJ Wavelength = 3.5 - 3.9 μm
Mean = 10.86
Std. Dev. = 3.26

FIGURE 13b. HISTOGRAM OF (TOTAL-AREA) DATA OVER NELLIS MOUNTAINS

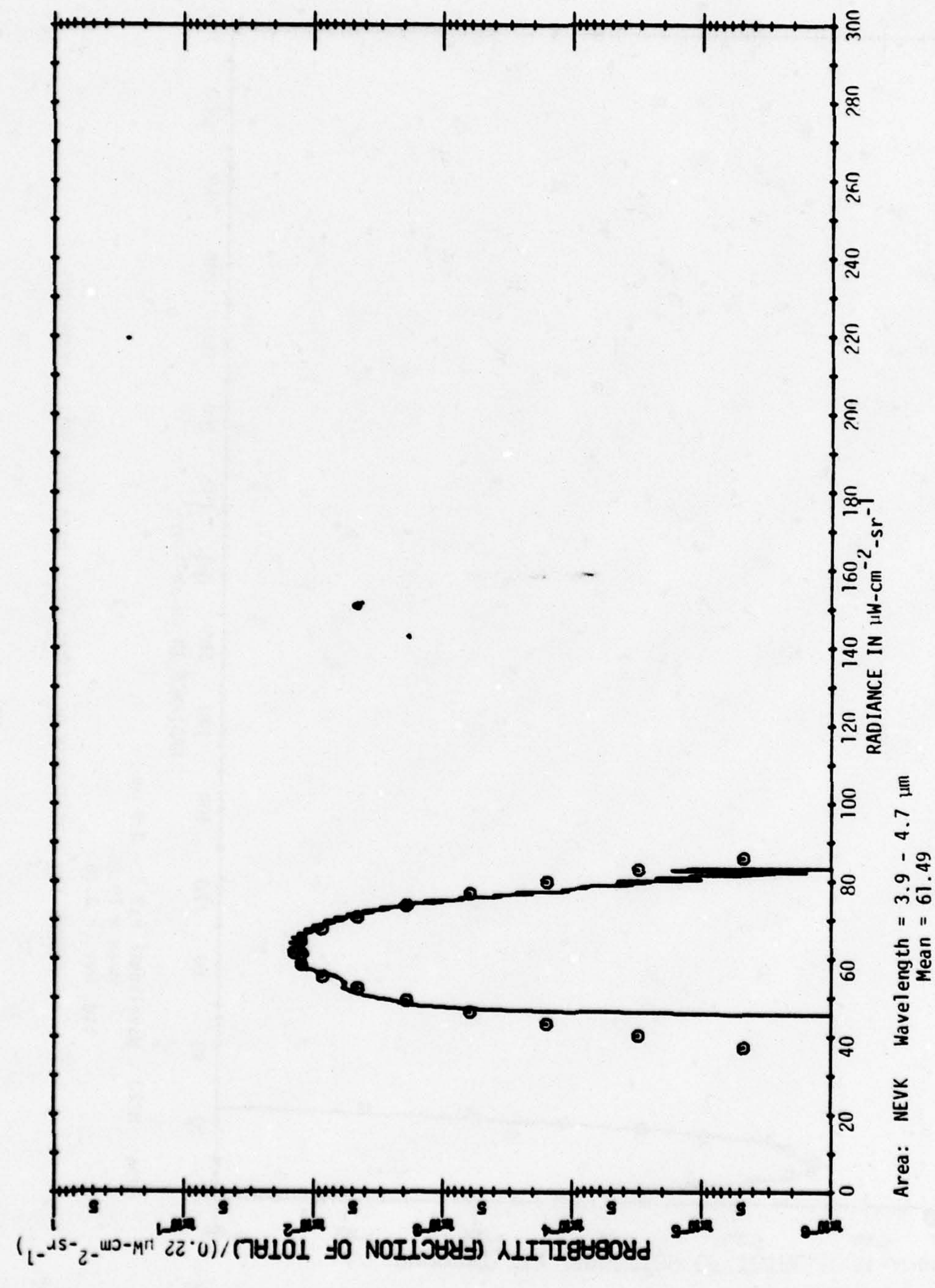

FIGURE 14a. HISTOGRAM OF (TOTAL-AREA) DATA OVER NELLIS MOUNTAINS

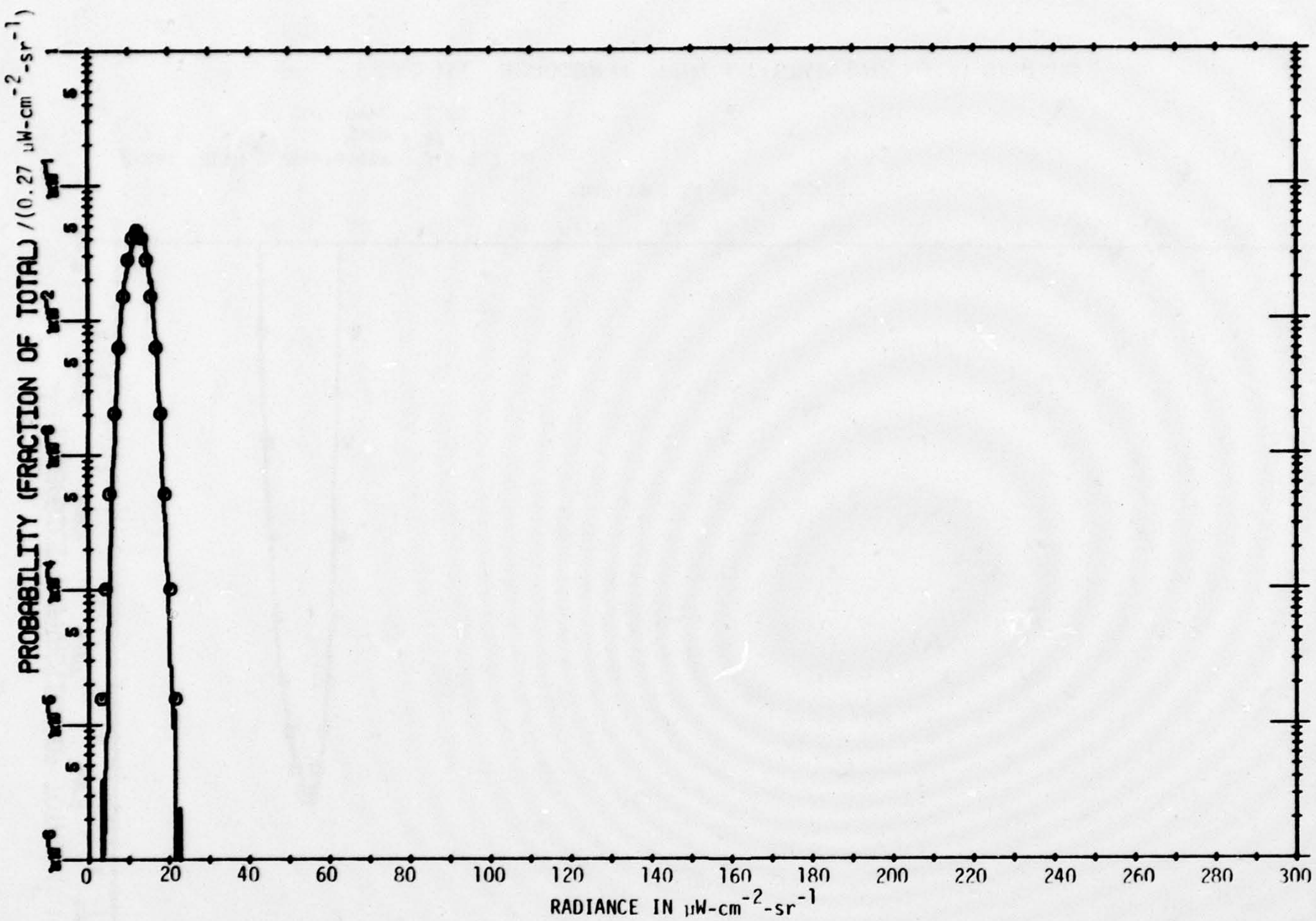

Area: NEVK Wavelength = 3.5 - 3.9 μm
Mean = 12.33
Std. Dev. = 2.31

FIGURE 14b. HISTOGRAM OF (TOTAL-AREA) DATA OVER NELLIS MOUNTAINS

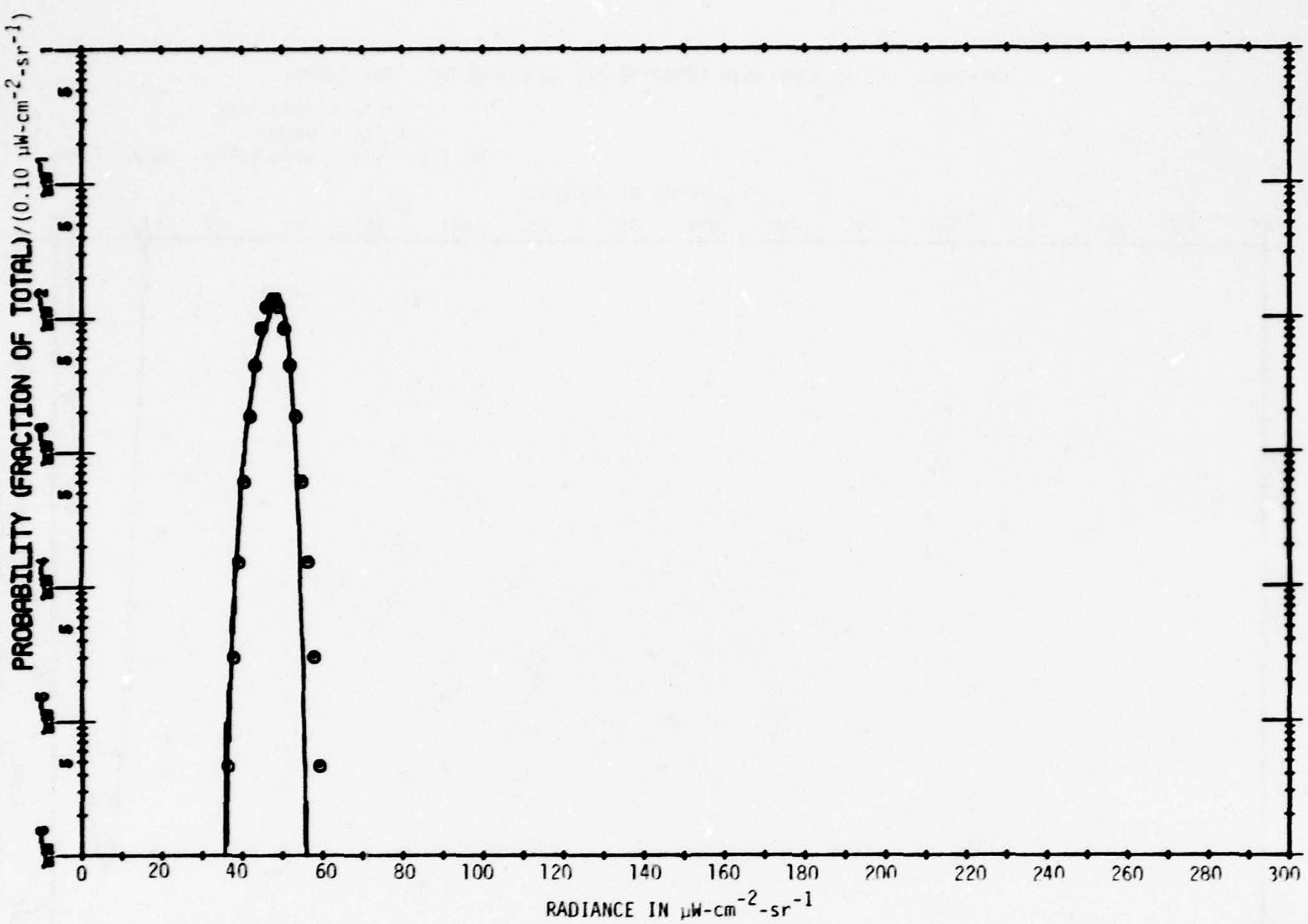

Area: NEVM Wavelength = 3.9-4.7 μm
Mean = 47.67
Std. Dev. = 2.85

FIGURE 15a. HISTOGRAM OF (TOTAL-AREA) DATA OVER NELLIS MOUNTAINS

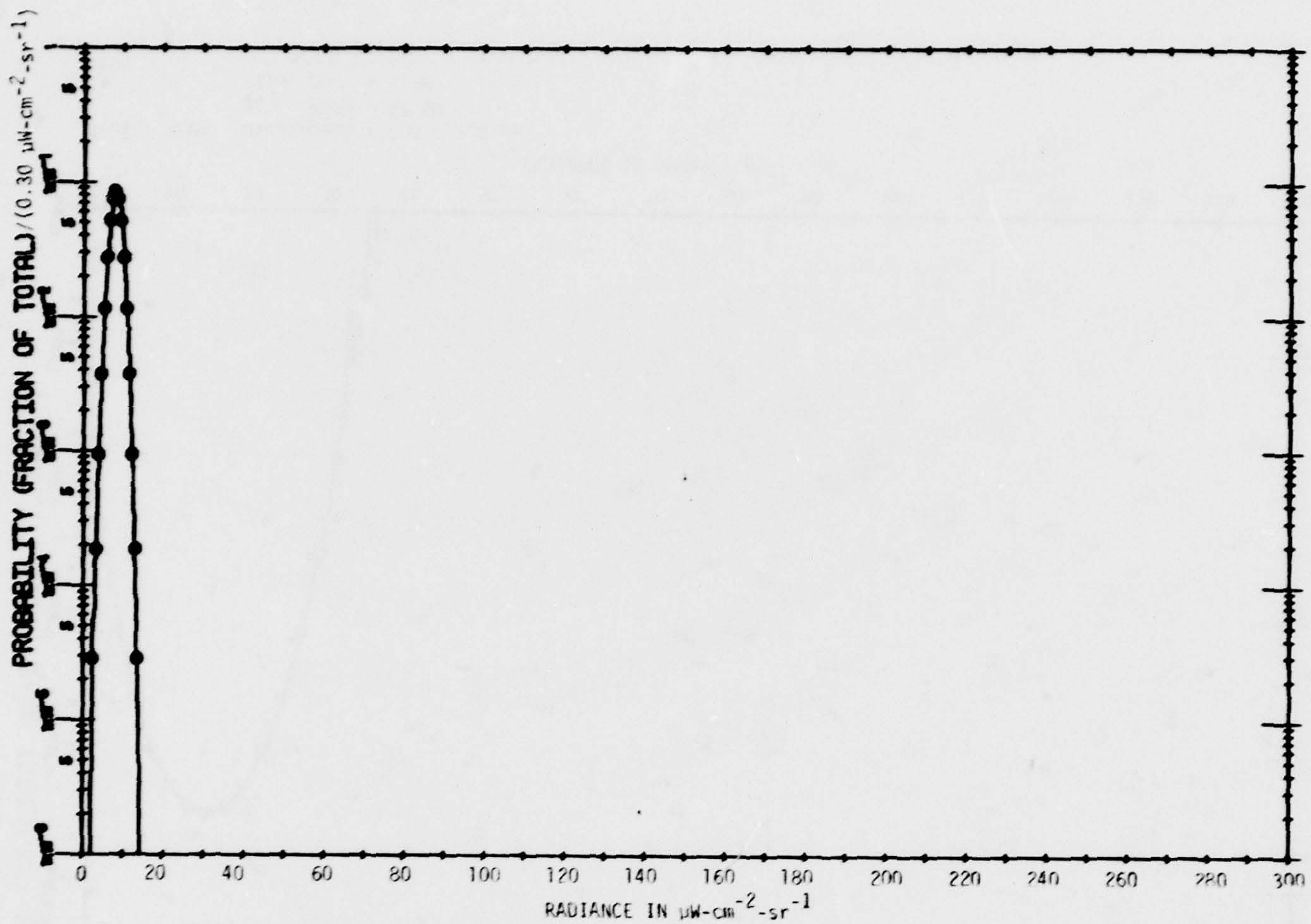

Area: NEVM Wavelength = 3.5-3.9 μm
Mean = 7.93
Std. Dev. = 1.40

FIGURE 15b. HISTOGRAM OF (TOTAL-AREA) DATA OVER NELLIS MOUNTAINS

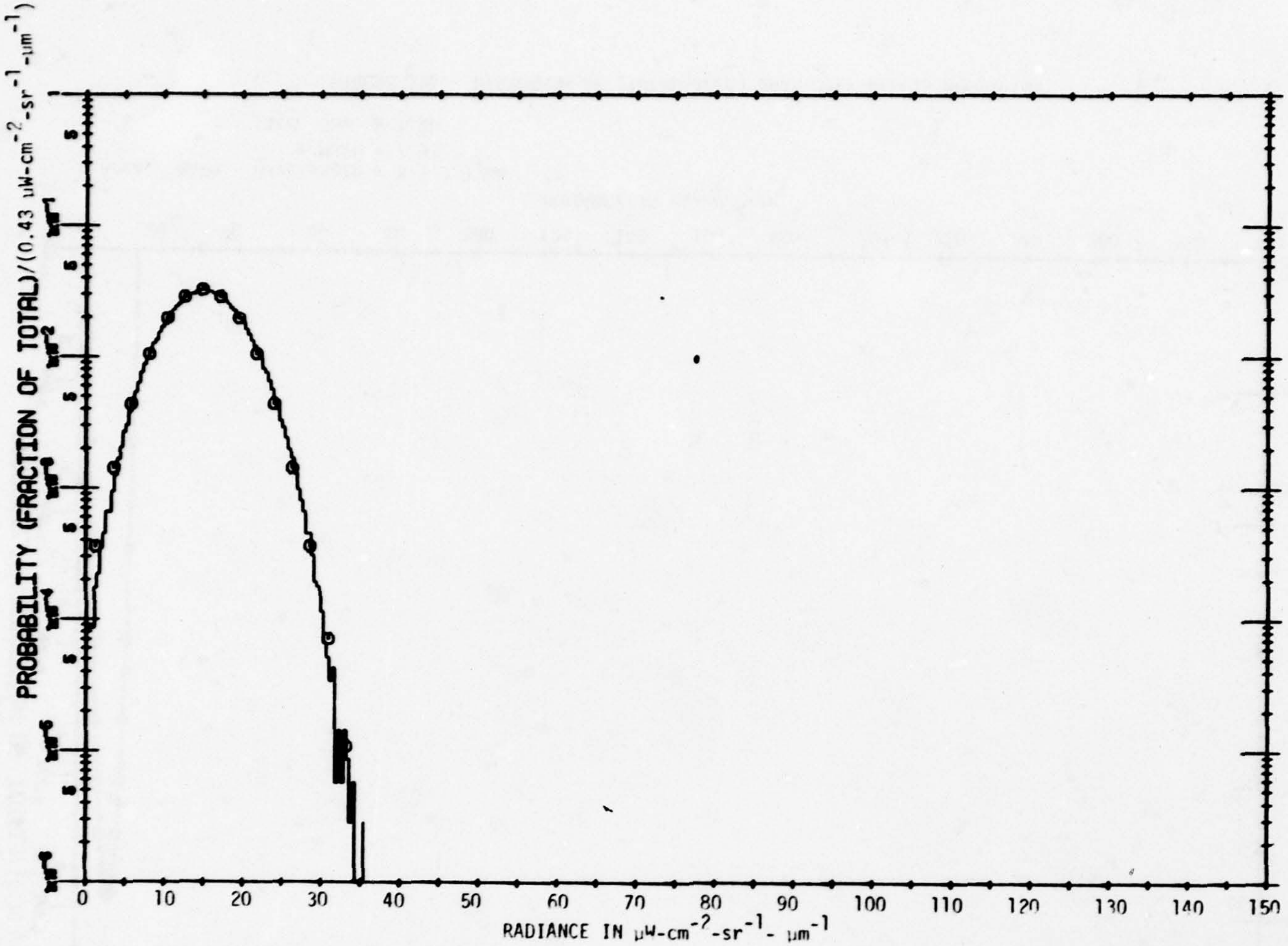

Area: NEVN Wavelength = 2.0 - 2.6 μm
Mean = 17.30
Std. Dev. = 5.28

FIGURE 16a. HISTOGRAM OF (TOTAL-AREA) DATA OVER NELLIS MOUNTAINS

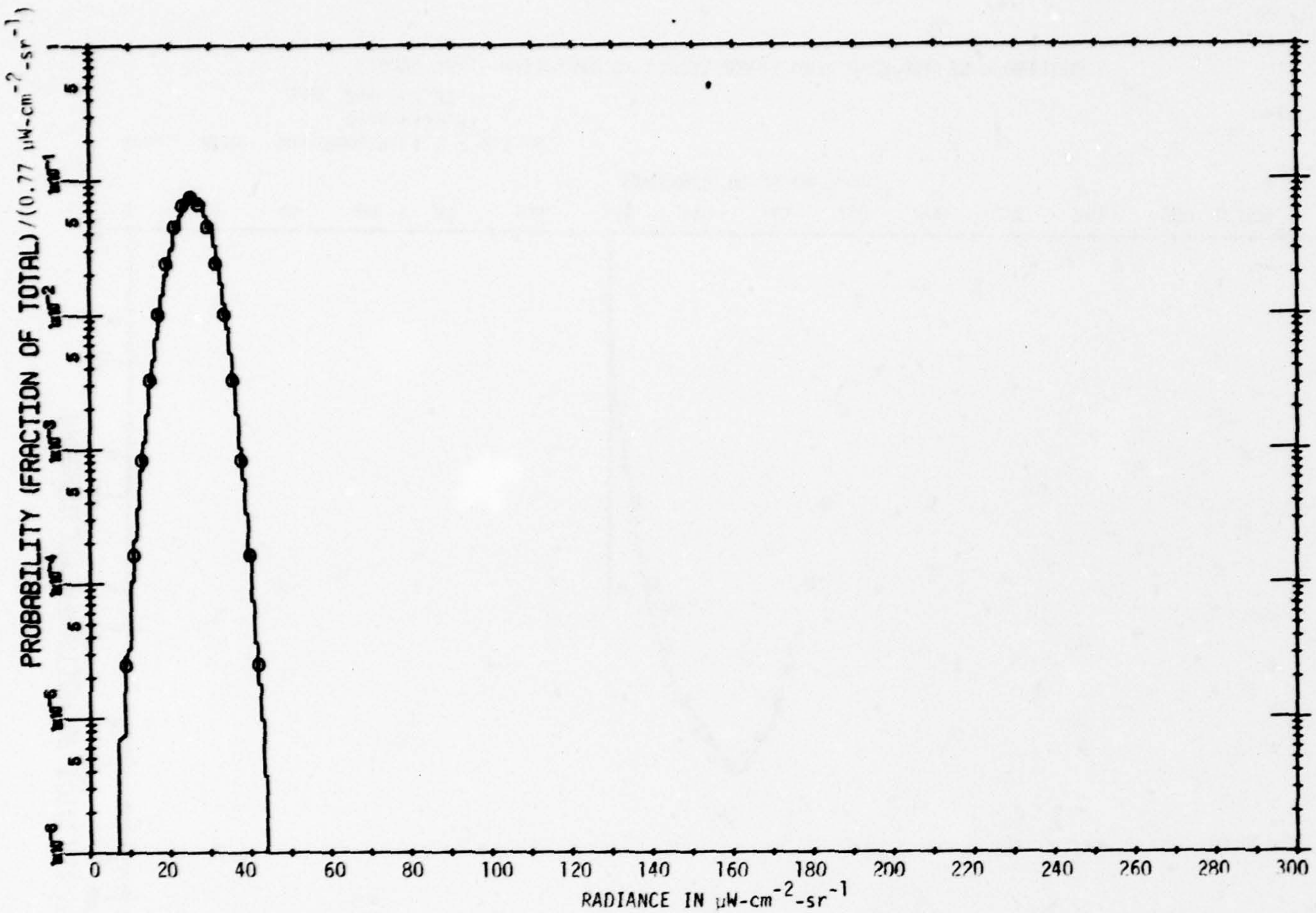

Area: NEVN Wavelength = 3.0 - 4.2 μm
Mean = 25.38
Std. Dev. = 4.13

FIGURE 16b. HISTOGRAM OF (TOTAL-AREA) DATA OVER NELLIS MOUNTAINS

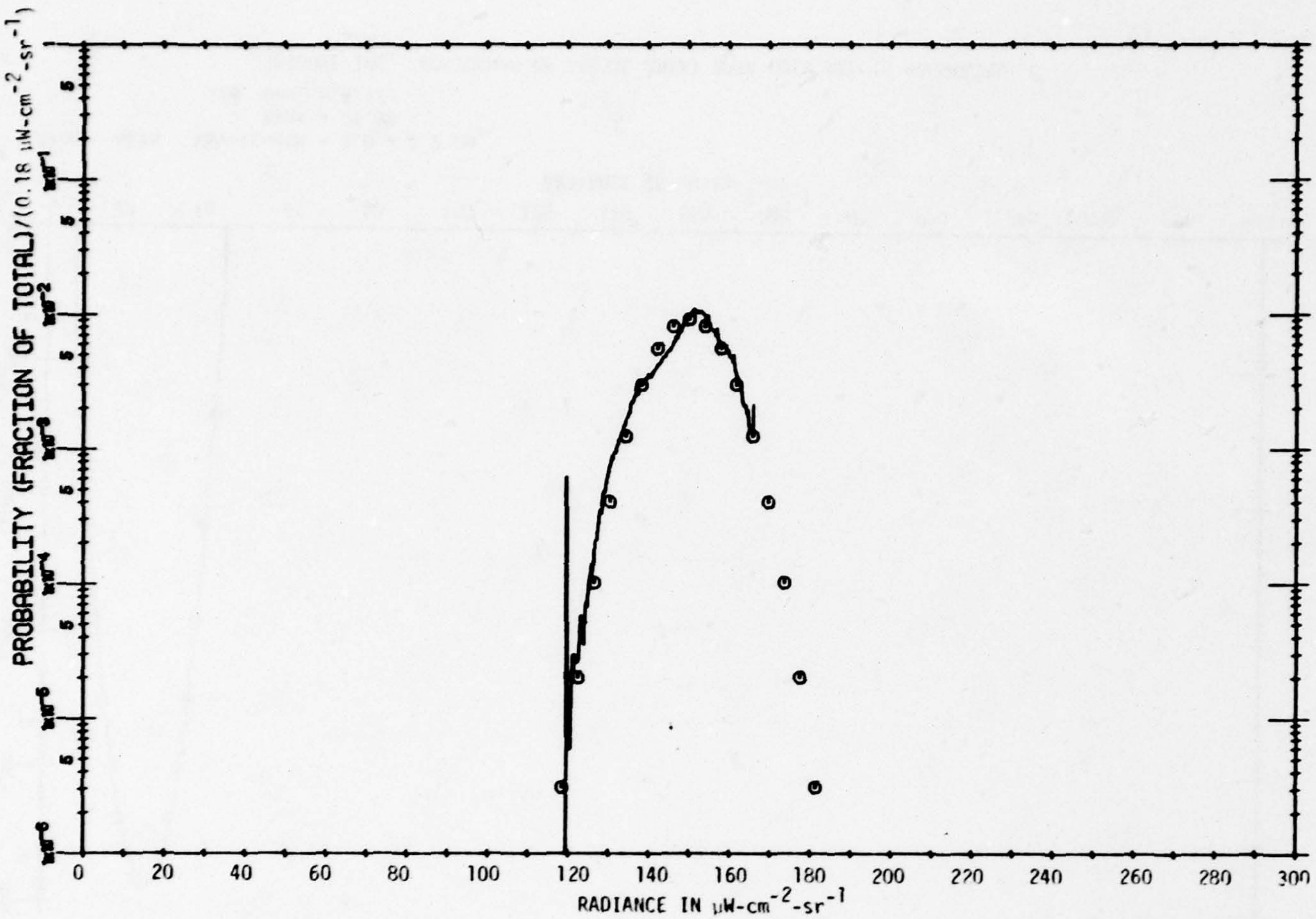

Area: NEVN Wavelength = 4.5 - 5.5 μm
Mean = 149.91
Std. Dev. = 7.83

FIGURE 16c. HISTOGRAM OF (TOTAL-AREA) DATA OVER NELLIS MOUNTAINS

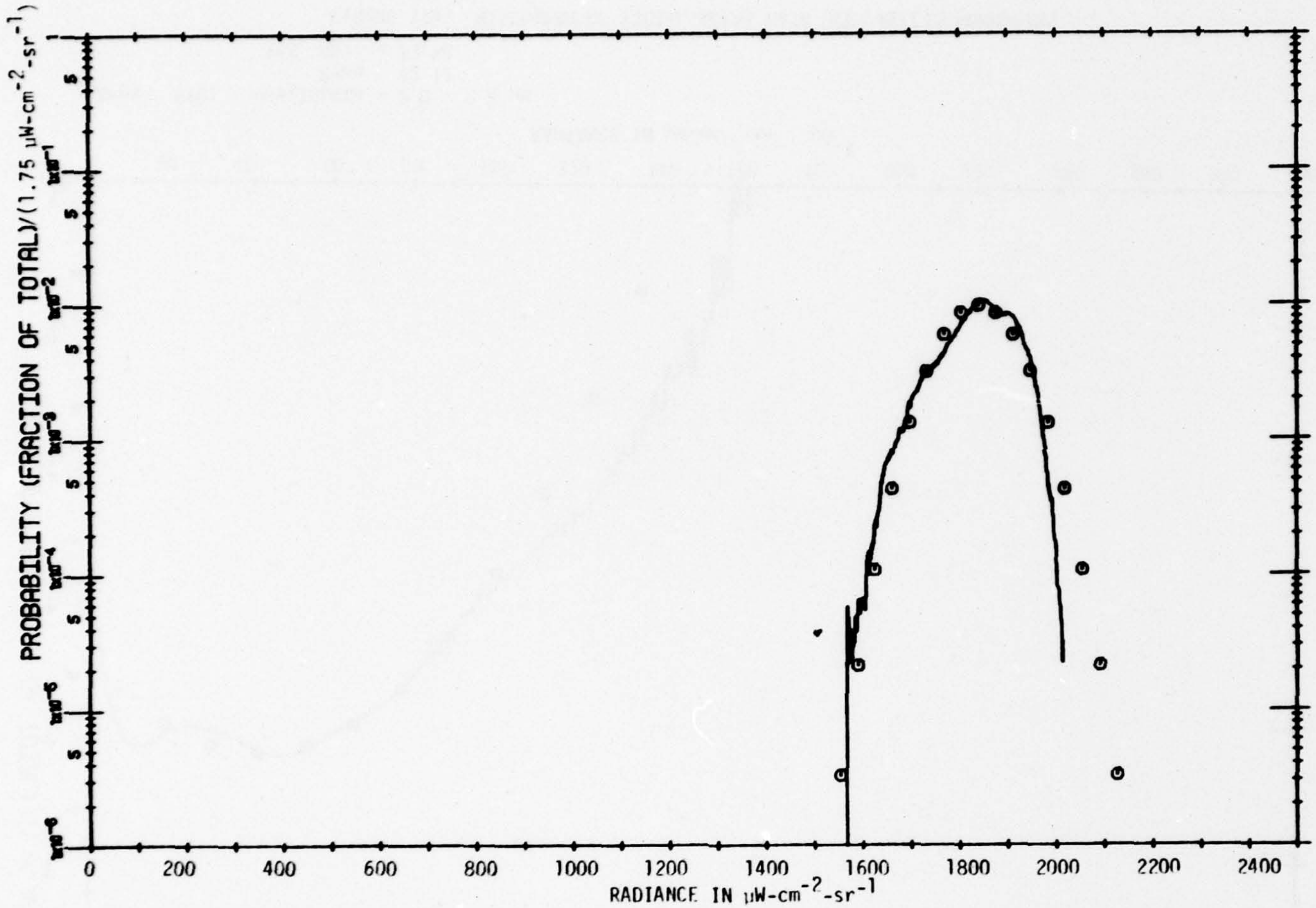

Area: NEVN Wavelength = 9.0 - 11.4 μm
Mean = 1840.59
Std. Dev. = 71.53

FIGURE 16d. HISTOGRAM OF (TOTAL-AREA) DATA OVER NELLIS MOUNTAINS

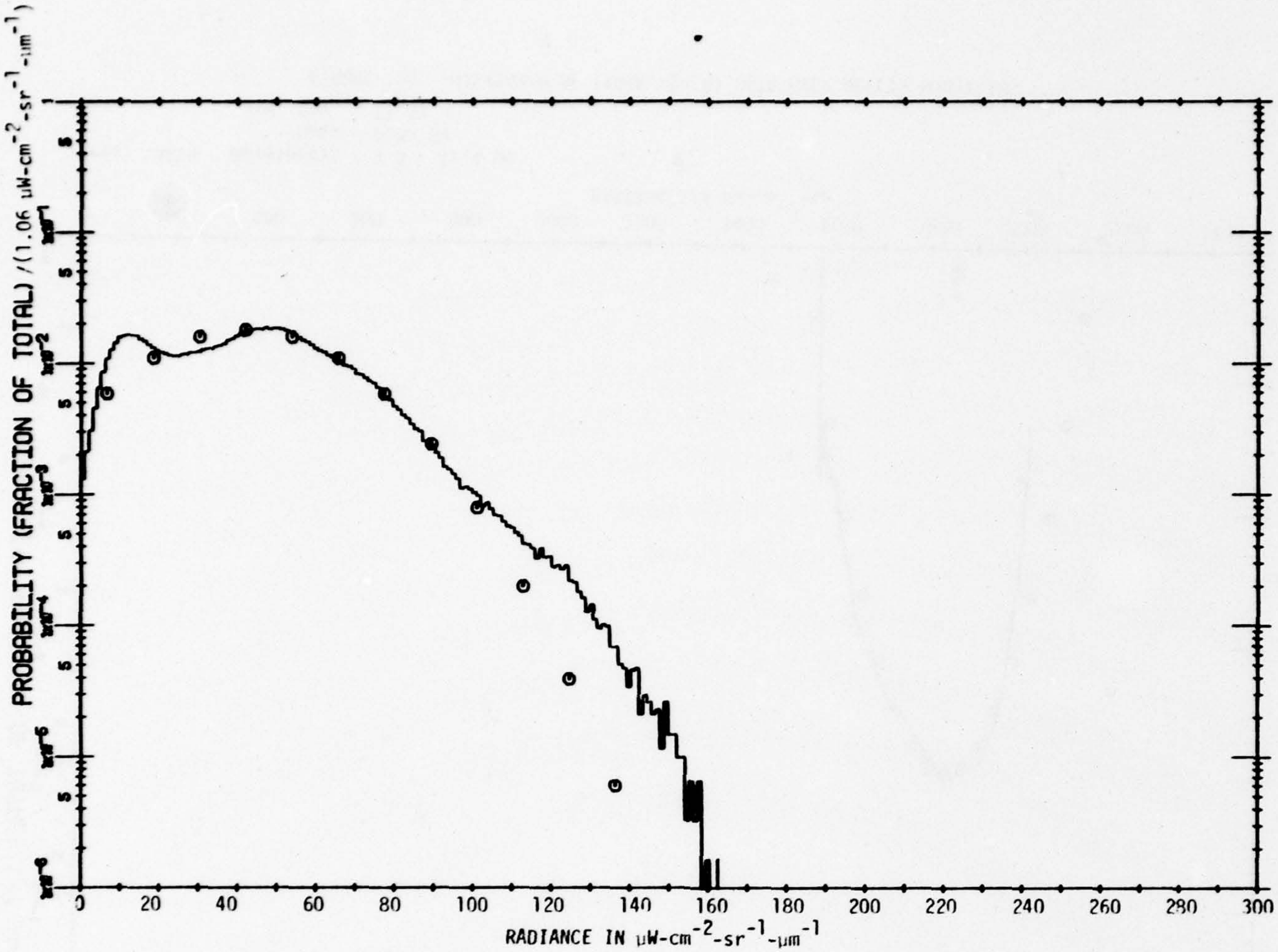

Area: NVG1 Wavelength = 2.0 - 2.6 μm
Mean = 42.12
Std. Dev. = 23.56

FIGURE 17a. HISTOGRAM OF (TOTAL-AREA) DATA OVER NELLIS MOUNTAINS

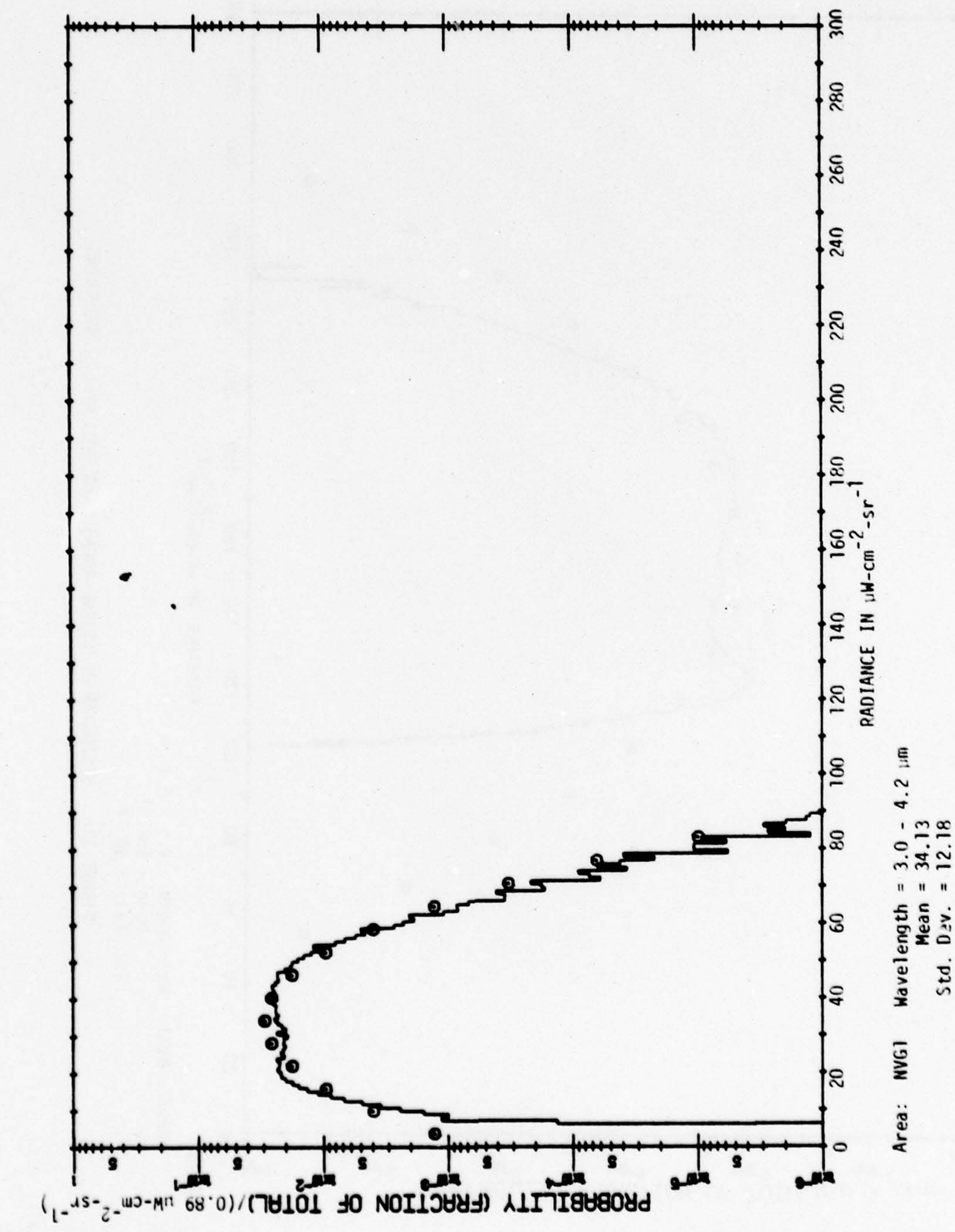

FIGURE 17b. HISTOGRAM OF (TOTAL-AREA) DATA OVER NELLIS MOUNTAINS

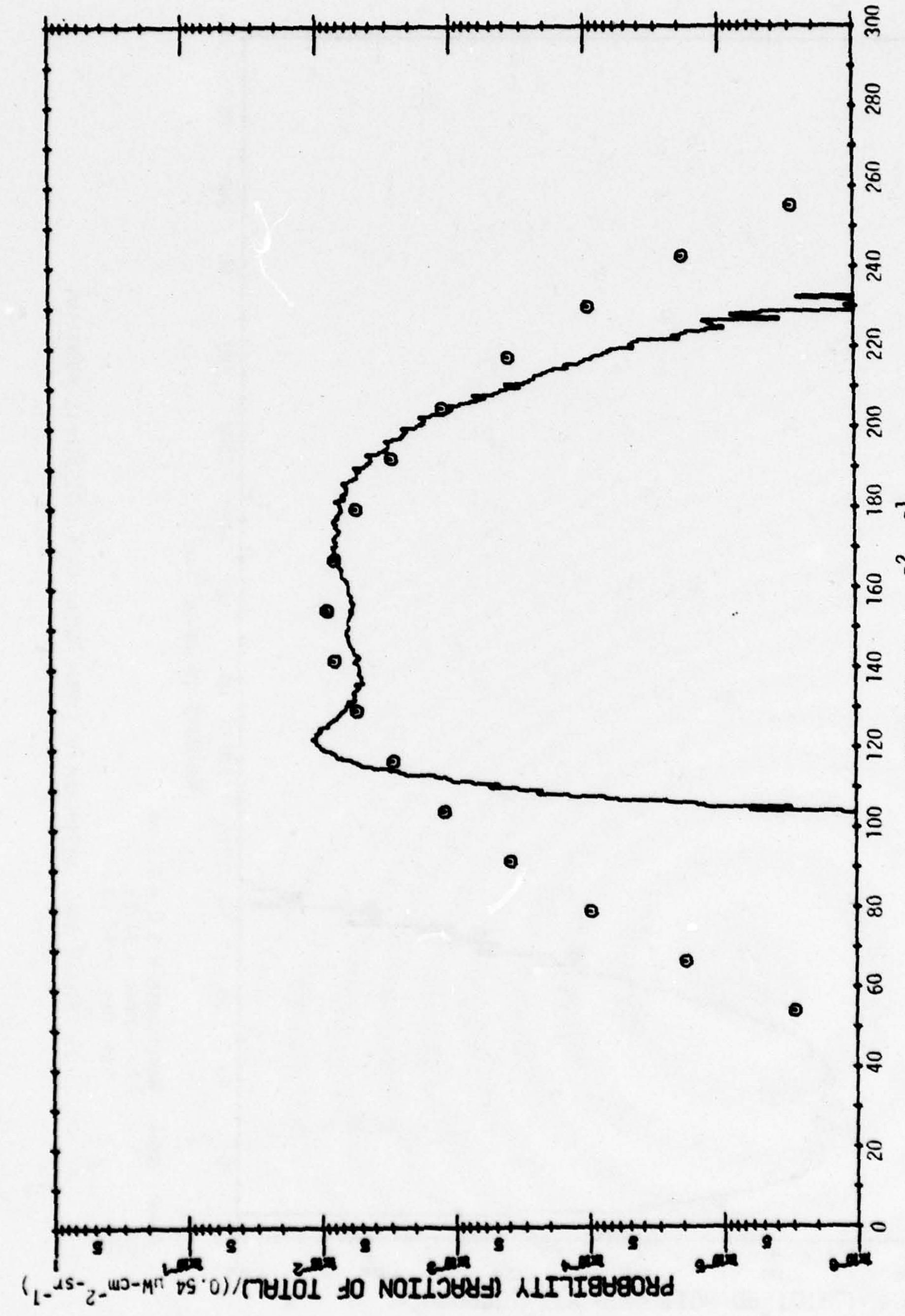

Area: NVG1 Wavelength = 4.5 - 5.5 µm
Mean = 154.51
Std. Dev. = 25.14

FIGURE 17c. HISTOGRAM OF (TOTAL-AREA) DATA OVER NELLIS MOUNTAINS

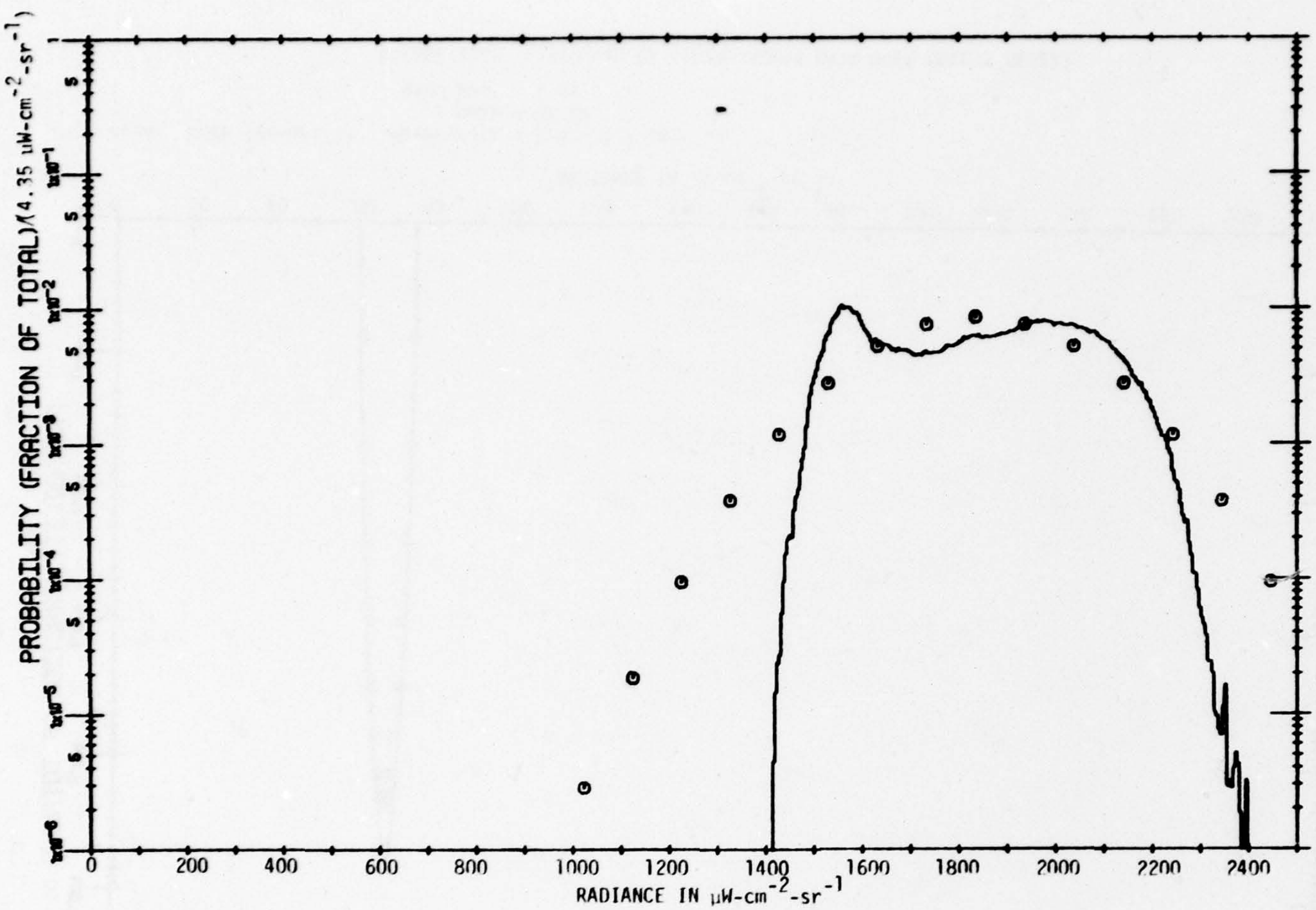

Area: NVG1 Wavelength = 9.0 - 11.4 μm
Mean = 1836.08
Std. Dev. = 203.25

FIGURE 17d. HISTOGRAM OF (TOTAL-AREA) DATA OVER NELLIS MOUNTAINS

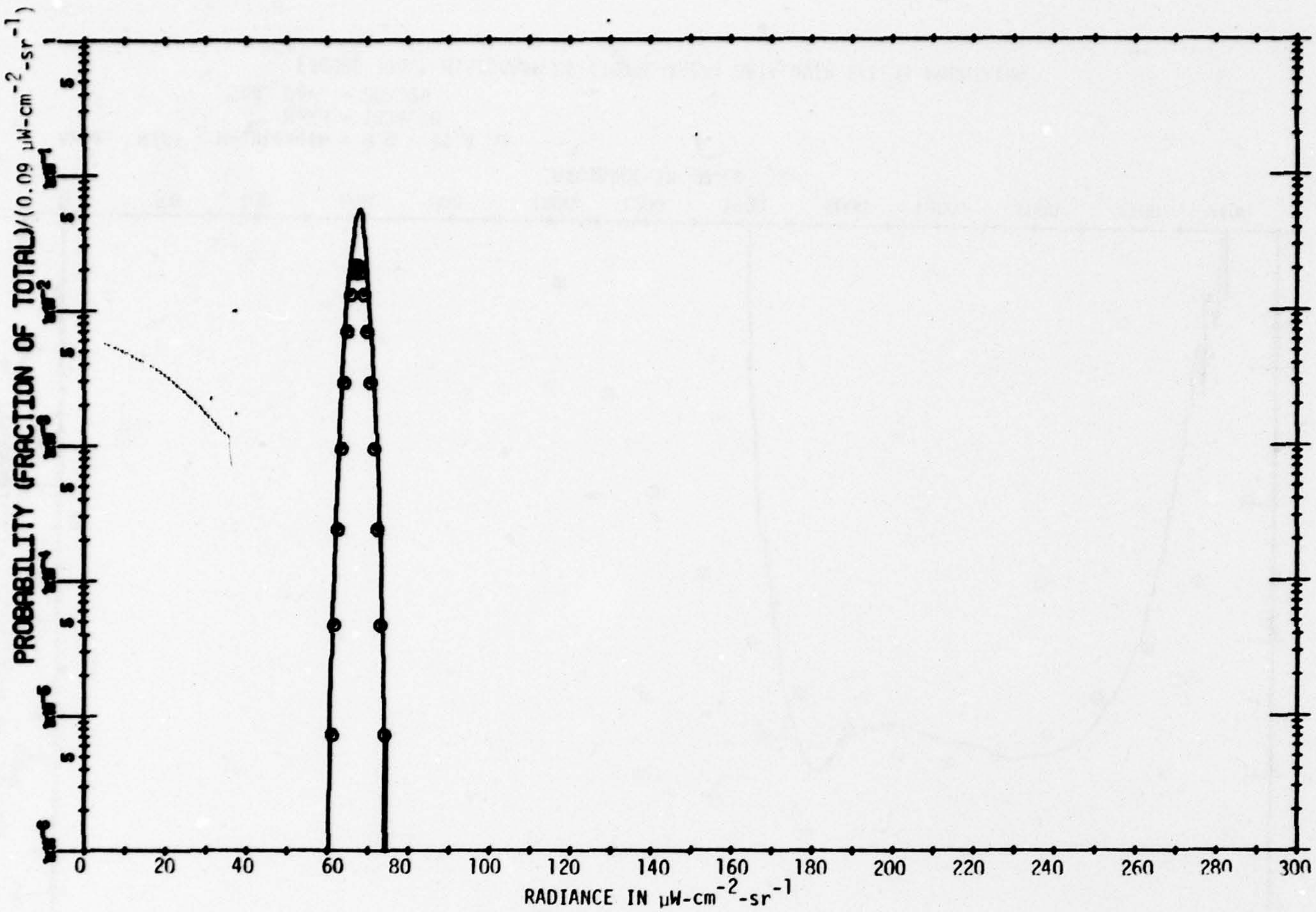

Area: NEVL (Desert 1) Wavelength = 3.9 - 4.7 μm
Mean = 67.64
Std. Dev. = 1.63

FIGURE 18a. HISTOGRAM OF (TOTAL-AREA) DATA OVER NELLIS DESERT

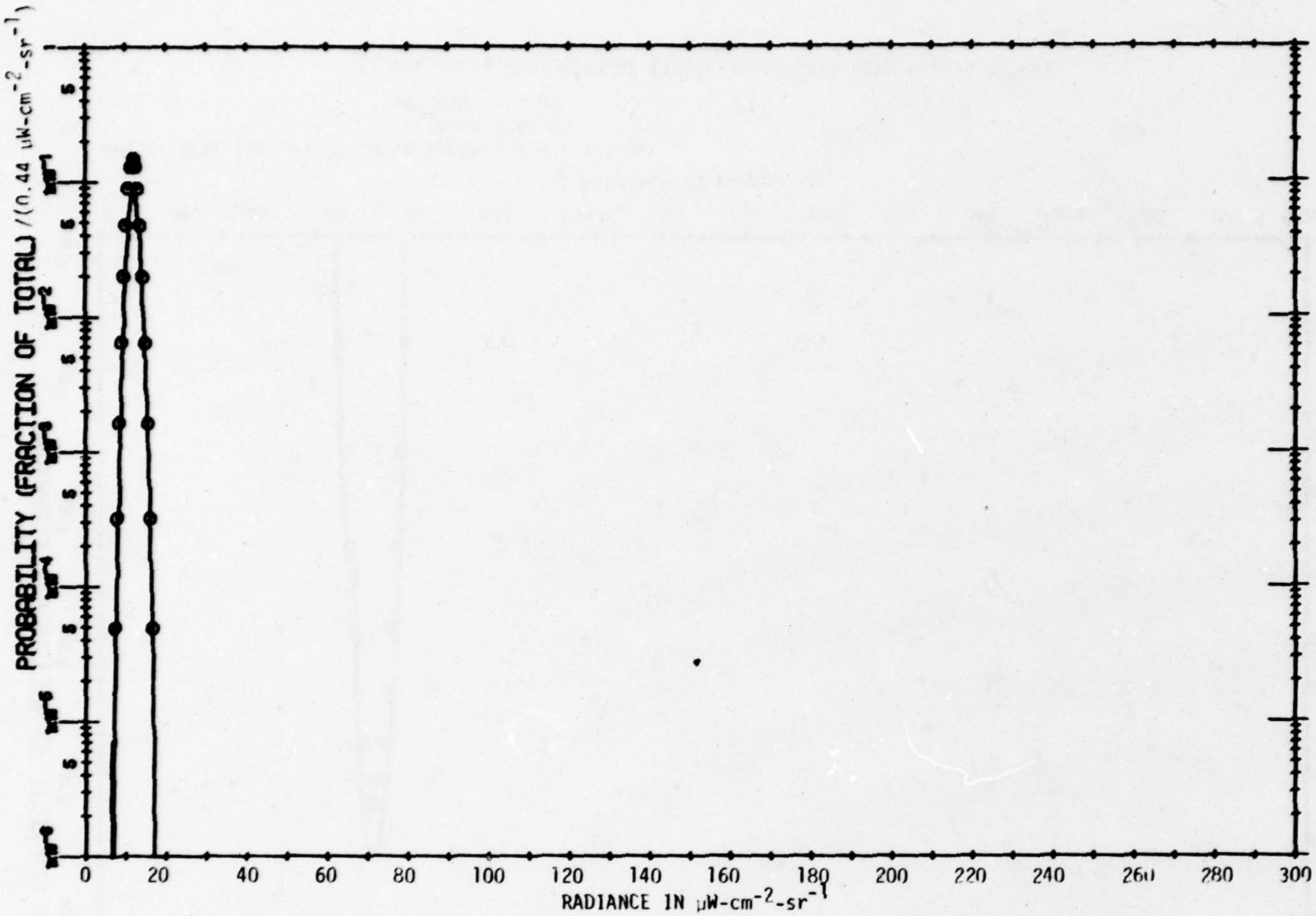

Area: NEVL (Desert 1) Wavelength = 3.5 - 3.9 μm
Mean = 11.94
Std. Dev. = 1.18

FIGURE 18b. HISTOGRAM OF (TOTAL-AREA) DATA OVER NELLIS DESERT

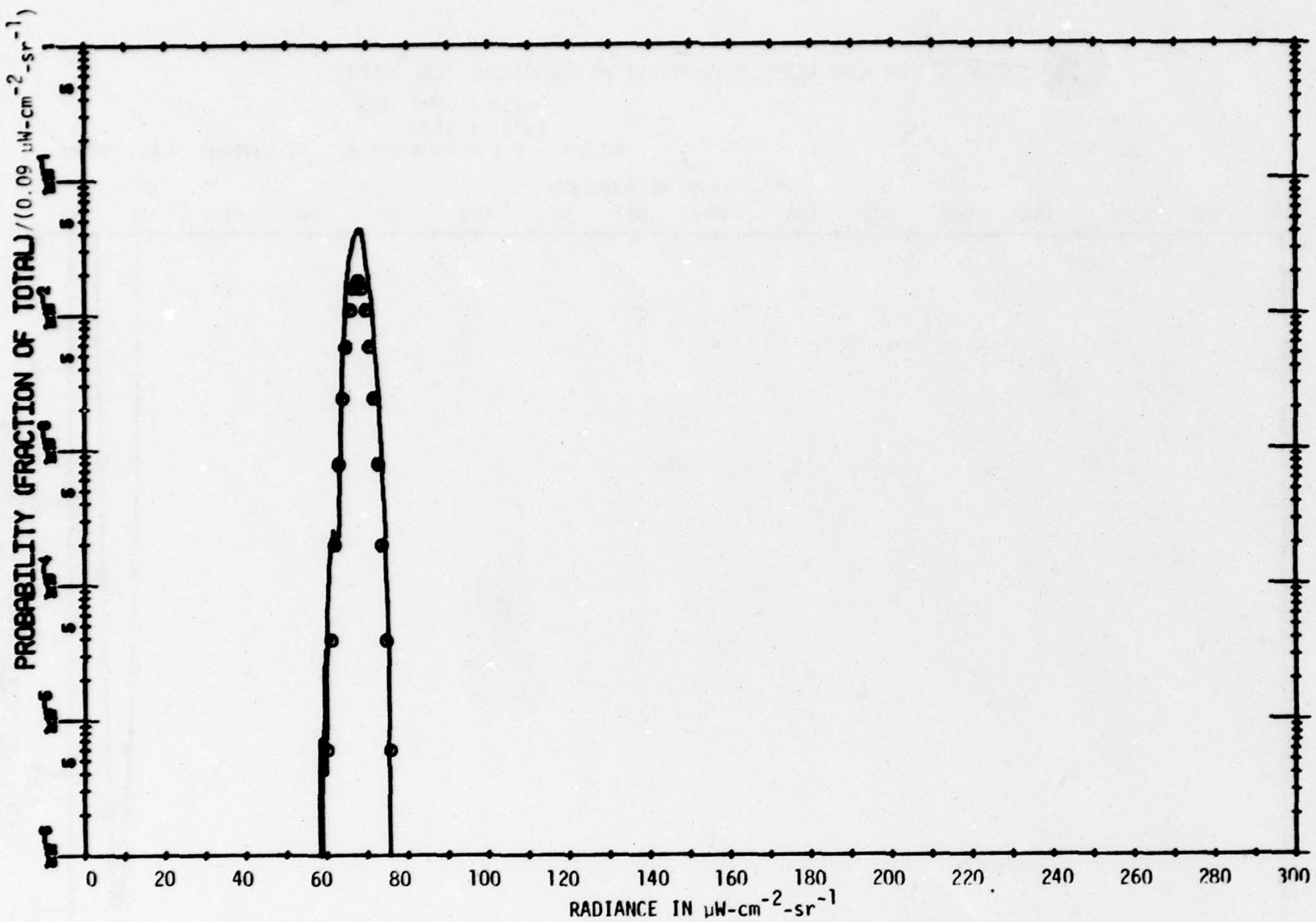

Area: NEVL (Desert 2) Wavelength = 3.9 - 4.7 μm
Mean = 67.93
Std. Dev. = 1.95

FIGURE 18c. HISTOGRAM OF (TOTAL-AREA) DATA OVER NELLIS DESERT

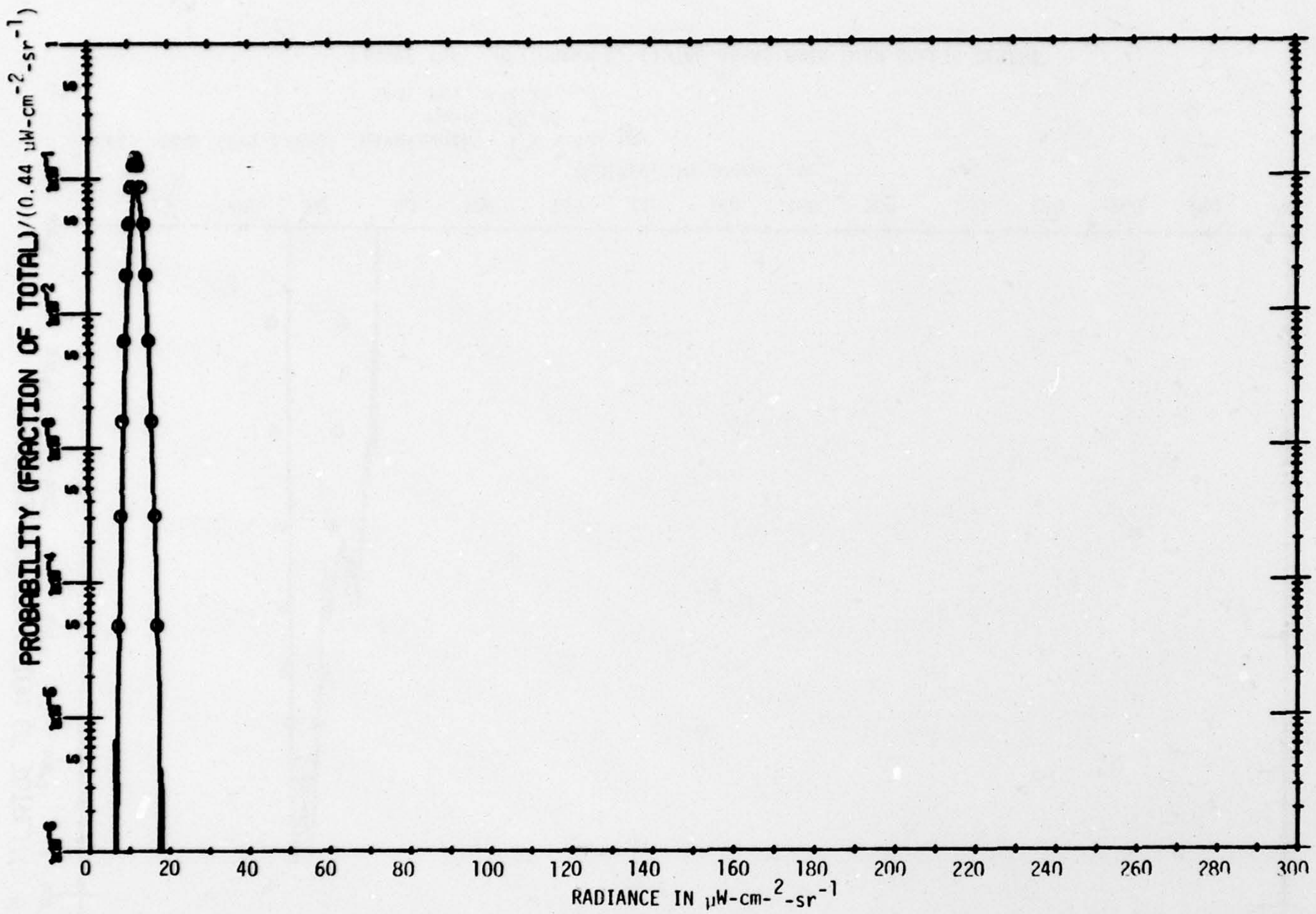

Area: NEVL (Desert 2) Wavelength = 3.5 - 3.9 μm
Mean = 11.97
Std. Dev. = 1.22

FIGURE 18d. HISTOGRAM OF (TOTAL-AREA) DATA OVER NELLIS DESERT

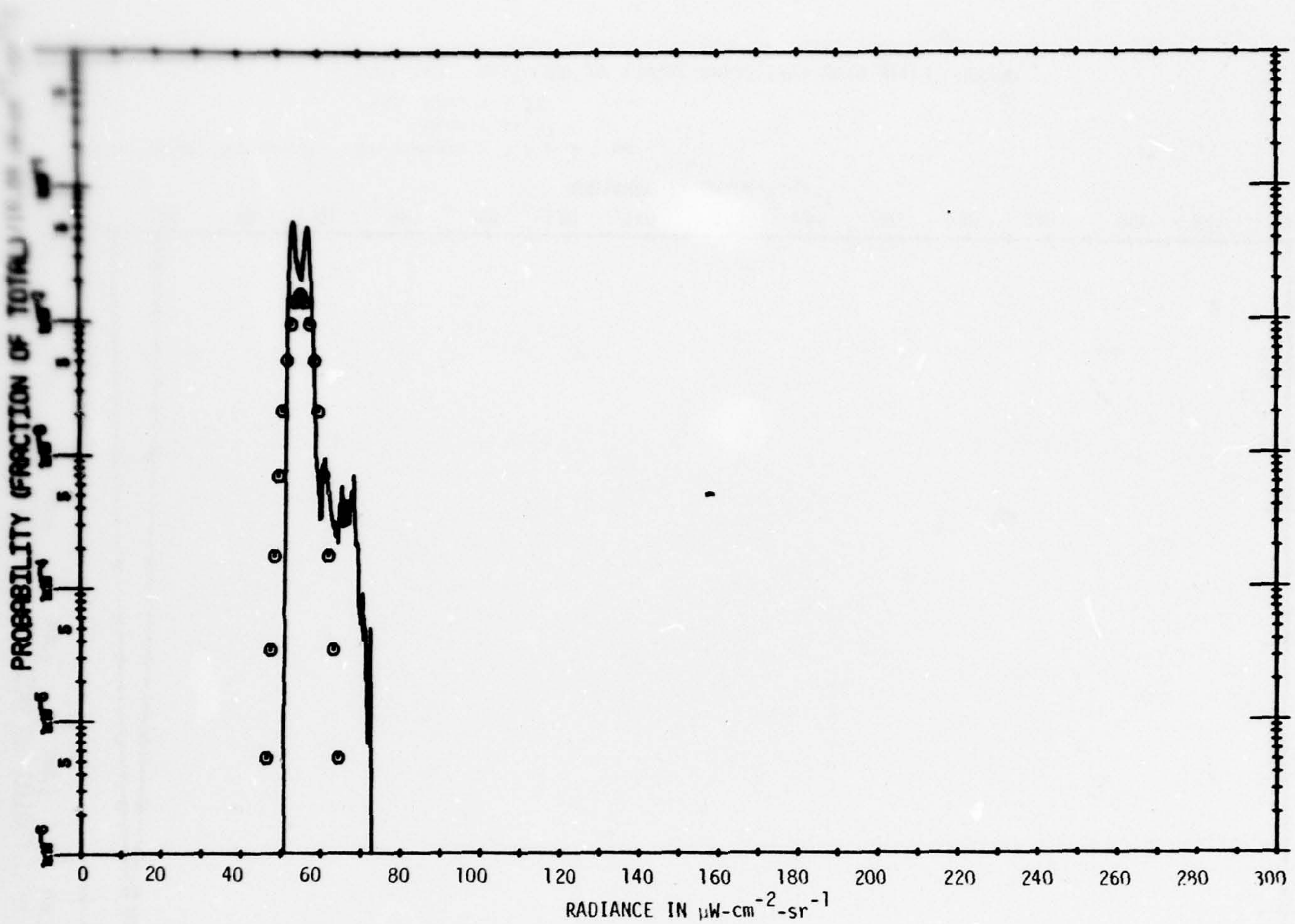

Area: NEVL (Dry Lake) Wavelength = 3.9 - 4.7 μm
Mean = 55.44
Std. Dev. = 2.25

FIGURE 18e. HISTOGRAM OF (TOTAL-AREA) DATA OVER NELLIS DESERT

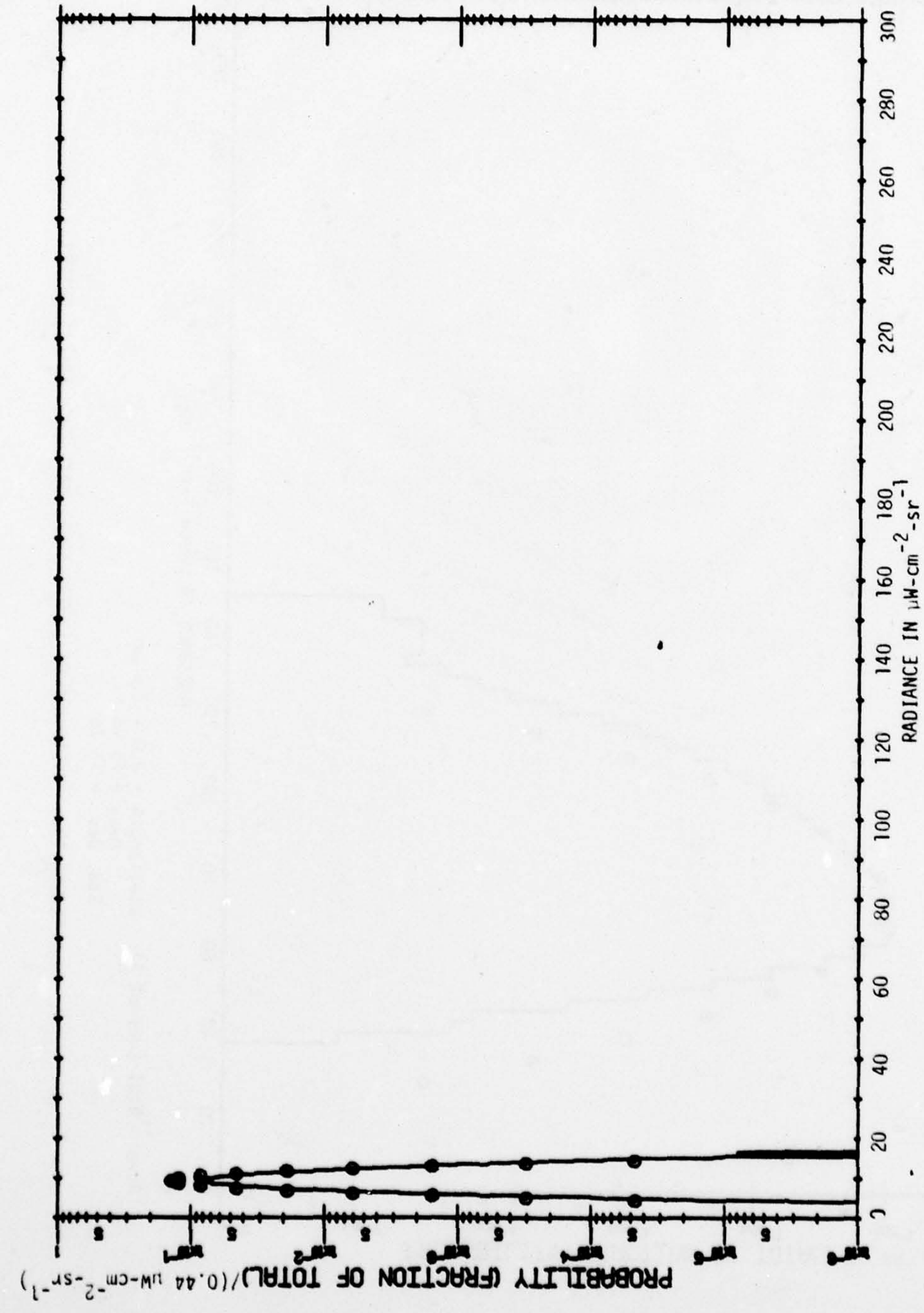

Area: NEVL (Dry Lake) Wavelength = 3.5 - 3.9 μm
Mean = 9.31
Std. Dev. = 1.25

FIGURE 18f. HISTOGRAM OF (TOTAL-AREA) DATA OVER NELLIS DESERT

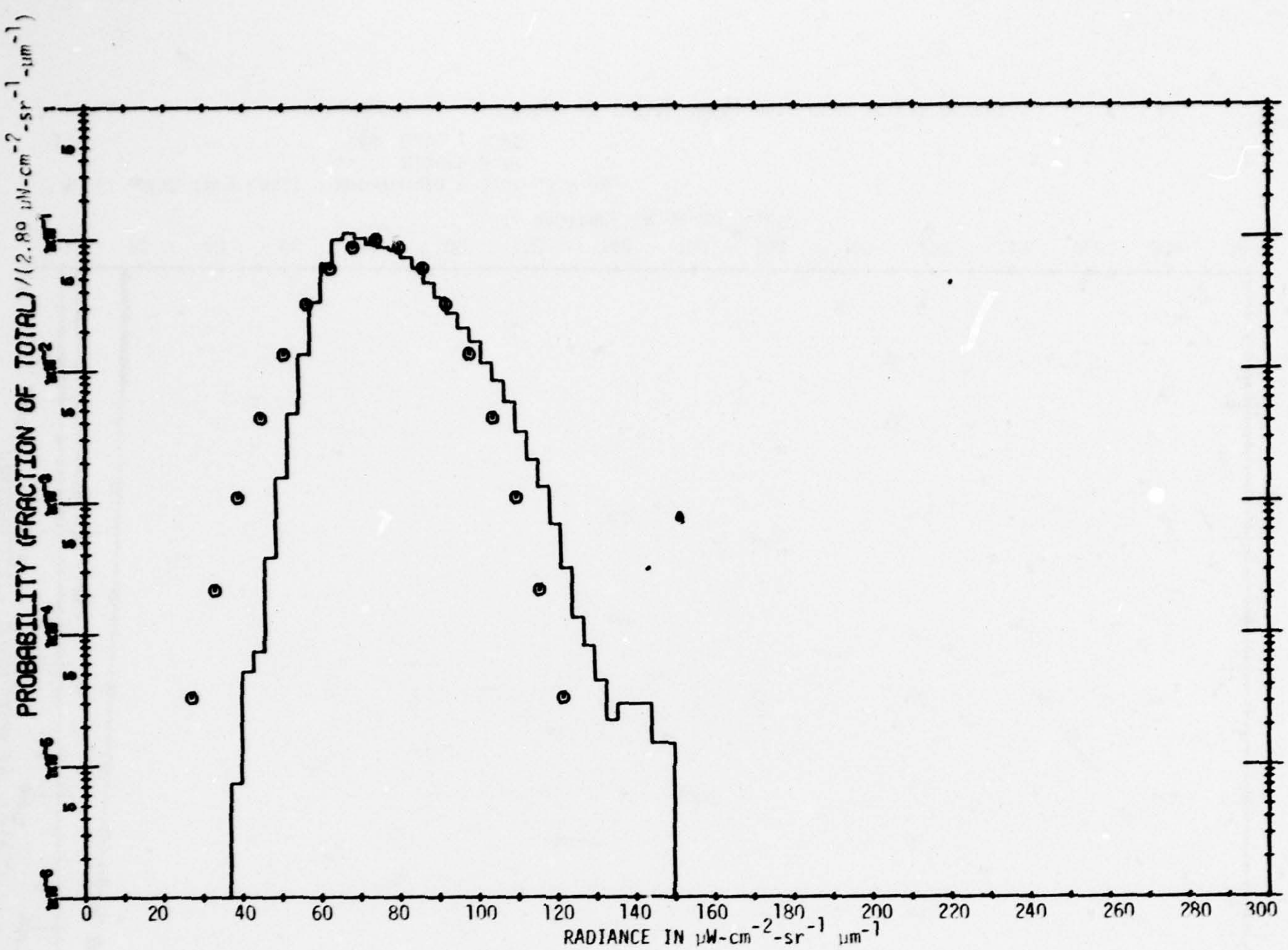

Area: NVH1 (Desert 1) Wavelength = 2.0 - 2.6 μm
Mean = 73.96
Std. Dev. = 11.75

FIGURE 19a. HISTOGRAM OF (TOTAL-AREA) DATA OVER NELLIS DESERT

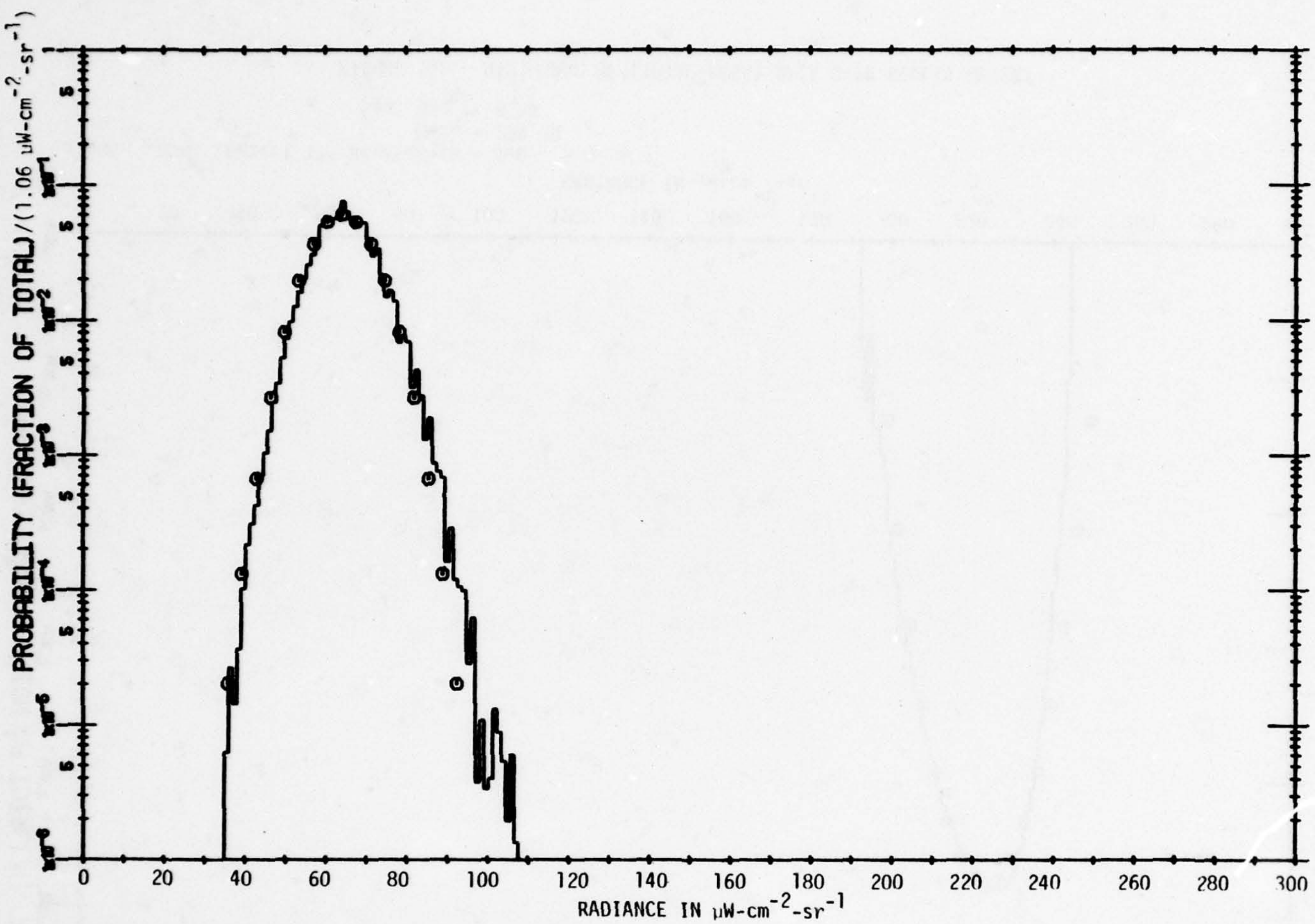

Area: NVH1 (Desert 1)   Wavelength = 3.0 - 4.2 μm
Mean = 64.19
Std. Dev. = 7.09

FIGURE 19b. HISTOGRAM OF (TOTAL-AREA) DATA OVER NELLIS DESERT

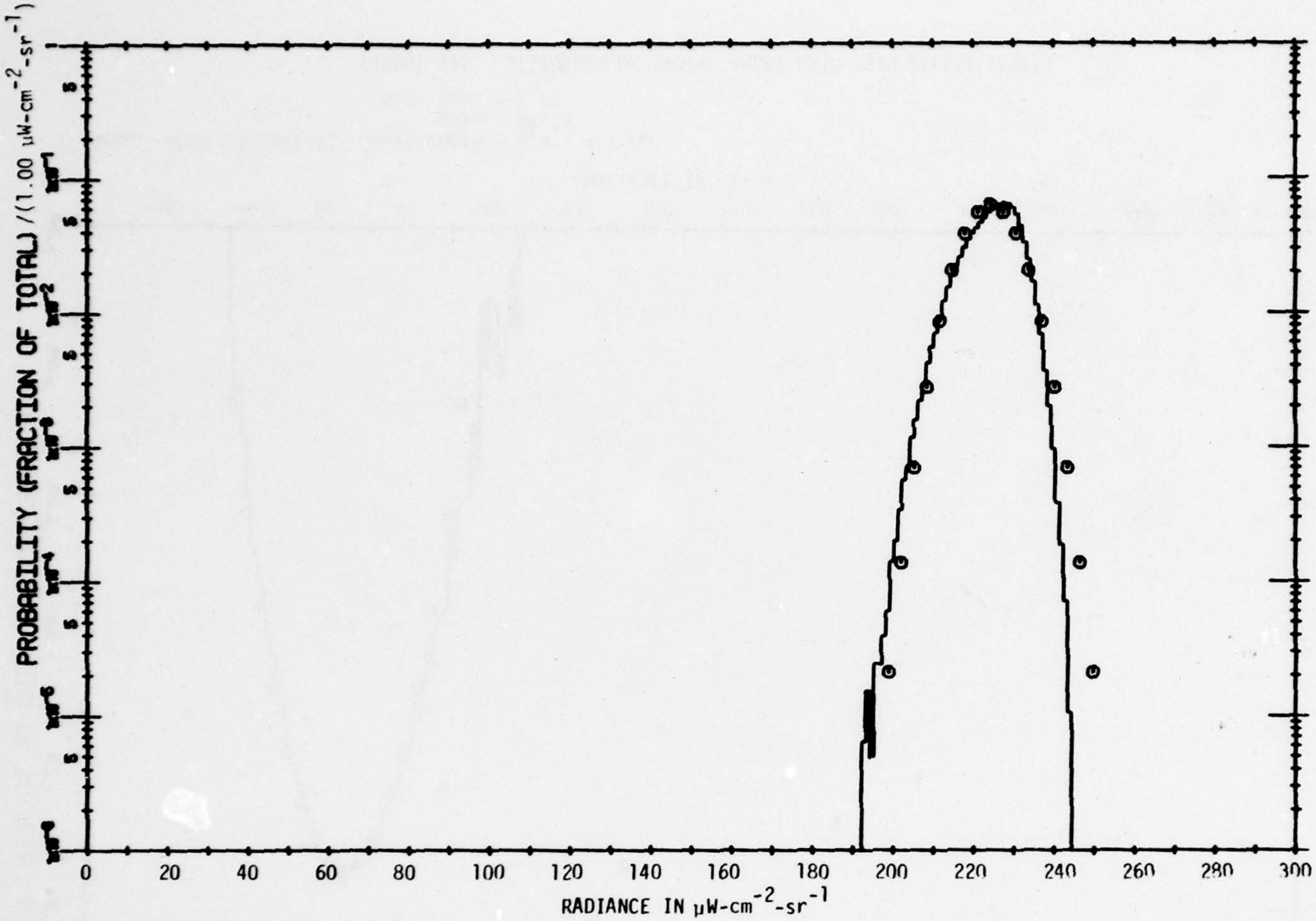

Area: NVH1 (Desert 1) Wavelength = 4.5 - 5.5 μm
Mean = 224.29
Std. Dev. = 6.34

FIGURE 19c. HISTOGRAM OF (TOTAL-AREA) DATA OVER NELLIS DESERT

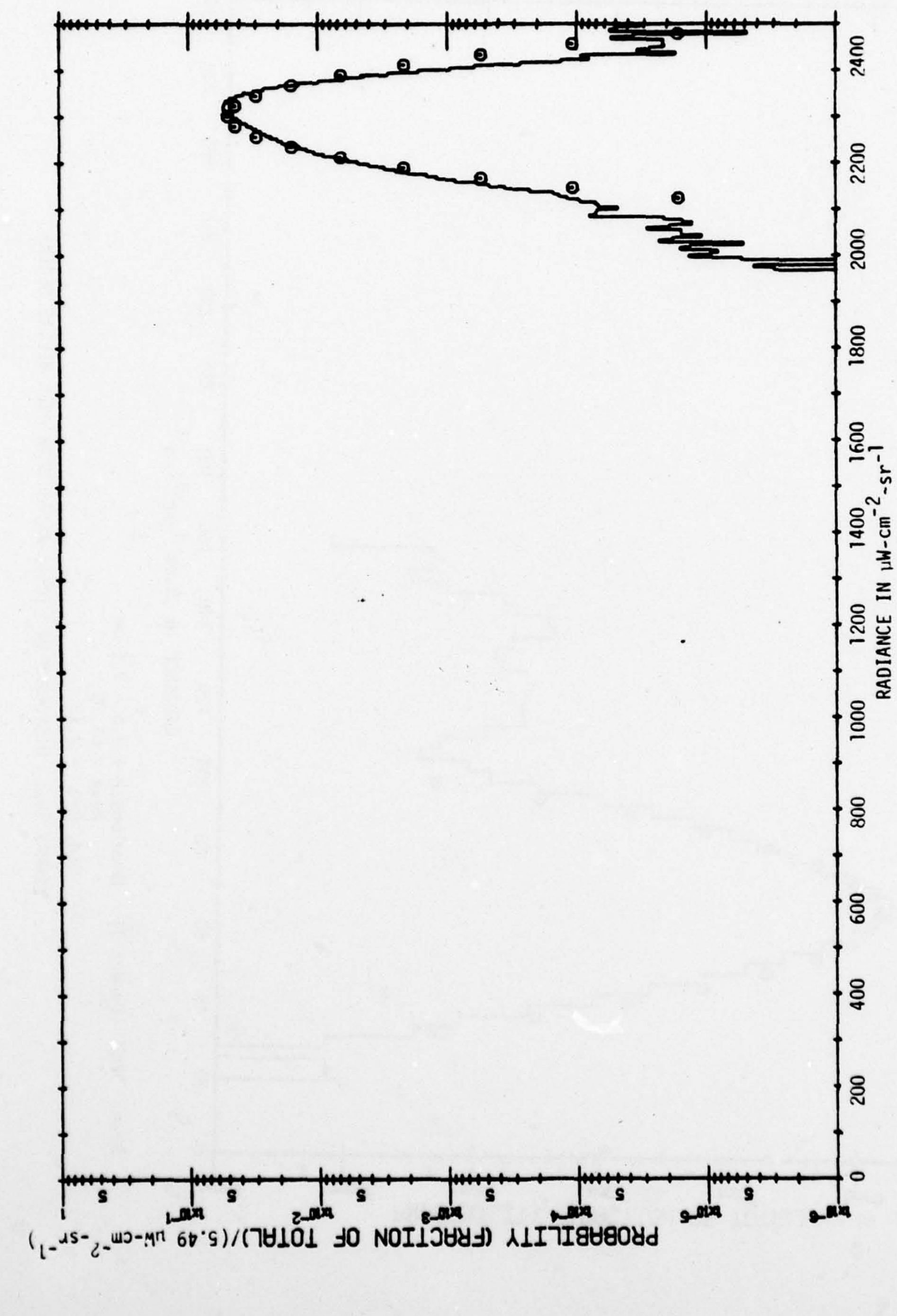

Area: NVH1 (Desert 1) Wavelength = 9.0 - 11.4 μm
Mean = 2300.58
Std. Dev. = 44.44

FIGURE 19d. HISTOGRAM OF (TOTAL-AREA) DATA OVER NELLIS DESERT

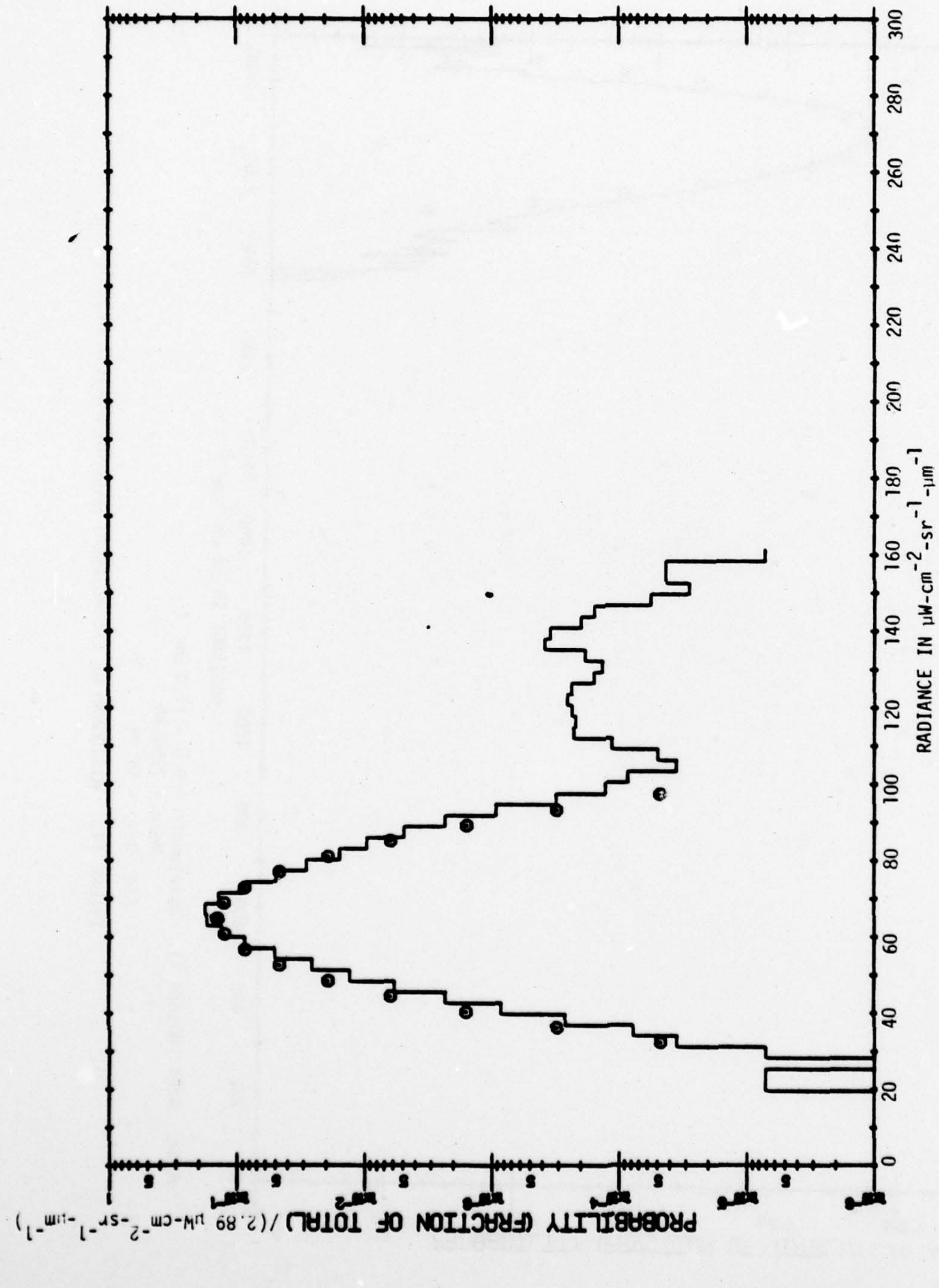

Area: NVHI (Desert 2) Wavelength = 2.0 - 2.6 µm
Mean = 64.70
Std. Dev. = 8.13

FIGURE 19e. HISTOGRAM OF (TOTAL-AREA) DATA OVER NELLIS DESERT

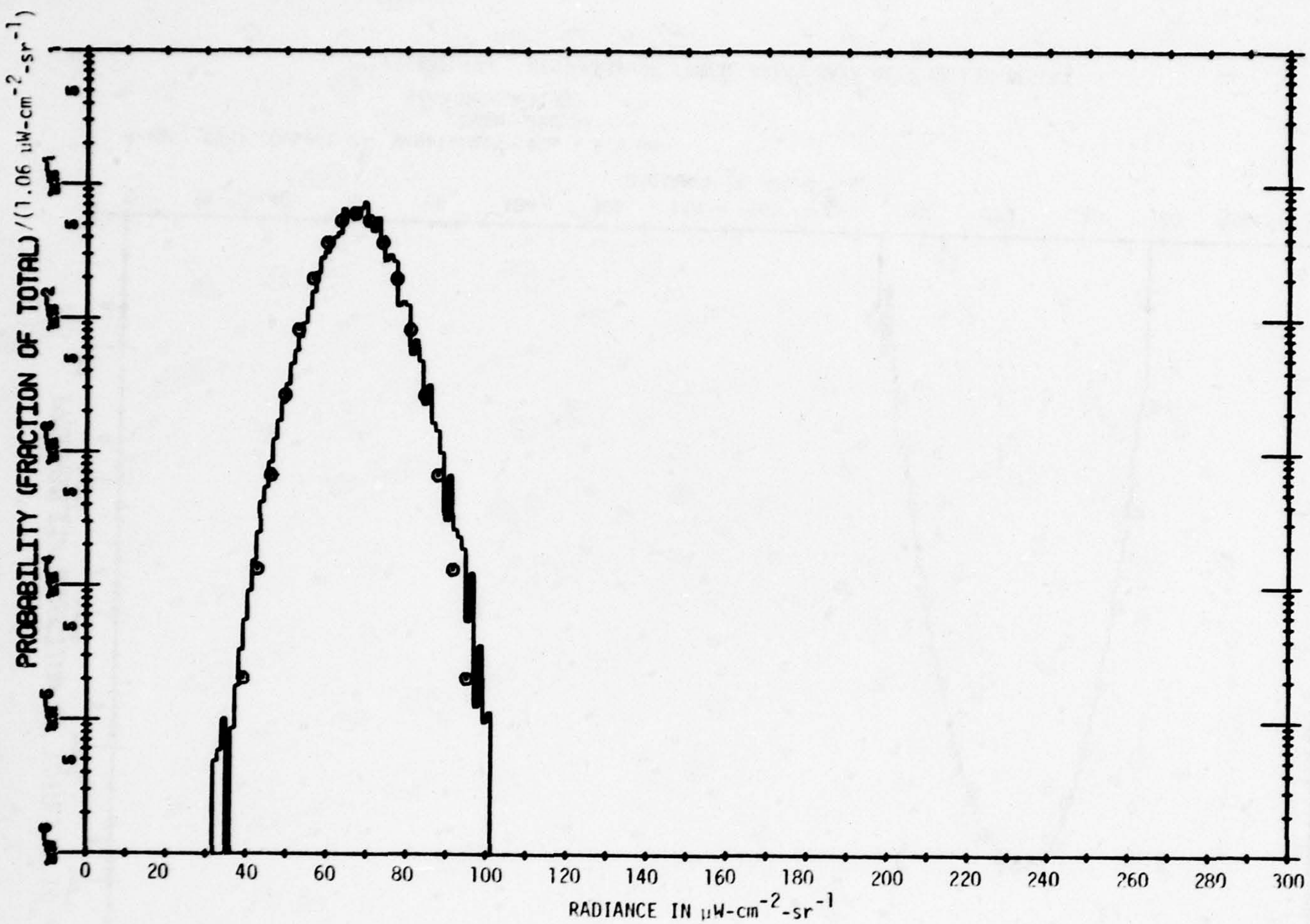

Area: NVH1 (Desert 2) Wavelength = 3.0 - 4.2 μm
Mean = 67.14
Std. Dev. = 6.97

FIGURE 19f. HISTOGRAM OF (TOTAL-AREA) DATA OVER NELLIS DESERT

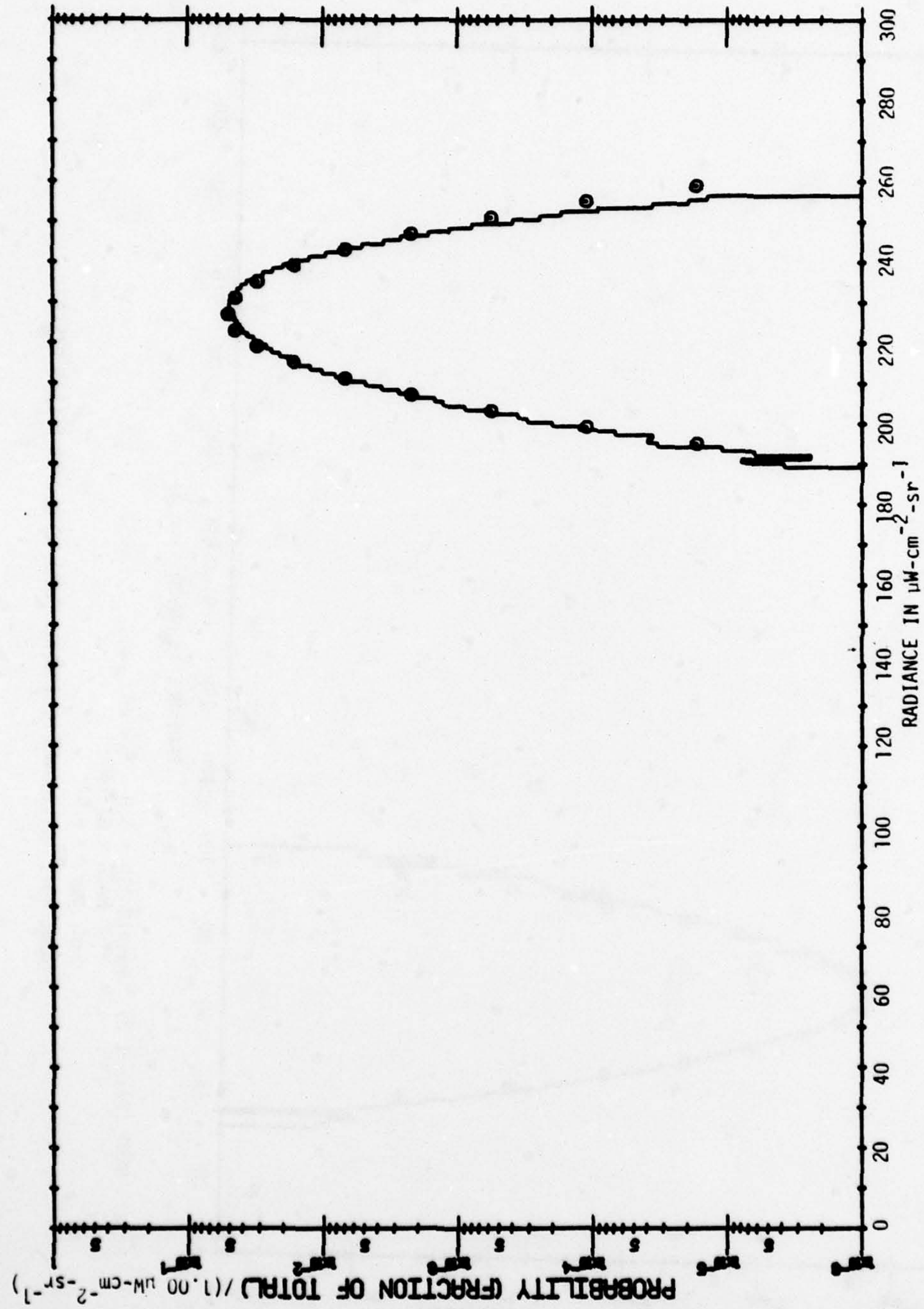

Area: NVH1 (Desert 2) Wavelength = 4.5 - 5.5 μm
Mean = 226.97
Std. Dev. = 7.98

FIGURE 19g. HISTOGRAM OF (TOTAL-AREA) DATA OVER NELLIS DESERT

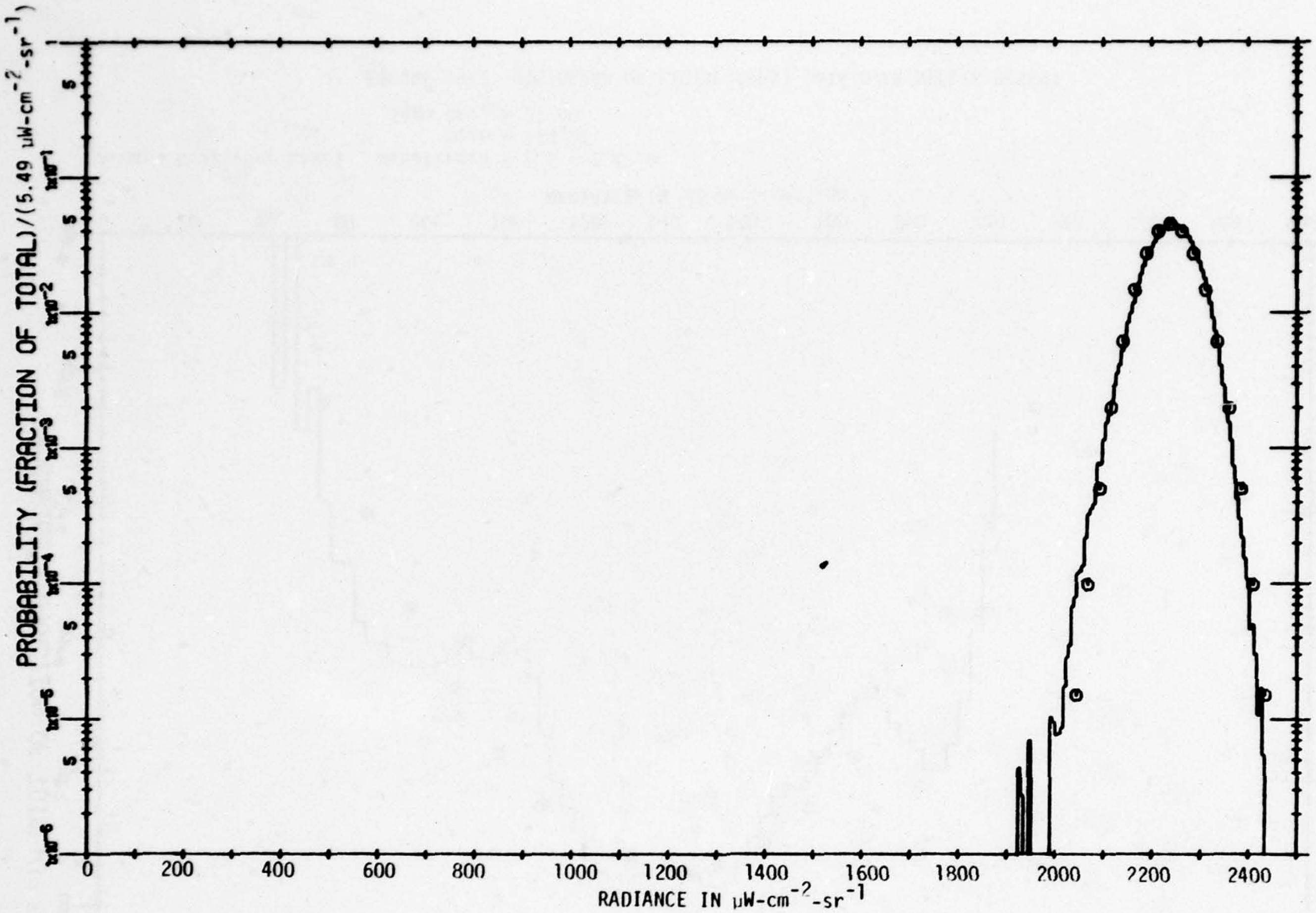

Area: NVH1 (Desert 2) Wavelength = 9.0 - 11.4 μm
Mean = 2238.24
Std. Dev. = 48.71

FIGURE 19h. HISTOGRAM OF (TOTAL-AREA) DATA OVER NELLIS DESERT

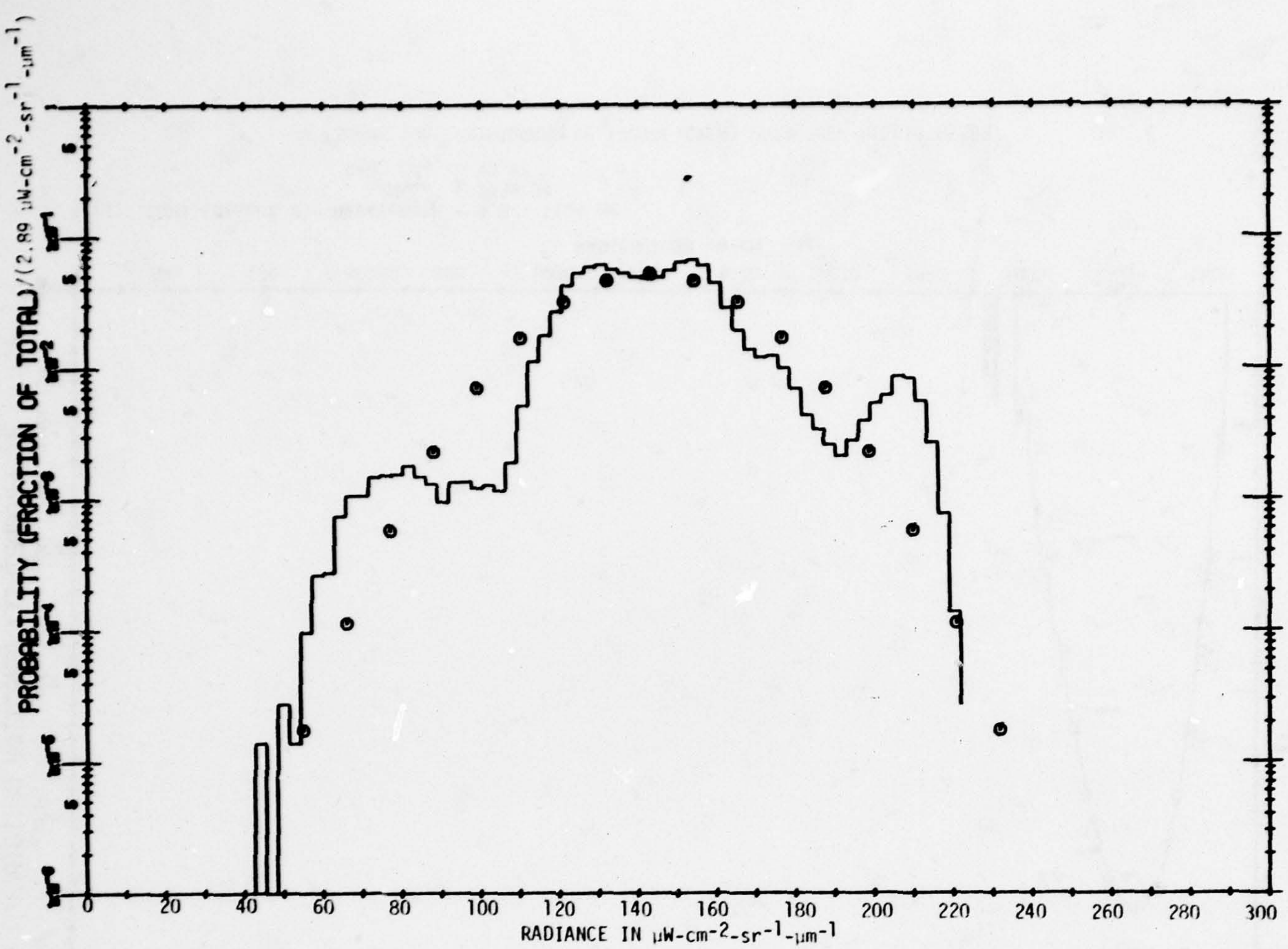

Area: NVH1 (Dry Lake) Wavelength = 2.0 - 2.6 μm
Mean = 143.24
Std. Dev. = 22.08

FIGURE 19i. HISTOGRAM OF (TOTAL-AREA) DATA OVER NELLIS DESERT

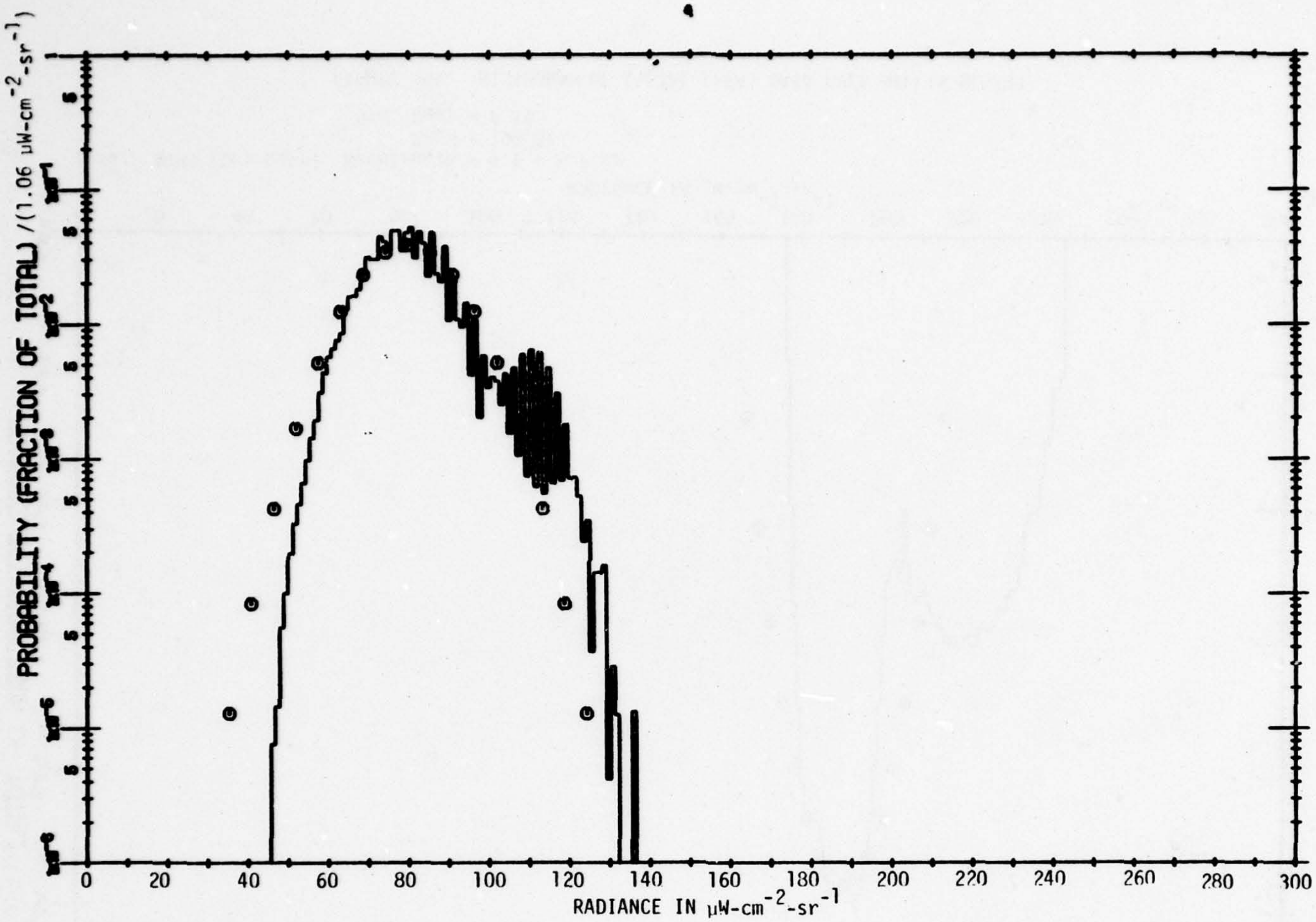

Area: NVH1 (Dry Lake)   Wavelength = 3.0 - 4.2 μm
Mean = 79.74
Std. Dev. = 11.11

FIGURE 19j. HISTOGRAM OF (TOTAL-AREA) DATA OVER NELLIS DESERT

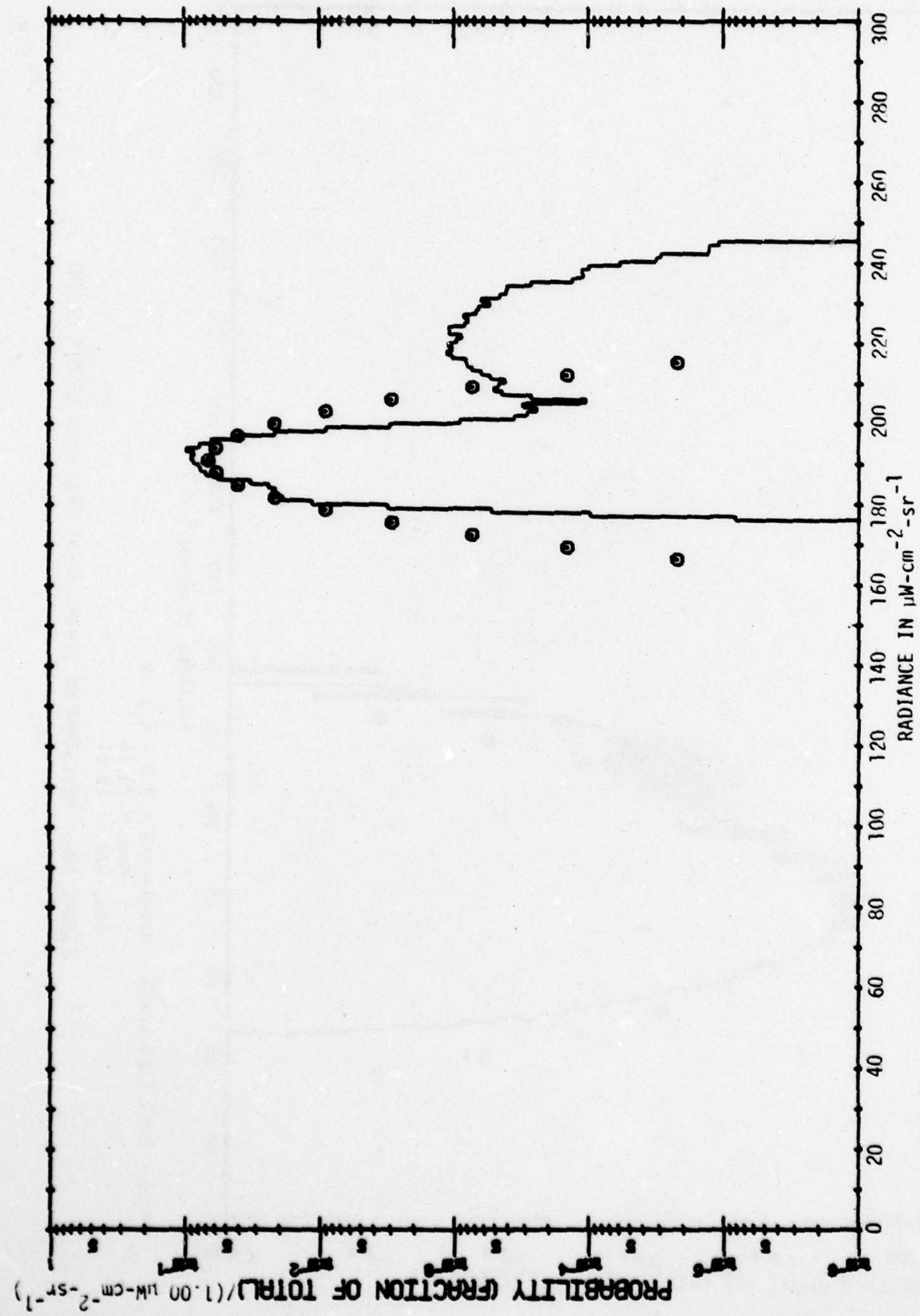

Area: NVHI (Dry Lake) Wavelength = 4.5 - 5.5 µm
Mean = 190.87
Std. Dev. = 6.19

FIGURE 19k. HISTOGRAM OF (TOTAL-AREA) DATA OVER NELLIS DESERT

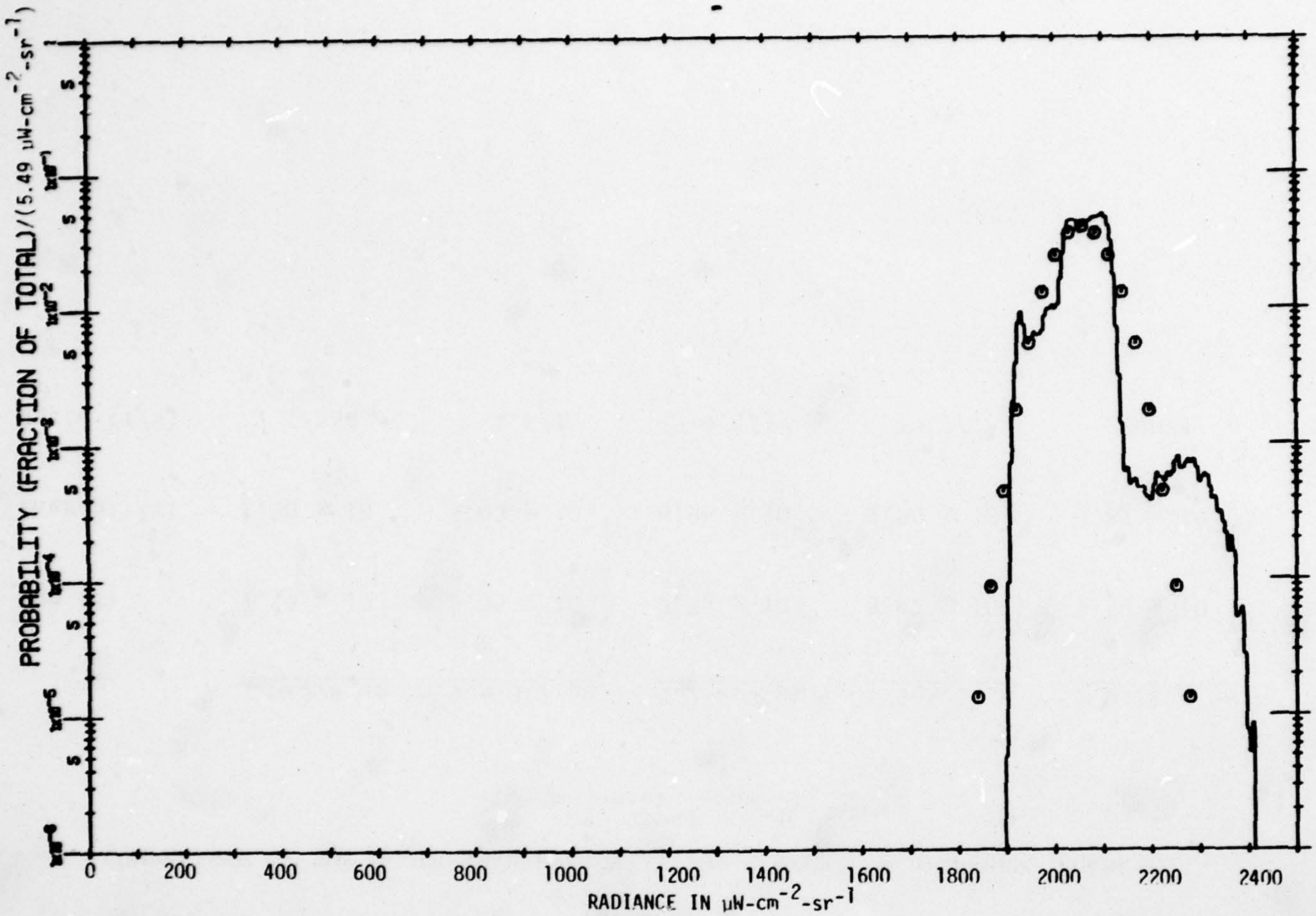

Area: NVH1 (Dry Lake) Wavelength = 9.0 - 11.4 μm
Mean = 2058.56
Std. Dev. = 54.89

FIGURE 19Z. HISTOGRAM OF (TOTAL-AREA) DATA OVER NELLIS DESERT

AD-A068 389 ENVIRONMENTAL RESEARCH INST OF MICHIGAN ANN ARBOR IN--ETC F/G 17/5
STATISTICAL ANALYSES OF TERRAIN DATA.(U)
FEB 79 A J LAROCCA, J R MAXWELL N60530-78-C-0009
UNCLASSIFIED ERIM-132300-2-F NL

2 OF 3

AD
A068389

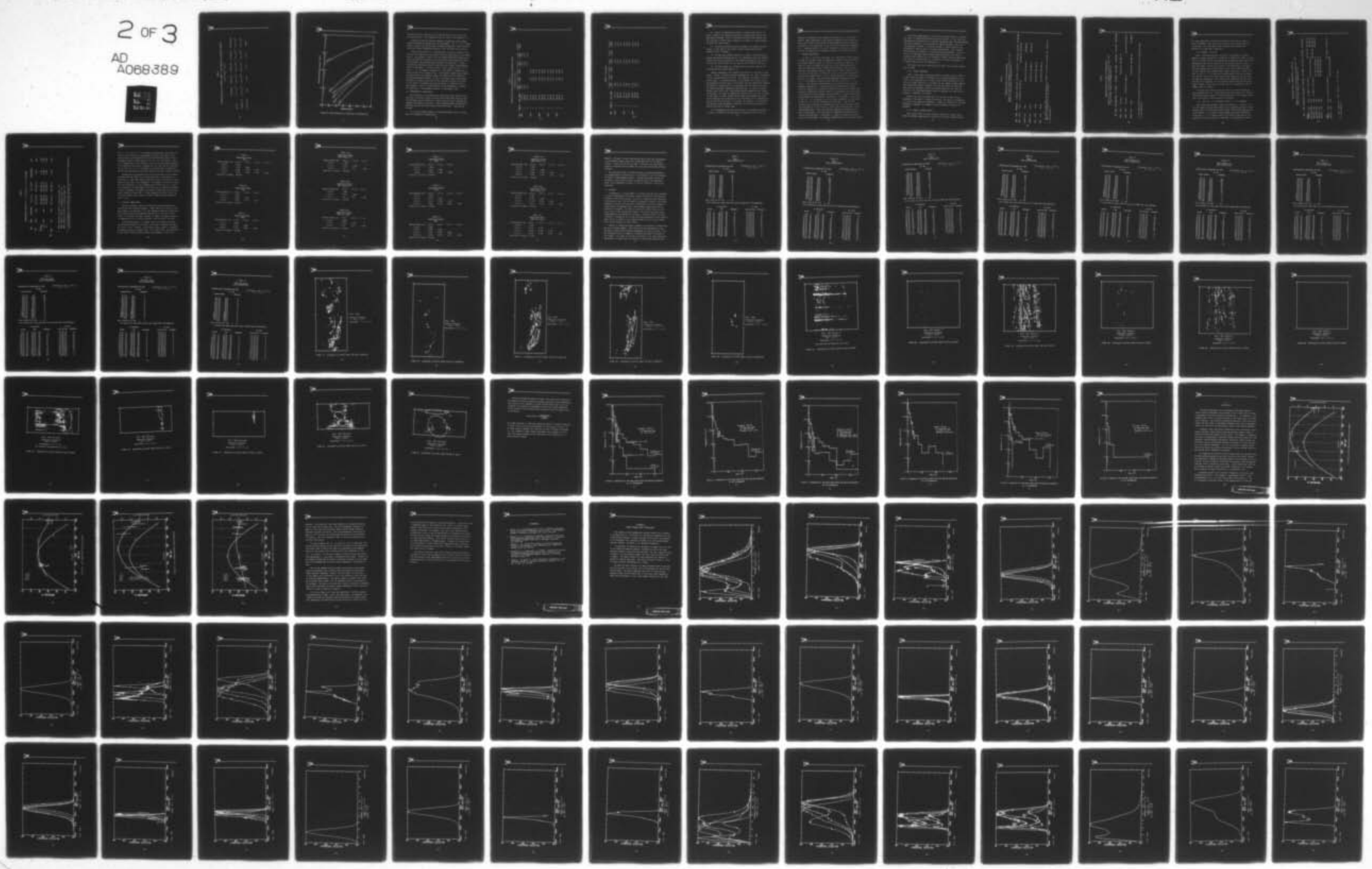

TABLE 3

COMPARISON OF SUN vs THERMAL ENERGY AT THE CENTERS OF DIFFERENT CHANNELS

($w\text{-}cm^{-2}\text{-}ster^{-1}\text{-}\mu m^{-1}$)

	2.0-2.6 μm	3.5-3.9 μm	3.9-4.7 μm	4.5-5.5 μm	9.0-11.4 μm
Sun (S)	7.15×10^{-5}	2.55×10^{-5}	7.36×10^{-6}	3.97×10^{-6}	2.59×10^{-7}
Thermal (T)	1.30×10^{-7}	4.03×10^{-5}	6.96×10^{-5}	7.80×10^{-5}	9.87×10^{-4}
Ratio (T/S)	1/550	1.6/1	9.5/1	19.7/1	3800/1

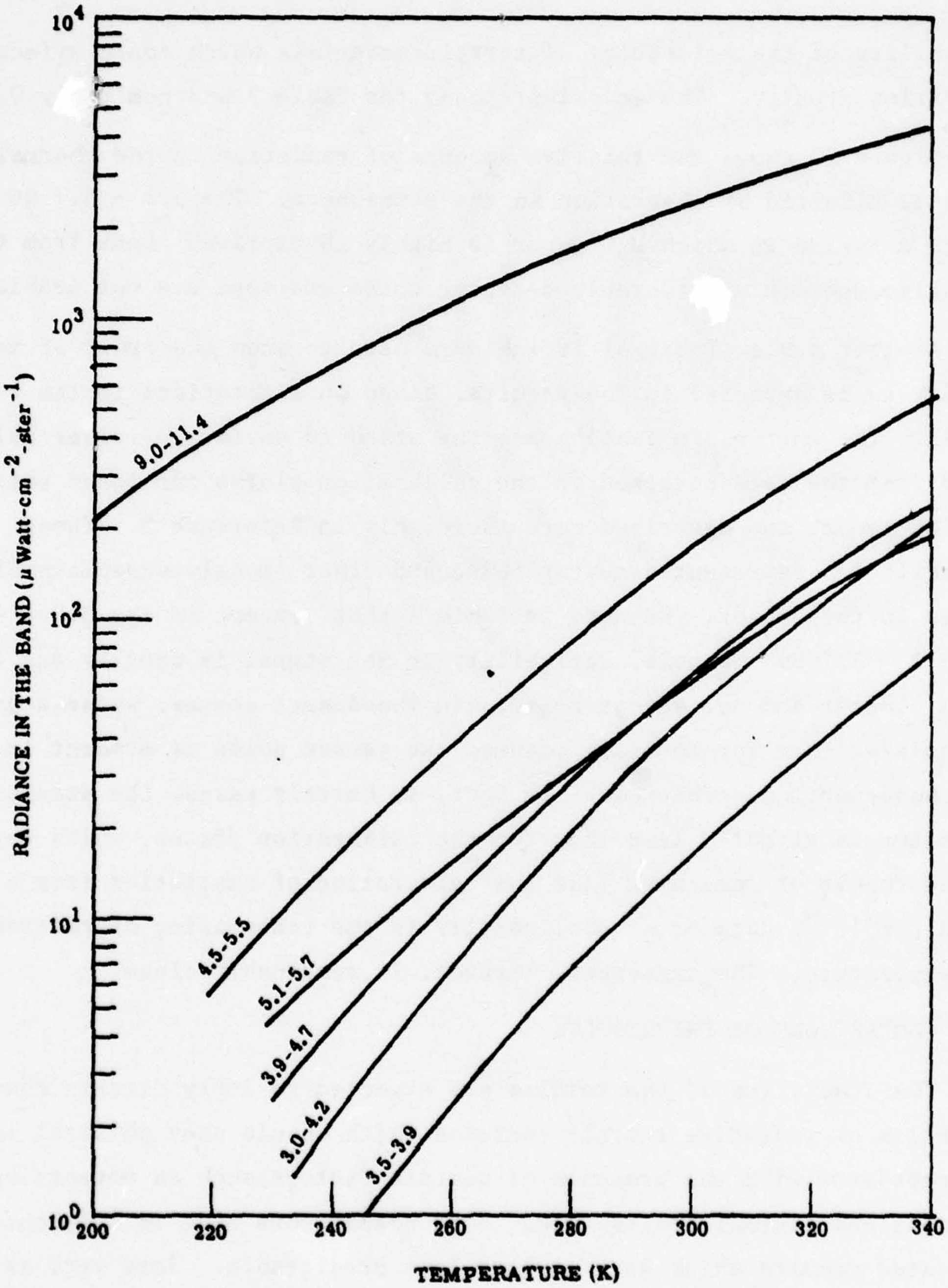

FIGURE 20. BAND RADIANCE AS A FUNCTION OF TEMPERATURE

variability of the emissivity of terrain materials which could affect the ratios greatly. The emissivity used for Table 3 was nominally 0.9.

Figure 20 shows the relative amounts of radiation in the thermal bands as affected by absorption in the atmosphere. The 5.1 - 5.7 μm band covers a region in which H_2O vapor is highly absorptive. Data from this band also contain considerable detector noise and some are not usable.

Another table (Table 4) is included here to show the order of variability to be expected in the results, based on limitations in the system itself. The entries in Table 4 are the standard deviation values calculated from the data obtained on the calibration plates mentioned earlier in this report and described more thoroughly in Reference 3. These variabilities represent detector noise and other (mostly unexplainable) noises in the sensor. We note in Table 2 that, except in the 3.0 - 4.2 and 5.1 - 5.7 μm channels, variability in the signal is usually due to scene clutter and not sensor noise. In the desert scenes, whose signals are quieter than for mountain scenes, the sensor noise is evident in the above-mentioned channels. In fact, in certain cases, the standard deviation is slightly less than for the calibration plates, which may be the result of something like the calculation of statistics from a small sample of data or of nonlinearity in the transposing of radiance to temperature. The agreement, however, is reasonably close.

3.2 COMPARISONS OF THE RESULTS

The statistics of the results are expected to imply certain characteristics of radiative terrain features which should obey physical laws in accordance with the presence of certain factors, such as meteorology, seasonal and diurnal cycles, etc. Some comparisons made in Reference 2 indicated results which were more-or-less predictable. Some were as follows:

(1) Certain signals showed an altitude dependence which is caused mainly by atmospheric transmittance.

TABLE 4

DERIVED NEΔT VALUES DETERMINED FROM CALIBRATION PLATES

(Temperature in K)

Run	Plate #	Ave. Temp.	3.0-4.2 (μm)	3.5-3.9 (μm)	3.9-4.7 (μm)	4.5-5.5 (μm)	5.1-5.7 (μm)	9.0-11.4 (μm)
NEVI	1	277.63	7.07			0.24	3.86	
	2	282.88	5.18			0.22	3.33	
	3	291.62	3.61			0.17	2.65	
NEVJ	1	277.47		4.75	0.33			
	2	283.44		3.56	0.26			
	3	291.35		2.54	0.21			
NEVK	1	277.44		4.26	0.32			
	2	283.18		3.32	0.26			
	3	291.33		2.30	0.20			
NEVL	1	277.71		3.89	0.27			
	2	287.85		2.55	0.26			
	3	291.35		2.19	0.22			
NEVM	1	280.45		3.75	0.29			
	2	282.59		3.39	0.26			
	3	287.44		2.74	0.22			

TABLE 4 (Continued)

Run	Plate #	Ave. Temp.	3.0–4.2 (μm)	3.5–3.9 (μm)	3.9–4.7 (μm)	4.5–5.5 (μm)	5.1–5.7 (μm)	9.0–11.4 (μm)
NEVN	1	279.43	3.88			0.17		0.11
	2	282.79	3.35			0.16		0.13
	3	284.37	3.11			0.15		0.10
NVG1	1	274.11	6.78			0.35		0.25
	2	284.37	3.94			0.24		0.21
	3	278.93	5.14			0.28		0.22
NVH1	1	283.09	6.76			0.28		0.34
	2	283.99	6.48			0.30		0.36
	3	289.37	4.95			0.23		0.29

(2) Clutter in mountainous scenery is greater than that in the desert, caused by the greater variability in mountainous terrain, and resulting in shadows. Note in the desert results in this report that the curve has a bimodal shape, probably as a result of a small mixture of desert and lake scenery.

(3) Correlations between spectral channels were higher for mountainous terrain than for the desert scenery, making manifest the dramatic effect of shadows.

(4) The mean and standard deviation of signals received when the scanner was pointed downward and at a 35° depression angle were similar, particularly when the altitude in the downward-looking case was such as to equal the slant distance to the scene in the forward-looking case.

(5) The mean signal for afternoon runs was usually greater than for morning runs by approximately 5 K.

Similar comparisons can be made in the results of the data in this report. Others, covering different parameters are also made, considering spatial and meteorological effects. One important observation is made at the outset. As mentioned above, it was agreed that because radiance distributions were more basic to the sensor and more immediately amenable to simulation, these would be incorporated into the report along with the usually presented temperature distributions. It should be noted, however, that, albeit the relationship between temperature and radiance is nonlinear, the range of temperatures observed in the scenery included in this report is small enough that the means and standard deviations of the radiances can be derived directly from those of the temperatures with little loss in accuracy. Of course, the accuracy is a function of the spectral range considered, being less for the shorter wavelength regions than for the longer ones.

It is recommended that the past practice of recording statistics in terms of temperature distributions be continued, even if they are

presented concomitantly with radiance distributions. It is so much easier to make comparisons in the results between spectral regions as long as the losses in the system and the atmosphere, and the spectral variability of the emissivity of the terrain are understood reasonably well. Comparing results in terms of temperature allows us to remove at least one important but manageable variable, the Planck function.

3.3 FURTHER COMPARISONS

In light of the above statements, the comparisons in this section are made in accordance with the temperature values collected in Table 2. For related radiance values, the reader is referred to Table 2a. It might be useful to remind the reader that these comparisons must be made with some reservation, considering the numerous factors which influence the measured radiance, many of which can be figured in the data only qualitatively, and some not at all. In all data measured in the spectral regions below 4 μm, the sun is influential to some extent. We note, for example, that the average apparent temperature in the 3.5 - 3.9 μm region is usually higher than that in the 3.9 - 4.7 μm region. From previous considerations, we are already aware that the apparent temperature is a strong function of many external factors. These two regions are of particular interest because they represent the region of transition below which the sun is influential and above which the influence is mostly thermal, except possibly in cases in which many strong glints are experienced. From Table 3, for example, we note that in the 3.5 - 3.9 μm region, the sun is still influential to some extent; in the 3.9 - 4.7 μm, its influence is on the wane. Just how much influence the sun exerts is determined not only by the spectral region and the amount of cloud cover, etc., but by the characteristics of the scattering surface. Thus, the apparent temperature determined from a given reading must be altered before any comparisons between spectral regions are meaningful. Furthermore, if there is significant absorption in the atmosphere, the apparent temperatures will be further altered.

Any future measurements to be made must attempt either to eliminate the effect of dominating influences such as sunlight, or take them into consideration quantitatively by specially measuring them. Notwithstanding the need to measure in certain bands for special reasons, there are a few atmospheric windows, or spectral regions, in which radiation can propagate for 1000 or 2000 ft virtually unattenuated. These regions should always be included in any multispectral measurement. As far as the sun is concerned, remote sensing specialists have lived with it (indeed, often depend on it) on reasonably friendly terms for many years. They simply try to know what it is doing at all times by measuring it in those bands which are influenced by it.

With these and other considerations in mind, the following comparisons are made.

3.3.1 FLIGHT DIRECTION

Table 5 lists those total-area values of scenery listed in Table 2 of this report and those of Reference 2 for which mountains were overflown in the afternoon with a scanner line-of-sight depression of 35°. As far as flight direction is concerned, we are tempted to make comparisons between the spectral regions, but find that except for what was said about sun influence, little is evident beyond the fact that the clutter for the northward-heading sensor is smaller than those for the easterly or southerly directions.

Based on the few data shown here, if one were to make a broad judgement of the effect of flight direction on the choice of parameters to select in an organized experiment, it might be considered of secondary importance, compared, for example, with the presence or absence of sunlight.

3.3.2 CLEAR vs OVERCAST SKIES

This latter effect is easily noted in the data of Table 6 which shows the average temperatures to be less for overcast conditions than

TABLE 5

COMPARISONS MADE ON FLIGHT DIRECTION*

Values at 2.0-2.6 μm are Radiance in $\mu w\text{-}cm^{-2}\text{-}ster^{-1}\text{-}\mu m^{-1}$
Values in other regions are Temperature in K

Run	Time	Direction	2.0-2.6μm	3.0-4.2μm	3.5-3.9μm	3.9-4.7μm	4.5-5.5μm	5.1-5.7μm	9.0-11.4μm
NEVI	1510	East	71.48±29.85	300.00±7.28			290.68±4.60	283.70±3.89	
NEVB**	1511	East			298.19±7.17	290.05±4.94		282.88±3.90	
NEVE**	1424	East			307.94±6.70	291.58±4.47		278.15±2.31	
NEVJ	1528	South			289.71±6.90	285.70±4.07			
NEVK	1543	North			293.06±4.33	288.34±2.53			

* All flights except NEVE are over mountains at 1000 ft. with depression angle 35°. NEVE is at 5000 ft. All flights are in the afternoon.

** From Reference 2.

TABLE 6

COMPARISONS MADE ON CLEAR VS OVERCAST SKY*

Values at 2.0 - 2.6 μm are Radiance in $\mu w\text{-}cm^{-2}\text{-}ster^{-1}\text{-}\mu m^{-1}$
Values in other regions are Temperatures in K

Run	Time	Sky Condition	2.0-2.6μm	3.0-4.2μm	3.5-3.9μm	3.9-4.7μm	4.5-5.5μm	9.0-11.4μm
NEVM	1022	Overcast			283.60±3.82	282.09±1.46		
NEVN	1044	Overcast	17.30±5.28	285.68±3.65			283.12±1.49	285.37±2.23
NEVF**	1034	Clear			296.76±9.94	286.49±5.68		287.08±6.53

* All flight directions eastward over mountains in the morning at 35° depression angle.

** From Reference 2.

for clear conditions, as expected, because of the lack of sunlight. Note, furthermore, that the clutter is less for an overcast than for a clear day. As in the above case, some data are borrowed from Reference 2 to make these comparisons.

3.3.3 DESERT: AM vs PM

Table 7 specifies the data of Table 2, 2a pertinent to desert imagery. A direct comparison is infeasible in these cases since, according to the flight record, the sunshine was essentially unobscured in the morning while the sky was overcast in the afternoon when the data for NEVL were taken. This fact is evident in the observation from Table 7 that the temperatures for NEVL are all lower than for NEVC and NVH1, in which the data were obtained under sunlit conditions. We note also that in the 2.0 - 2.6 μm region the contribution by the sun is greater over the dry lake than over the desert which seems to result at times in negative correlations. This verifies the observation by the flight crew that the brightness from the lake was greater than that from the desert regions. The effect is evident also in a comparison of the IR imagery shown in Figure 3.

One notes also from the data from certain of these regions that the correlations are low. This seems to be characteristic of relatively low-contrast areas in which a large contribution to the standard deviation in the data is from the noise in the sensor.

3.3.4 THE 4.5 - 5.5 μm REGION vs THE 9.0 - 11.4 μm REGION

Data from these spectral regions are singled out in Table 8. Of all the regions included these should yield comparable apparent temperatures, since the effects are mainly thermal except where sunglint may be influential. It is best to avoid making any serious comparisons using the 5.1 - 5.7 μm band because of the noise in the detector and because of the severe effect of atmosphere on attenuating the signal.

TABLE 7

COMPARISONS MADE ON DESERT DATA*, AM VS PM

Values at 2.0 2.6 μm are Radiance in $\mu w\text{-}cm^{-2}\text{-}ster^{-1}\text{-}\mu m^{-1}$
Values in other regions are Temperature in K

Run	Time	Direction	2.0-2.6μm	3.0-4.2μm	3.5-3.9μm	3.9-4.7μm	4.5-5.5μm	9.0-11.4μm
Desert								
NVH1(D1)	1051	East	64.70±8.11	308.60±2.65			295.38±1.08	297.01±1.34
NEVC(D1)**	1056	West			309.56±2.49	297.41±1.24		298.75±1.35
NVH1(D2)	1051	East	73.96±11.75	307.45±2.77			295.02±0.86	298.72±1.20
NEVC(D2)**	1056	West			315.14±2.95	298.85±1.25		298.58±1.45
NEVL(D1)	1554	East			292.66±2.28	290.95±0.73		
NEVL(D2)	1554	East			292.60±2.20	290.84±0.62		
Lake								
NVH1(L)	1051	East	143.24±22.09	312.90±3.51			290.16±0.91	291.94±1.57
NEVL(L)	1554	East			287.11±2.89	285.83±0.98		

* (D1) = Desert #1; (D2) = Desert #2; (L) = Dry Lake

** From Reference 2.

TABLE 8

COMPARISONS* MADE ON 4.5 - 5.5 μm and 9.0 - 11.4 μm REGIONS

Run	Time	Direction	4.5 - 5.5	9.0 - 11.4	Correlation	τ**
NVG1	0926	West	283.73±4.66	285.06±6.35	0.914	0.95
NVH1(D1)			295.02±0.86	298.72±1.20	0.584	0.89
(D2)	1051	East	295.38±1.08	297.01±1.34	0.568	0.95
(L)			290.16±0.91	291.94±1.57	0.902	0.94
NEVN	1044	East	283.12±1.49	285.37±2.23	0.910	0.92

* NVG1, mountains at 1750 ft., depression angle = 90°

NVH1, desert at 1000 ft., depression angle = 35°

NEVN, mountains at 1000 ft., depression angle = 35°

** τ is the atmospheric transmittance that accounts for the difference in temperatures between the values at 4.5 - 5.5 μm and 9.0 - 11.4 μm.

The 4.5 - 5.5 and 9.0 - 11.4 μm bands are sufficiently noise-free (see Table 4) that, except for unaccountable factors, they should yield results which are identical except for the attenuating effect of the atmosphere (which is quite small in the 9.0 - 11.4 μm region). Thus if the temperature in this region is taken as the true terrain temperature (neglecting the effect of emissivity), we note that the reduction in the value for 4.5 - 5.5 μm admits of an attenuation of almost 10%. The derived transmittance values are shown in the last column of Table 8.

Assuming that the emissivities in the two regions are not grossly different and that there is not sufficient haze to cause much of a difference, we note that small attenuations indicate a relatively small amount of H_2O vapor in the atmosphere. According to the data of Taylor and Yates (Reference 4), the transmission in 1000 ft due to 1.1 mm of precipitable H_2O is approximately 65%, which in the maritime atmosphere of their experiment is probably considerably higher than in the experimental regions at Nellis AFB. A crude comparison with the Taylor and Yates data implies that the water content during the measurement was about 0.2 mm.

3.4 SPECTRAL CORRELATIONS

Tables 9 through 16 show the correlations obtained between the results from the different channels. These tables are produced in the same format as in Reference 2 for easy comparison with those data which were taken during the same general time period as the data in this report. The tables are shown, however, in terms of radiances instead of temperature; but, as noted previously, the differences are small.

We have noted above, for example, that in low-contrast scenery, the uncorrelated noise of the sensor could tend to dominate the apparent scene clutter. However, in the desert scenery, where, as opposed to mountain scenery, we might expect to see this effect, the variability in the results is high enough to make any judgements of this kind

TABLE 9

CORRELATION MATRIX

NEVI

Spectral Band (μm)	2.0-2.6	3.0-4.2	4.5-5.5	5.1-5.7
2.0-2.6	1.000			
3.0-4.2	0.740	1.000		
4.5-5.5	0.612	0.804	1.000	
5.1-5.7	0.287	0.408	0.438	1.000
Total No. of Pixels:	349,600			

TABLE 10

CORRELATION MATRIX

NEVJ

Spectral Band (μm)	3.9-4.7	3.5-3.9	2.0-2.6
3.9-4.7	1.000		
3.5-3.9	0.850	1.000	
2.0-2.6	0.839	0.779	1.000
Total No. of Pixels:	349,600		

TABLE 11

CORRELATION MATRIX

NEVK

Spectral Band (μm)	3.9-4.7	3.5-3.9	2.0-2.6
3.9-4.7	1.000		
3.5-3.9	0.751	1.000	
2.0-2.6	0.701	0.657	1.000
Total No. of Pixels:	349,600		

TABLE 12(a)

CORRELATION MATRIX
NEVL (Desert #1)

Spectral Band (μm)	3.9-4.7	3.5-3.9	5.1-5.7
3.9-4.7	1.000		
3.5-3.9	0.157	1.000	
5.1-5.7	N.A.	N.A.	1.000
Total No. of Pixels:	136,400		

TABLE 12(b)

CORRELATION MATRIX
NEVL (Desert #2)

Spectral Band (μm)	3.9-4.7	3.5-3.9	5.1-5.7
3.9-4.7	1.000		
3.5-3.9	0.323	1.000	
5.1-5.7	N.A.	N.A.	1.000
Total No. of Pixels:	141,200		

TABLE 12(c)

CORRELATION MATRIX
NEVL (Dry Lake)

Spectral Band (μm)	3.9-4.7	3.5-3.9	5.1-5.7
3.9-4.7	1.000		
3.5-3.9	0.391	1.000	
5.1-5.7	N.A.	N.A.	1.000
Total No. of Pixels:	72,400		

TABLE 13

CORRELATION MATRIX
NEVM

Spectral Band (μm)	3.9-4.7	3.5-3.9	2.0-2.6
3.9-4.7	1.000		
3.5-3.9	0.491	1.000	
2.0-2.6	0.529	0.286	1.000
Total No. of Pixels:	349,600		

TABLE 14

CORRELATION MATRIX
NEVN

Spectral Band (μm)	2.0-2.6	3.0-4.2	4.5-5.5	9.0-11.4
2.0-2.6	1.000			
3.0-4.2	0.255	1.000		
4.5-5.5	0.413	0.539	1.000	
9.0-11.4	0.398	0.565	0.910	1.000
Total No. of Pixels:	349,600			

TABLE 15

CORRELATION MATRIX
NVG1

Spectral Band (μm)	2.0-2.6	3.0-4.2	4.5-5.5	9.0-11.4
2.0-2.6	1.000			
3.0-4.2	0.837	1.000		
4.5-5.5	0.793	0.894	1.000	
9.0-11.4	0.810	0.899	0.983	1.000
Total No. of Pixels:	610,400			

TABLE 16(a)

CORRELATION MATRIX
NVH1 (Desert #1)

Spectral Band (μm)	2.0-2.6	3.0-4.2	4.5-5.5	9.0-11.4
2.0-2.6	1.000			
3.0-4.2	0.408	1.000		
4.5-5.5	0.015	0.188	1.000	
9.0-11.4	-0.001	0.102	0.584	1.000
Total No. of Pixels:	136,400			

TABLE 16(b)

CORRELATION MATRIX
NVH1 (Desert #2)

Spectral Band (μm)	2.0-2.6	3.0-4.2	4.5-5.5	9.0-11.4
2.0-2.6	1.000			
3.0-4.2	0.336	1.000		
4.5-5.5	0.343	0.308	1.000	
9.0-11.4	0.378	0.240	0.568	1.000
Total No. of Pixels:	141,200			

TABLE 16(c)

CORRELATION MATRIX
NVH1 (Dry Lake)

Spectral Band (μm)	2.0-2.6	3.0-4.2	4.5-5.5	9.0-11.4
2.0-2.6	1.000			
3.0-4.2	0.737	1.000		
4.5-5.5	-0.830	-0.487	1.000	
9.0-11.4	-0.935	-0.690	0.902	1.000
Total No. of Pixels:	72,400			

suspect. The most, in fact, that can be said is that the correlations in the mountain scenery tend to be larger than those in the desert scenery. In the case of the dry lake, on occasion, the correlations reverse to negative values between the reflective and thermal infrared channels.

One important reason, from the viewpoint of making measurements, for seeking spectral correlations is to establish a basis for reducing the number of measurement channels. Barring any special reasons for choosing a certain spectral band, one should choose the measurement bands in the atmospheric windows to avoid the influence of molecular absorption.

3.5 ELLIPSES

In Reference 2, a large number of "ellipse pictures" were presented to show the methodology for giving a simple pictorial of the statistics involved in the various scenes. In brief, as explained more thoroughly in References 2 and 3, the ellipses are designed to imitate, with simple geometrical figures, the areas and orientations of all scene elements, constructed of contiguous pixels, with apparent temperatures above a preselected threshold. In order to remove the effect of noise in the scene, and to avoid unnecessary clutter, only areas larger than those corresponding to two pixels were selected. They are actually recorded in Tables 17 through 26, but it has not been established in this analysis which are due to noise in the scanner and which are real scene events which could contribute to false alarms.

Figures 21 through 29 present a sample of the results to demonstrate the use of ellipse imagery. The figures are self-explanatory in that the areas covered and the physical parameters are given in Table 1, and the threshold levels (in numbers of standard deviations) are shown on the figures. The reader is referred to Reference 2 for some qualitative discussions on scenery which are similar to the scenery analyzed here.

TABLE 17

NEVN
AREA DISTRIBUTIONS

DISTRIBUTION OF RECOGNIZED HOT SPOT

$\left(\begin{array}{c} \text{Threshold} = \text{Ave.} + 2.50\ \sigma \\ 2.0 - 2.6\ \mu m \end{array} \right)$

BY AREA

SQUARE METERS			FREQUENCY
8.0	TO	10.0	69
10.0	TO	15.0	45
15.0	TO	20.0	36
20.0	TO	25.0	21
25.0	TO	30.0	2
30.0	TO	35.0	8
35.0	TO	40.0	2
40.0	TO	45.0	3
45.0	TO	50.0	3
50.0	TO	75.0	4
75.0	TO	100.0	1
100.0	TO	150.0	0
150.0	TO	200.0	0
200.0	TO	250.0	0
250.0	TO	300.0	1
300.0	TO	400.0	1
400.0	TO	500.0	0
	OVER	500.0	0

TOTAL NUMBER OF HOT SPOT = 196

1089 FEATURES WITH AREAS LESS THAN 8.00 SQ. METERS WERE ALSO RECOGNIZED

BY PERIMETER

METERS			FEET			FREQUENCY
0	TO	7	0	TO	22	0
7	TO	10	22	TO	32	0
10	TO	12	32	TO	39	0
12	TO	14	39	TO	45	4
14	TO	16	45	TO	52	19
16	TO	17	52	TO	55	13
17	TO	20	55	TO	65	42
20	TO	22	65	TO	72	29
22	TO	24	72	TO	78	10
24	TO	26	78	TO	85	4
26	TO	28	85	TO	91	16
28	TO	30	91	TO	98	7
30	TO	32	98	TO	104	9
32	TO	39	104	TO	127	11
39	TO	45	127	TO	147	9
45	TO	55	147	TO	180	8
55	TO	71	180	TO	232	8
71	TO	100	232	TO	328	4
OVER		100	OVER		328	3

BY SHAPE

SHAPE FACTOR			FREQUENCY
0.0	TO	1.0	0
1.0	TO	1.1	0
1.1	TO	1.2	6
1.2	TO	1.3	0
1.3	TO	1.4	23
1.4	TO	1.5	1
1.5	TO	1.6	29
1.6	TO	1.7	9
1.7	TO	1.8	44
1.8	TO	1.9	2
1.9	TO	2.0	16
2.0	TO	2.4	47
2.4	TO	2.6	6
2.6	TO	2.8	3
2.8	TO	3.0	5
3.0	TO	3.5	2
3.5	TO	4.0	1
4.0	TO	4.5	0
OVER		4.5	2

TABLE 18

NEVN
AREA DISTRIBUTIONS

(Threshold = Ave. + 1.50 σ
2.0 - 2.6 μm)

DISTRIBUTION OF RECOGNIZED HOT SPOT

BY AREA

SQUARE METERS	FREQUENCY
8.0 TO 10.0	286
10.0 TO 15.0	126
15.0 TO 20.0	141
20.0 TO 25.0	69
25.0 TO 30.0	26
30.0 TO 35.0	40
35.0 TO 40.0	7
40.0 TO 45.0	19
45.0 TO 50.0	18
50.0 TO 75.0	38
75.0 TO 100.0	18
100.0 TO 150.0	18
150.0 TO 200.0	13
200.0 TO 250.0	6
250.0 TO 300.0	2
300.0 TO 400.0	5
400.0 TO 500.0	2
OVER 500.0	12

TOTAL NUMBER OF HOT SPOT = 846

3248 FEATURES WITH AREAS LESS THAN 8.00 SQ. METERS WERE ALSO RECOGNIZED

BY PERIMETER

METERS	FEET	FREQUENCY
0 TO 7	0 TO 22	0
7 TO 10	22 TO 32	0
10 TO 12	32 TO 39	0
12 TO 14	39 TO 45	13
14 TO 16	45 TO 52	92
16 TO 17	52 TO 55	47
17 TO 20	55 TO 65	172
20 TO 22	65 TO 72	86
22 TO 24	72 TO 78	22
24 TO 26	78 TO 85	19
26 TO 28	85 TO 91	48
28 TO 30	91 TO 98	29
30 TO 32	98 TO 104	28
32 TO 39	104 TO 127	53
39 TO 45	127 TO 147	38
45 TO 55	147 TO 180	45
55 TO 71	180 TO 232	36
71 TO 100	232 TO 328	40
OVER 100	OVER 328	78

BY SHAPE

SHAPE FACTOR	FREQUENCY
0.0 TO 1.0	0
1.0 TO 1.1	0
1.1 TO 1.2	18
1.2 TO 1.3	4
1.3 TO 1.4	111
1.4 TO 1.5	5
1.5 TO 1.6	127
1.6 TO 1.7	20
1.7 TO 1.8	145
1.8 TO 1.9	19
1.9 TO 2.0	52
2.0 TO 2.4	145
2.4 TO 2.6	45
2.6 TO 2.8	31
2.8 TO 3.0	22
3.0 TO 3.5	34
3.5 TO 4.0	19
4.0 TO 4.5	18
OVER 4.5	31

TABLE 19

NEVN
AREA DISTRIBUTIONS

DISTRIBUTION OF RECOGNIZED HOT SPOT
BY AREA

(Threshold = Ave. + 1.50 σ
4.5 - 5.5 μm)

SQUARE METERS			FREQUENCY
8.0	TO	10.0	66
10.0	TO	15.0	50
15.0	TO	20.0	44
20.0	TO	25.0	25
25.0	TO	30.0	13
30.0	TO	35.0	13
35.0	TO	40.0	3
40.0	TO	45.0	5
45.0	TO	50.0	8
50.0	TO	75.0	17
75.0	TO	100.0	11
100.0	TO	150.0	18
150.0	TO	200.0	7
200.0	TO	250.0	8
250.0	TO	300.0	1
300.0	TO	400.0	2
400.0	TO	500.0	5
	OVER	500.0	22

TOTAL NUMBER OF HOT SPOT = 318

539 FEATURES WITH AREAS LESS THAN 8.00 SQ. METERS WERE ALSO RECOGNIZED

BY PERIMETER

METERS			FEET			FREQUENCY
0	TO	7	0	TO	22	0
7	TO	10	22	TO	32	0
10	TO	12	32	TO	39	0
12	TO	14	39	TO	45	3
14	TO	16	45	TO	52	28
16	TO	17	52	TO	55	19
17	TO	20	55	TO	65	46
20	TO	22	65	TO	72	21
22	TO	24	72	TO	78	12
24	TO	26	78	TO	85	3
26	TO	28	85	TO	91	22
28	TO	30	91	TO	98	11
30	TO	32	98	TO	104	9
32	TO	39	104	TO	127	24
39	TO	45	127	TO	147	13
45	TO	55	147	TO	180	13
55	TO	71	180	TO	232	21
71	TO	100	232	TO	328	19
OVER		100	OVER		328	54

BY SHAPE

SHAPE FACTOR			FREQUENCY
0.0	TO	1.0	0
1.0	TO	1.1	0
1.1	TO	1.2	7
1.2	TO	1.3	3
1.3	TO	1.4	32
1.4	TO	1.5	4
1.5	TO	1.6	55
1.6	TO	1.7	8
1.7	TO	1.8	40
1.8	TO	1.9	12
1.9	TO	2.0	21
2.0	TO	2.4	64
2.4	TO	2.6	10
2.6	TO	2.8	6
2.8	TO	3.0	4
3.0	TO	3.5	19
3.5	TO	4.0	9
4.0	TO	4.5	9
	OVER	4.5	15

TABLE 20

NEVN
AREA DISTRIBUTIONS

(Threshold = Ave. + 1.00 σ)
9.0 - 11.4 μm

DISTRIBUTION OF RECOGNIZED HOT SPOT

BY AREA

SQUARE METERS		FREQUENCY
8.0 TO	10.0	63
10.0 TO	15.0	41
15.0 TO	20.0	49
20.0 TO	25.0	23
25.0 TO	30.0	7
30.0 TO	35.0	11
35.0 TO	40.0	1
40.0 TO	45.0	5
45.0 TO	50.0	4
50.0 TO	75.0	21
75.0 TO	100.0	11
100.0 TO	150.0	11
150.0 TO	200.0	8
200.0 TO	250.0	0
250.0 TO	300.0	1
300.0 TO	400.0	6
400.0 TO	500.0	2
OVER	500.0	20

TOTAL NUMBER OF HOT SPOT = 284

349 FEATURES WITH AREAS LESS THAN 8.00 SQ. METERS WERE ALSO RECOGNIZED

BY PERIMETER

METERS	FEET	FREQUENCY
0 TO 7	0 TO 22	0
7 TO 10	22 TO 32	0
10 TO 12	32 TO 39	0
12 TO 14	39 TO 45	5
14 TO 16	45 TO 52	36
16 TO 17	52 TO 55	21
17 TO 20	55 TO 65	35
20 TO 22	65 TO 72	20
22 TO 24	72 TO 78	17
24 TO 26	78 TO 85	8
26 TO 28	85 TO 91	15
28 TO 30	91 TO 98	10
30 TO 32	98 TO 104	8
32 TO 39	104 TO 127	16
39 TO 45	127 TO 147	10
45 TO 55	147 TO 180	15
55 TO 71	180 TO 232	14
71 TO 100	232 TO 328	15
OVER 100	OVER 328	39

BY SHAPE

SHAPE FACTOR	FREQUENCY
0.0 TO 1.0	1
1.0 TO 1.1	0
1.1 TO 1.2	13
1.2 TO 1.3	2
1.3 TO 1.4	47
1.4 TO 1.5	8
1.5 TO 1.6	54
1.6 TO 1.7	14
1.7 TO 1.8	36
1.8 TO 1.9	12
1.9 TO 2.0	23
2.0 TO 2.4	23
2.4 TO 2.6	9
2.6 TO 2.8	8
2.8 TO 3.0	6
3.0 TO 3.5	7
3.5 TO 4.0	7
4.0 TO 4.5	6
OVER 4.5	8

TABLE 21

NVH1 (Desert #1)
AREA DISTRIBUTIONS

DISTRIBUTION OF RECOGNIZED HOT SPOT

(Threshold = Ave. + 2.00 σ
3.0 - 4.2 μm)

BY AREA

SQUARE METERS		FREQUENCY
8.0 TO	10.0	176
10.0 TO	15.0	88
15.0 TO	20.0	84
20.0 TO	25.0	31
25.0 TO	30.0	18
30.0 TO	35.0	10
35.0 TO	40.0	10
40.0 TO	45.0	9
45.0 TO	50.0	5
50.0 TO	75.0	14
75.0 TO	100.0	6
100.0 TO	150.0	6
150.0 TO	200.0	2
200.0 TO	250.0	0
250.0 TO	300.0	0
300.0 TO	400.0	0
400.0 TO	500.0	0
OVER	500.0	0

TOTAL NUMBER OF HOT SPOT = 459

1770 FEATURES WITH AREAS LESS THAN 8.00 SQ. METERS WERE ALSO RECOGNIZED

BY PERIMETER

METERS		FEET		FREQUENCY
0 TO	7	0 TO	22	1
7 TO	10	22 TO	32	0
10 TO	12	32 TO	39	0
12 TO	14	39 TO	45	68
14 TO	16	45 TO	52	98
16 TO	17	52 TO	55	16
17 TO	20	55 TO	65	91
20 TO	22	65 TO	72	32
22 TO	24	72 TO	78	11
24 TO	26	78 TO	85	25
26 TO	28	85 TO	91	12
28 TO	30	91 TO	98	19
30 TO	32	98 TO	104	6
32 TO	39	104 TO	127	21
39 TO	45	127 TO	147	13
45 TO	55	147 TO	180	15
55 TO	71	180 TO	232	14
71 TO	100	232 TO	328	11
OVER	100	OVER	328	6

BY SHAPE

SHAPE FACTOR	FREQUENCY
0.0 TO 1.0	1
1.0 TO 1.1	0
1.1 TO 1.2	76
1.2 TO 1.3	58
1.3 TO 1.4	97
1.4 TO 1.5	19
1.5 TO 1.6	58
1.6 TO 1.7	22
1.7 TO 1.8	33
1.8 TO 1.9	6
1.9 TO 2.0	22
2.0 TO 2.4	39
2.4 TO 2.6	12
2.6 TO 2.8	8
2.8 TO 3.0	1
3.0 TO 3.5	5
3.5 TO 4.0	1
4.0 TO 4.5	1
OVER 4.5	0

TABLE 22

NVH1 (Desert #1)
AREA DISTRIBUTIONS

DISTRIBUTION OF RECOGNIZED HOT SPOT

BY AREA

(Threshold = Ave. + 1.50 σ
4.5 - 5.5 μm)

SQUARE METERS			FREQUENCY
8.0	TO	10.0	155
10.0	TO	15.0	119
15.0	TO	20.0	146
20.0	TO	25.0	61
25.0	TO	30.0	28
30.0	TO	35.0	30
35.0	TO	40.0	10
40.0	TO	45.0	19
45.0	TO	50.0	15
50.0	TO	75.0	35
75.0	TO	100.0	19
100.0	TO	150.0	21
150.0	TO	200.0	4
200.0	TO	250.0	1
250.0	TO	300.0	6
300.0	TO	400.0	0
400.0	TO	500.0	3
	OVER	500.0	0

TOTAL NUMBER OF HOT SPOT = 672

1102 FEATURES WITH AREAS LESS THAN 8.00 SQ. METERS WERE ALSO RECOGNIZED

BY PERIMETER

METERS	FEET	FREQUENCY
0 TO 7	0 TO 22	0
7 TO 10	22 TO 32	0
10 TO 12	32 TO 39	0
12 TO 14	39 TO 45	8
14 TO 16	45 TO 52	89
16 TO 17	52 TO 55	43
17 TO 20	55 TO 65	110
20 TO 22	65 TO 72	48
22 TO 24	72 TO 78	38
24 TO 26	78 TO 85	14
26 TO 28	85 TO 91	47
28 TO 30	91 TO 98	26
30 TO 32	98 TO 104	39
32 TO 39	104 TO 127	50
39 TO 45	127 TO 147	26
45 TO 55	147 TO 180	36
55 TO 71	180 TO 232	28
71 TO 100	232 TO 328	33
OVER 100	OVER 328	37

BY SHAPE

SHAPE FACTOR	FREQUENCY
0.0 TO 1.0	1
1.0 TO 1.1	0
1.1 TO 1.2	24
1.2 TO 1.3	9
1.3 TO 1.4	107
1.4 TO 1.5	21
1.5 TO 1.6	121
1.6 TO 1.7	34
1.7 TO 1.8	78
1.8 TO 1.9	18
1.9 TO 2.0	46
2.0 TO 2.4	122
2.4 TO 2.6	25
2.6 TO 2.8	18
2.8 TO 3.0	5
3.0 TO 3.5	24
3.5 TO 4.0	7
4.0 TO 4.5	9
OVER 4.5	3

TABLE 23

NVH1 (Desert #1)
AREA DISTRIBUTIONS

(Threshold = Ave. + 2.00 σ
9.0 - 11.4 μm)

DISTRIBUTION OF RECOGNIZED HOT SPOT
BY AREA

SQUARE METERS		FREQUENCY
8.0 TO	10.0	126
10.0 TO	15.0	62
15.0 TO	20.0	76
20.0 TO	25.0	36
25.0 TO	30.0	12
30.0 TO	35.0	17
35.0 TO	40.0	2
40.0 TO	45.0	4
45.0 TO	50.0	1
50.0 TO	75.0	9
75.0 TO	100.0	2
100.0 TO	150.0	1
150.0 TO	200.0	3
200.0 TO	250.0	1
250.0 TO	300.0	0
300.0 TO	400.0	0
400.0 TO	500.0	0
OVER	500.0	1

TOTAL NUMBER OF HOT SPOT = 353

860 FEATURES WITH AREAS LESS THAN 8.00 SQ. METERS WERE ALSO RECOGNIZED

BY PERIMETER

METERS	FEET	FREQUENCY
0 TO 7	0 TO 22	0
7 TO 10	22 TO 32	2
10 TO 12	32 TO 39	0
12 TO 14	39 TO 45	1
14 TO 16	45 TO 52	69
16 TO 17	52 TO 55	31
17 TO 20	55 TO 65	72
20 TO 22	65 TO 72	28
22 TO 24	72 TO 78	21
24 TO 26	78 TO 85	5
26 TO 28	85 TO 91	24
28 TO 30	91 TO 98	18
30 TO 32	98 TO 104	14
32 TO 39	104 TO 127	31
39 TO 45	127 TO 147	9
45 TO 55	147 TO 180	9
55 TO 71	180 TO 232	9
71 TO 100	232 TO 328	4
OVER 100	OVER 328	6

BY SHAPE

SHAPE FACTOR	FREQUENCY
0.0 TO 1.0	2
1.0 TO 1.1	0
1.1 TO 1.2	9
1.2 TO 1.3	6
1.3 TO 1.4	74
1.4 TO 1.5	6
1.5 TO 1.6	79
1.6 TO 1.7	12
1.7 TO 1.8	60
1.8 TO 1.9	15
1.9 TO 2.0	24
2.0 TO 2.4	43
2.4 TO 2.6	10
2.6 TO 2.8	6
2.8 TO 3.0	1
3.0 TO 3.5	2
3.5 TO 4.0	2
4.0 TO 4.5	1
OVER 4.5	1

TABLE 24

NVH1 (Dry Lake)
AREA DISTRIBUTIONS

(Threshold = Ave. + 1.00 σ
3.0 - 4.2 μm)

DISTRIBUTION OF RECOGNIZED HOT SPOT

BY AREA

SQUARE METERS			FREQUENCY
8.0	TO	10.0	161
10.0	TO	15.0	74
15.0	TO	20.0	86
20.0	TO	25.0	45
25.0	TO	30.0	12
30.0	TO	35.0	17
35.0	TO	40.0	7
40.0	TO	45.0	12
45.0	TO	50.0	9
50.0	TO	75.0	16
75.0	TO	100.0	5
100.0	TO	150.0	6
150.0	TO	200.0	5
200.0	TO	250.0	2
250.0	TO	300.0	0
300.0	TO	400.0	0
400.0	TO	500.0	0
	OVER	500.0	3

TOTAL NUMBER OF HOT SPOT = 460

1536 FEATURES WITH AREAS LESS THAN 8.00 SQ. METERS WERE ALSO RECOGNIZED

BY PERIMETER

METERS	FEET	FREQUENCY
0 TO 7	0 TO 22	0
7 TO 10	22 TO 32	0
10 TO 12	32 TO 39	0
12 TO 14	39 TO 45	46
14 TO 16	45 TO 52	72
16 TO 17	52 TO 55	15
17 TO 20	55 TO 65	84
20 TO 22	65 TO 72	42
22 TO 24	72 TO 78	16
24 TO 26	78 TO 85	11
26 TO 28	85 TO 91	23
28 TO 30	91 TO 98	17
30 TO 32	98 TO 104	8
32 TO 39	104 TO 127	33
39 TO 45	127 TO 147	19
45 TO 55	147 TO 180	24
55 TO 71	180 TO 232	15
71 TO 100	232 TO 328	14
OVER 100	OVER 328	21

BY SHAPE

SHAPE FACTOR	FREQUENCY
0.0 TO 1.0	0
1.0 TO 1.1	0
1.1 TO 1.2	51
1.2 TO 1.3	36
1.3 TO 1.4	71
1.4 TO 1.5	16
1.5 TO 1.6	53
1.6 TO 1.7	11
1.7 TO 1.8	52
1.8 TO 1.9	10
1.9 TO 2.0	19
2.0 TO 2.4	69
2.4 TO 2.6	24
2.6 TO 2.8	14
2.8 TO 3.0	6
3.0 TO 3.5	13
3.5 TO 4.0	6
4.0 TO 4.5	5
OVER 4.5	4

TABLE 25

NVH1 (Dry Lake)
AREA DISTRIBUTIONS

DISTRIBUTION OF RECOGNIZED HOT SPOT

BY AREA

(Threshold = Ave. + 1.50 σ
4.5 - 5.5 μm)

SQUARE METERS			FREQUENCY
8.0	TO	10.0	3
10.0	TO	15.0	1
15.0	TO	20.0	1
20.0	TO	25.0	0
25.0	TO	30.0	0
30.0	TO	35.0	0
35.0	TO	40.0	0
40.0	TO	45.0	0
45.0	TO	50.0	0
50.0	TO	75.0	0
75.0	TO	100.0	0
100.0	TO	150.0	0
150.0	TO	200.0	0
200.0	TO	250.0	0
250.0	TO	300.0	0
300.0	TO	400.0	0
400.0	TO	500.0	0
	OVER	500.0	2

TOTAL NUMBER OF HOT SPOT = 7

54 FEATURES WITH AREAS LESS THAN 8.00 SQ. METERS WERE ALSO RECOGNIZED

BY PERIMETER

METERS	FEET	FREQUENCY
0 TO 7	0 TO 22	1
7 TO 10	22 TO 32	1
10 TO 12	32 TO 39	1
12 TO 14	39 TO 45	0
14 TO 16	45 TO 52	1
16 TO 17	52 TO 55	0
17 TO 20	55 TO 65	1
20 TO 22	65 TO 72	0
22 TO 24	72 TO 78	0
24 TO 26	78 TO 85	0
26 TO 28	85 TO 91	0
28 TO 30	91 TO 98	0
30 TO 32	98 TO 104	0
32 TO 39	104 TO 127	0
39 TO 45	127 TO 147	0
45 TO 55	147 TO 180	0
55 TO 71	180 TO 232	0
71 TO 100	232 TO 328	0
OVER 100	OVER 328	2

BY SHAPE

SHAPE FACTOR	FREQUENCY
0.0 TO 1.0	3
1.0 TO 1.1	0
1.1 TO 1.2	0
1.2 TO 1.3	0
1.3 TO 1.4	1
1.4 TO 1.5	0
1.5 TO 1.6	1
1.6 TO 1.7	0
1.7 TO 1.8	0
1.8 TO 1.9	0
1.9 TO 2.0	0
2.0 TO 2.4	0
2.4 TO 2.6	0
2.6 TO 2.8	0
2.8 TO 3.0	0
3.0 TO 3.5	0
3.5 TO 4.0	1
4.0 TO 4.5	0
OVER 4.5	1

TABLE 26

NVH1 (Dry Lake)
AREA DISTRIBUTIONS

DISTRIBUTION OF RECOGNIZED HOT SPOT

BY AREA

(Threshold = Ave. + 1.50 σ
9.0 - 11.4 um)

SQUARE METERS			FREQUENCY
8.0	TO	10.0	6
10.0	TO	15.0	3
15.0	TO	20.0	3
20.0	TO	25.0	0
25.0	TO	30.0	0
30.0	TO	35.0	0
35.0	TO	40.0	0
40.0	TO	45.0	0
45.0	TO	50.0	1
50.0	TO	75.0	0
75.0	TO	100.0	0
100.0	TO	150.0	0
150.0	TO	200.0	0
200.0	TO	250.0	0
250.0	TO	300.0	1
300.0	TO	400.0	0
400.0	TO	500.0	0
	OVER	500.0	4

TOTAL NUMBER OF HOT SPOT = 18

6 FEATURES WITH AREAS LESS THAN 8.00 SQ. METERS WERE ALSO RECOGNIZED

BY PERIMETER

METERS			FEET			FREQUENCY
0	TO	7	0	TO	22	1
7	TO	10	22	TO	32	4
10	TO	12	32	TO	39	1
12	TO	14	39	TO	45	3
14	TO	16	45	TO	52	0
16	TO	17	52	TO	55	0
17	TO	20	55	TO	65	4
20	TO	22	65	TO	72	0
22	TO	24	72	TO	78	0
24	TO	26	78	TO	85	0
26	TO	28	85	TO	91	0
28	TO	30	91	TO	98	0
30	TO	32	98	TO	104	0
32	TO	39	104	TO	127	0
39	TO	45	127	TO	147	0
45	TO	55	147	TO	180	0
55	TO	71	180	TO	232	1
71	TO	100	232	TO	328	0
OVER		100	OVER		328	4

BY SHAPE

SHAPE FACTOR			FREQUENCY
0.0	TO	1.0	7
1.0	TO	1.1	0
1.1	TO	1.2	4
1.2	TO	1.3	2
1.3	TO	1.4	1
1.4	TO	1.5	0
1.5	TO	1.6	0
1.6	TO	1.7	0
1.7	TO	1.8	0
1.8	TO	1.9	0
1.9	TO	2.0	0
2.0	TO	2.4	2
2.4	TO	2.6	0
2.6	TO	2.8	1
2.8	TO	3.0	0
3.0	TO	3.5	0
3.5	TO	4.0	0
4.0	TO	4.5	0
OVER		4.5	1

Area: NEVN

Radiance Threshold
= Ave. + 1.50 σ

Wavelength = 2.0 - 2.6 μm

FIGURE 21a. EQUIVALENT ELLIPTICAL AREAS FOR NELLIS MOUNTAINS

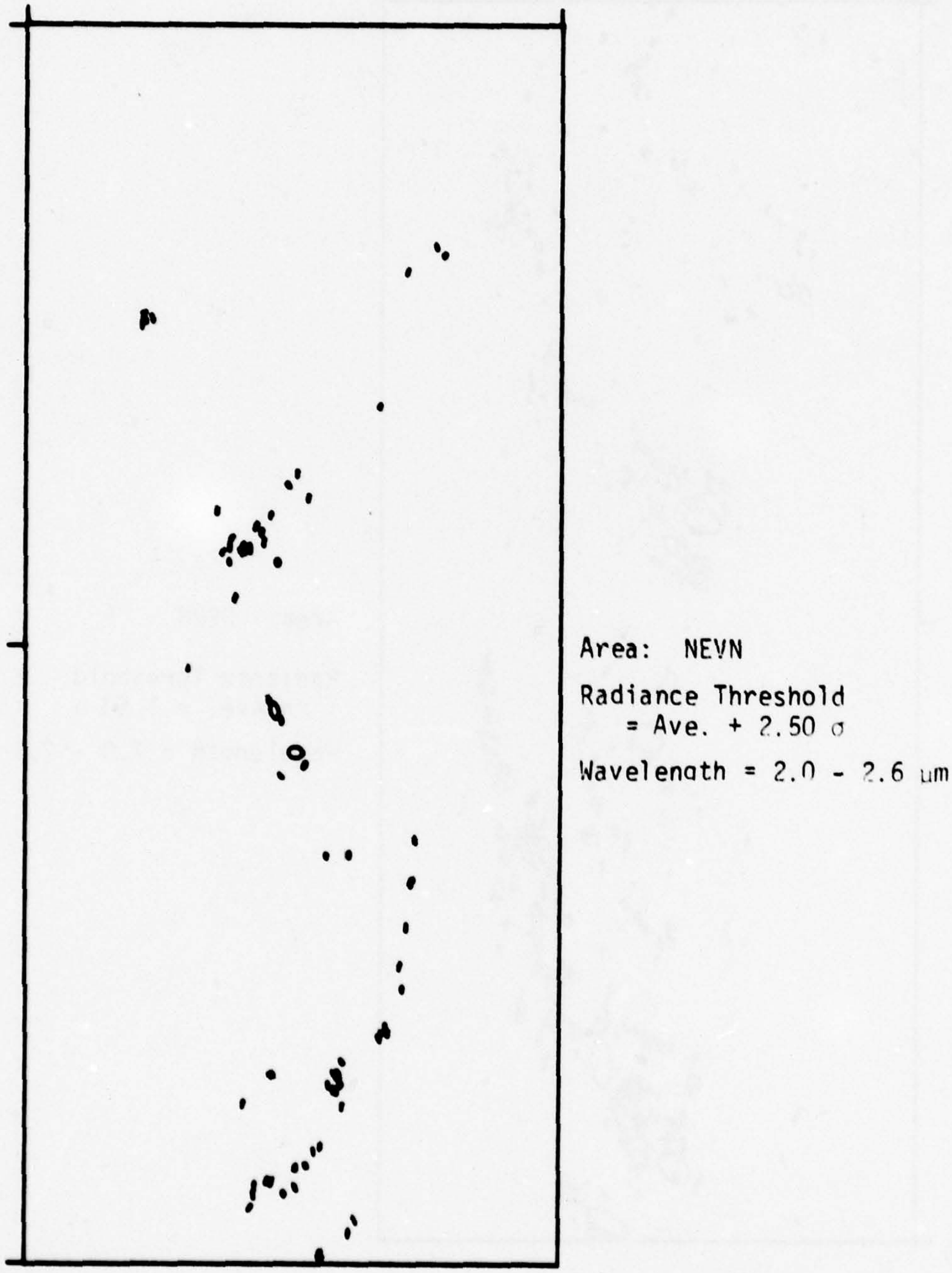

FIGURE 21b. EQUIVALENT ELLIPTICAL AREAS FOR NELLIS MOUNTAINS

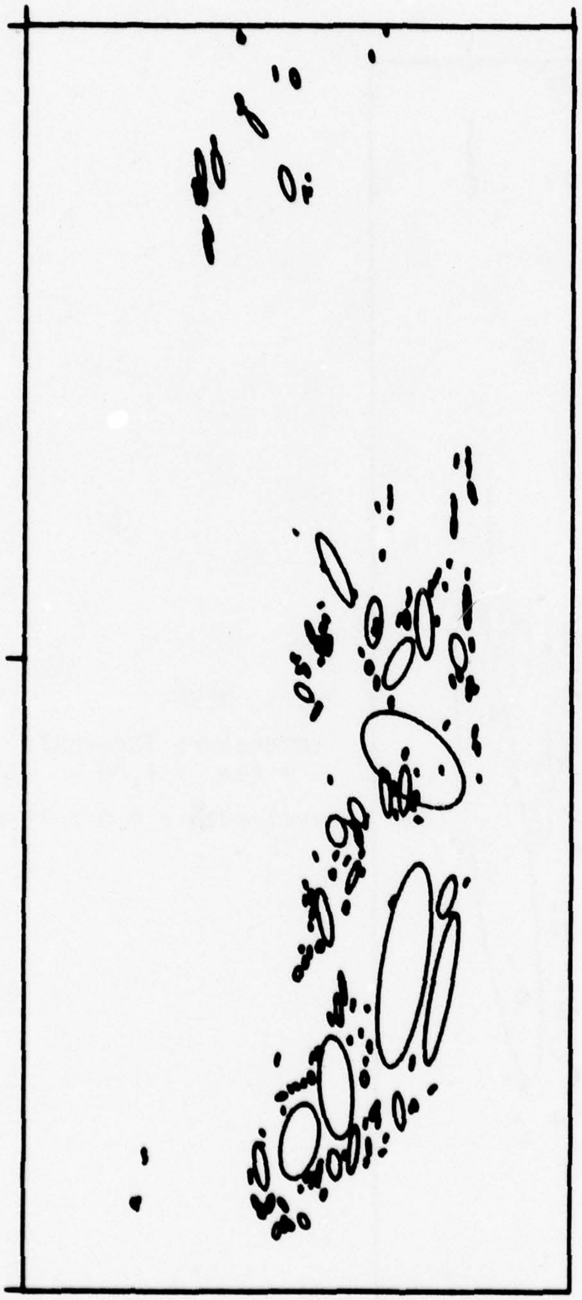

Area: NEVN

Temperature Threshold
= Ave. + 1.50 σ

Wavelength = 4.5 - 5.5 μm

FIGURE 22. EQUIVALENT ELLIPTICAL AREAS FOR NELLIS MOUNTAINS

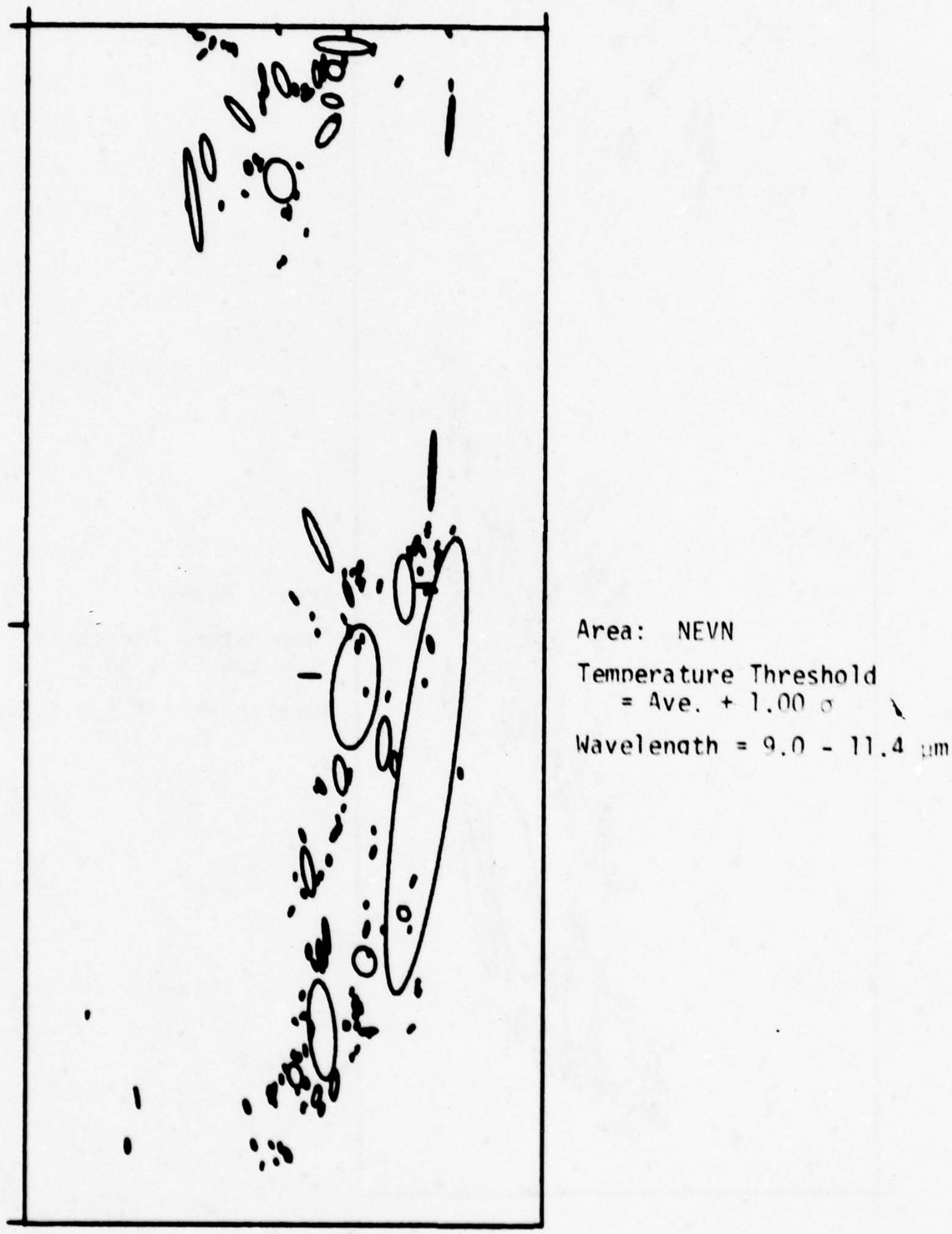

FIGURE 23a. EQUIVALENT ELLIPTICAL AREAS FOR NELLIS MOUNTAINS

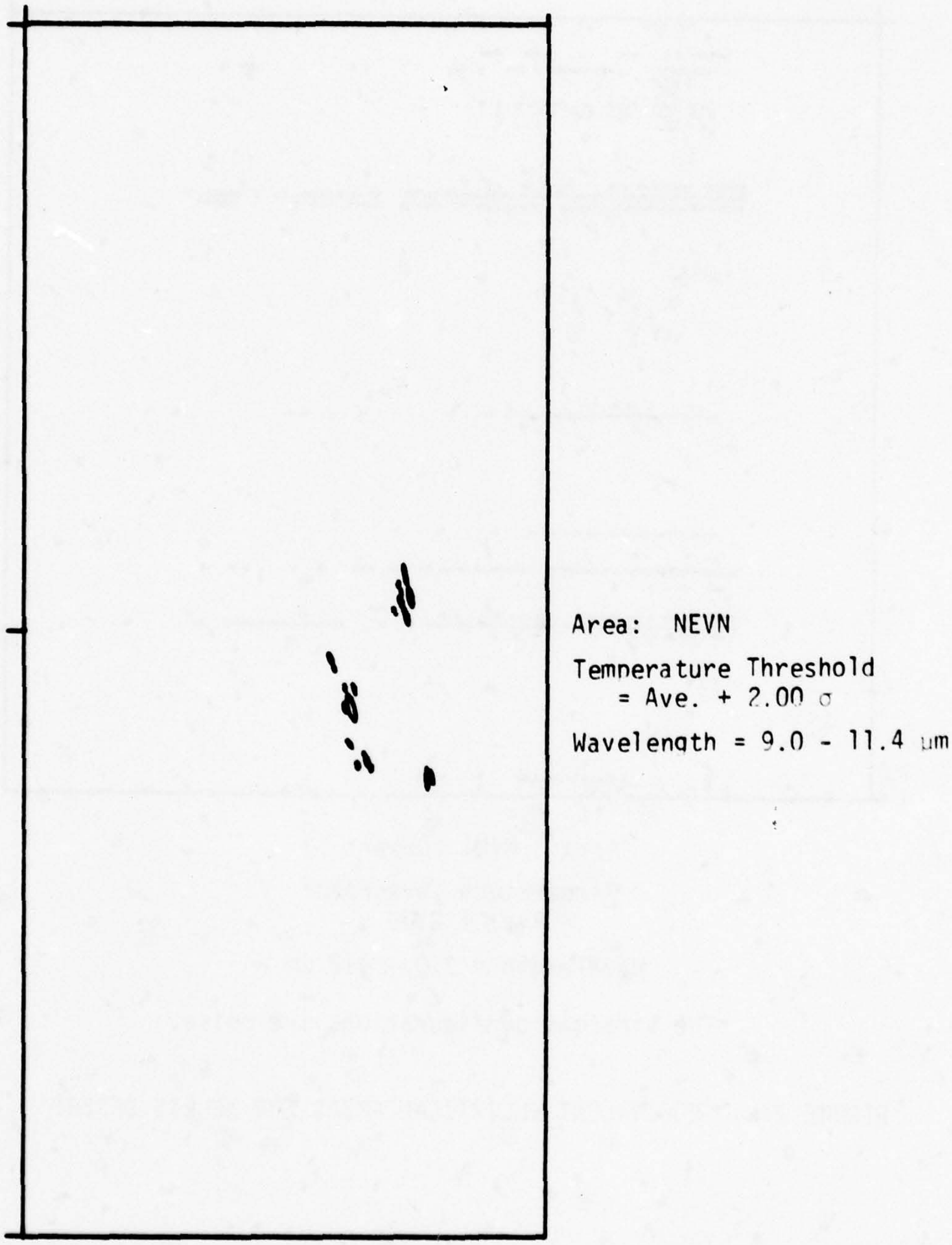

FIGURE 23b. EQUIVALENT ELLIPTICAL AREAS FOR NELLIS MOUNTAINS

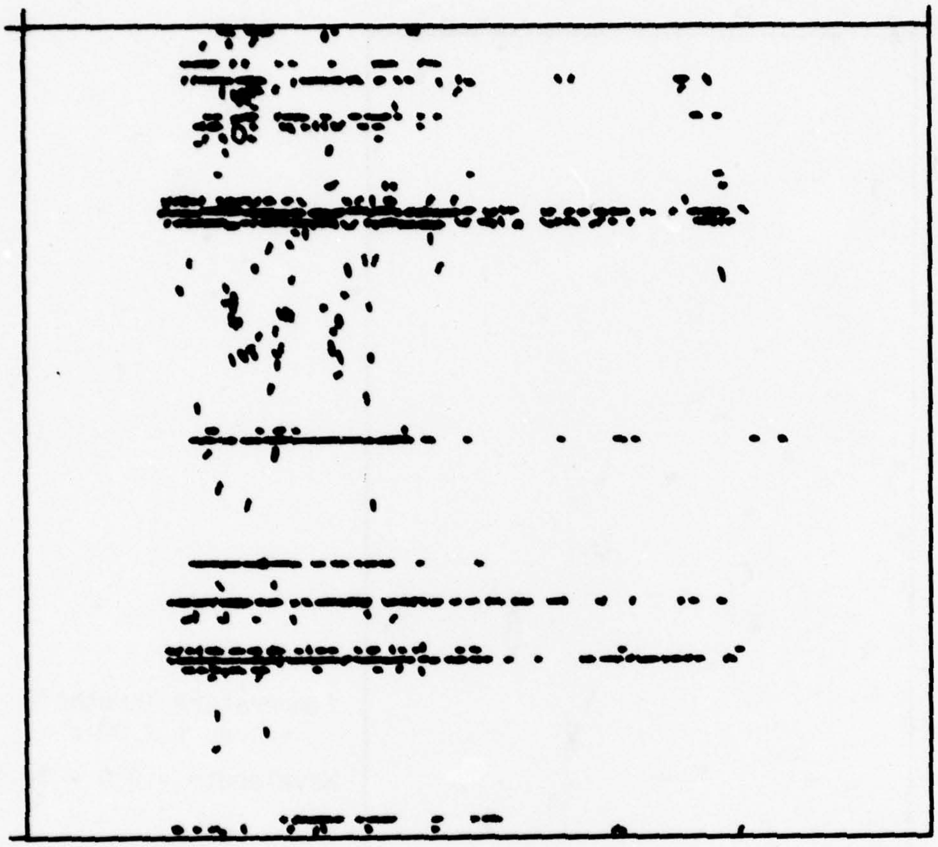

Area: NVH1 (Desert 1)

Temperature Threshold*
= Ave. + 2.00 σ

Wavelength = 3.0 - 4.2 μm

*The straight configurations are noise.

FIGURE 24a. EQUIVALENT ELLIPTICAL AREAS FOR NELLIS DESERT

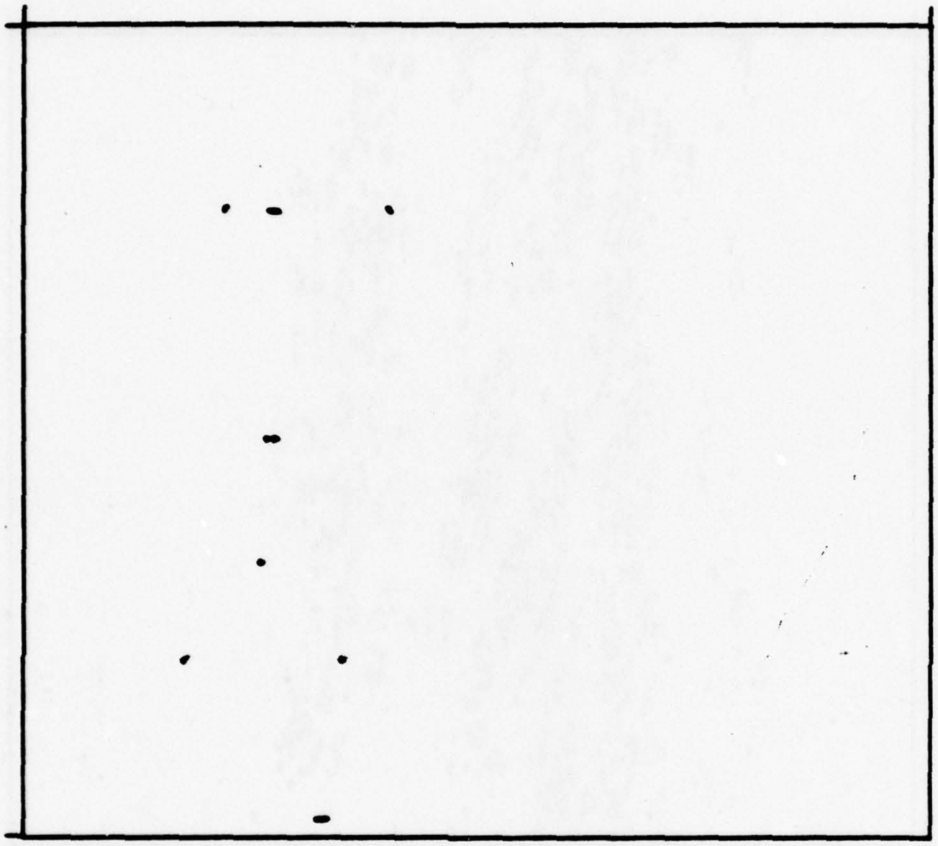

Area: NVH1 (Desert 1)

Temperature Threshold
= Ave. + 3.00 σ

Wavelength = 3.0 - 4.2 μm

FIGURE 24b. EQUIVALENT ELLIPTICAL AREAS FOR NELLIS DESERT

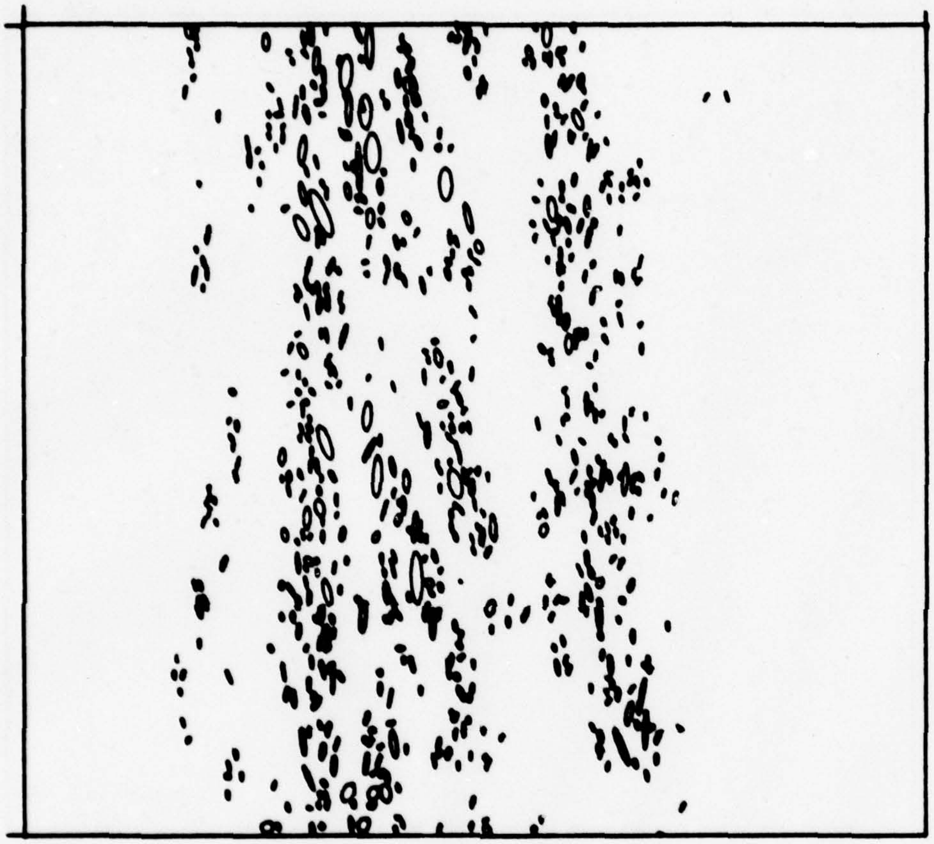

Area: NVH1 (Desert 1)

Temperature Threshold
= Ave. + 1.50 σ

Wavelength = 4.5 - 5.5 μm

FIGURE 25a. EQUIVALENT ELLIPTICAL AREAS FOR NELLIS DESERT

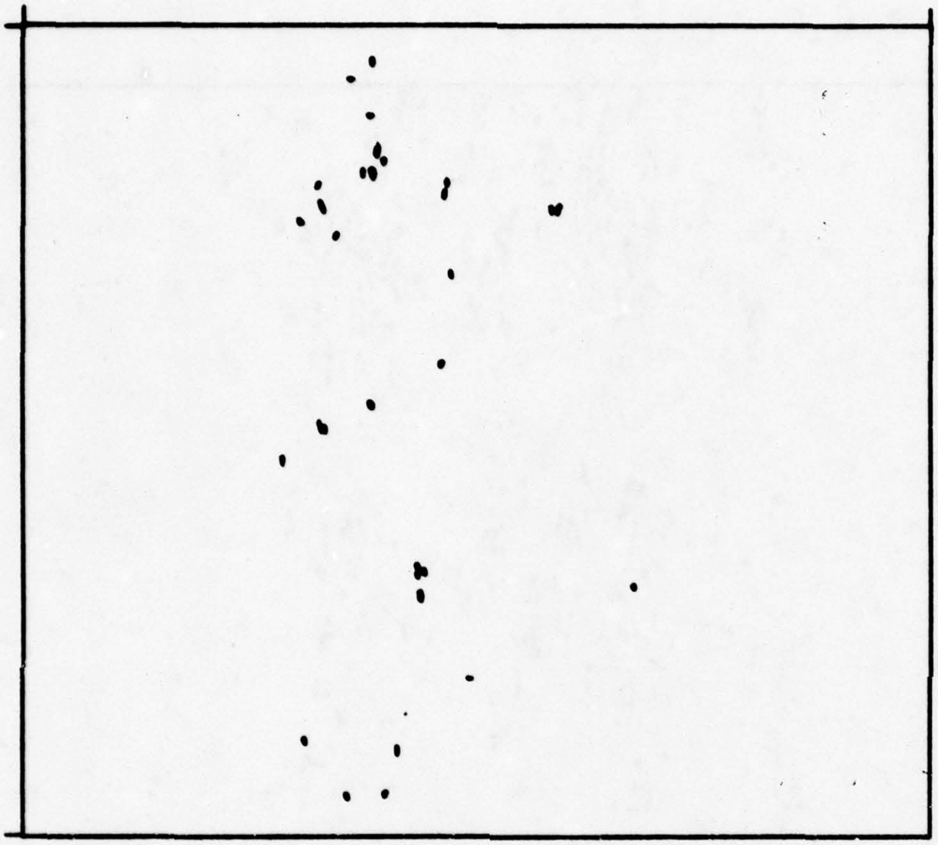

Area: NVH1 (Desert 1)

Temperature Threshold
= Ave. + 2.00 σ

Wavelength = 4.5 - 5.5 μm

FIGURE 25b. EQUIVALENT ELLIPTICAL AREAS FOR NELLIS DESERT

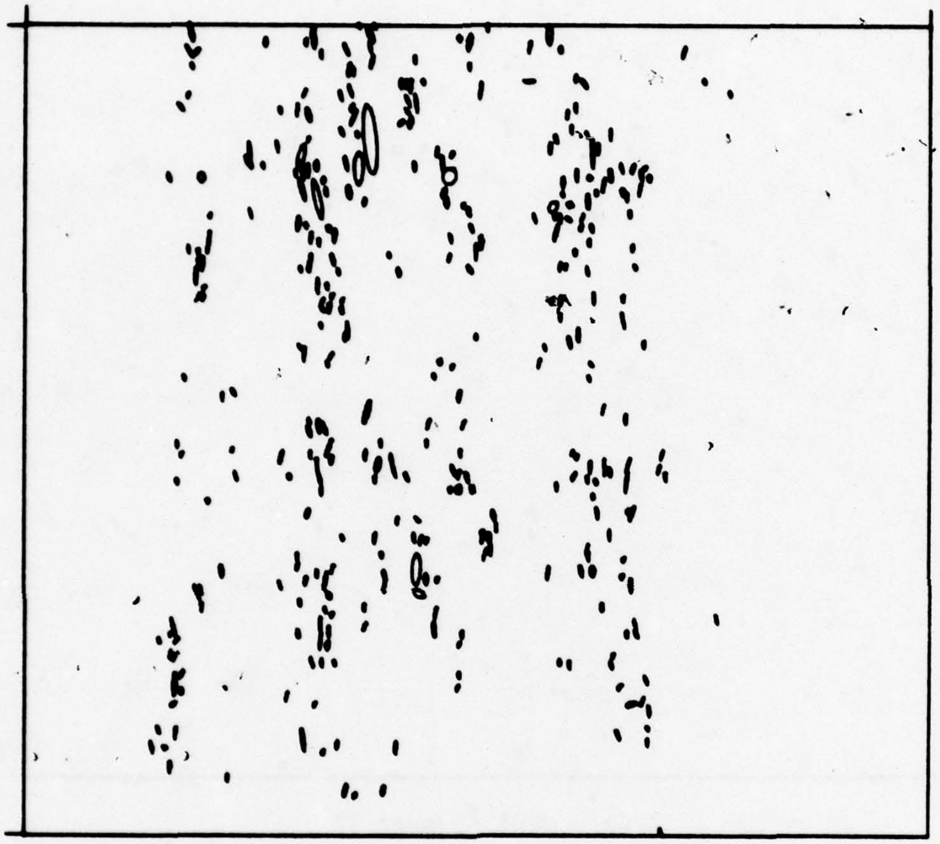

Area: NVH1 (Desert 1)

Temperature Threshold
= Ave. + 2.00 σ

Wavelength = 9.0 - 11.4 μm

FIGURE 26a. EQUIVALENT ELLIPTICAL AREAS FOR NELLIS DESERT

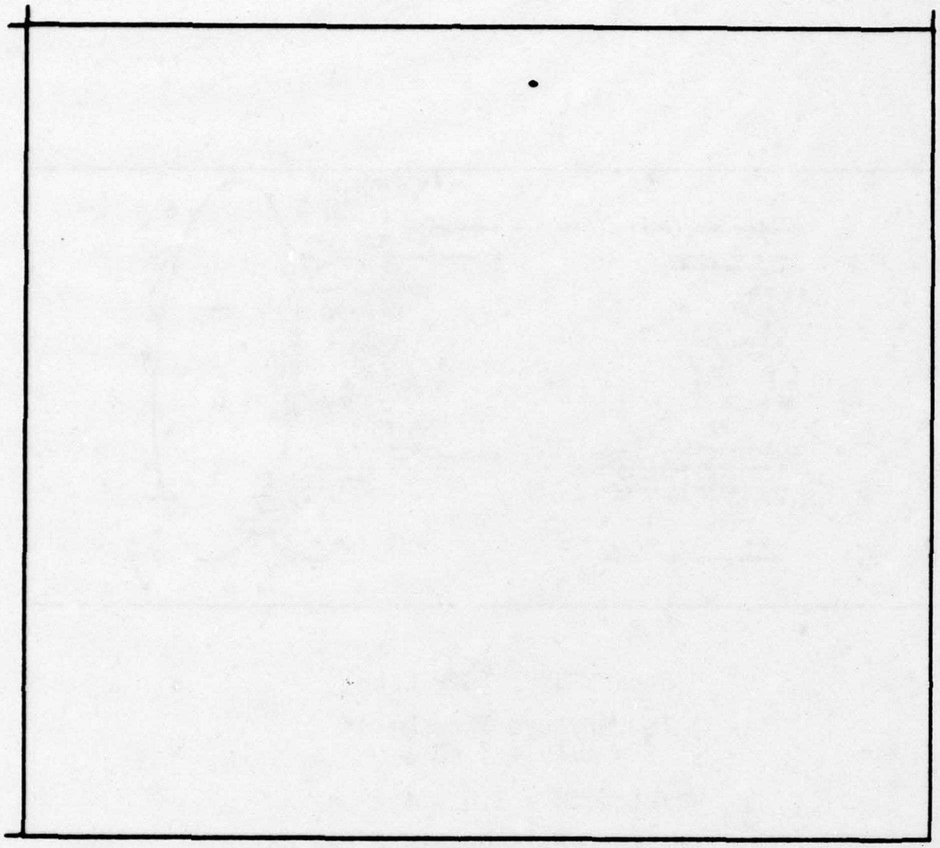

Area: NVH1 (Desert 1)

Temperature Threshold
= Ave. + 3.00 σ

Wavelength = 9.0 - 11.4 μm

FIGURE 26b. EQUIVALENT ELLIPTICAL AREAS FOR NELLIS DESERT

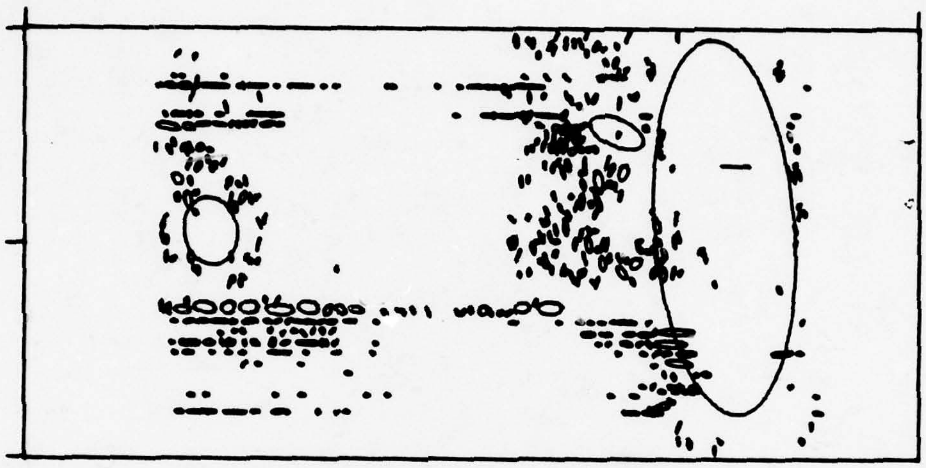

Area: NVH1 (Dry Lake)

Temperature Threshold*
= Ave. + 1.00 σ

Wavelength = 3.0 - 4.2 μm

*The straight configurations are noise.

FIGURE 27a. EQUIVALENT ELLIPTICAL AREAS FOR NELLIS DESERT

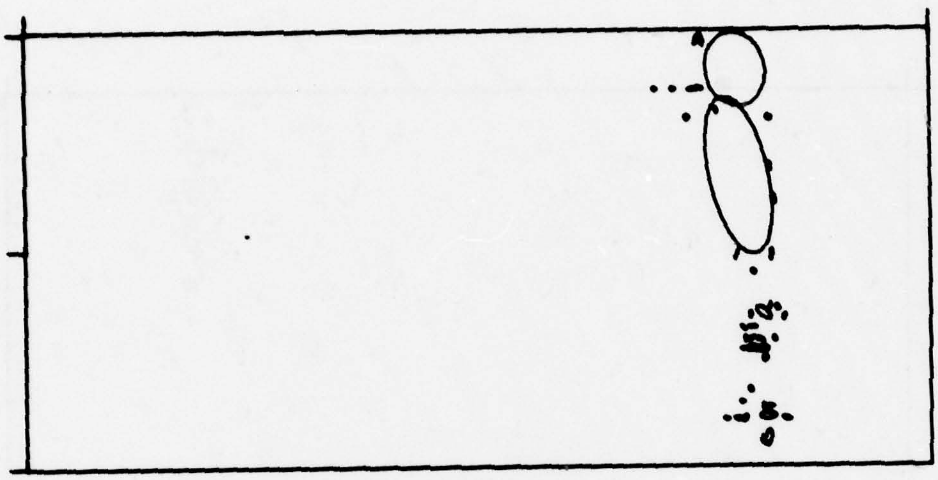

Area: NVH1 (Dry Lake)

Temperature Threshold
= Ave. + 2.00 σ

Wavelength = 3.0 - 4.2 μm

FIGURE 27b. EQUIVALENT ELLIPTICAL AREAS FOR NELLIS DESERT

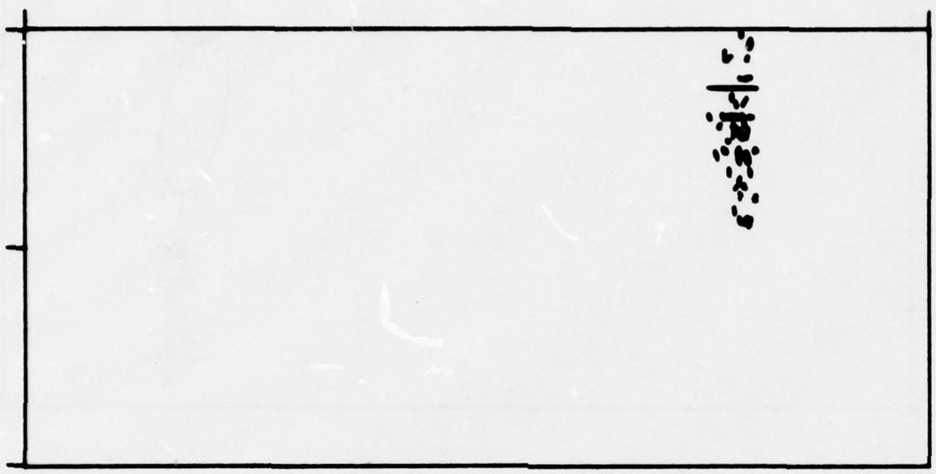

Area: NVH1 (Dry Lake)

Temperature Threshold
= Ave. + 3.00 σ

Wavelength = 3.0 - 4.2 μm

FIGURE 27c. EQUIVALENT ELLIPTICAL AREAS FOR NELLIS DESERT

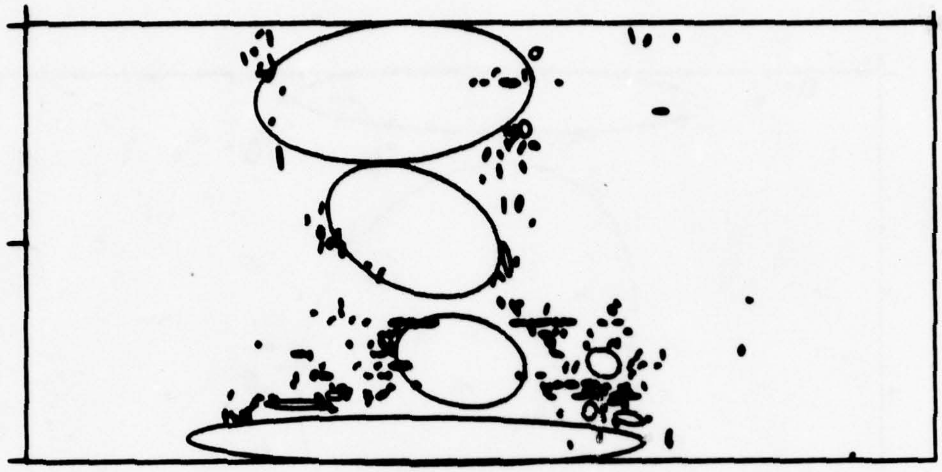

Area: NVH1 (Dry Lake)

Temperature Threshold
= Ave. + 0.50 σ

Wavelength = 4.5 - 5.5 μm

FIGURE 28. EQUIVALENT ELLIPTICAL AREAS FOR NELLIS DESERT

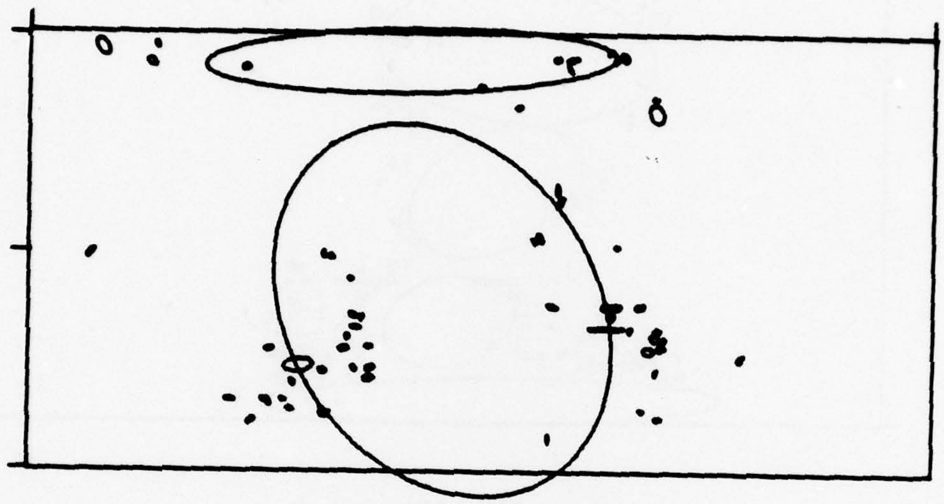

Area: NVH1 (Dry Lake)

Temperature Threshold
= Ave. + 0.50 σ

Wavelength = 9.0 - 11.4 μm

FIGURE 29. EQUIVALENT ELLIPTICAL AREAS FOR NELLIS DESERT

Tables 17 through 26 amplify on some of the qualitative statistics discernable from the pictures by including quantitative data enumerating such factors as the frequency at which various sized areas occur, the frequency of occurrence of perimeters of the actual areas represented by the ellipses, and the shape factor frequency, where the shape factor is defined by:

$$\text{Shape Factor} = \frac{\text{perimeter}/2\pi}{\sqrt{\text{area}/\pi}}$$

No attempt was made to cause the figures and tables to overlap completely. In order to give a pictorial presentation of these data, we show a few of those showing frequency as a function of area in Figures 30 through 35. The ordinate in these figures represents the frequency of occurrence per square kilometer of the area given on the abscissa in a 5 square meter increment.

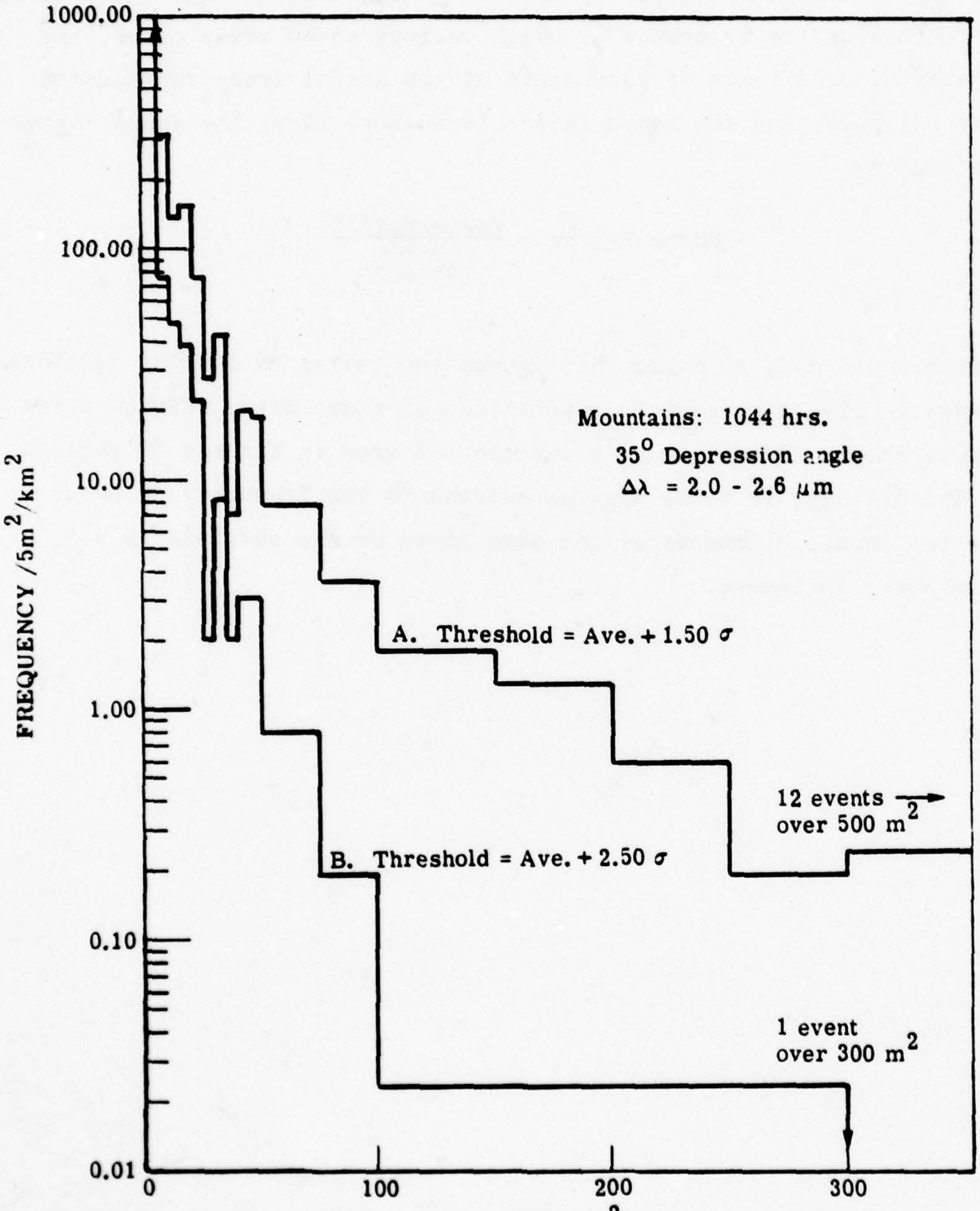

FIGURE 30. FREQUENCY OF FEATURE (AREA) SIZES PER SQUARE KILOMETER IN 5-m^2 INCREMENTS

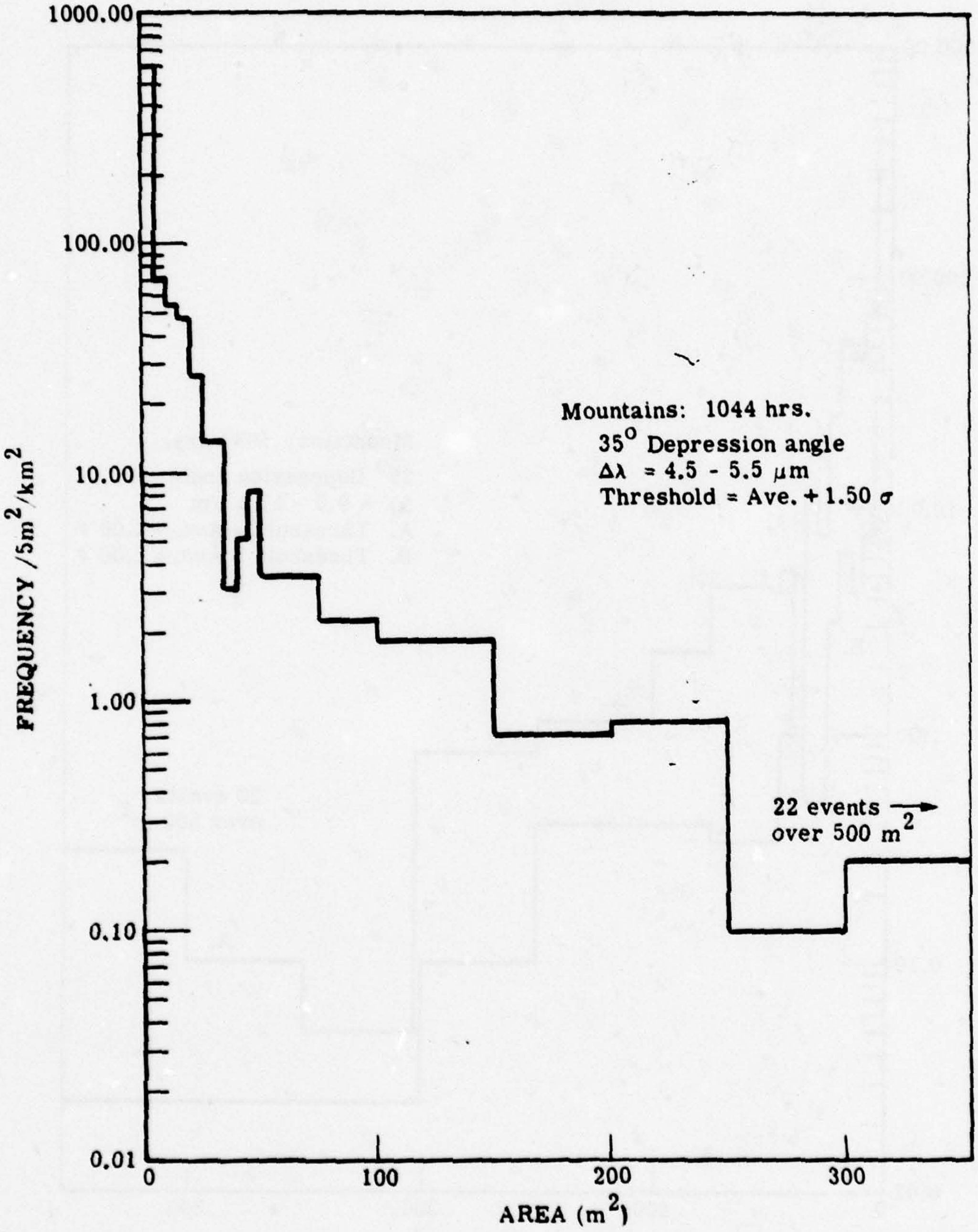

FIGURE 31. FREQUENCY OF FEATURE (AREA) SIZES PER SQUARE KILOMETER IN 5-m^2 INCREMENTS

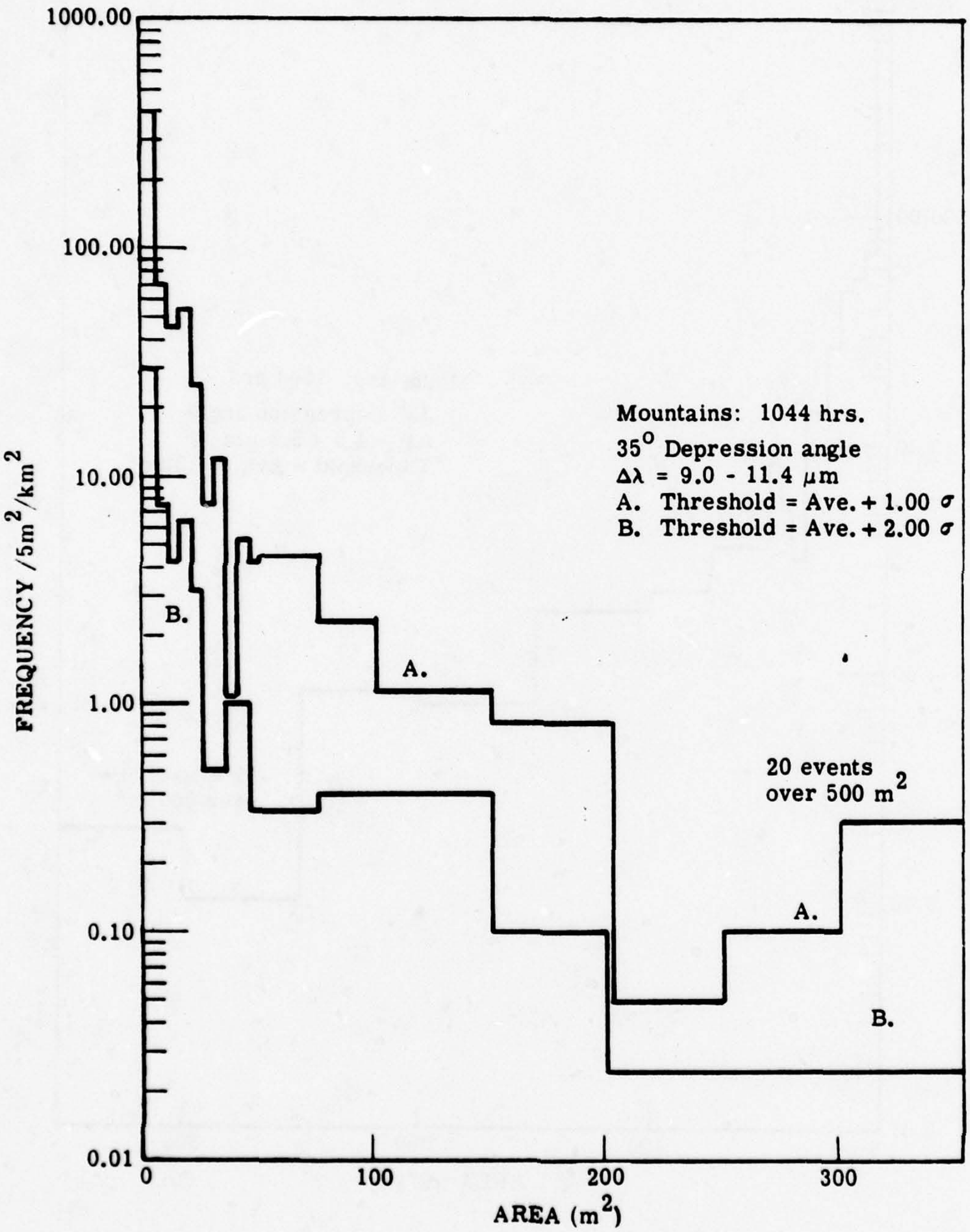

FIGURE 32. FREQUENCY OF FEATURE (AREA) SIZES PER SQUARE KILOMETER IN 5-m^2 INCREMENTS

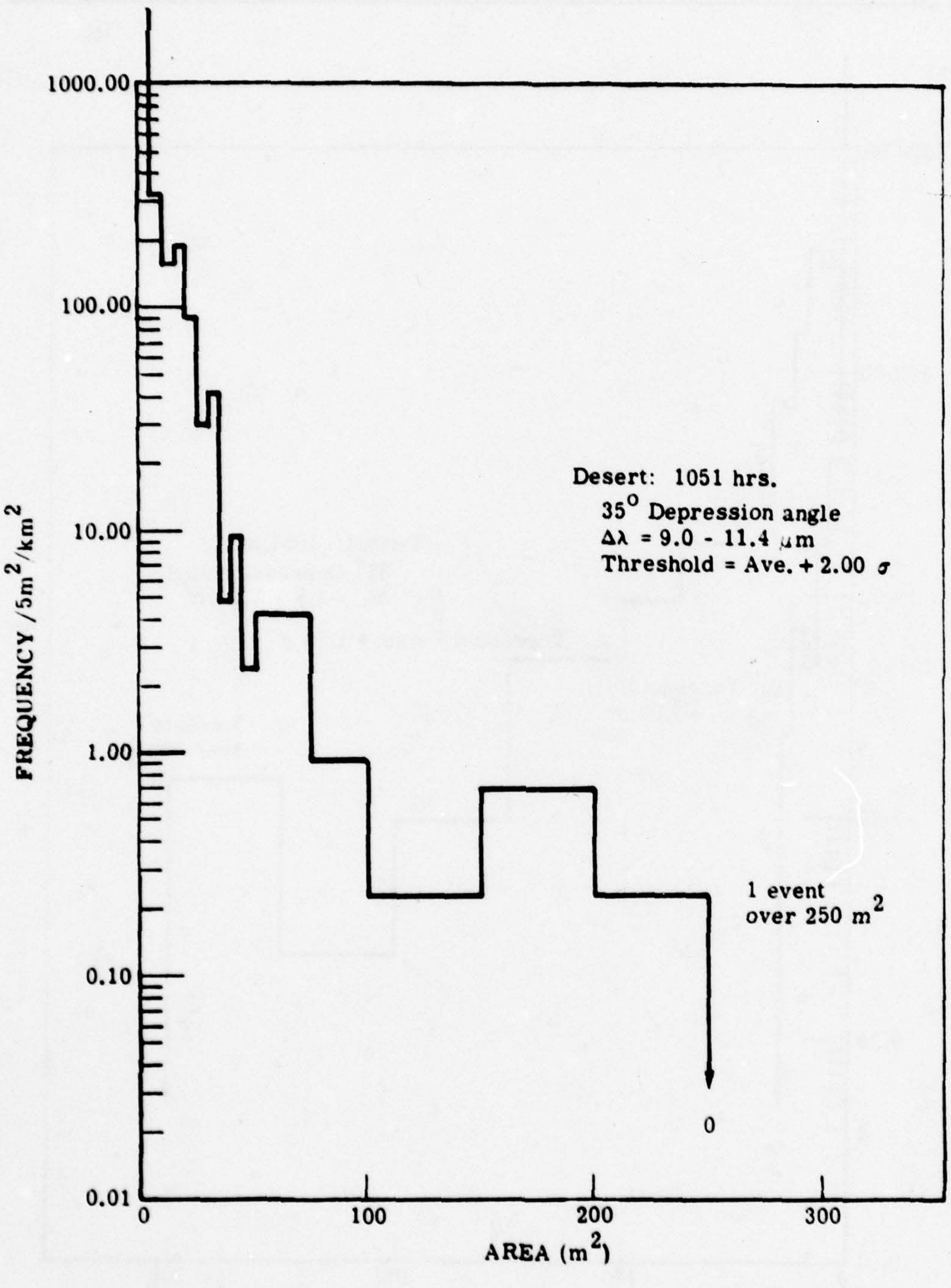

FIGURE 33. FREQUENCY OF FEATURE (AREA) SIZES PER SQUARE KILOMETER IN 5-m^2 INCREMENTS

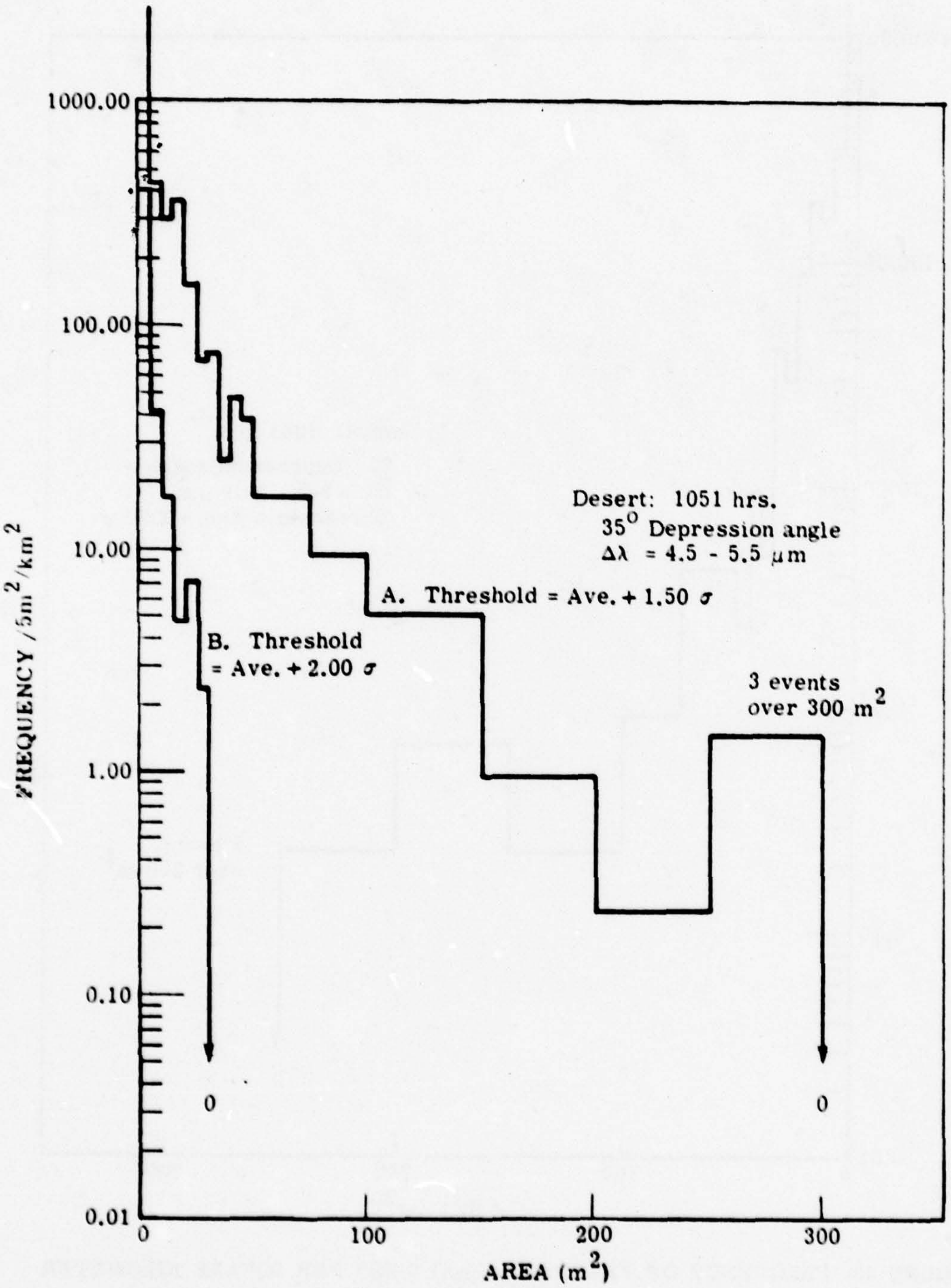

FIGURE 34. FREQUENCY OF FEATURE (AREA) SIZES PER SQUARE KILOMETER IN 5-m^2 INCREMENTS

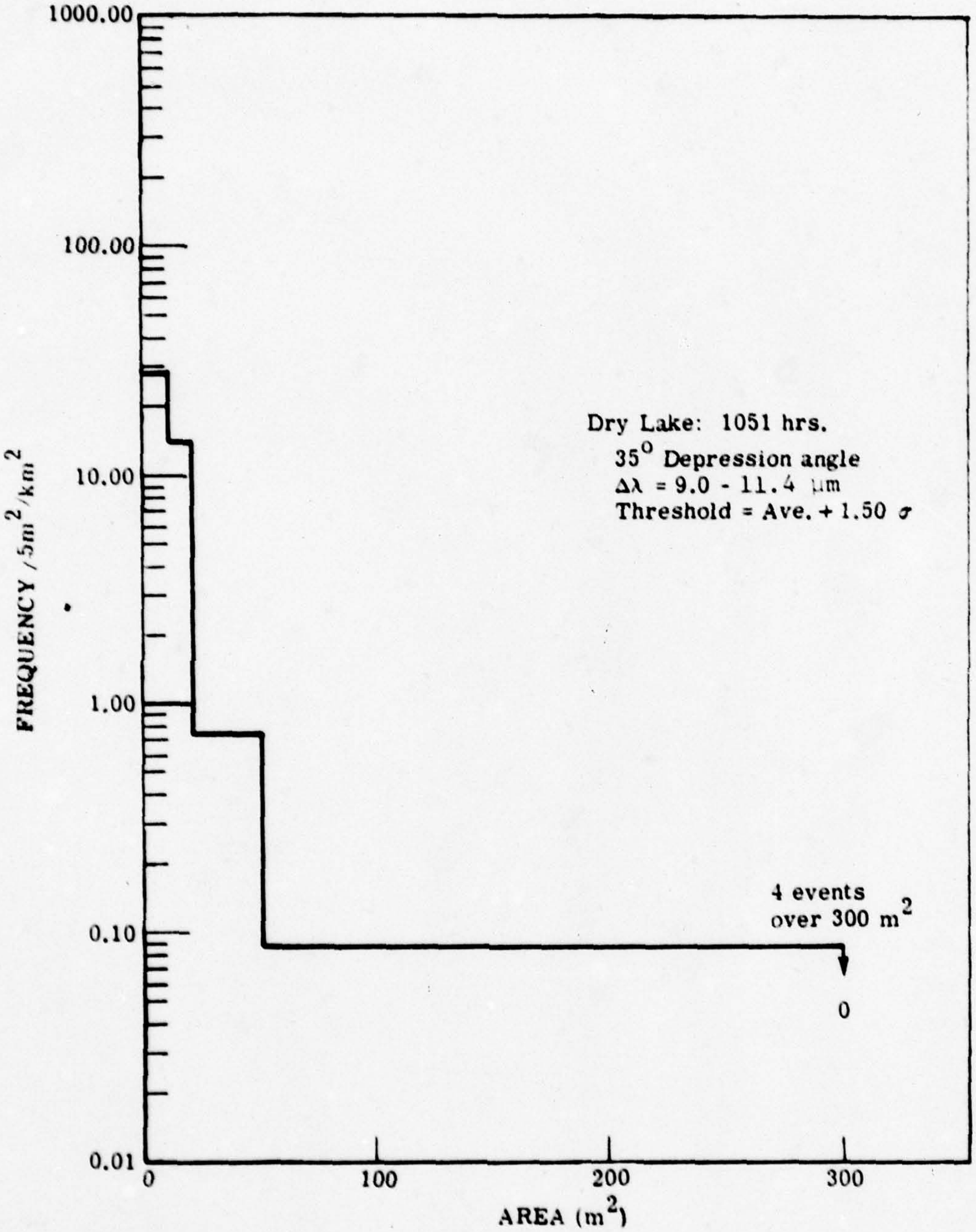

FIGURE 35. FREQUENCY OF FEATURE (AREA) SIZES PER SQUARE KILOMETER IN 5-m^2 INCREMENTS

4.0
CONCLUSIONS

Statistical analyses of the IR radiation from mountainous and desert terrain backgrounds are discussed in this report, which is meant to supplement the results reported in Reference 2. In Reference 2, the comments which refer to similar analyses in this report are, of course, still pertinent. The particular statistics analyzed in this study were chosen with the intent of providing information which will be generally useful, but which will be particularly useful to the systems designer.

Parameters other than those in Reference 2 were centralized in the present analysis, some of which indicated definite trends, others of which less typify the details in the scenery. For example, a comparison of results corresponding to different flight directions, especially over mountains, showed definite differences, indicating certain trends, but the effect was not sufficiently dramatic to single out flight direction as a very sensitive parameter. In fact, if we were to measure events which occur beyond the limits of the sensor's current dynamic range, we may perhaps see no significant difference.

The comparison of clear vs overcast skies yields the expected result of lower average temperature and less clutter for the latter; however, the comparison of morning vs afternoon results over the desert is not as fruitful, as can be observed from Figure 36, because so many parameters come into play on relatively little data. A more significant trend can be observed in Figure 37 where the diurnal variation in the mountain data is exactly as would be predicted on a geological scale.

In Figures 36 and 37, the letters correspond to the various runs designated in Table 1. (For example, L corresponds to NEVL.) Runs corresponding to B, C, D, E and F were taken from Reference 2. The x's correspond to the mean values of the temperatures for different

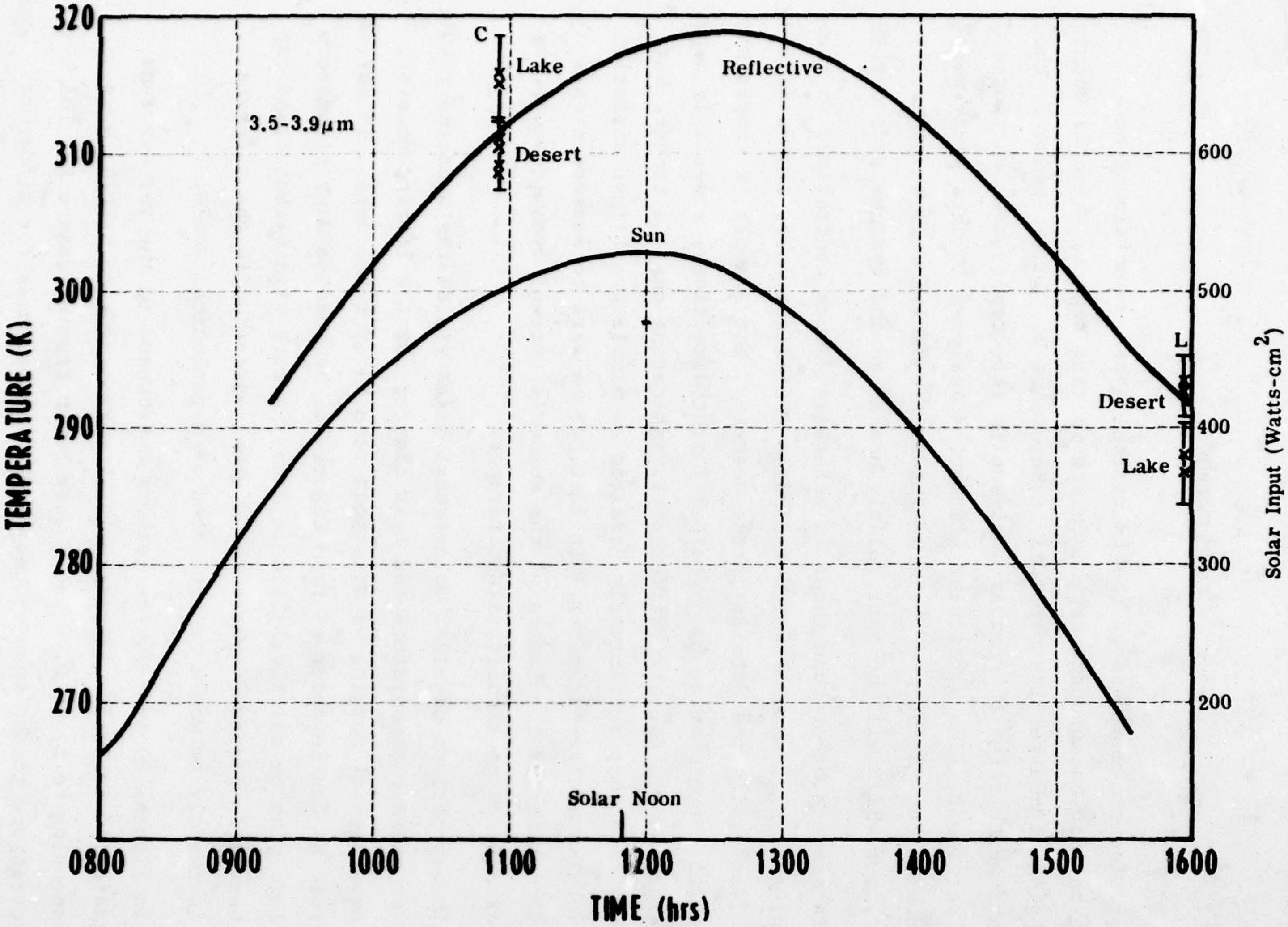

FIGURE 36a. DATA COMPILATION FOR NELLIS DESERT

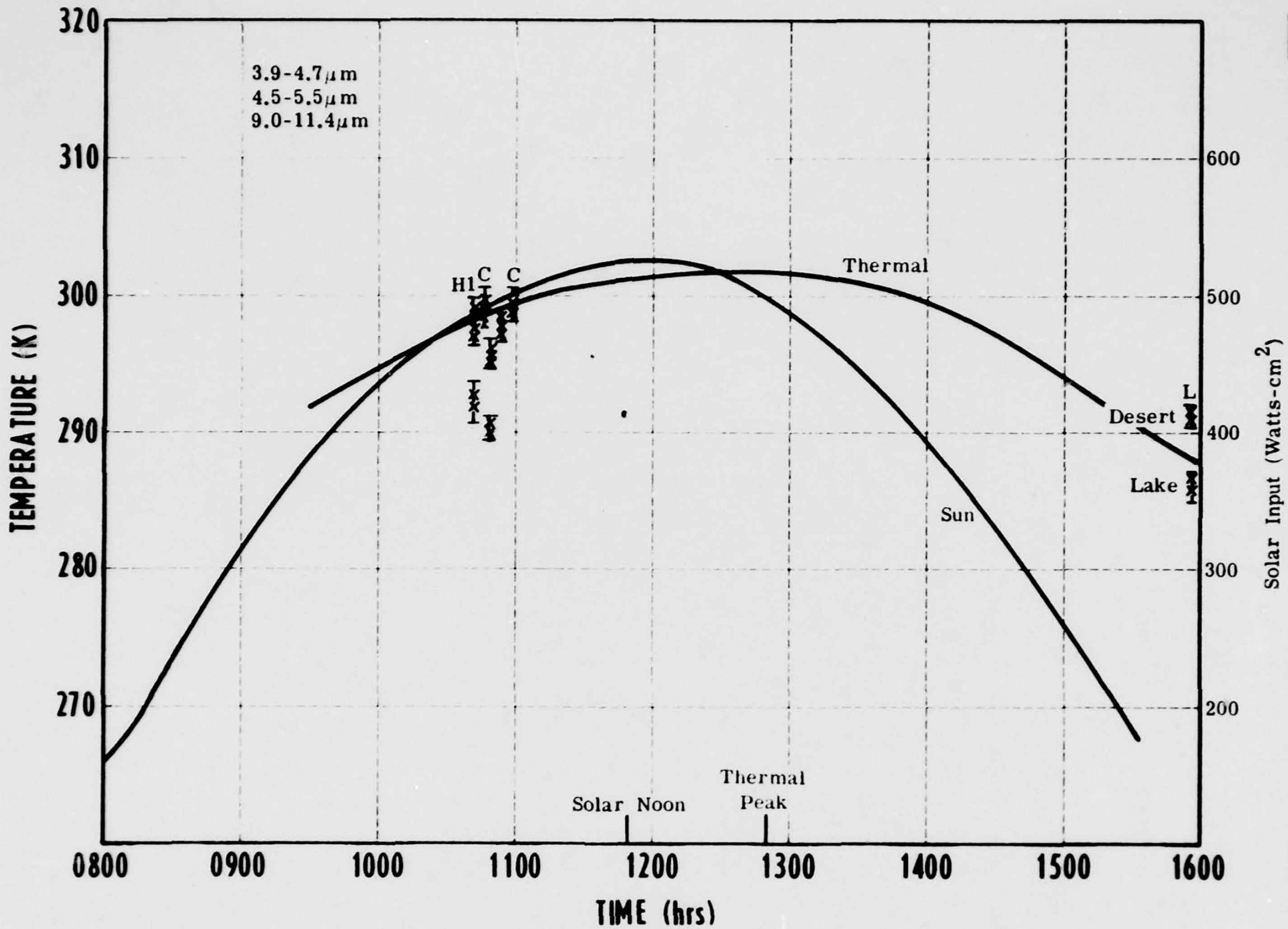

FIGURE 36b. DATA COMPILATION FOR NELLIS DESERT

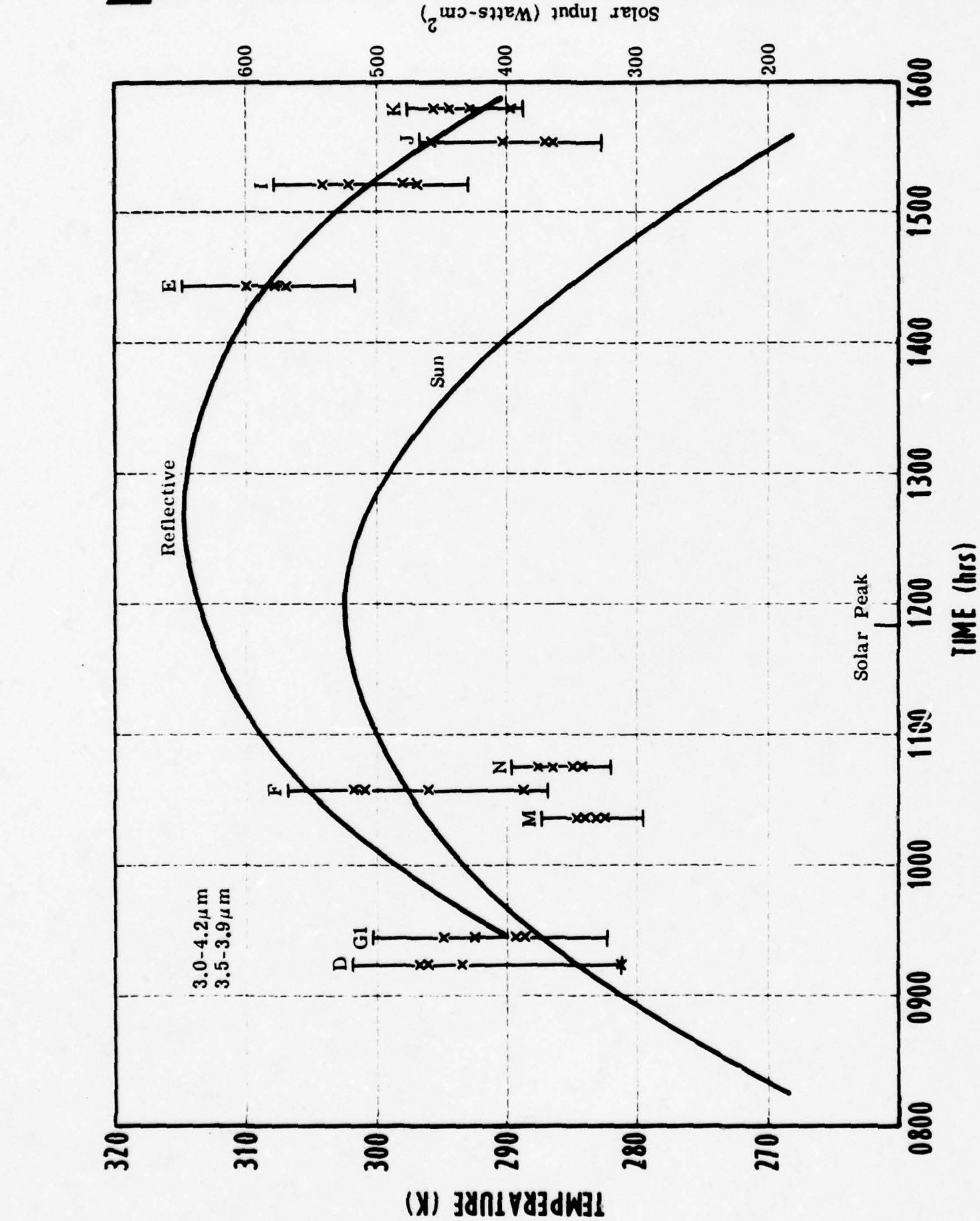

FIGURE 37a. DATA COMPILATION FOR NELLIS MOUNTAINS

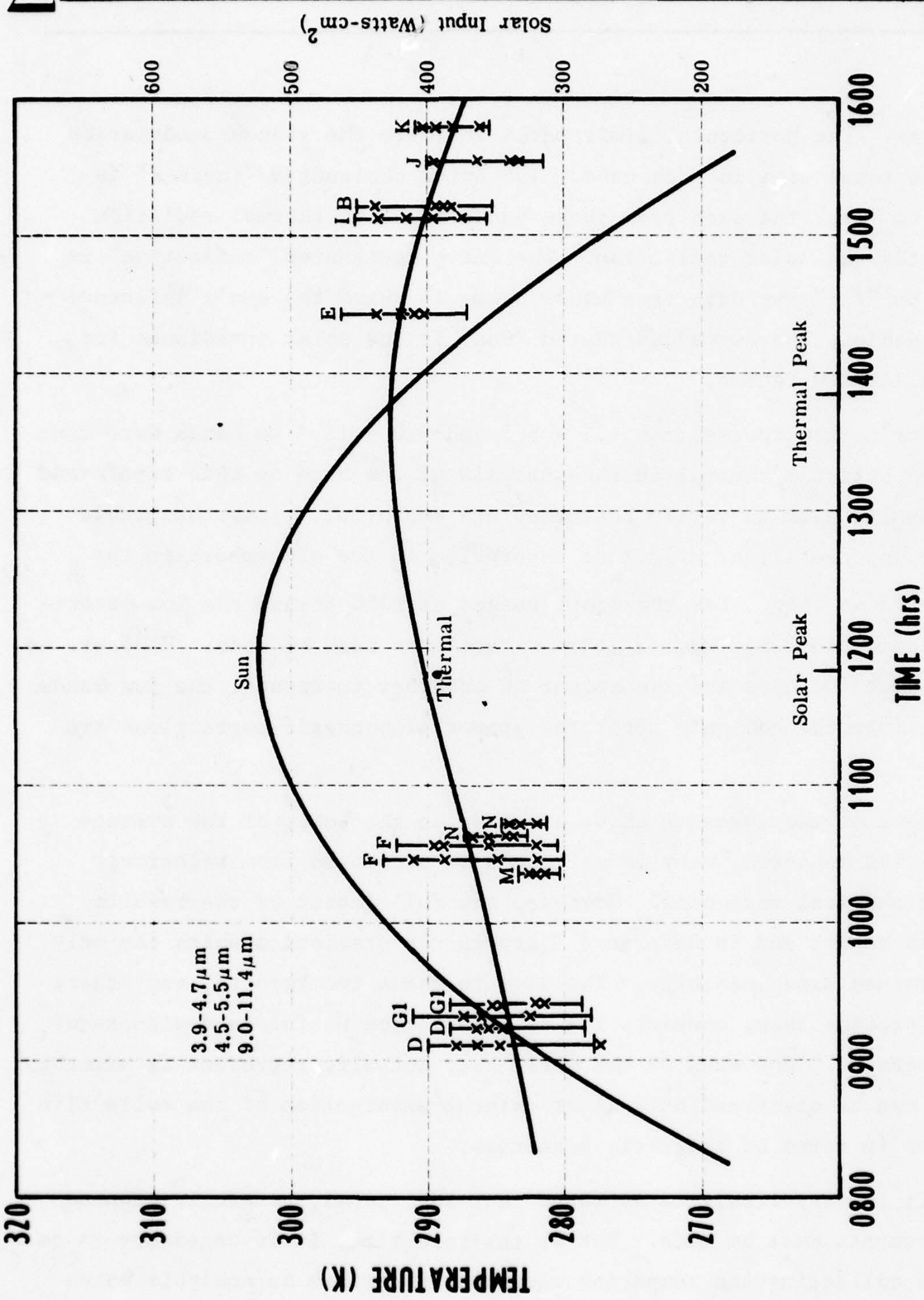

FIGURE 37b. DATA COMPILATION FOR NELLIS MOUNTAINS

subareas. The horizontal limit marks indicate the standard deviation for the total area in each case. The curve designated "thermal" is meant to "fit" the data from those bands in which thermal radiation dominates the solar reflection. The curve designated "reflective" is meant to "fit" the data from those bands in which the sun's influence is sizeable. The curve designated "sun" is the solar irradiance for the Nellis AFB region.

For most purposes, the 4.5 - 5.5 and 9.0 - 11.4 μm bands were considered strictly thermal in the analysis of the data in this report and the results seem to verify that they are essentially interchangeable except for the slight effect of absorption in the atmosphere in the 4.5 - 5.5 μm band. For the short ranges of 1000 ft and the low desert-type humidities, no discernible alterations need be made. However, as the ranges increase and the amount of absorber increases, the two bands may be interchanged only after the proper atmospheric corrections are made.

Most of the comments above are made on the basis of the average quantities measured, many of which can be predicted from relatively simple physical reasoning. However, the full impact of the results in this report and in Reference 2 are in the statistics which can only be obtained experimentally. The data in these two reports, and others which precede them, convey a lot of information useful to designers of IR equipment. How much of the world they actually represent is something which can be discerned only after careful examination of the collective results in terms of realistic scenarios.

It is very likely to be found that additional, carefully planned measurements must be made. But at the same time, it is necessary to go beyond collecting and comparing results and perform an analysis which will demonstrate the deficiencies in the collection of data up to this

point and guide the planning of future measurements. We believe we have a reasonable grasp of the statistics in a variety of terrain types. However, more effort will be put in later into attempting to find seasonal variations, for example. Also very little data have been gathered over water to help us make definitive statements about glint. We have not yet pointed the sensor skyward to learn about the effects of clouds and sky gradients. Even in the terrain cases, we have not yet made observations at skimming angles. Although the results have not been dramatic, we have shown that changing the sensor elevation by 35° effects some change in the data. Perhaps at shallower angles, the results will be dramatic.

We believe, therefore, that a two-pronged program is necessary: one being to collect and synthesize all of the data already available; the other being to make measurements which will fill the gaps in the background base to satisfy effectively the requirements of the sensor designer.

REFERENCES

1. Beard, J., J. Braithwaite and R. Turner, "Infrared Background Survey and Analysis," ERIM Report No. 118000-1-F, Environmental Research Institute of Michigan, Ann Arbor, June 1976.

2. Maxwell, J. R., "Statistical Analyses of Selected Terrain and Water Background Measurement Data," ERIM Report No. 132300-1-F, Environmental Research Institute of Michigan, Ann Arbor, July 1978, and

   Maxwell, J. R., Statistical Analysis of Terrain Backgrounds, Volume 22, Proceedings of IRIS, ERIM Report No. 127200-7-X, February 1978, pp. 101-129.

3. Spellicy, R., J. Beard and J. R. Maxwell, "Statistical Analysis of Terrain Background Measurements Data," ERIM Report No. 120500-12-F, Environmental Research Institute of Michigan, Ann Arbor, March 1977.

4. Taylor, J. H. and H. W. Yates, Atmospheric Transmission in the Infrared, Journal of the Optical Society of America, Vol. 47, No. 3, 1957, pp. 223-226.

APPENDIX A
LINEAR SUBAREA PLOTS (HISTOGRAMS)

The figures in this appendix are plotted linearly as a function of radiance for 2.6 - 2.0 μm and as a function of temperature for the other spectral regions. Consult the body of the report for log-plots of the statistics as a function of radiance for the long wavelength spectral regions. See Table 1 for pertinent parameters.

In each case, the subareas are plotted on a single curve for each of the respective spectral regions, followed by plots in the same spectral regions of the total area analyzed. The total areas are given in Table 1. In the mountain scenes, the total area was divided into 4 regions. The desert scenes are first subdivided into Desert #1, Desert #2, and Dry Lake areas. The sizes are shown in Table 1. Each of these is further subdivided into 2 areas.

We point out here, because it is more noticeable than in the log-plots in the body of the report, that the histograms for the dry lake has two humps. We believe, however, that this is caused as much perhaps by data from the desert part of the scene, which managed to sneak into the analysis, as by a true bimodal structure of the lake.

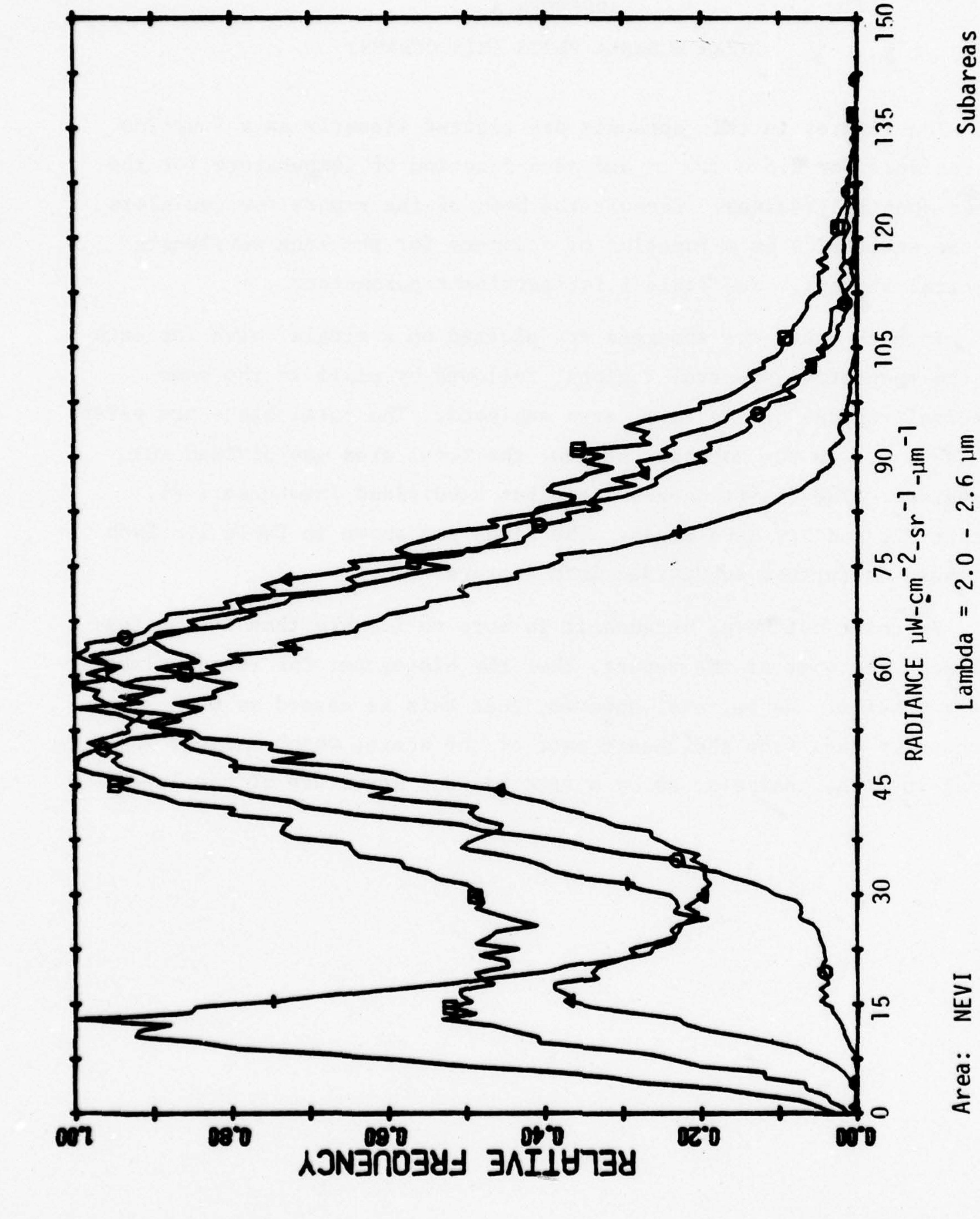
RELATIVE FREQUENCY
0.00
0.20
0.40
0.60
0.80
1.00
RADIANCE µW-cm^-2-sr^-1-µm^-1
0
15
30
45
60
75
90
105
120
135
150
Area: NEVI
Lambda = 2.0 - 2.6 µm
Subareas

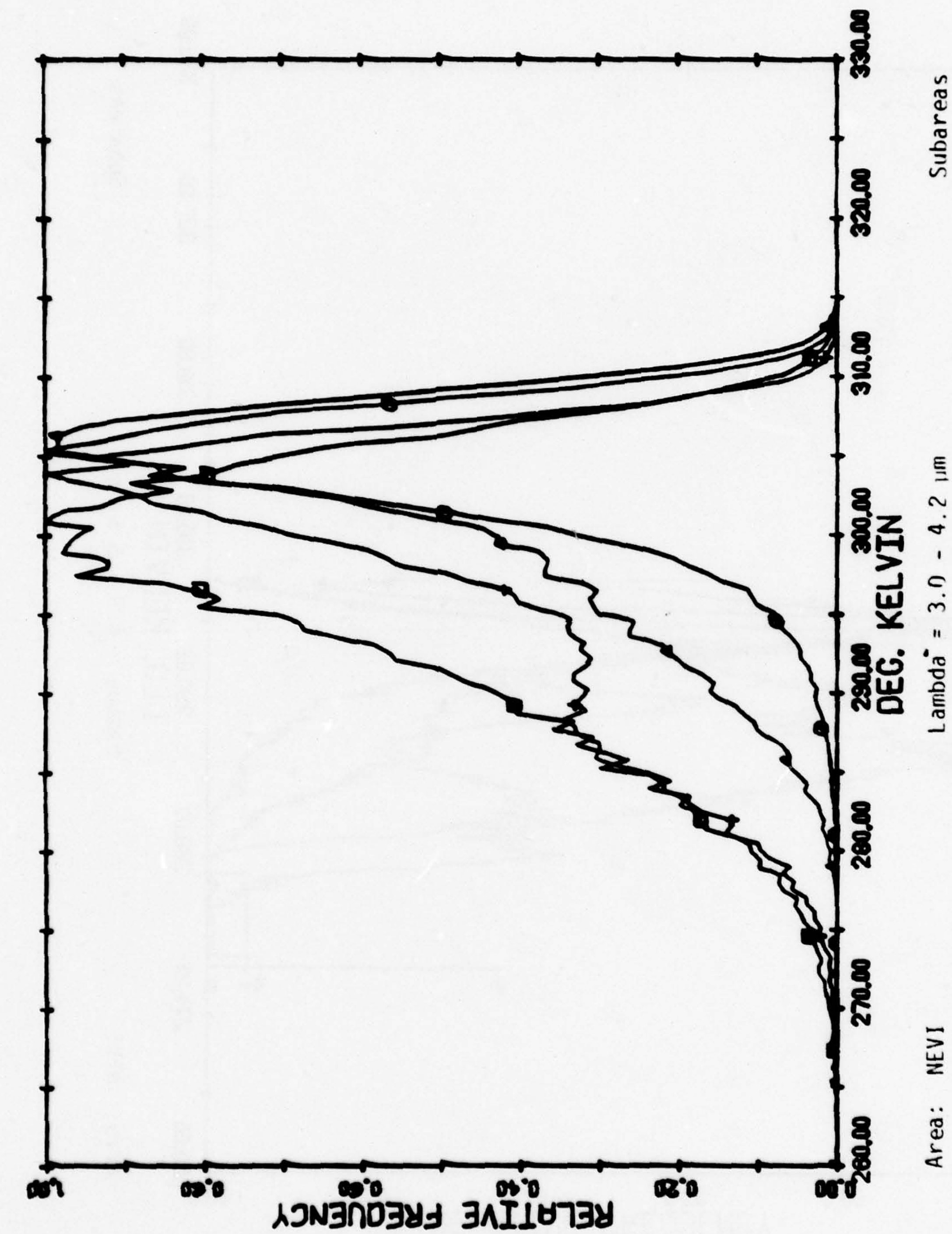
RELATIVE FREQUENCY
0.00
0.20
0.40
0.60
0.80
1.00
260.00
270.00
280.00
290.00
300.00
310.00
320.00
330.00
DEG. KELVIN
Area: NEVI
Lambda = 3.0 - 4.2 μm
Subareas

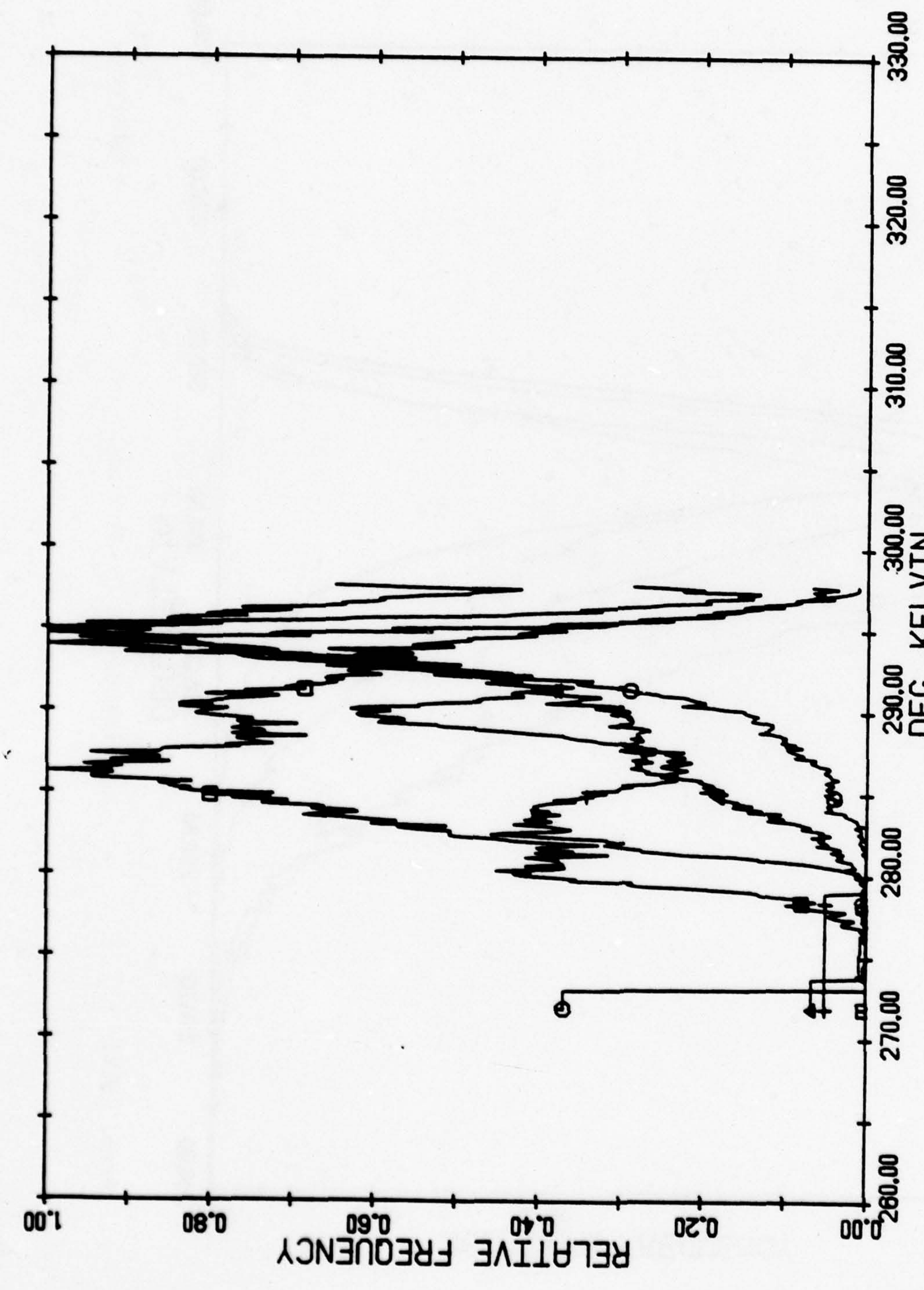

Area: NEVI Lambda = 4.5 - 5.5 μm Subareas

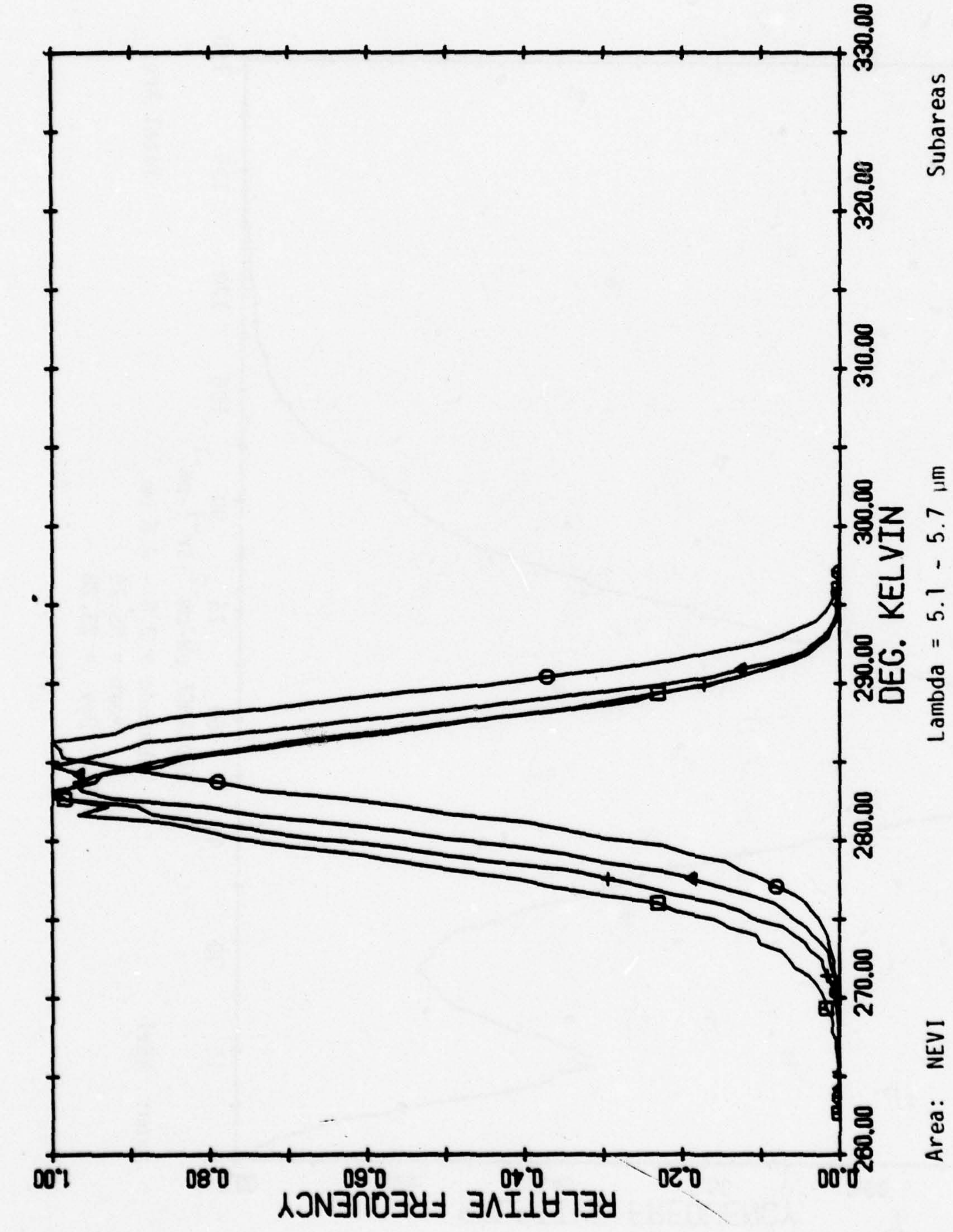

RELATIVE FREQUENCY
0.00
0.20
0.40
0.60
0.80
1.00
DEG. KELVIN
260.00
270.00
280.00
290.00
300.00
310.00
320.00
330.00
Area: NEVI
Lambda = 5.1 - 5.7 μm
Subareas

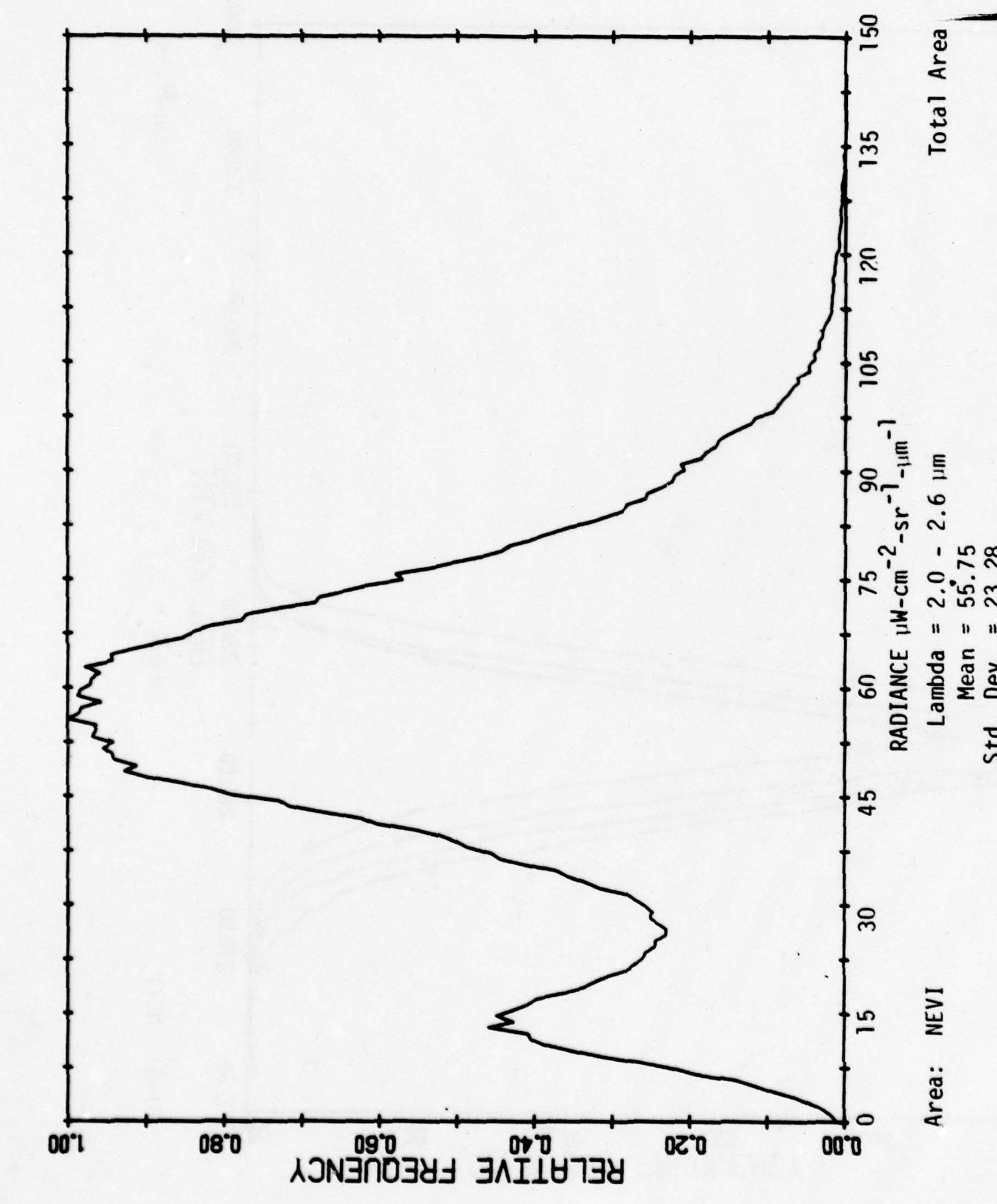
RELATIVE FREQUENCY
0.00
0.20
0.40
0.60
0.80
1.00
0
15
30
45
60
75
90
105
120
135
150
RADIANCE μW-cm^-2-sr^-1-μm^-1
Area: NEVI
Total Area
Lambda = 2.0 - 2.6 μm
Mean = 55.75
Std. Dev. = 23.28

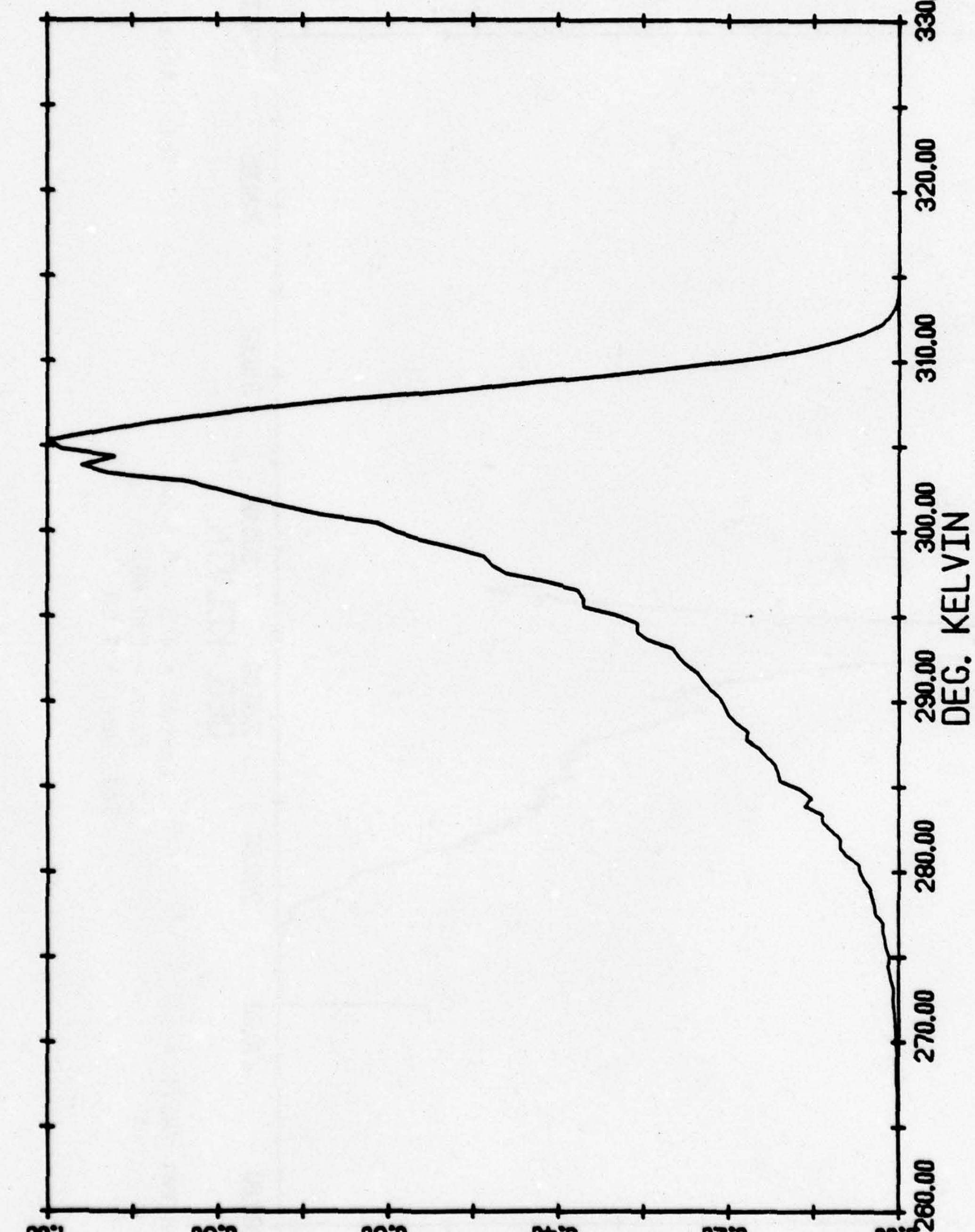

Area: NEVI

Lambda = 3.0 - 4.2 µm
Mean = 300.00
Std. Dev. = 7.28

Total Area

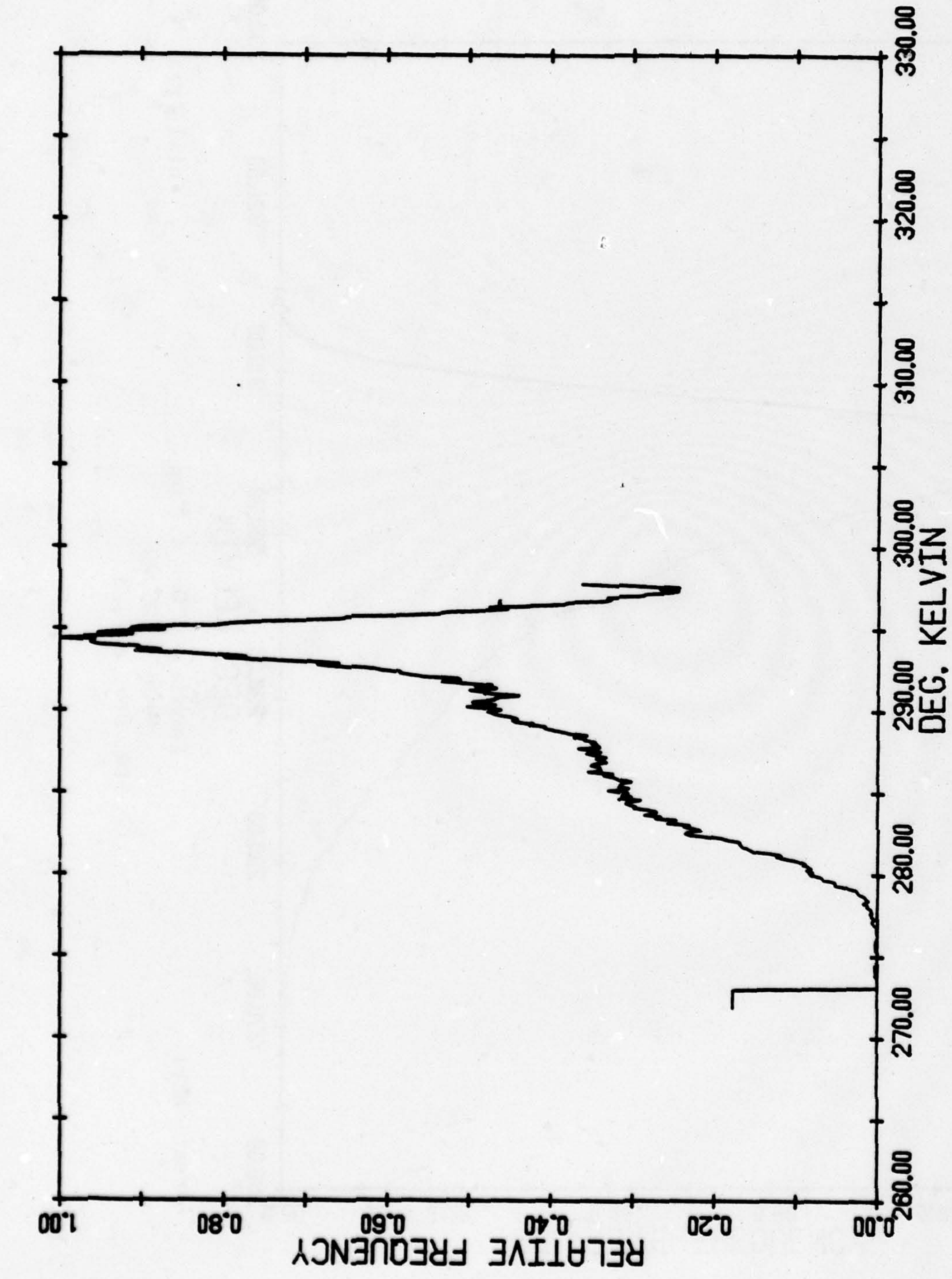

Area: NEVI

Lambda = 4.5 - 5.5 μm
Mean = 290.68
Std. Dev. = 4.60

Total Area

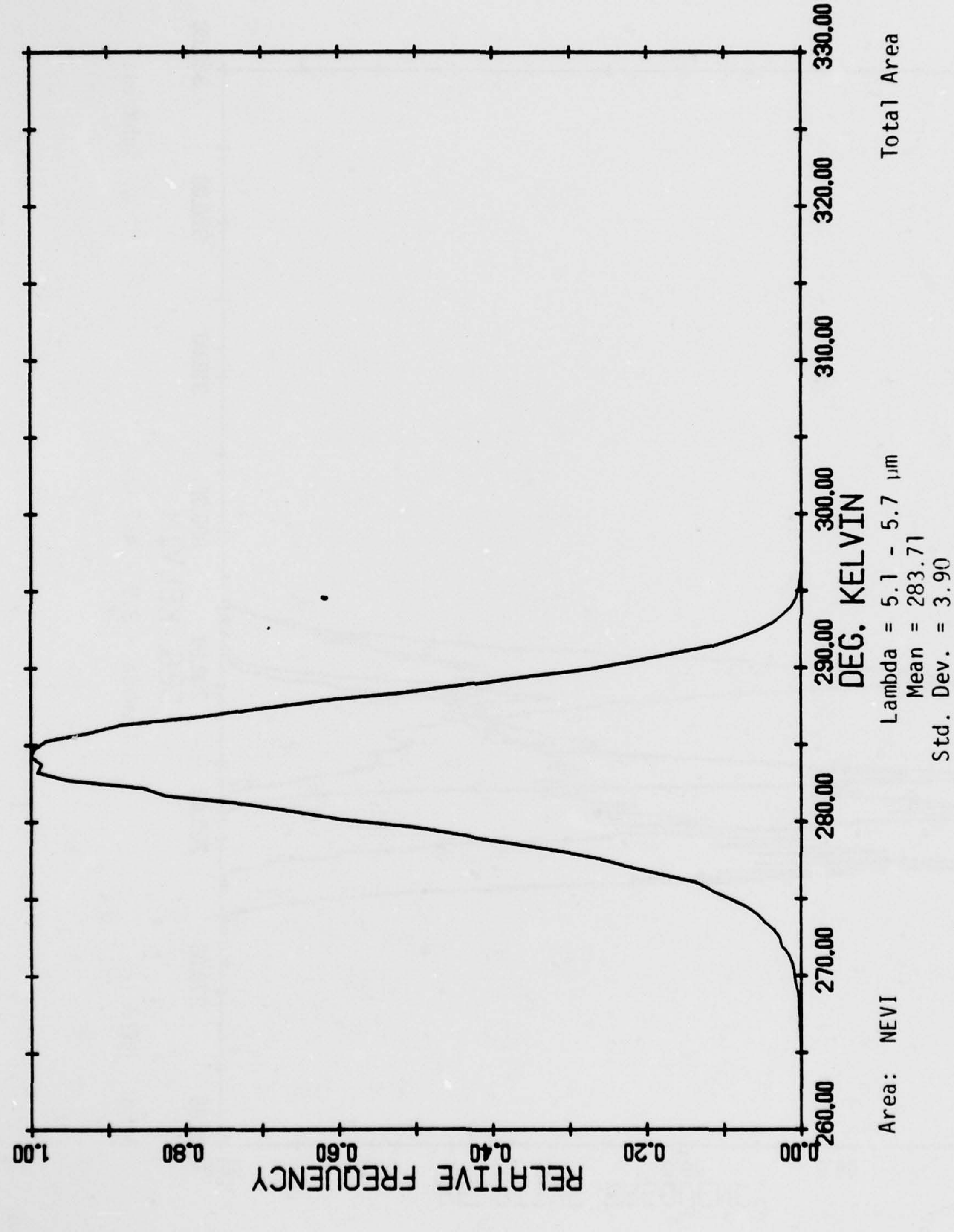

RELATIVE FREQUENCY
0.00
0.20
0.40
0.60
0.80
1.00
260.00
270.00
280.00
290.00
300.00
310.00
320.00
330.00
DEG. KELVIN
Lambda = 5.1 - 5.7 µm
Mean = 283.71
Std. Dev. = 3.90
Area: NEVI
Total Area

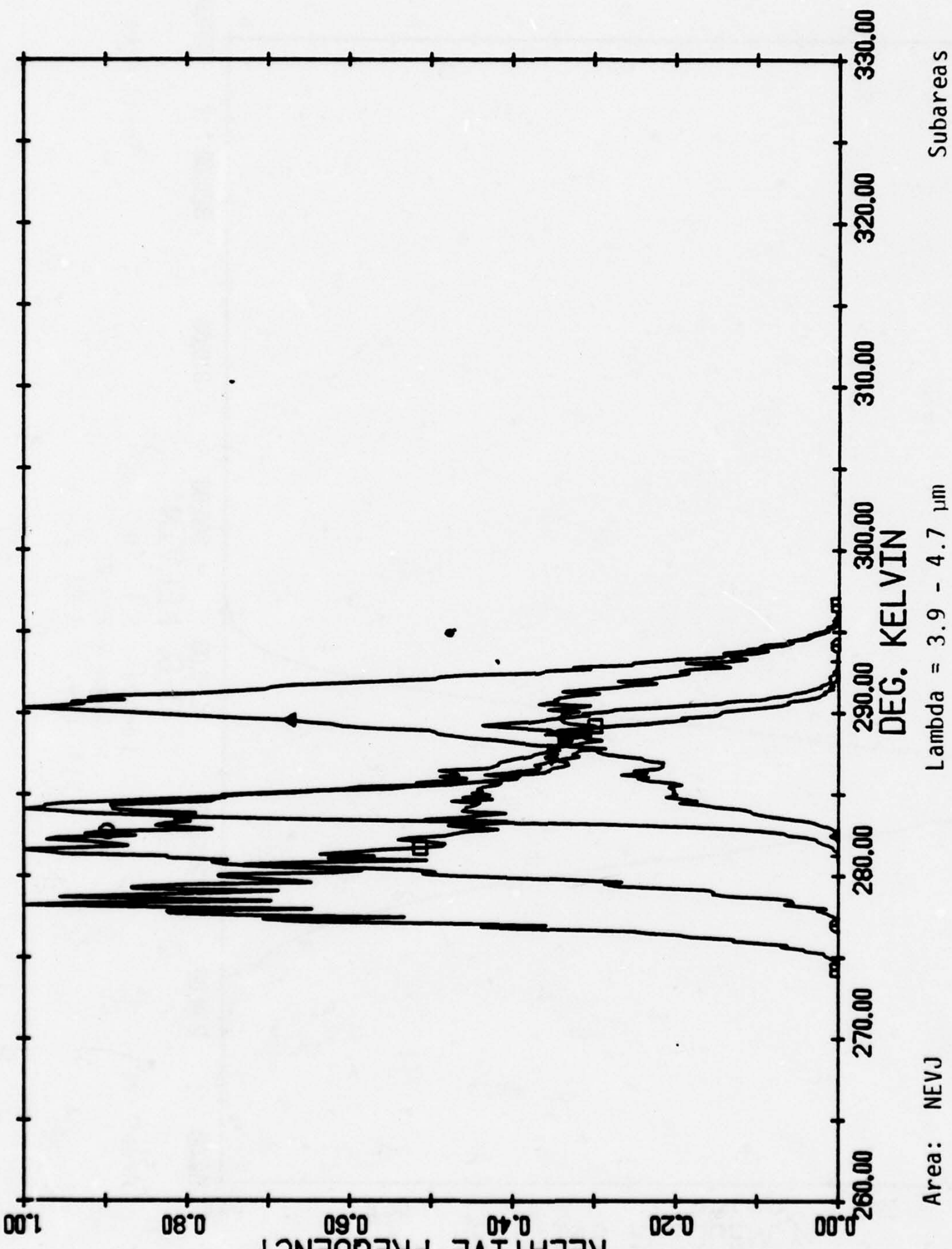
RELATIVE FREQUENCY
0.00
0.20
0.40
0.60
0.80
1.00
DEG. KELVIN
260.00
270.00
280.00
290.00
300.00
310.00
320.00
330.00
Area: NEVJ
Lambda = 3.9 - 4.7 µm
Subareas

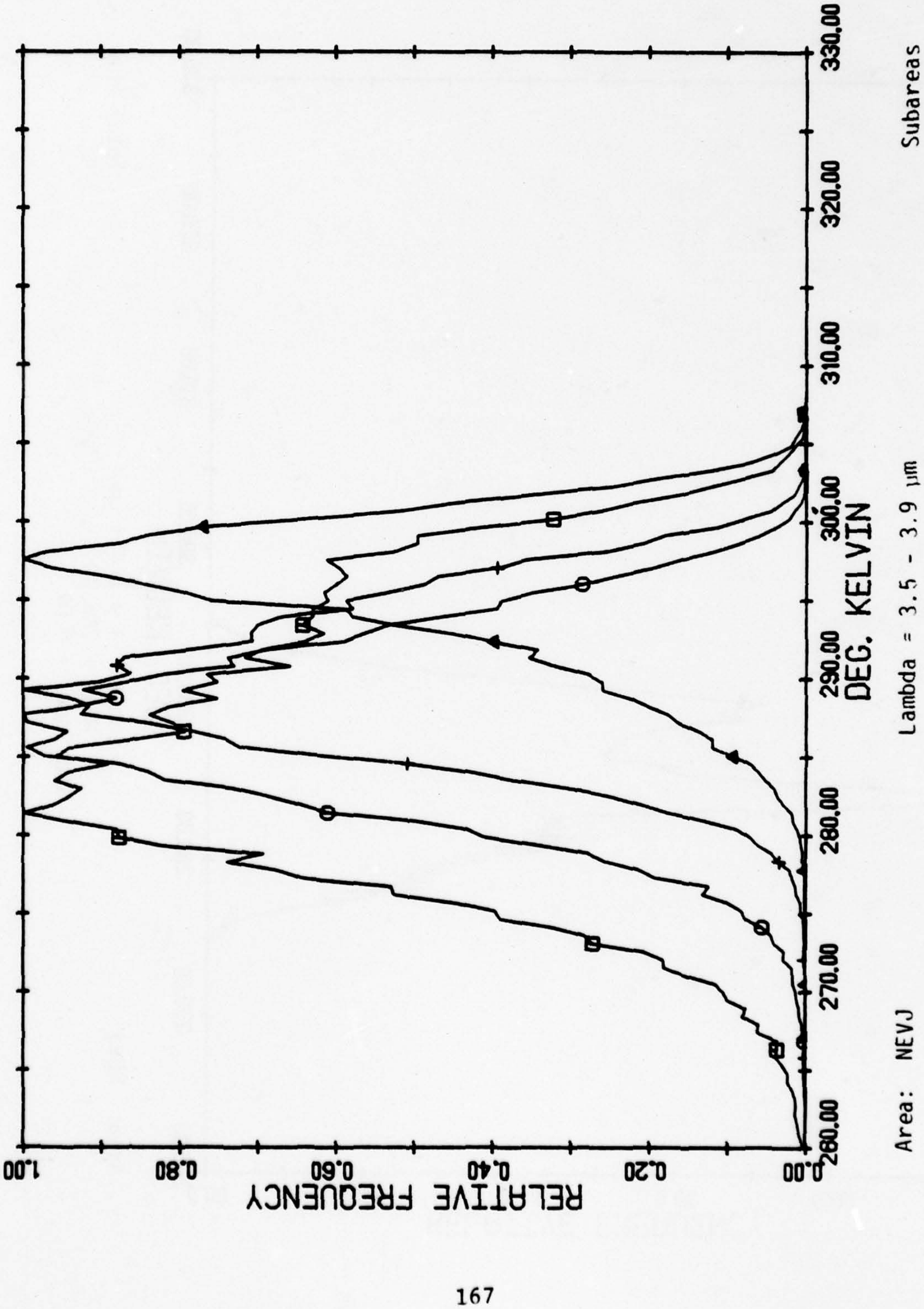
RELATIVE FREQUENCY
1.00
0.80
0.60
0.40
0.20
0.00
260.00
270.00
280.00
290.00
300.00
310.00
320.00
330.00
DEG. KELVIN
Area: NEVJ
Lambda = 3.5 - 3.9 μm
Subareas

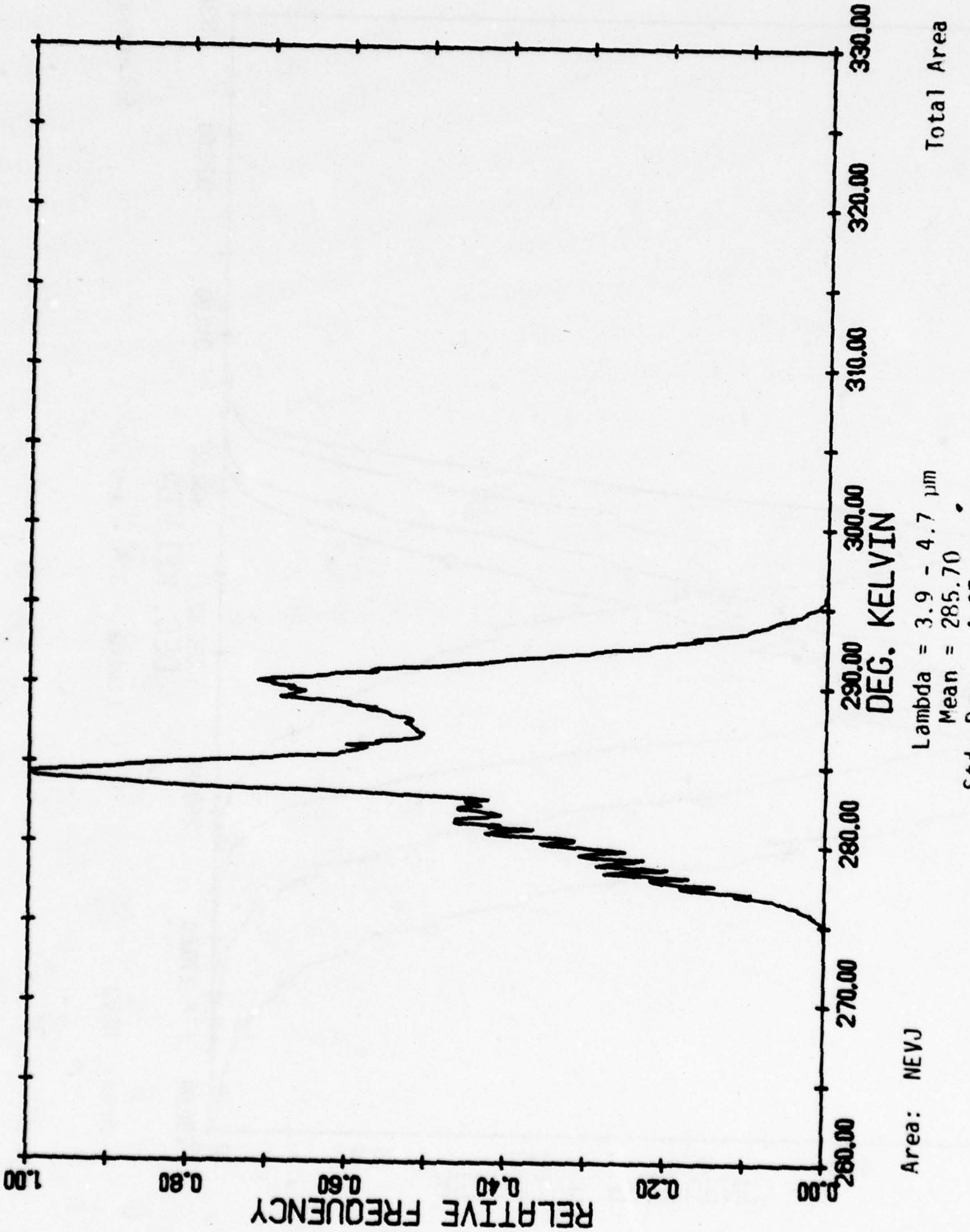
RELATIVE FREQUENCY
0.00
0.20
0.40
0.60
0.80
1.00
DEG. KELVIN
260.00
270.00
280.00
290.00
300.00
310.00
320.00
330.00
Lambda = 3.9 - 4.7 μm
Mean = 285.70
Std. Dev. = 4.07
Area: NEVJ
Total Area

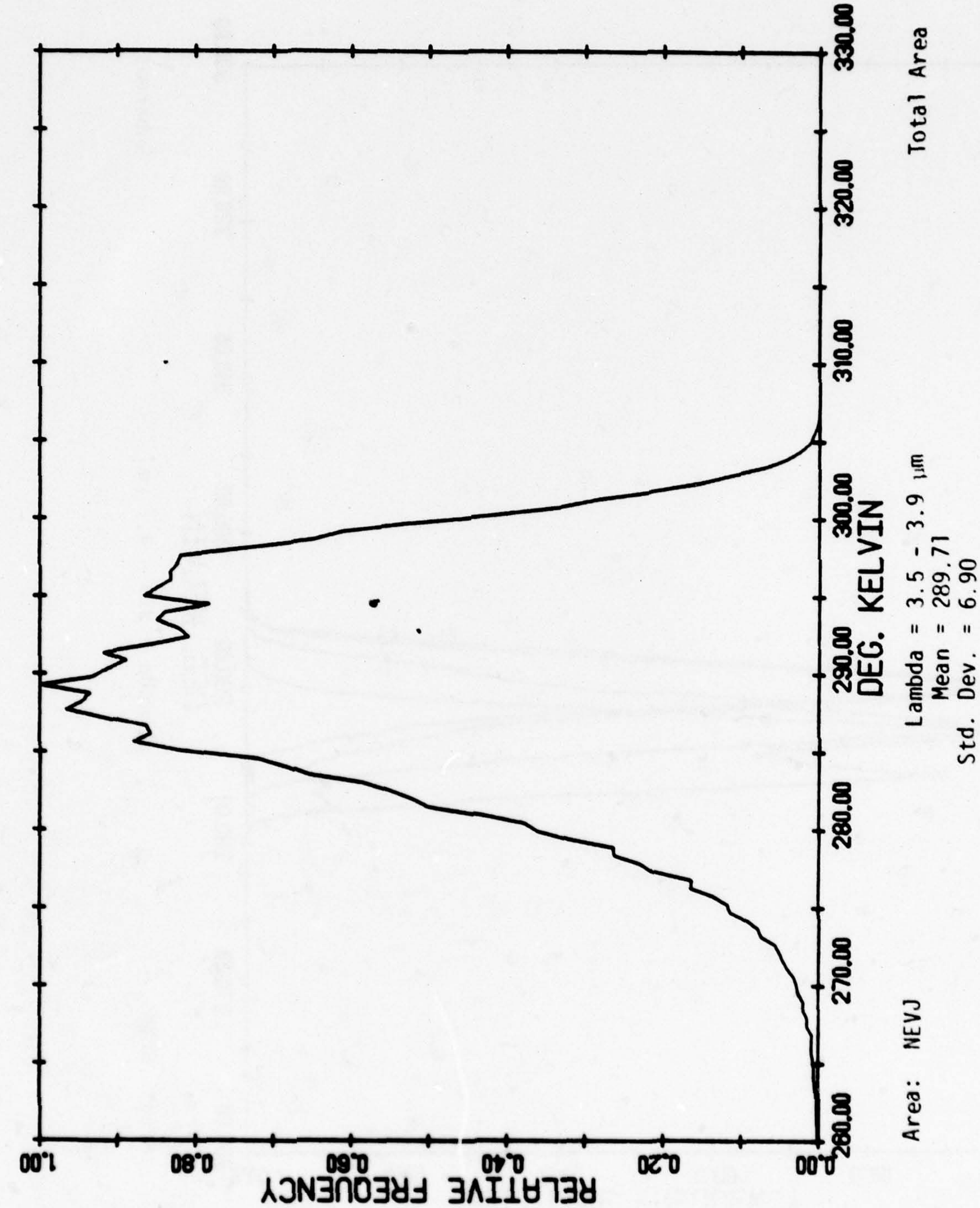
RELATIVE FREQUENCY
0.00
0.20
0.40
0.60
0.80
1.00
DEG. KELVIN
260.00
270.00
280.00
290.00
300.00
310.00
320.00
330.00
Area: NEVJ
Lambda = 3.5 - 3.9 μm
Mean = 289.71
Std. Dev. = 6.90
Total Area

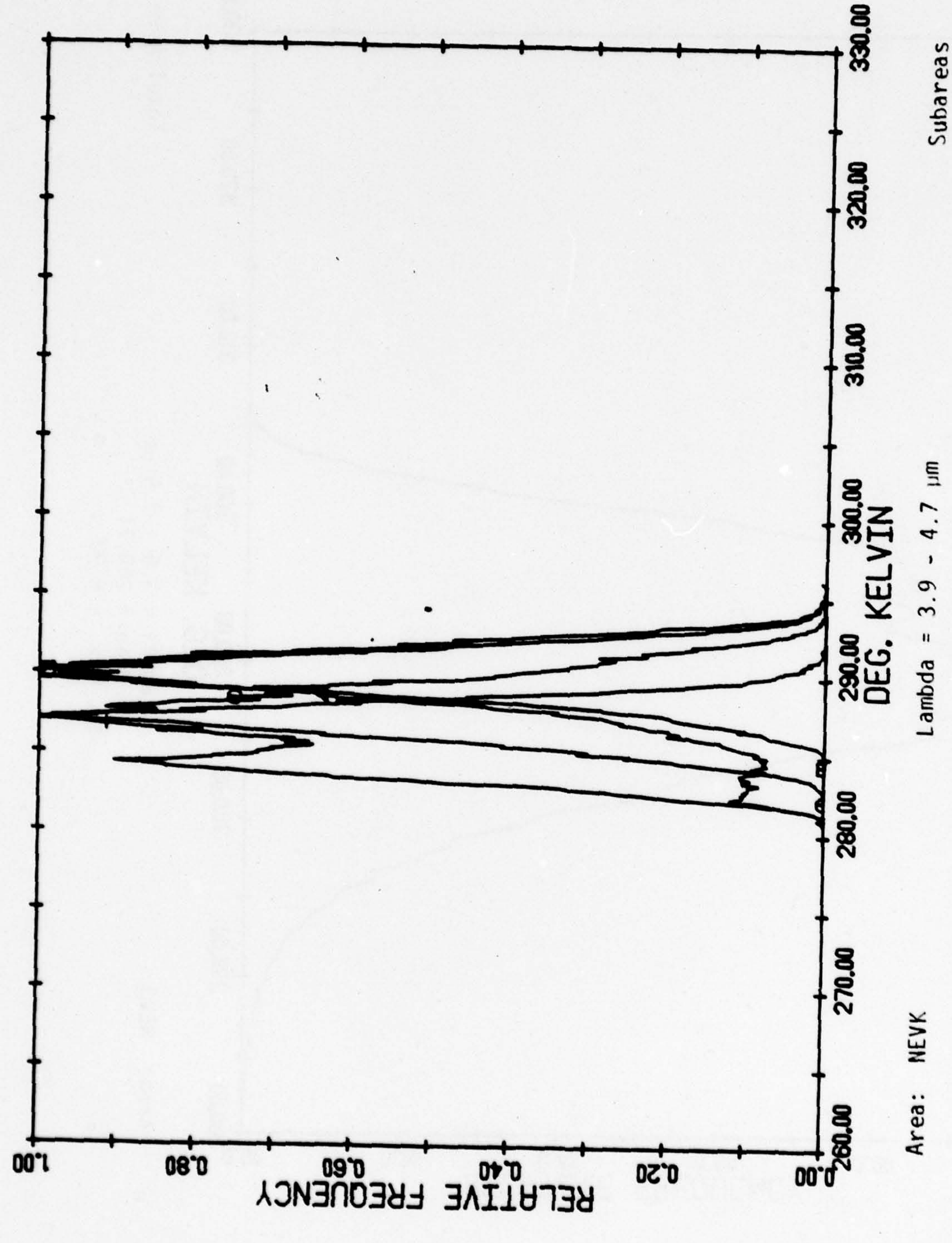
RELATIVE FREQUENCY
0.00
0.20
0.40
0.60
0.80
1.00
DEG. KELVIN
260.00
270.00
280.00
290.00
300.00
310.00
320.00
330.00
Area: NEVK
Lambda = 3.9 - 4.7 µm
Subareas

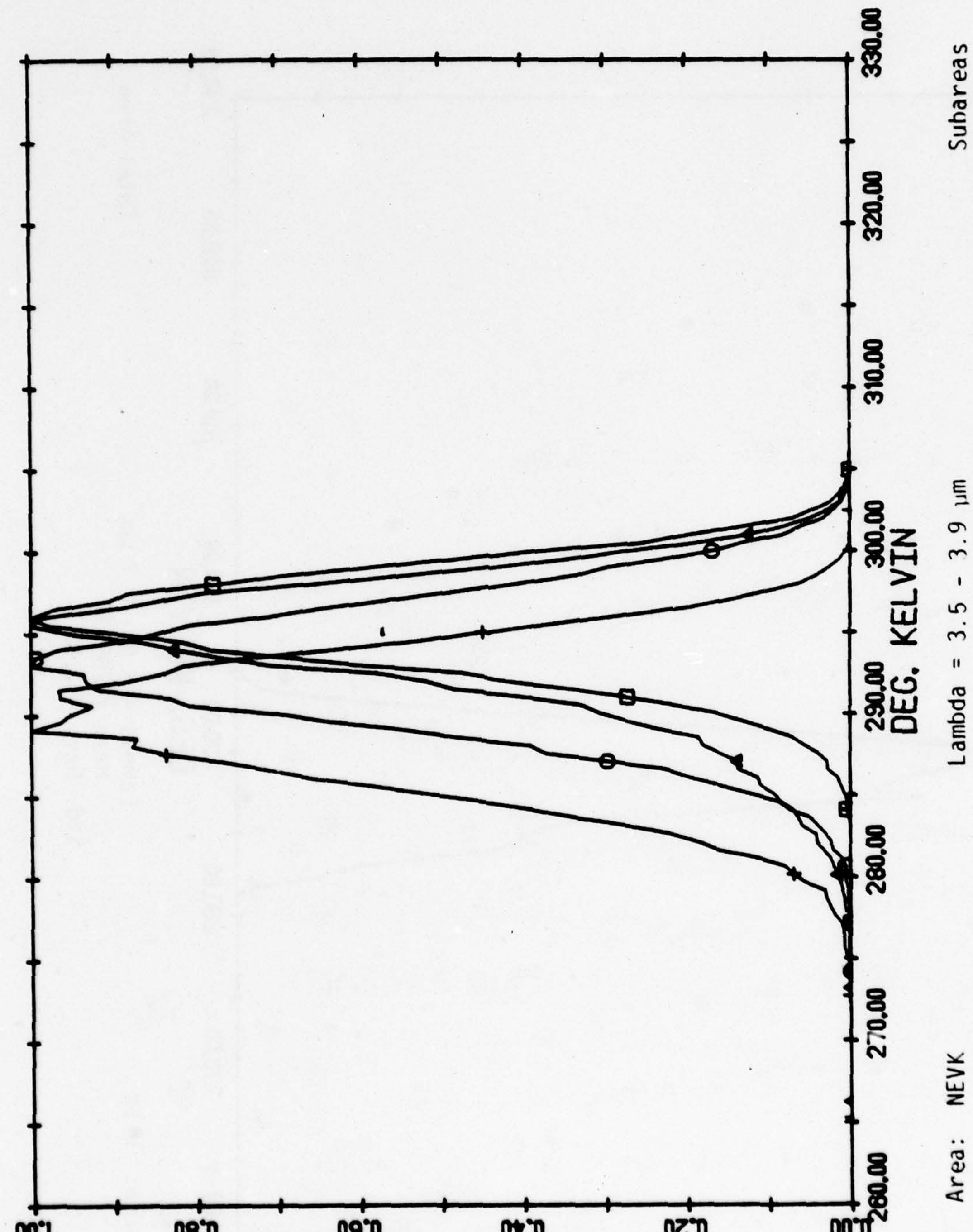
RELATIVE FREQUENCY
0.00
0.20
0.40
0.60
0.80
1.00
DEG. KELVIN
260.00
270.00
280.00
290.00
300.00
310.00
320.00
330.00
Area: NEVK
Lambda = 3.5 - 3.9 µm
Subareas

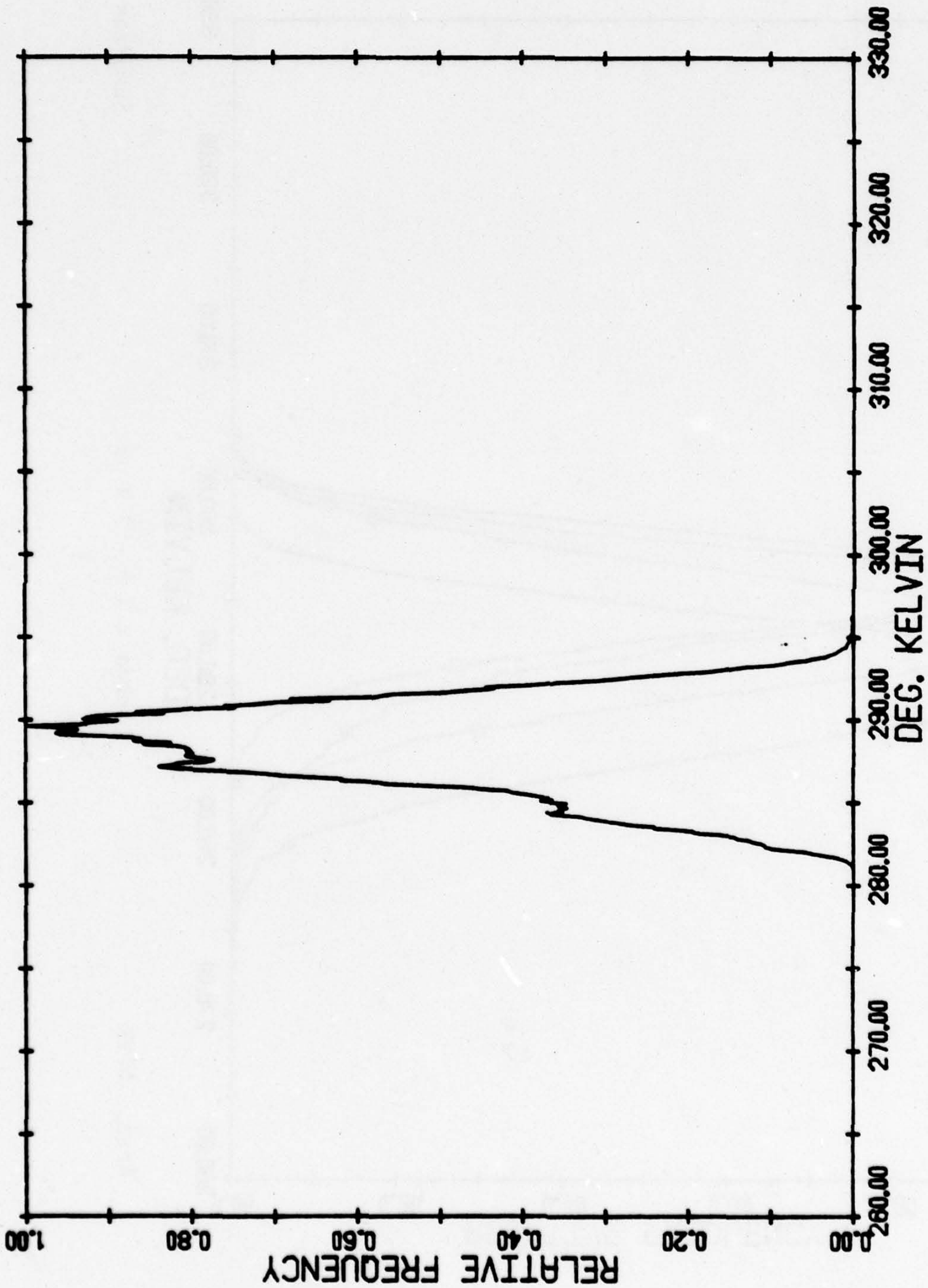

Area: NEVK

Lambda = 3.9 - 4.7 μm
Mean = 288.34
Std. Dev. = 2.53

Total Area

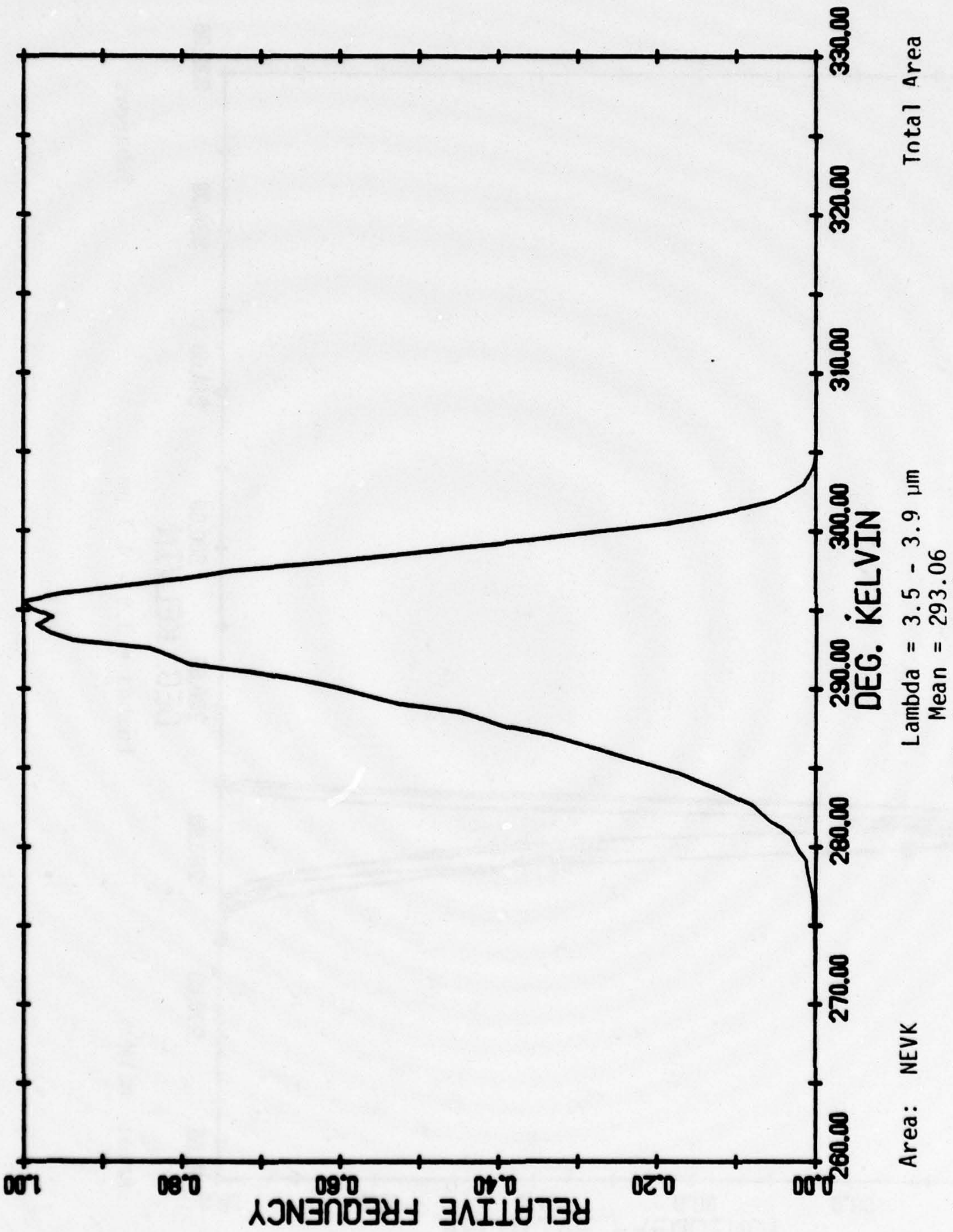
RELATIVE FREQUENCY
0.00
0.20
0.40
0.60
0.80
1.00
260.00
270.00
280.00
290.00
300.00
310.00
320.00
330.00
DEG. KELVIN
Area: NEVK
Total Area
Lambda = 3.5 - 3.9 µm
Mean = 293.06
Std. Dev. = 4.34

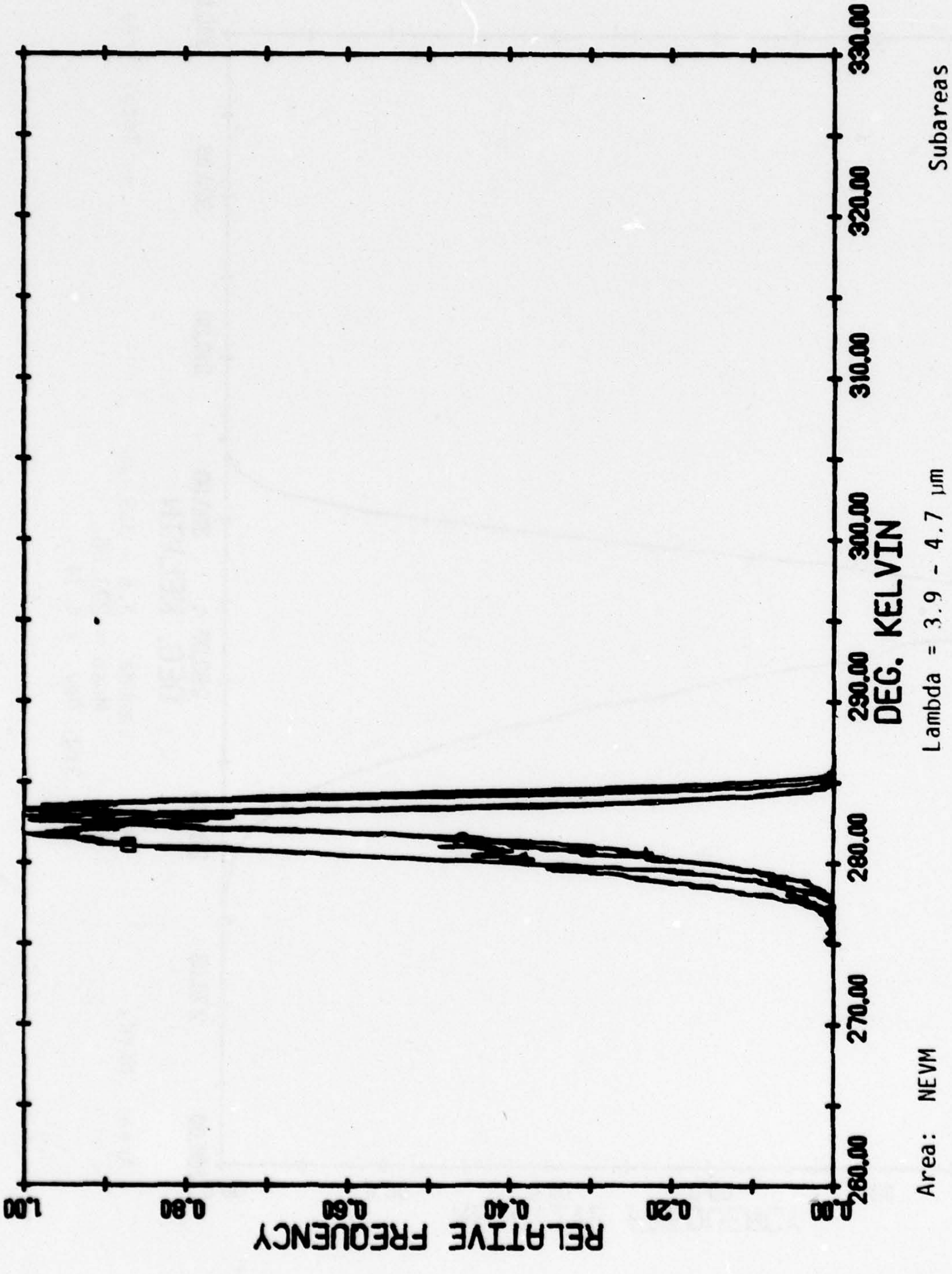
RELATIVE FREQUENCY
0.00
0.20
0.40
0.60
0.80
1.00
260.00
270.00
280.00
290.00
300.00
310.00
320.00
330.00
DEG. KELVIN
Lambda = 3.9 - 4.7 μm
Area: NEVM
Subareas

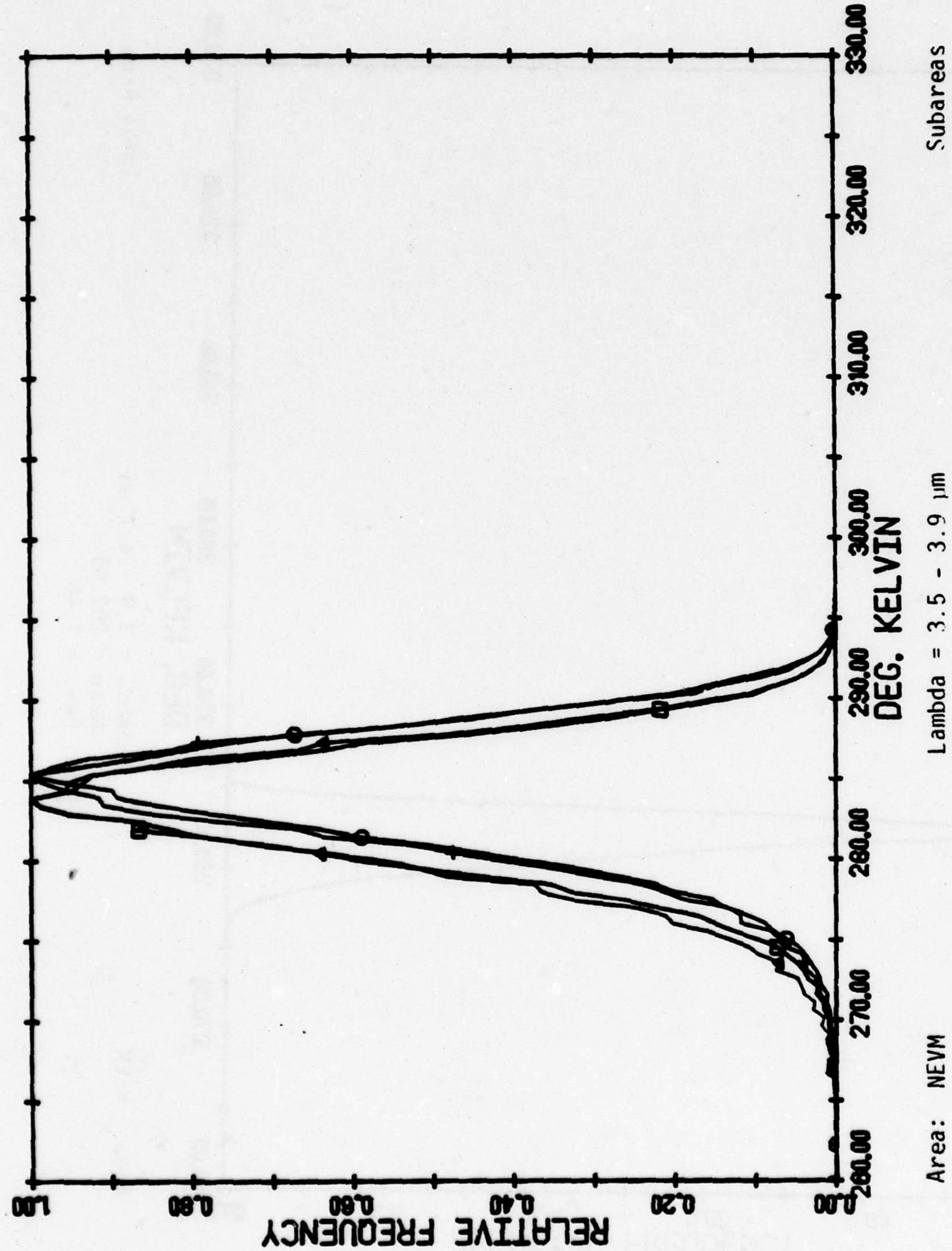
RELATIVE FREQUENCY
0.00
0.20
0.40
0.60
0.80
1.00
DEG. KELVIN
260.00
270.00
280.00
290.00
300.00
310.00
320.00
330.00
Area: NEVM
Lambda = 3.5 - 3.9 μm
Subareas

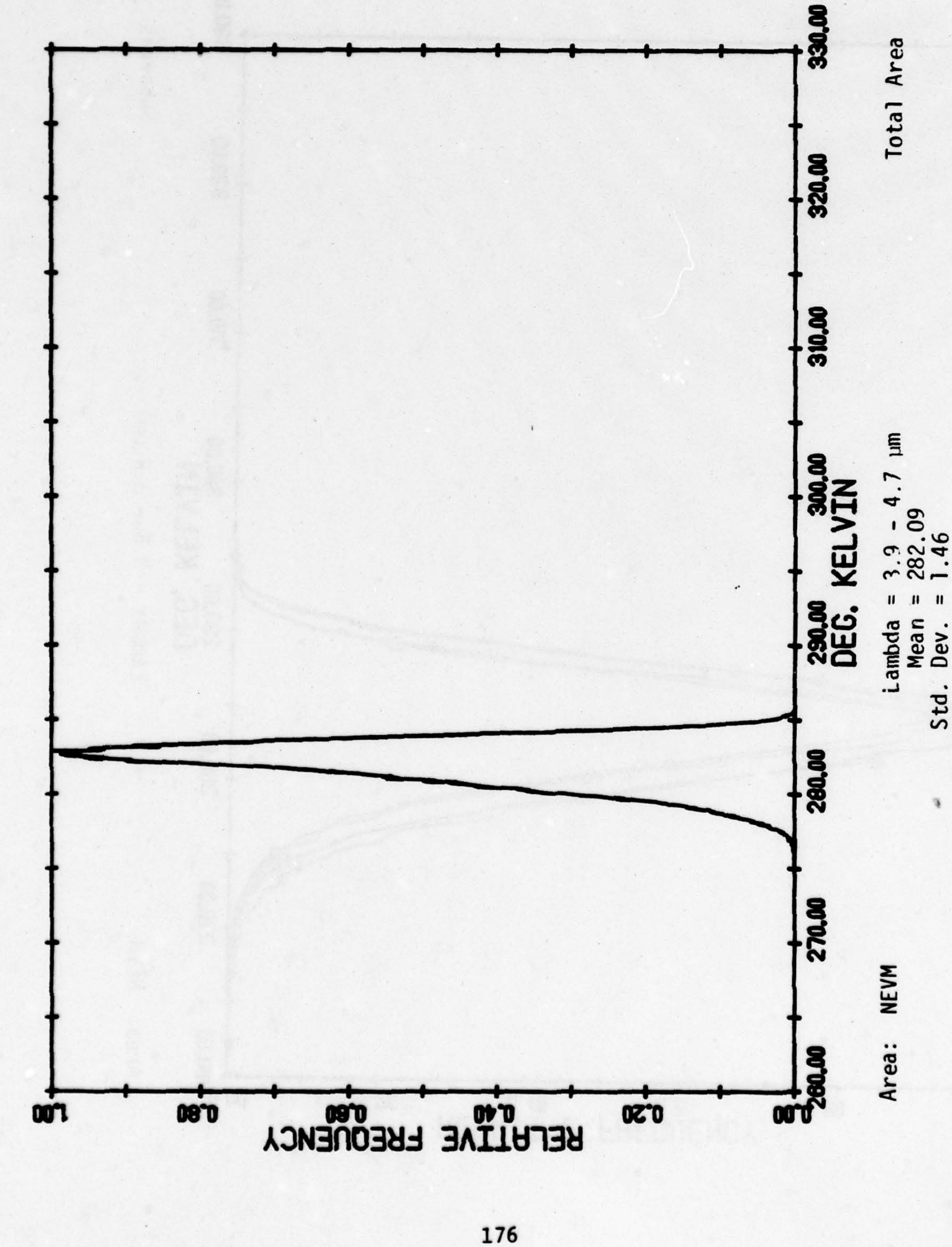
Area: NEVM
Total Area
Lambda = 3.9 - 4.7 μm
Mean = 282.09
Std. Dev. = 1.46
DEG. KELVIN
260.00
270.00
280.00
290.00
300.00
310.00
320.00
330.00
RELATIVE FREQUENCY
0.00
0.20
0.40
0.60
0.80
1.00

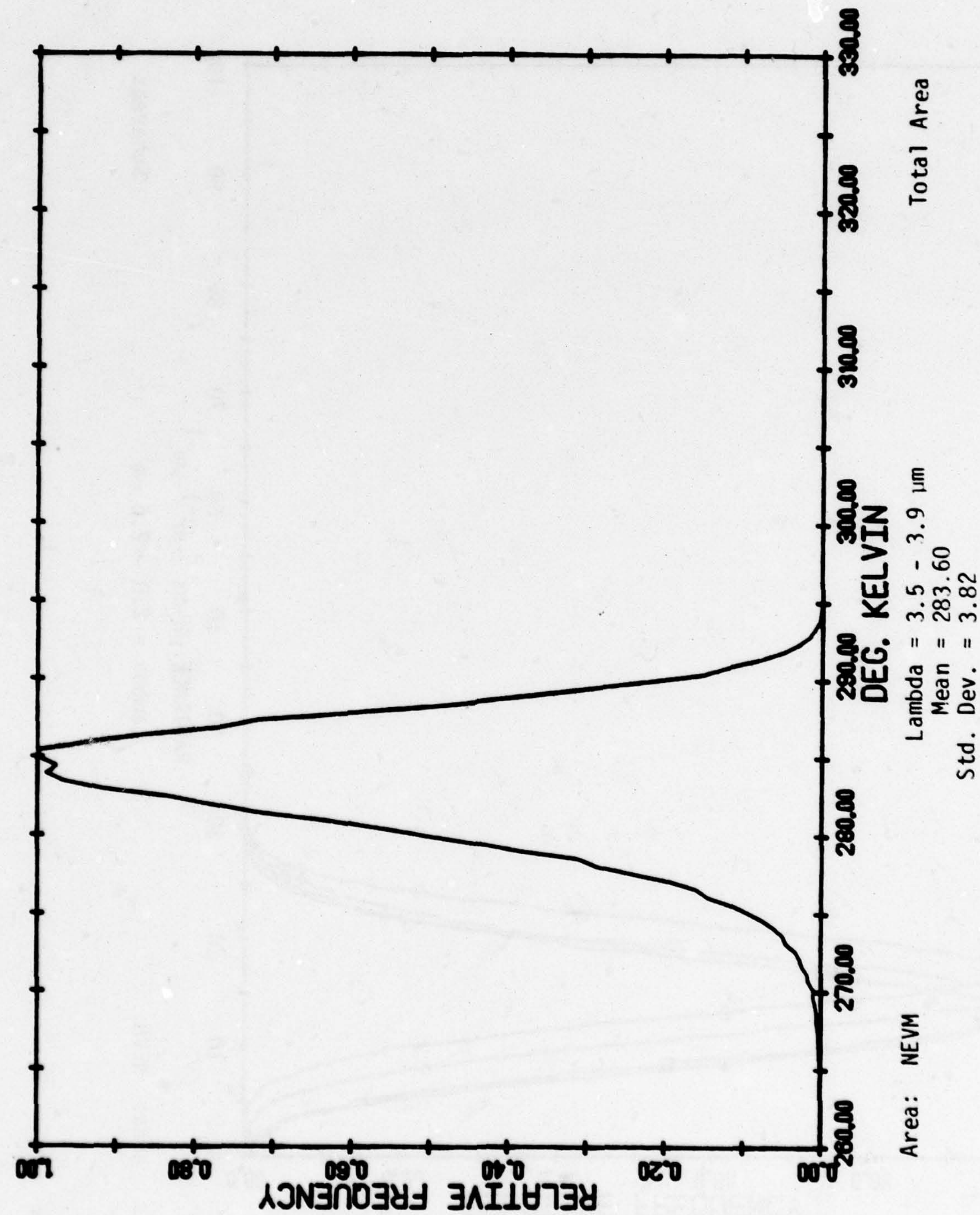
RELATIVE FREQUENCY
0.00
0.20
0.40
0.60
0.80
1.00
DEG. KELVIN
260.00
270.00
280.00
290.00
300.00
310.00
320.00
330.00
Area: NEVM
Total Area
Lambda = 3.5 - 3.9 µm
Mean = 283.60
Std. Dev. = 3.82

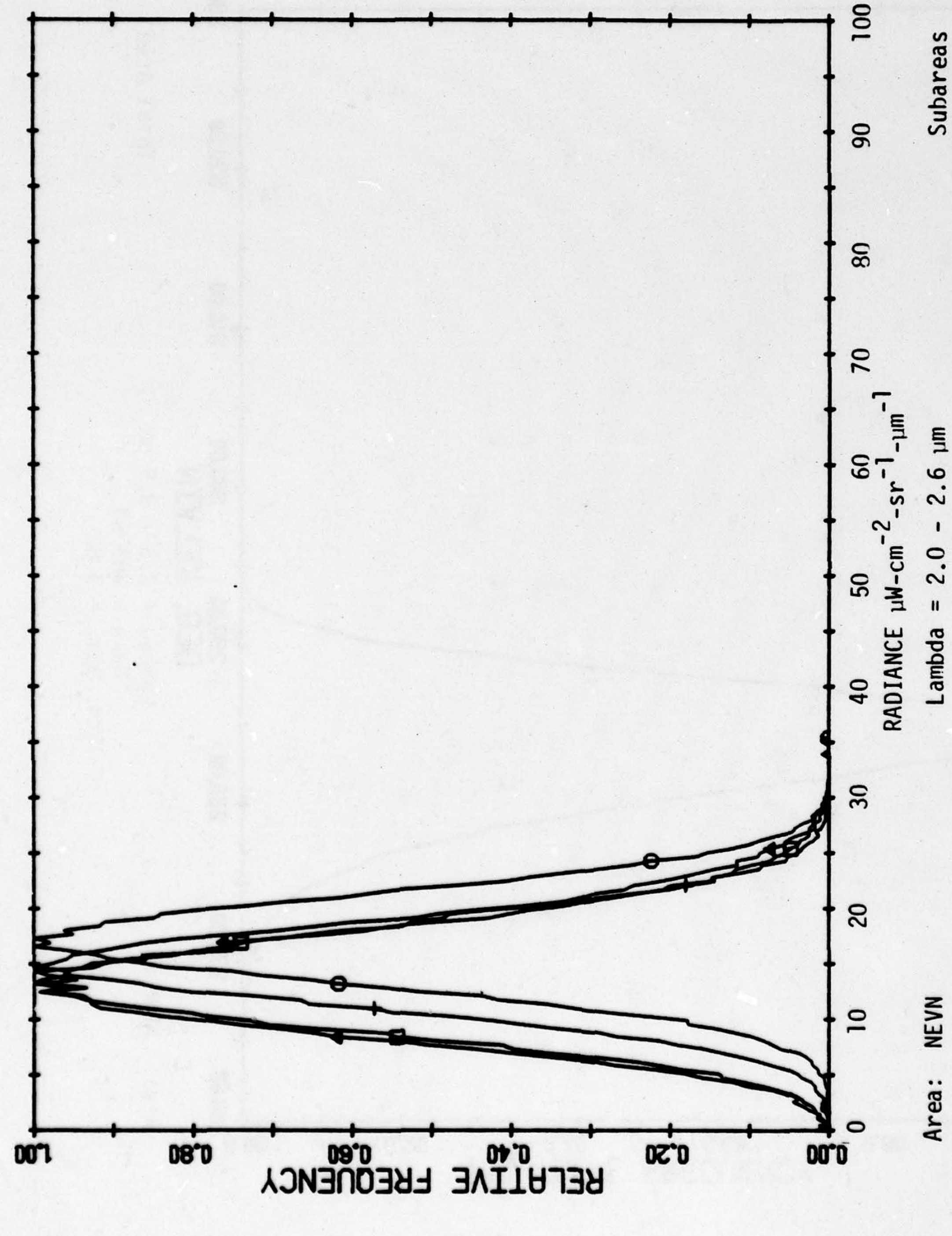
RELATIVE FREQUENCY
0.00
0.20
0.40
0.60
0.80
1.00
0
10
20
30
40
50
60
70
80
90
100
RADIANCE μW-cm-2-sr-1-μm-1
Lambda = 2.0 - 2.6 μm
Area: NEVN
Subareas

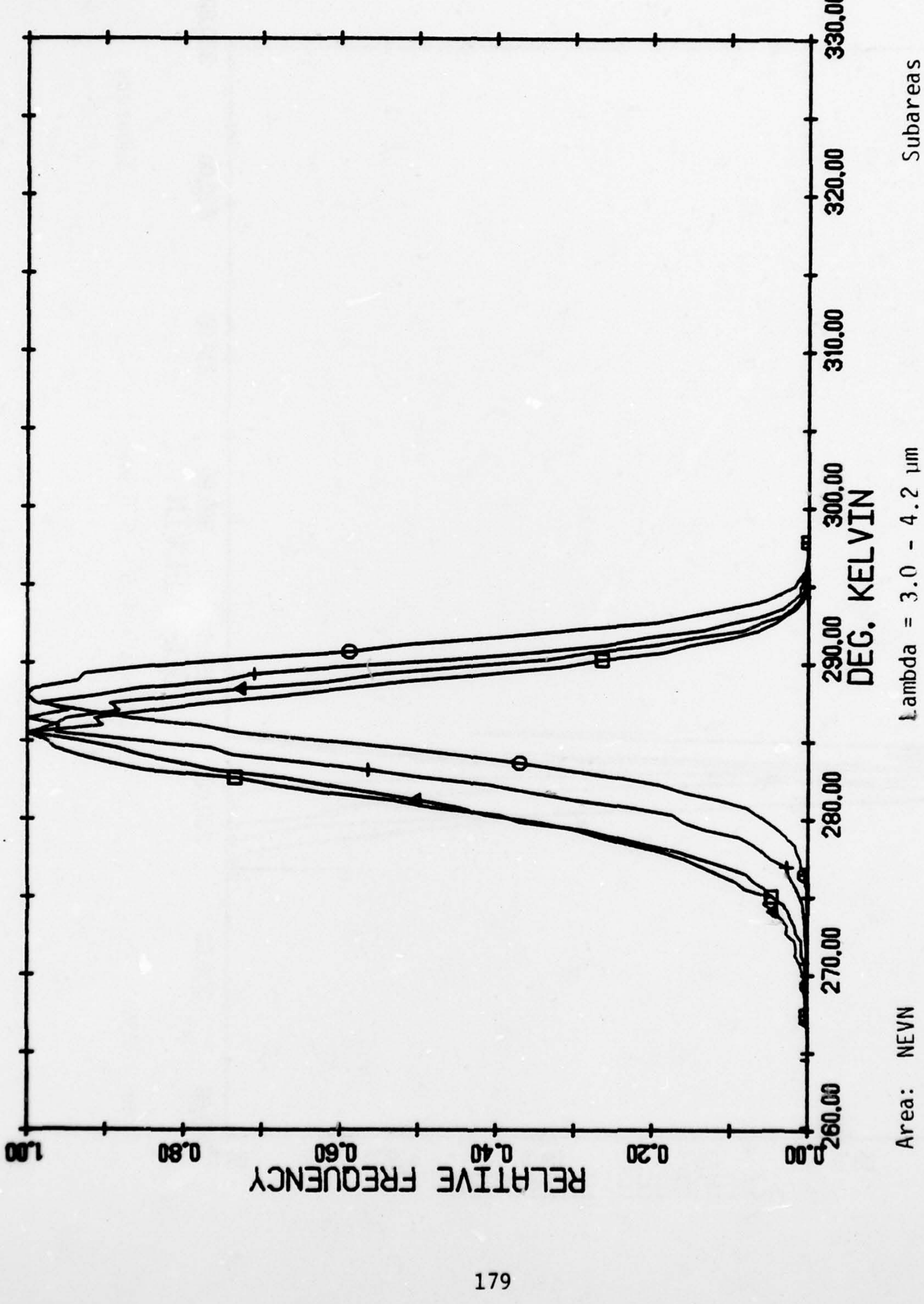
RELATIVE FREQUENCY
0.00
0.20
0.40
0.60
0.80
1.00
DEG. KELVIN
260.00
270.00
280.00
290.00
300.00
310.00
320.00
330.00
Area: NEVN
Lambda = 3.0 - 4.2 µm
Subareas

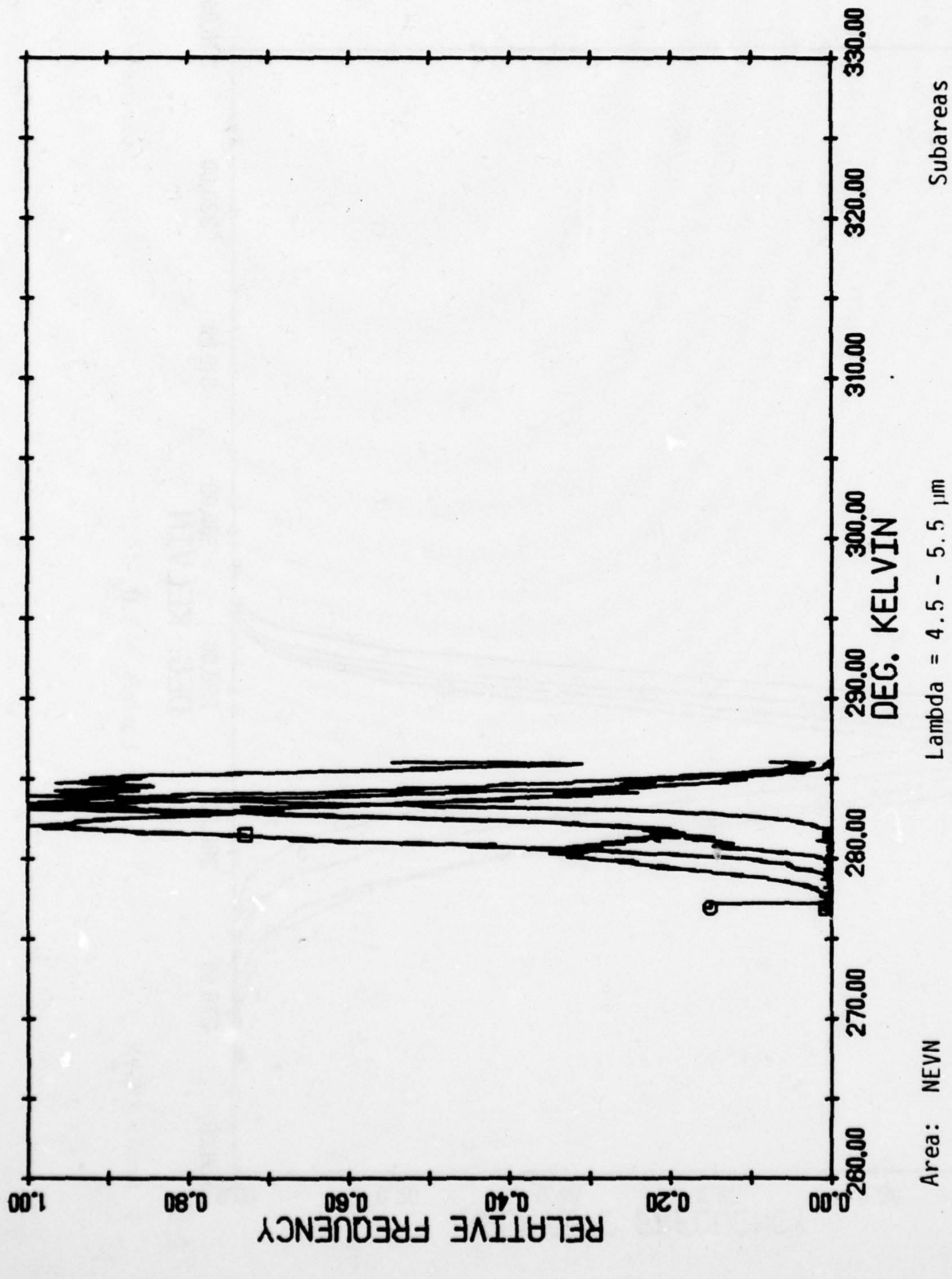
RELATIVE FREQUENCY
0.00
0.20
0.40
0.60
0.80
1.00
DEG. KELVIN
260.00
270.00
280.00
290.00
300.00
310.00
320.00
330.00
Area: NEVN
Lambda = 4.5 - 5.5 μm
Subareas

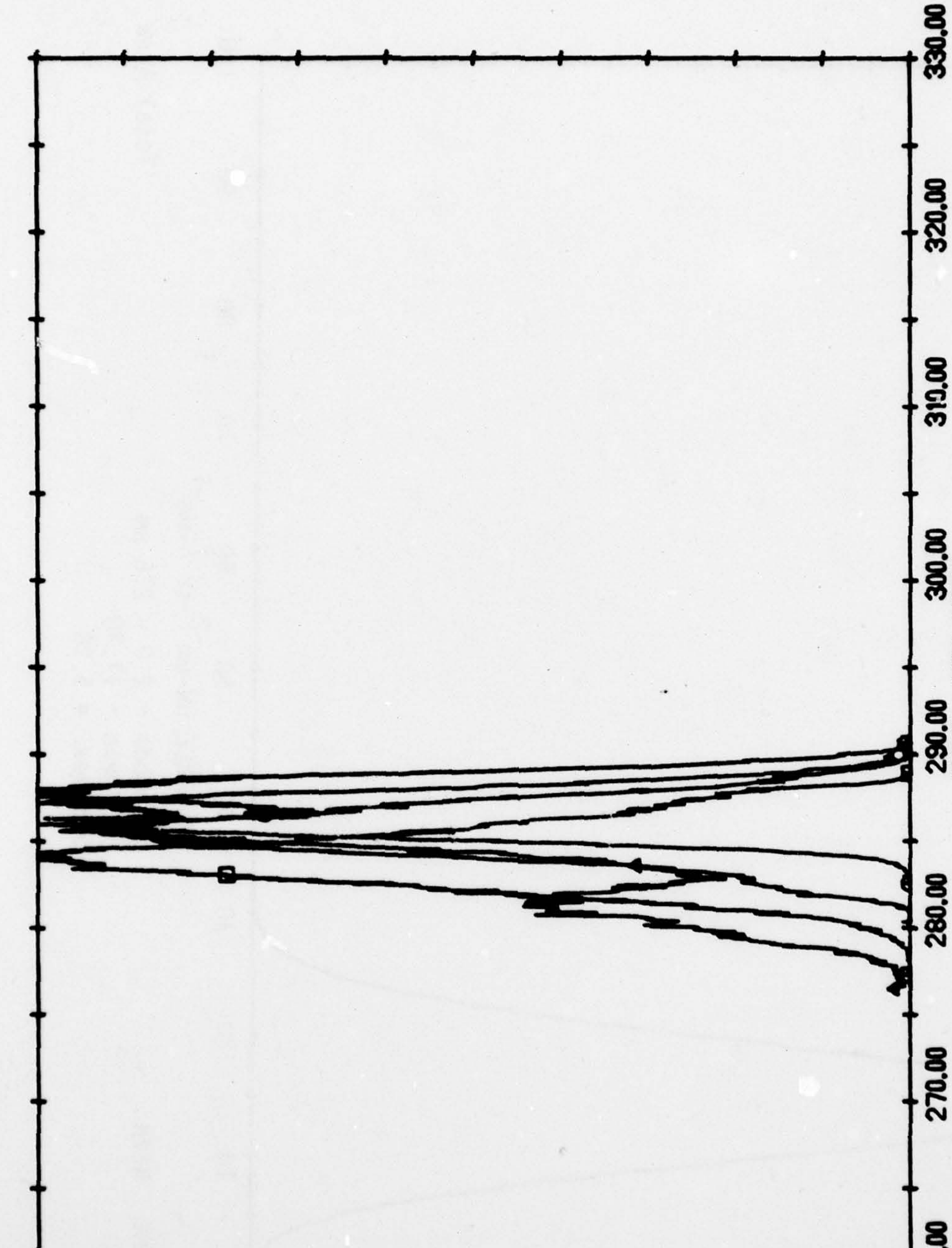

Area: NEVN Lambda = 9.0 - 11.4 μm Subareas

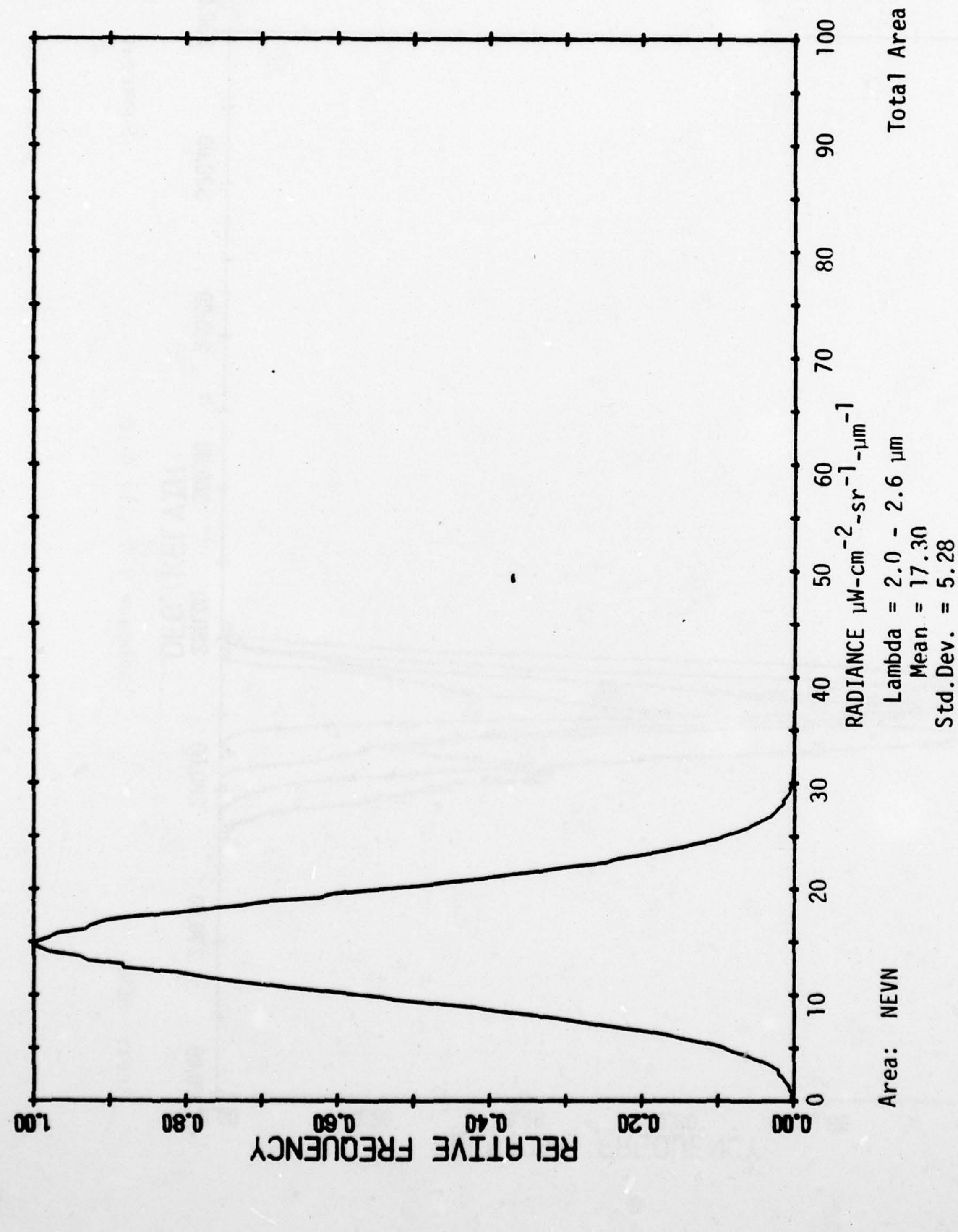
RELATIVE FREQUENCY
0.00
0.20
0.40
0.60
0.80
1.00
0
10
20
30
40
50
60
70
80
90
100
RADIANCE μW-cm^{-2}-sr^{-1}-μm^{-1}
Area: NEVN
Lambda = 2.0 - 2.6 μm
Mean = 17.30
Std.Dev. = 5.28
Total Area

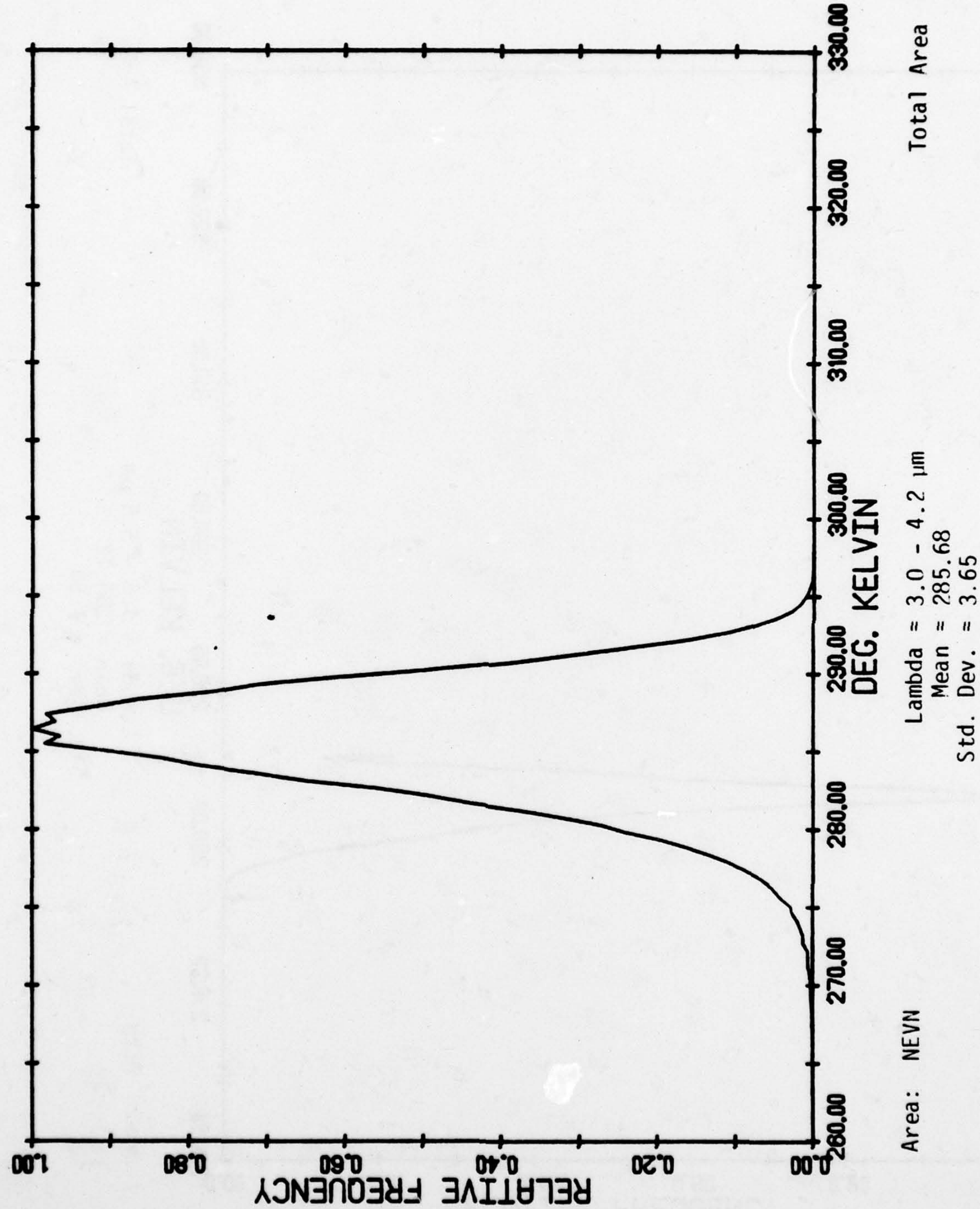
RELATIVE FREQUENCY
0.00
0.20
0.40
0.60
0.80
1.00
DEG. KELVIN
260.00
270.00
280.00
290.00
300.00
310.00
320.00
330.00
Area: NEVN
Lambda = 3.0 - 4.2 µm
Mean = 285.68
Std. Dev. = 3.65
Total Area

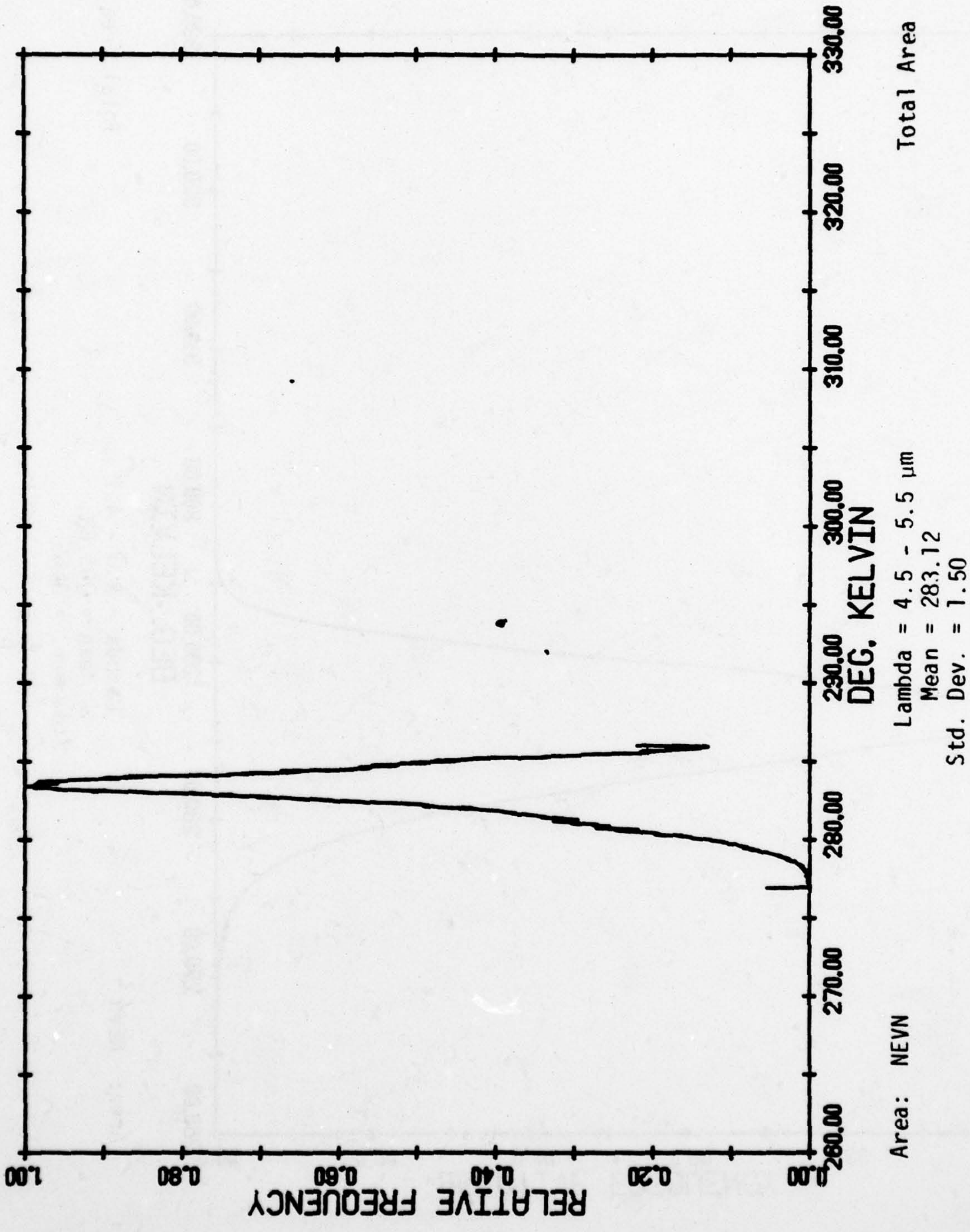

RELATIVE FREQUENCY
0.00
0.20
0.40
0.60
0.80
1.00
260.00
270.00
280.00
290.00
300.00
310.00
320.00
330.00
DEG. KELVIN
Area: NEVN
Total Area
Lambda = 4.5 - 5.5 µm
Mean = 283.12
Std. Dev. = 1.50

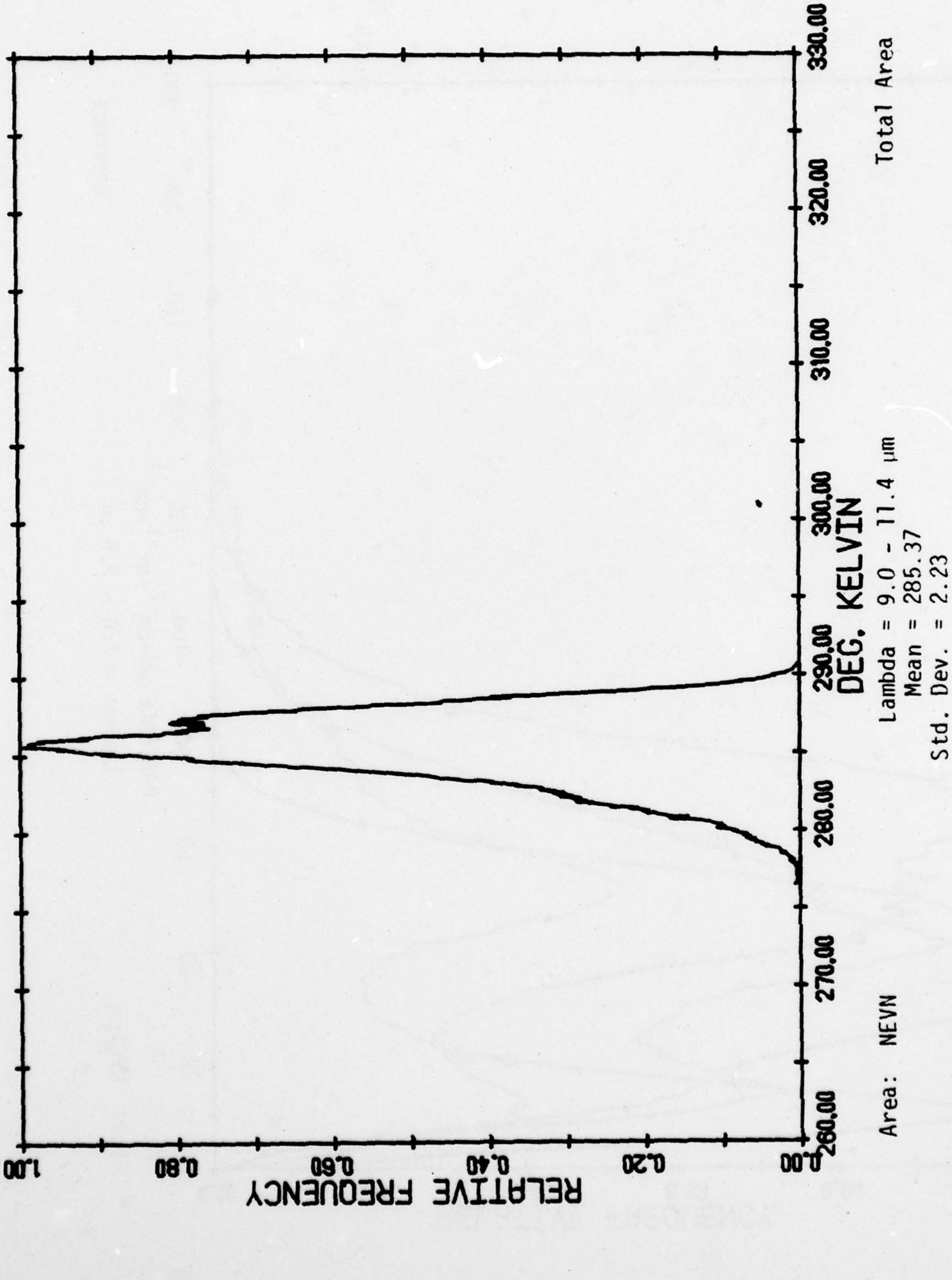

RELATIVE FREQUENCY
0.00
0.20
0.40
0.60
0.80
1.00
DEG. KELVIN
260.00
270.00
280.00
290.00
300.00
310.00
320.00
330.00
Lambda = 9.0 - 11.4 μm
Mean = 285.37
Std. Dev. = 2.23
Area: NEVN
Total Area

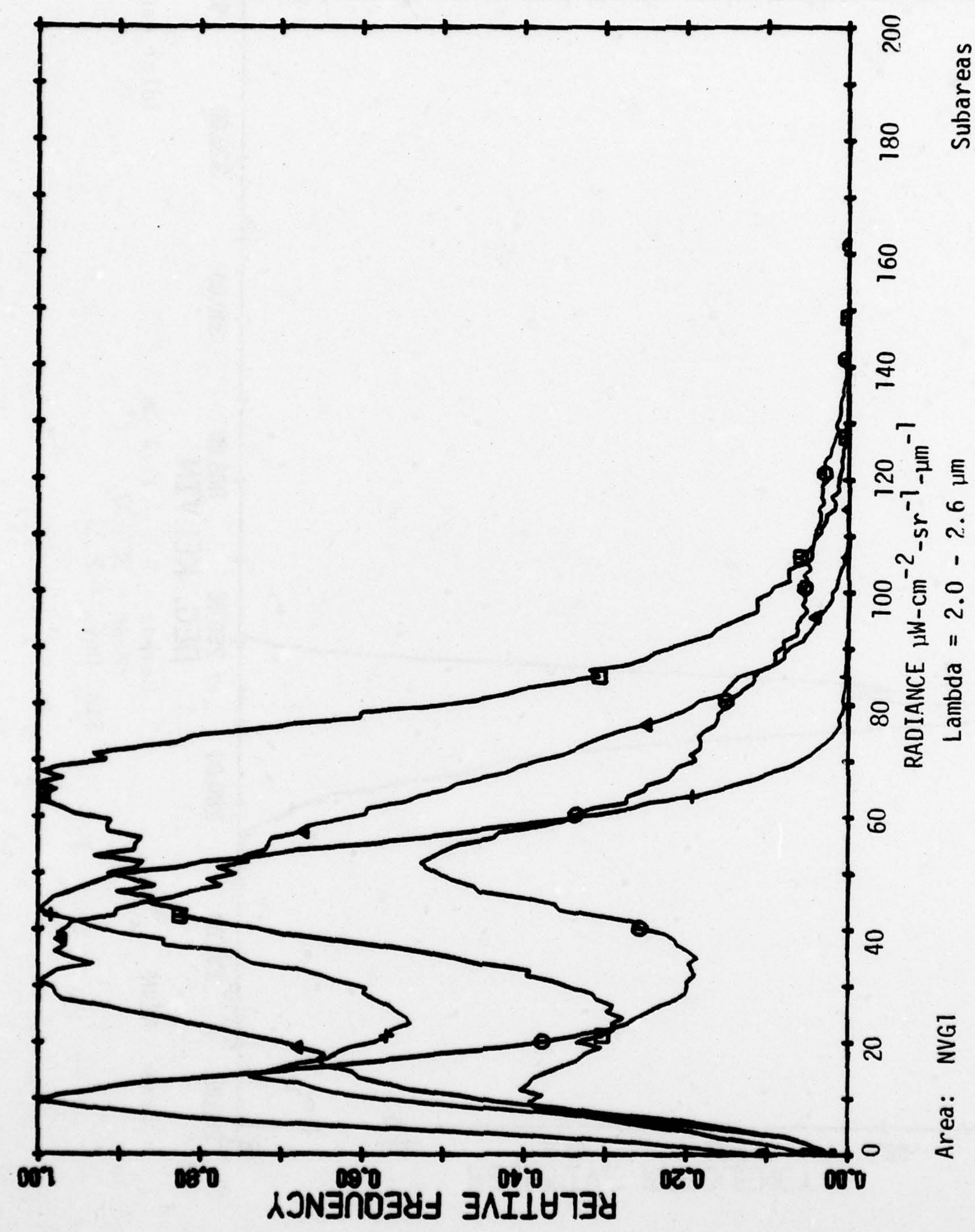

RELATIVE FREQUENCY
0.00
0.20
0.40
0.60
0.80
1.00
0
20
40
60
80
100
120
140
160
180
200
RADIANCE µW-cm^-2-sr^-1-µm^-1
Lambda = 2.0 - 2.6 µm
Area: NVG1
Subareas

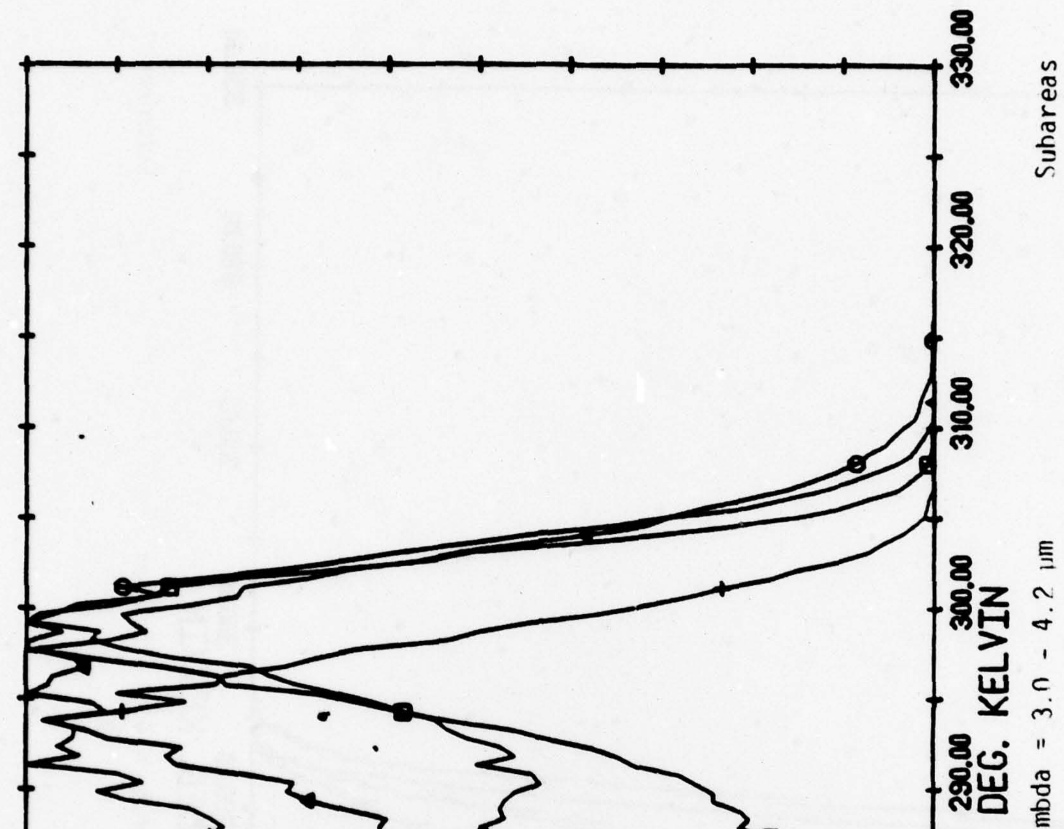
RELATIVE FREQUENCY
0.00
0.20
0.40
0.60
0.80
1.00
260.00
270.00
280.00
290.00
300.00
310.00
320.00
330.00
DEG. KELVIN
Area: NVG1
Lambda = 3.0 - 4.2 μm
Subareas

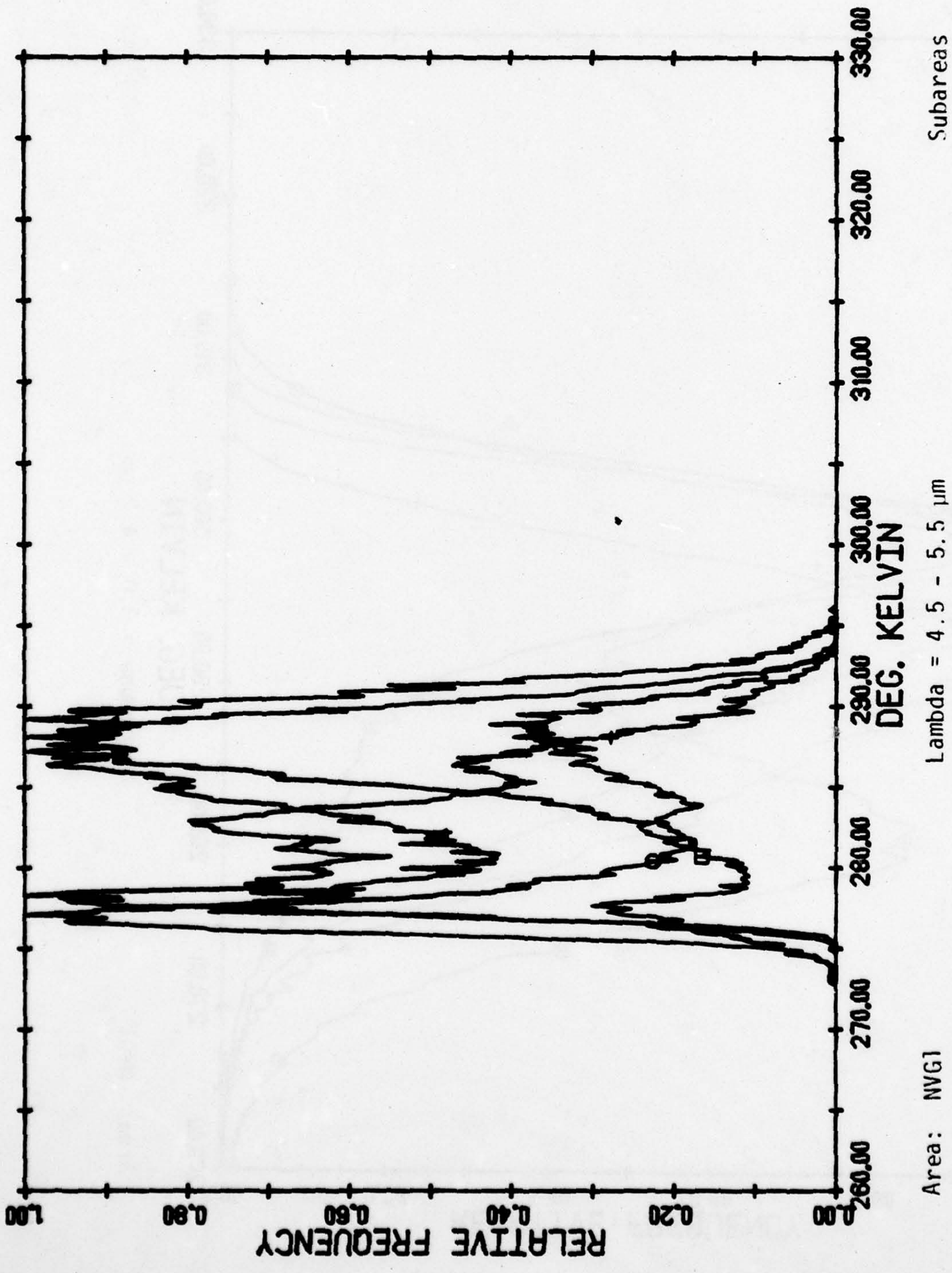
RELATIVE FREQUENCY
0.00
0.20
0.40
0.60
0.80
1.00
260.00
270.00
280.00
290.00
300.00
310.00
320.00
330.00
DEG. KELVIN
Lambda = 4.5 - 5.5 μm
Area: NVG1
Subareas

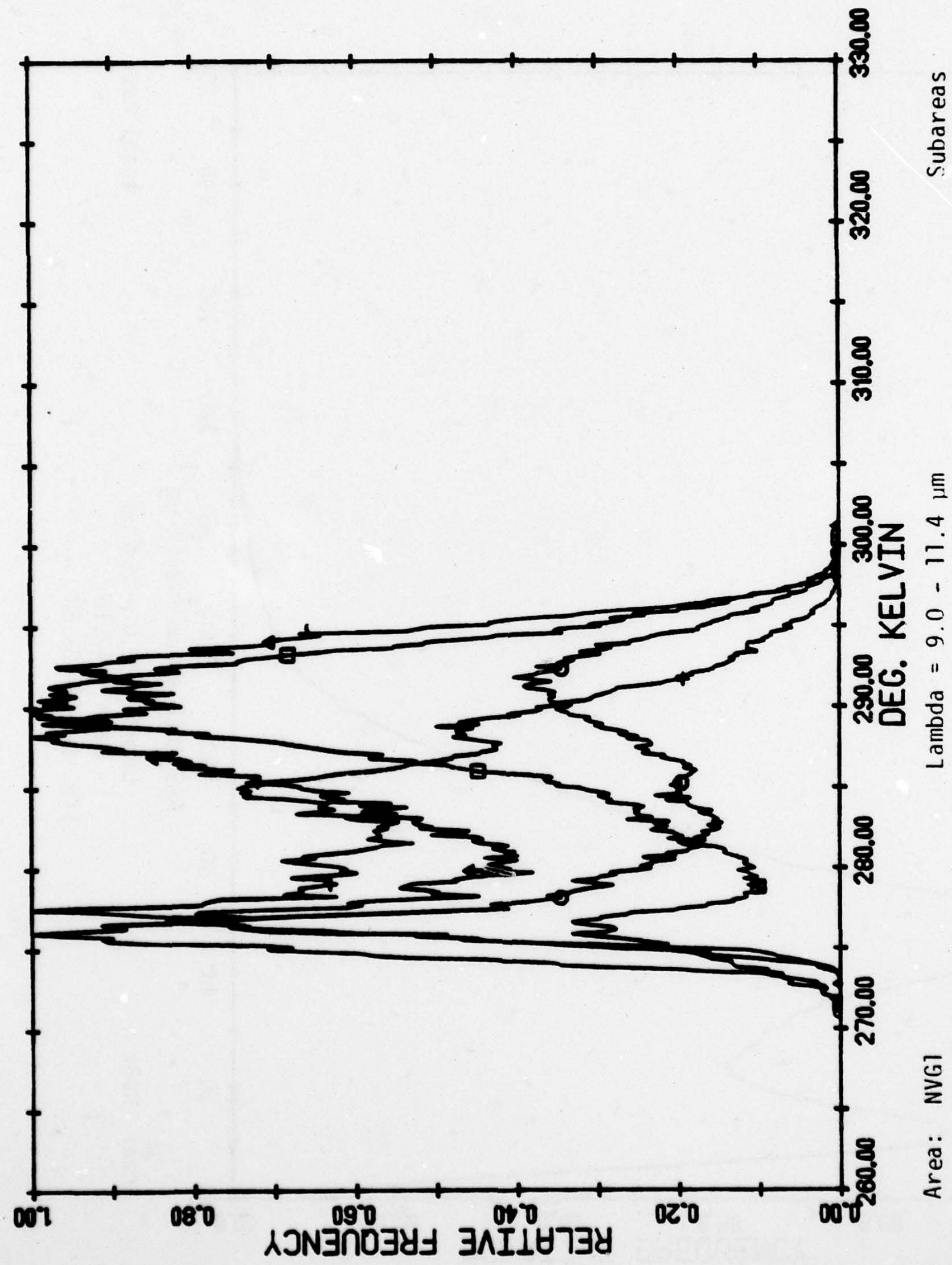
RELATIVE FREQUENCY
0.00
0.20
0.40
0.60
0.80
1.00
DEG. KELVIN
260.00
270.00
280.00
290.00
300.00
310.00
320.00
330.00
Area: NVG1
Lambda = 9.0 - 11.4 μm
Subareas

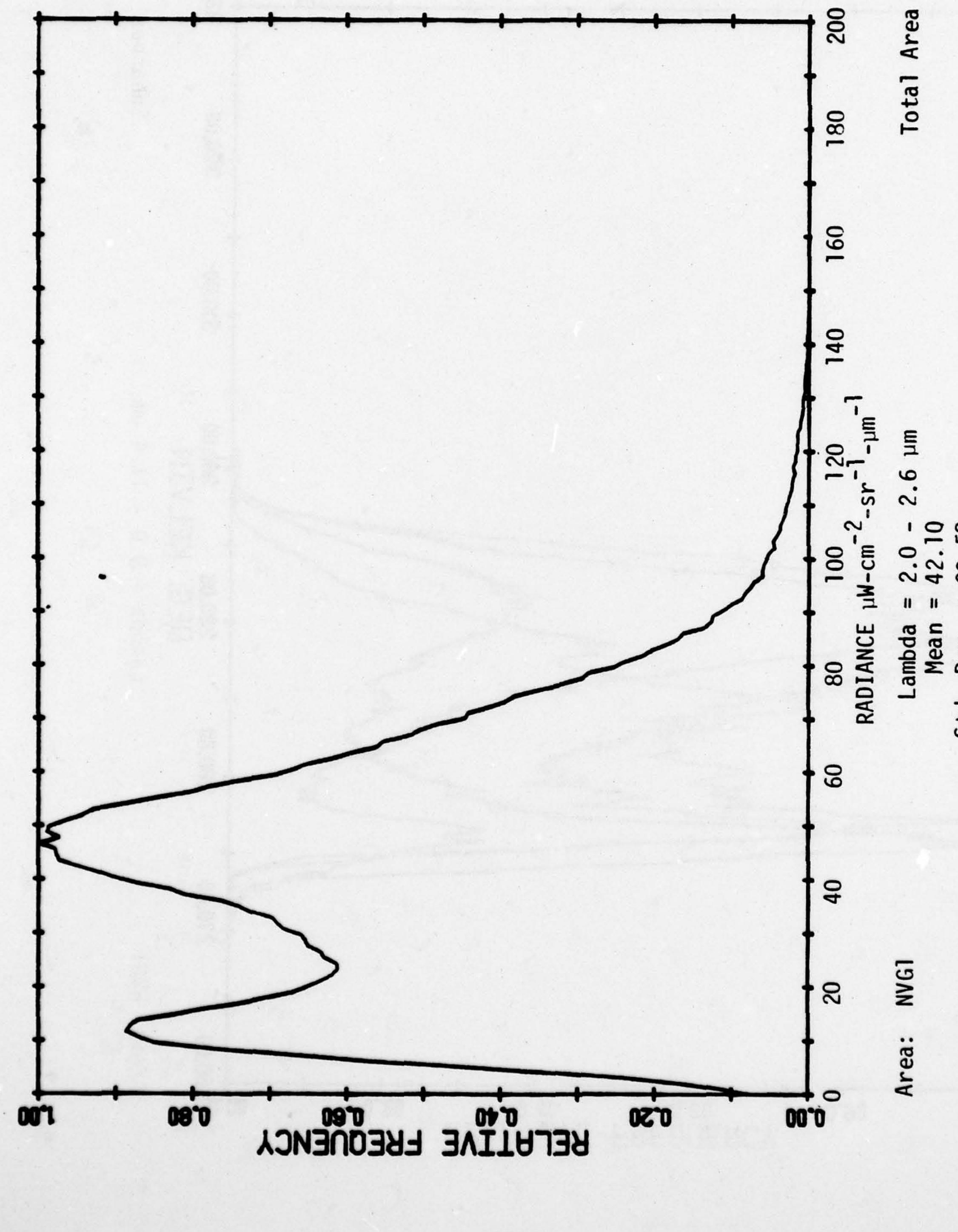
RELATIVE FREQUENCY
0.00
0.20
0.40
0.60
0.80
1.00
0
20
40
60
80
100
120
140
160
180
200
RADIANCE μW-cm^-2-sr^-1-μm^-1
Area: NVG1
Lambda = 2.0 - 2.6 μm
Mean = 42.10
Std. Dev. = 23.58
Total Area

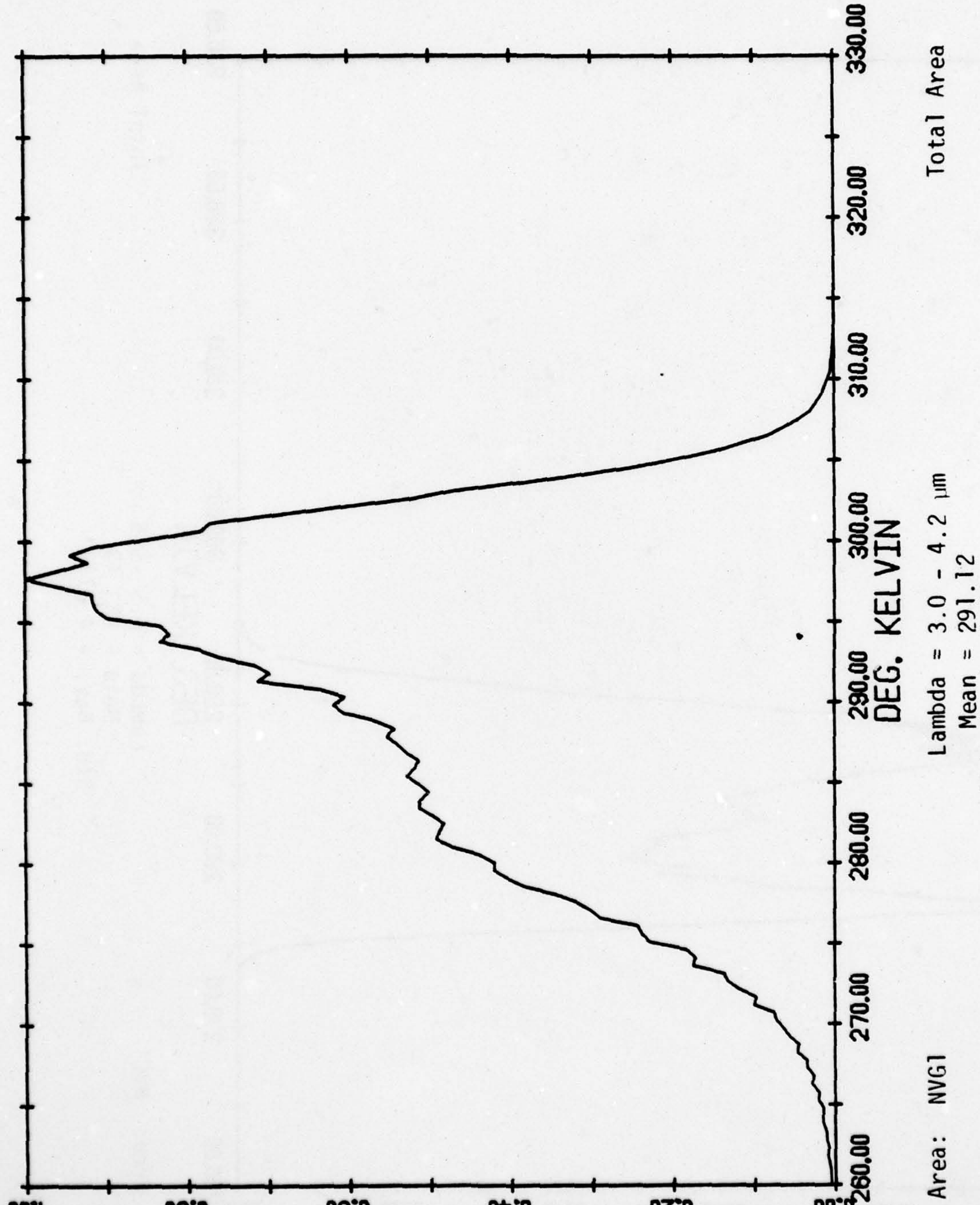
RELATIVE FREQUENCY
0.00
0.20
0.40
0.60
0.80
1.00
DEG. KELVIN
260.00
270.00
280.00
290.00
300.00
310.00
320.00
330.00
Area: NVG1
Total Area
Lambda = 3.0 - 4.2 μm
Mean = 291.12
Std. Dev. = 8.89

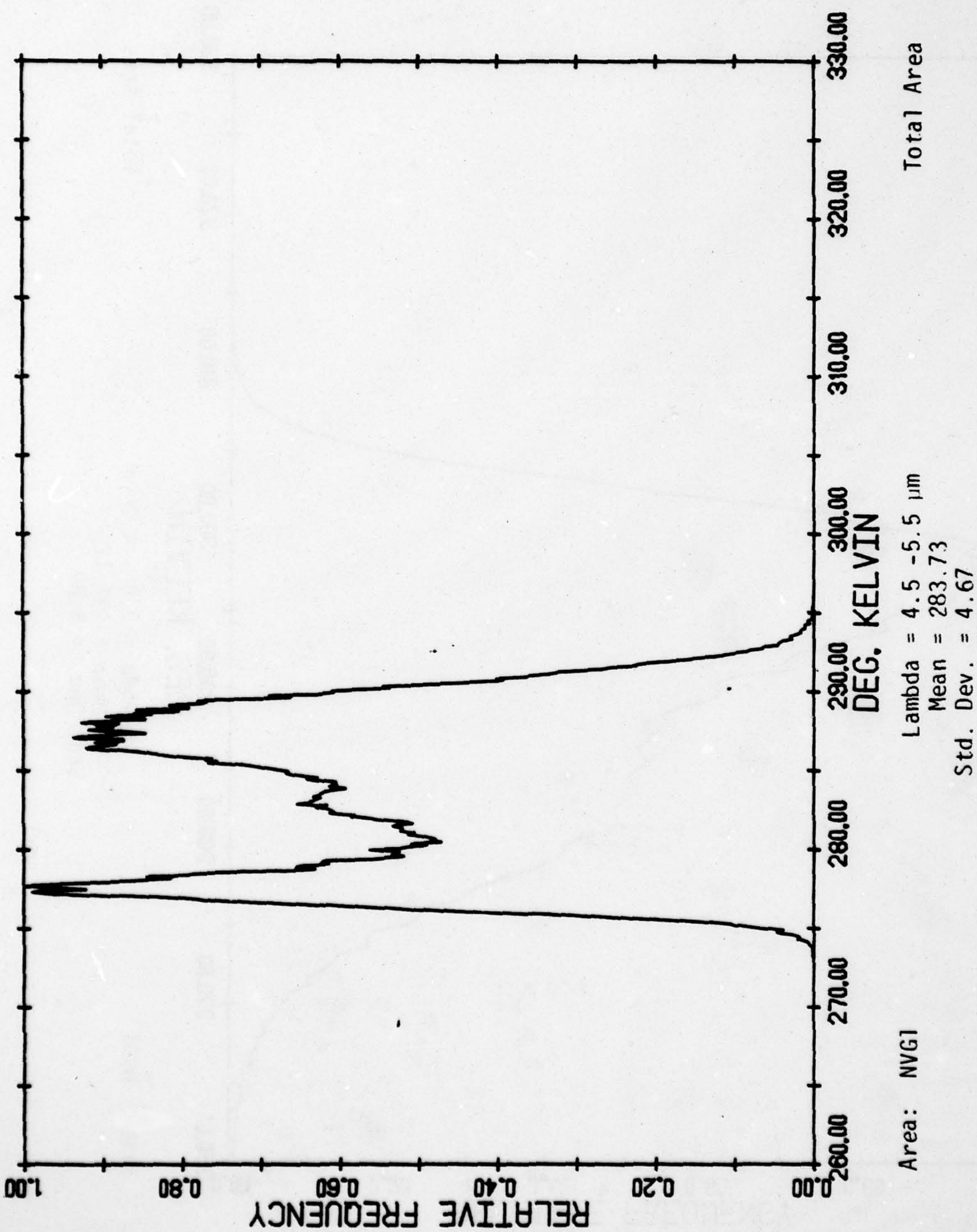
RELATIVE FREQUENCY
0.00
0.20
0.40
0.60
0.80
1.00
260.00
270.00
280.00
290.00
300.00
310.00
320.00
330.00
DEG. KELVIN
Area: NVG1
Lambda = 4.5 -5.5 μm
Mean = 283.73
Std. Dev. = 4.67
Total Area

AD-A068 389 ENVIRONMENTAL RESEARCH INST OF MICHIGAN ANN ARBOR IN--ETC F/G 17/5
STATISTICAL ANALYSES OF TERRAIN DATA.(U)
FEB 79 A J LAROCCA, J R MAXWELL N60530-78-C-0009
UNCLASSIFIED ERIM-132300-2-F NL

3 OF 3
AD
A068389

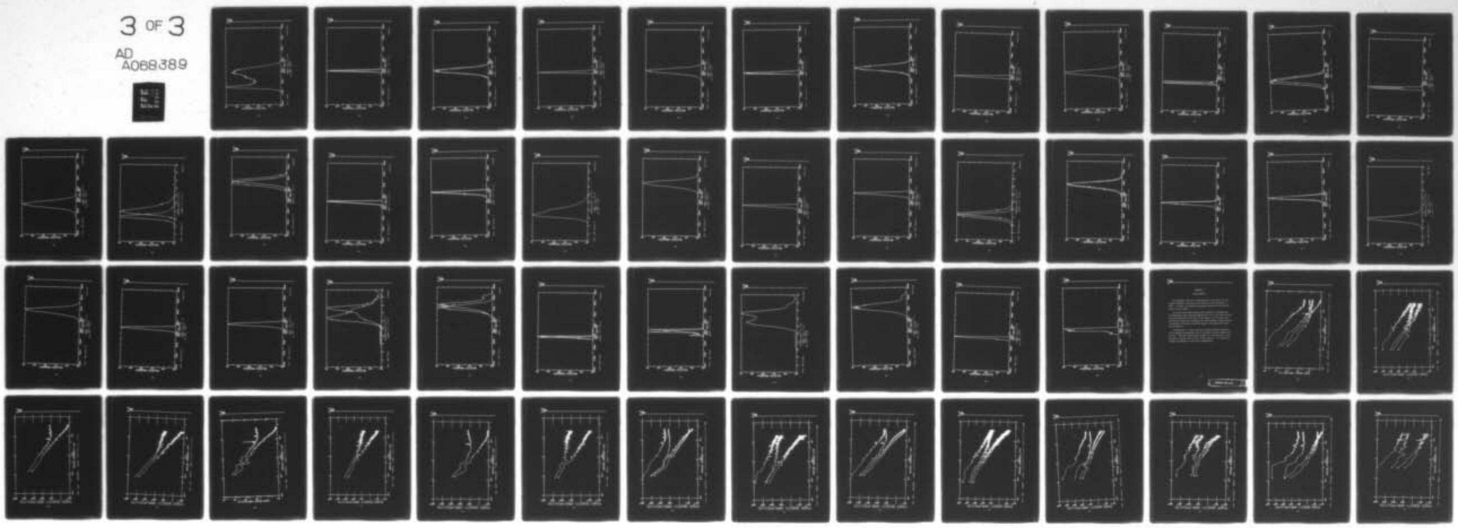

END
DATE
FILMED
6-79
DDC

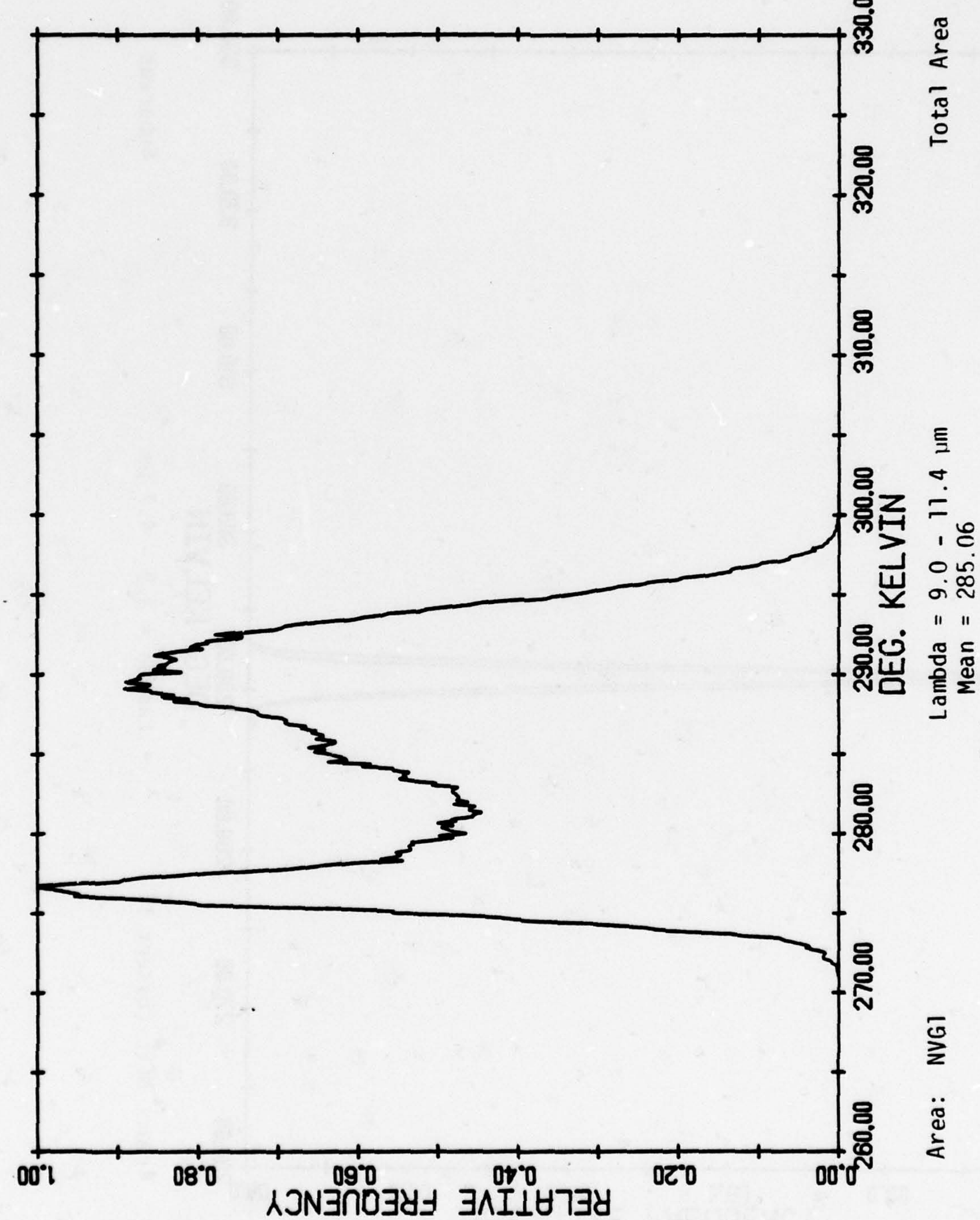

RELATIVE FREQUENCY
0.00
0.20
0.40
0.60
0.80
1.00
DEG. KELVIN
260.00
270.00
280.00
290.00
300.00
310.00
320.00
330.00
Area: NVG1
Lambda = 9.0 - 11.4 μm
Mean = 285.06
Std. Dev. = 6.35
Total Area

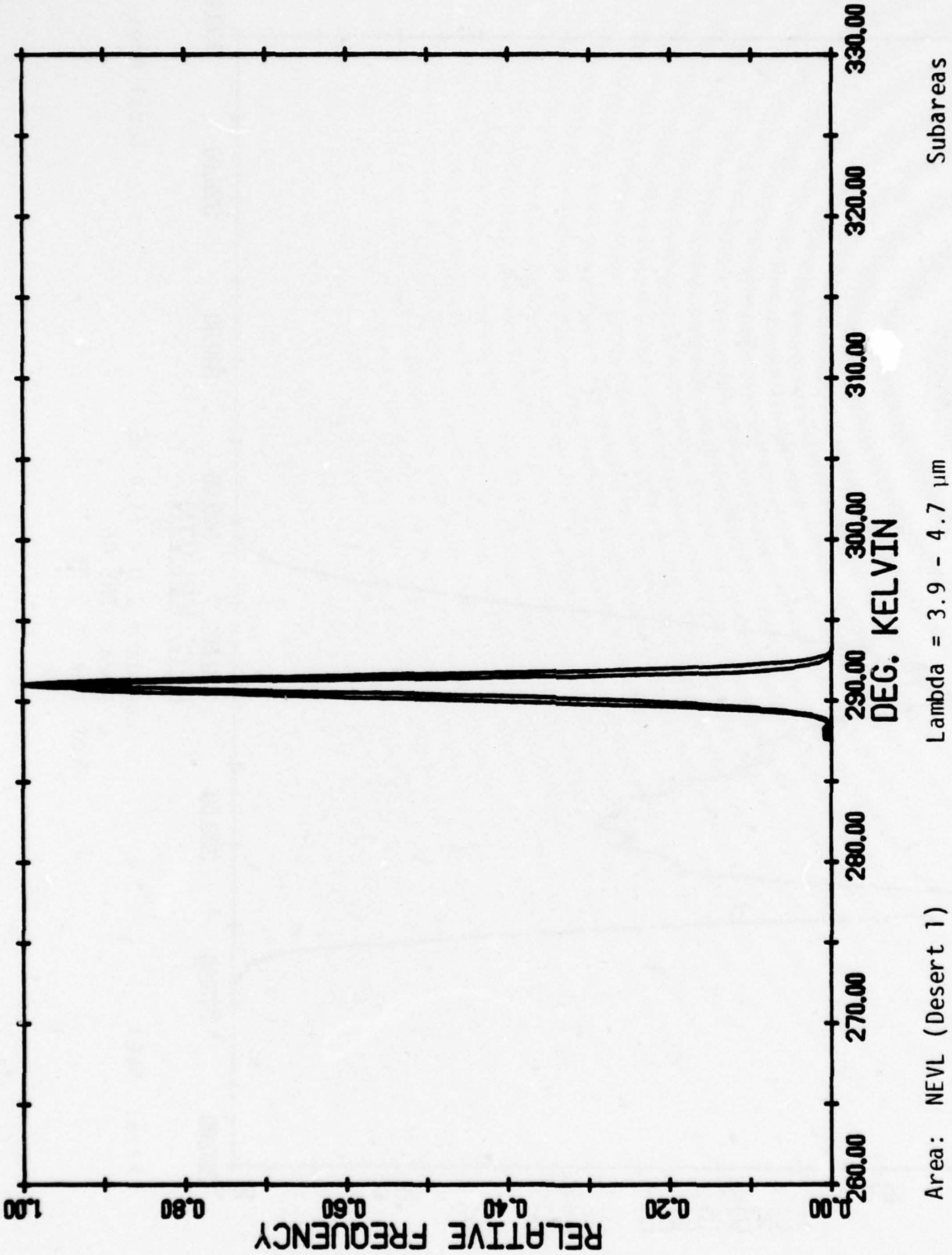
RELATIVE FREQUENCY
1.00
0.80
0.60
0.40
0.20
0.00
260.00
270.00
280.00
290.00
300.00
310.00
320.00
330.00
DEG. KELVIN
Area: NEVL (Desert 1)
Lambda = 3.9 - 4.7 µm
Subareas

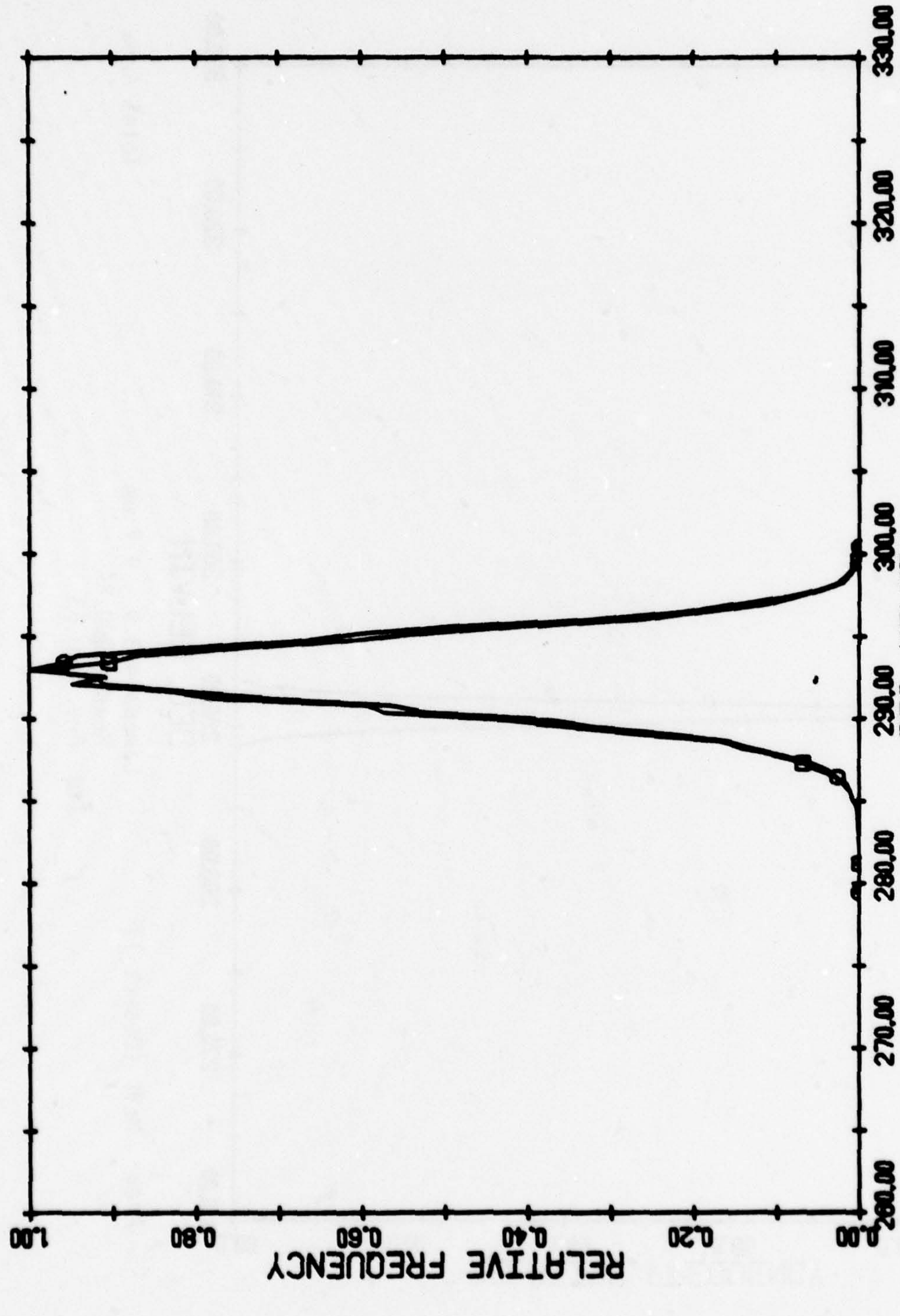

Area: NEVL (Desert 1) Lambda = 3.5 - 3.9 μm Subareas

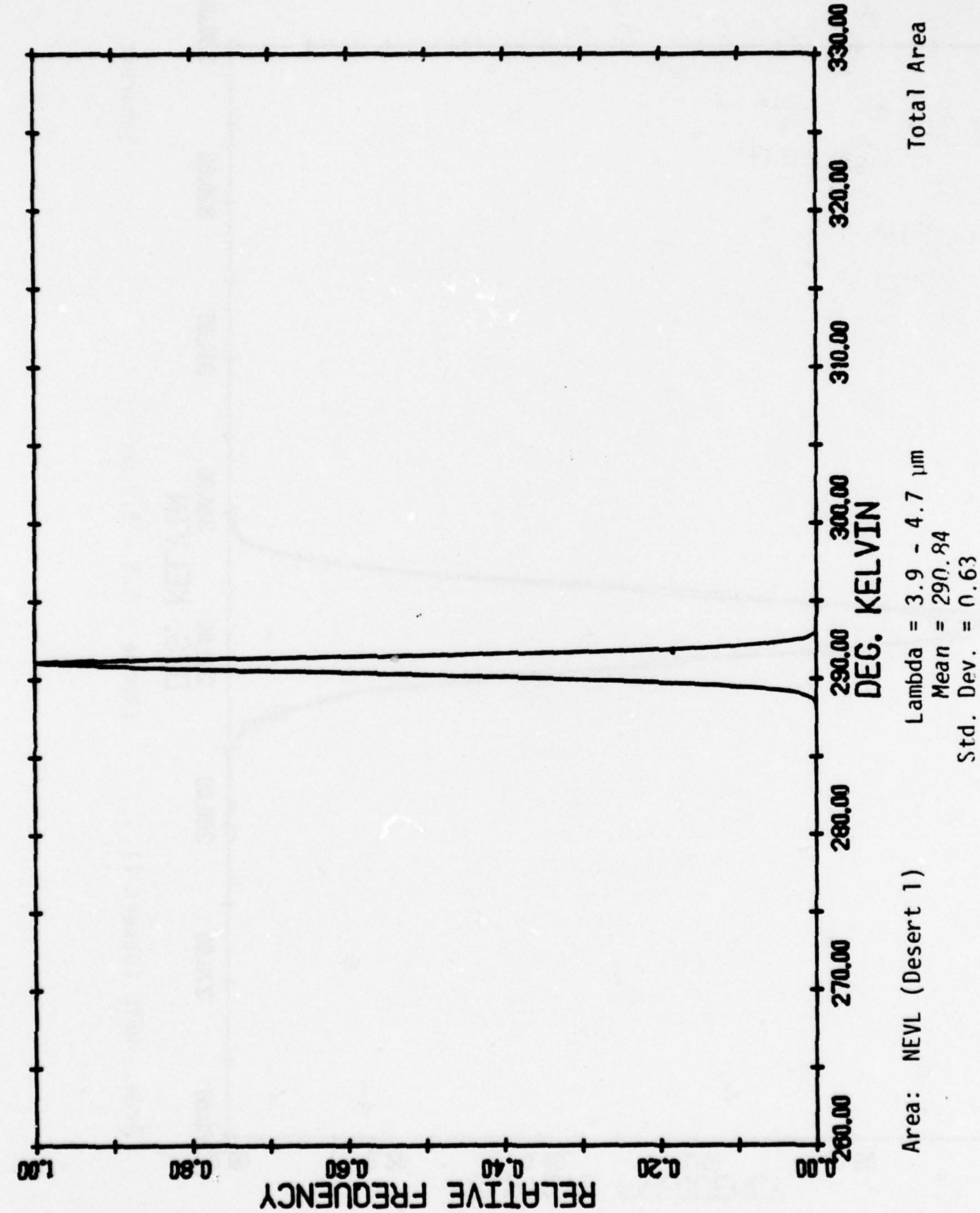
RELATIVE FREQUENCY
0.00
0.20
0.40
0.60
0.80
1.00
260.00
270.00
280.00
290.00
300.00
310.00
320.00
330.00
DEG. KELVIN
Area: NEVL (Desert 1)
Lambda = 3.9 - 4.7 µm
Mean = 290.84
Std. Dev. = 0.63
Total Area

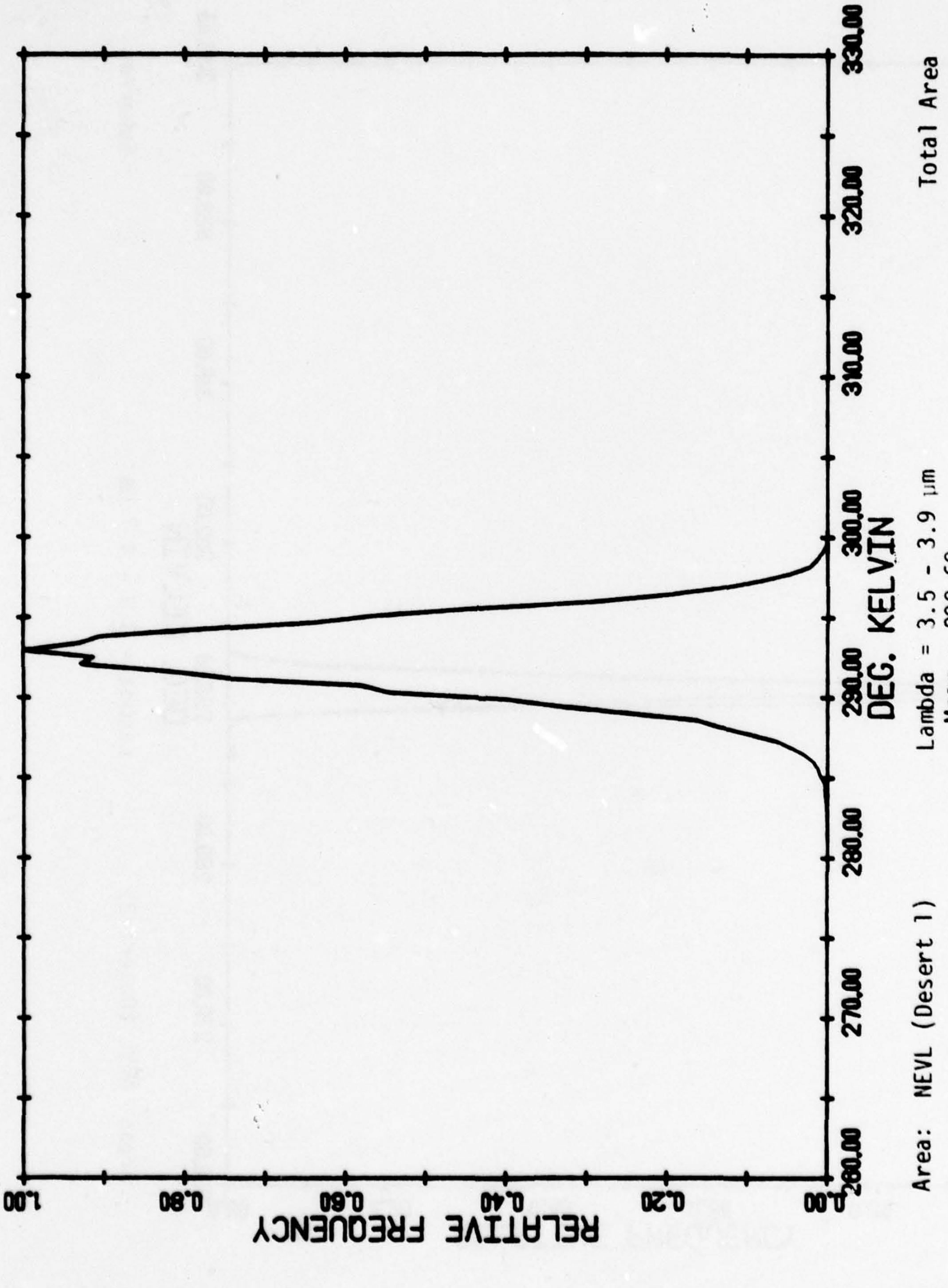
RELATIVE FREQUENCY
1.00
0.80
0.60
0.40
0.20
0.00
260.00
270.00
280.00
290.00
300.00
310.00
320.00
330.00
DEG. KELVIN
Area: NEVL (Desert 1)
Lambda = 3.5 - 3.9 µm
Mean = 292.60
Std. Dev. = 2.21
Total Area

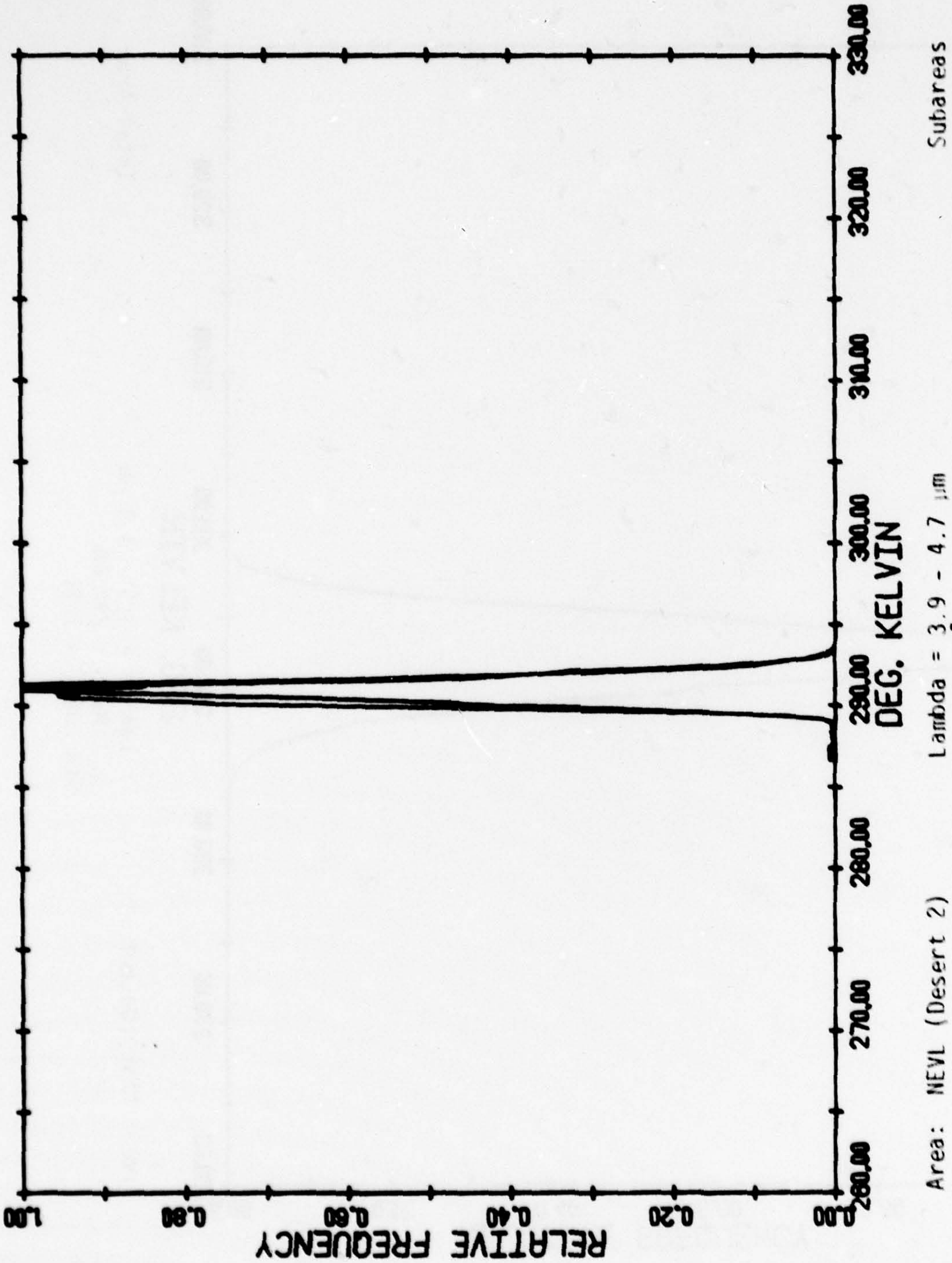
RELATIVE FREQUENCY
0.00
0.20
0.40
0.60
0.80
1.00
DEG. KELVIN
260.00
270.00
280.00
290.00
300.00
310.00
320.00
330.00
Area: NEVL (Desert 2)
Lambda = 3.9 - 4.7 µm
Subareas

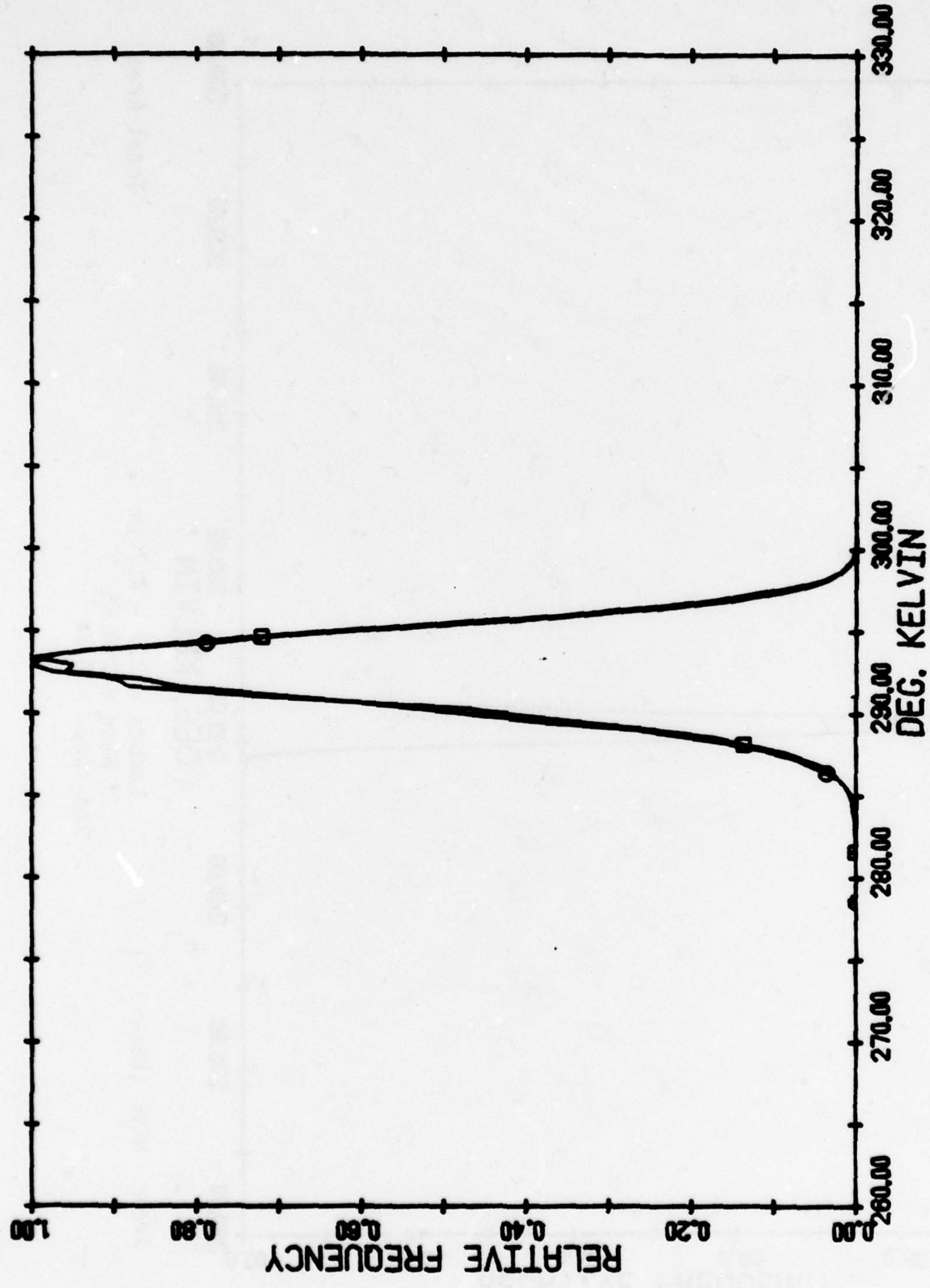

Area: NEVL (Desert 2) Lambda = 3.5 - 3.9 μm Subareas

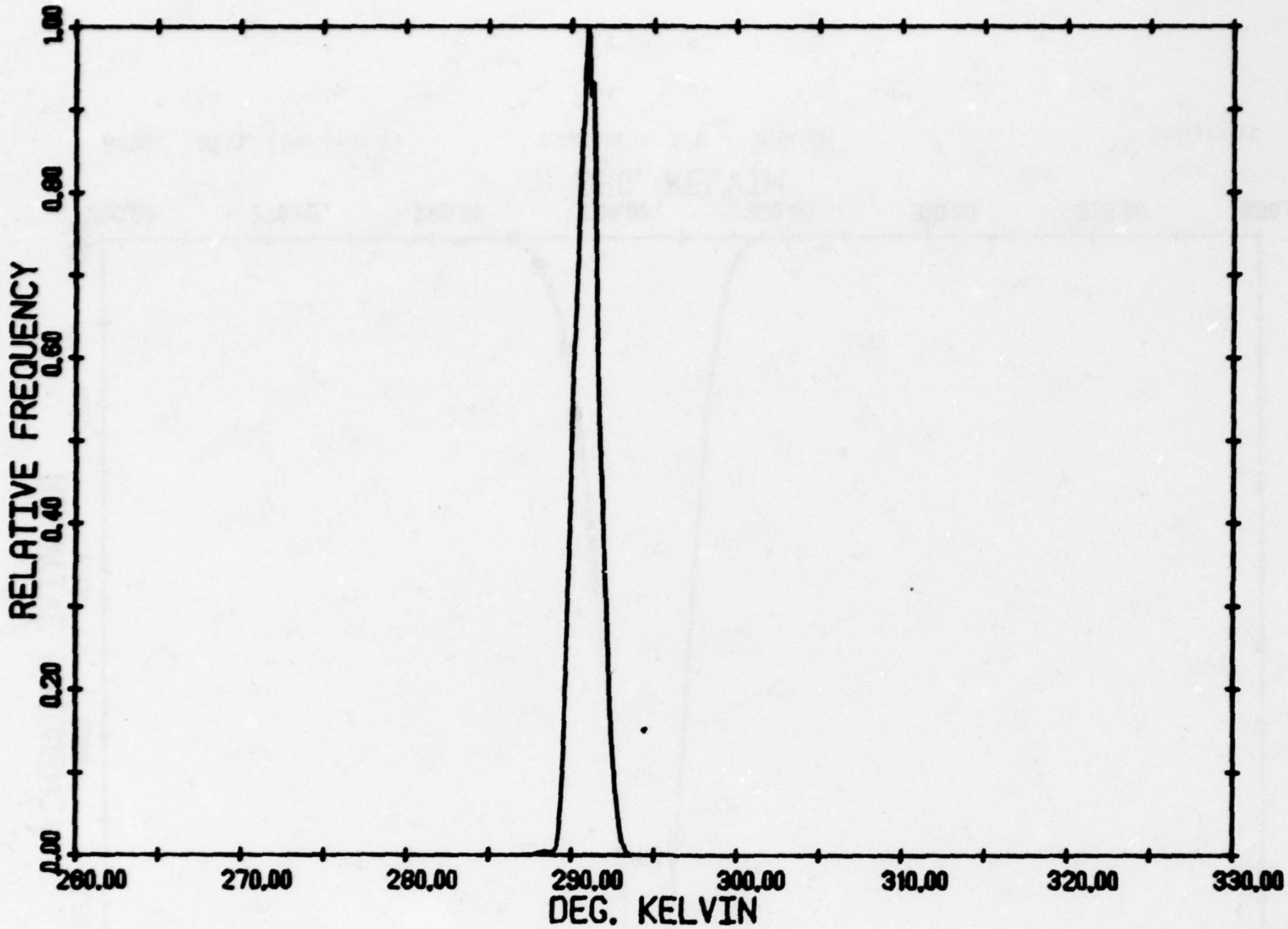

Area: NEVL (Desert 2)

Lambda = 3.9 - 4.7 μm
Mean = 290.95
Std. Dev. = 0.74

Total Area

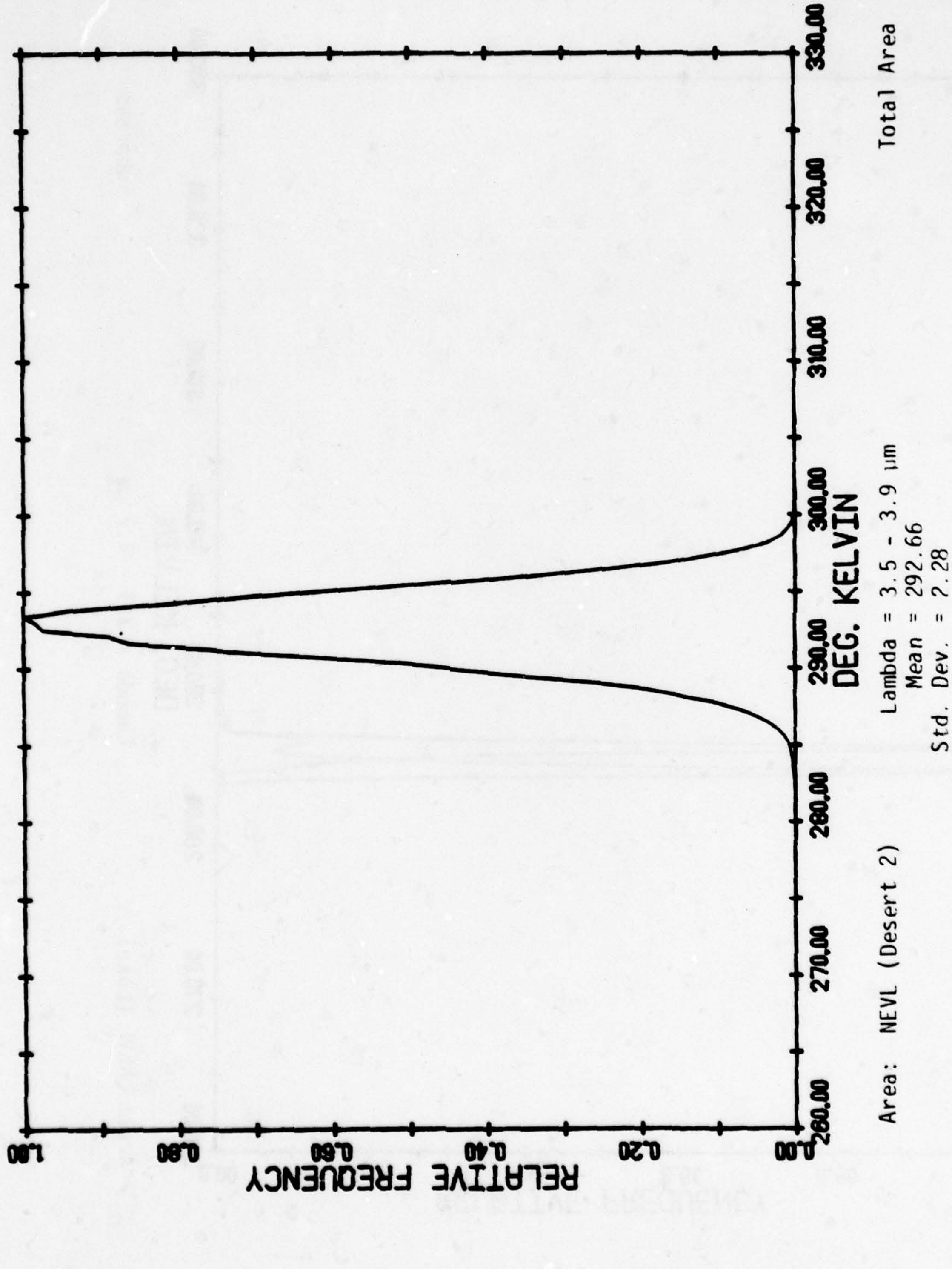
RELATIVE FREQUENCY
1.00
0.80
0.60
0.40
0.20
0.00
260.00
270.00
280.00
290.00
300.00
310.00
320.00
330.00
DEG. KELVIN
Area: NEVL (Desert 2)
Total Area
Lambda = 3.5 - 3.9 μm
Mean = 292.66
Std. Dev. = 2.28

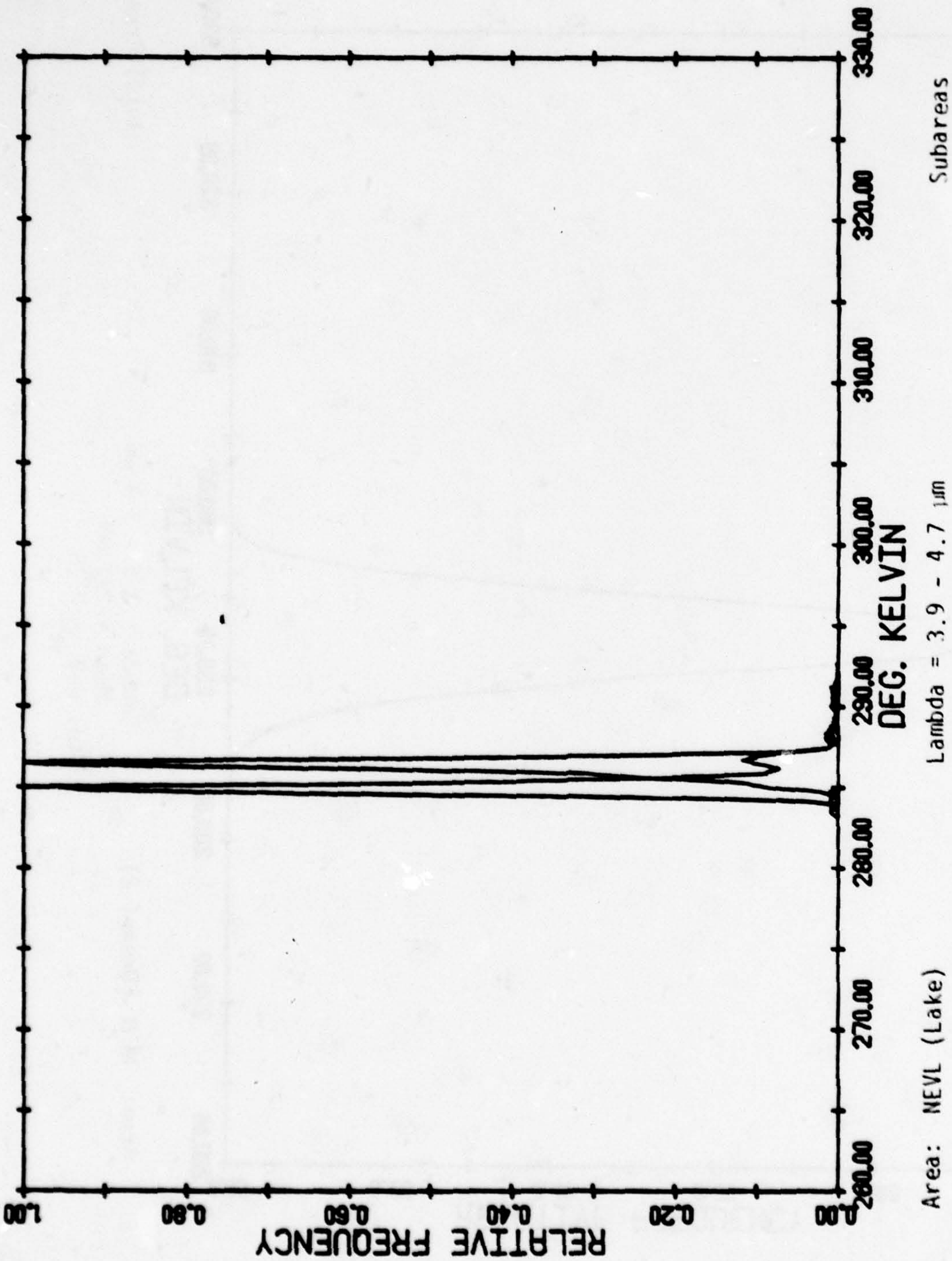
RELATIVE FREQUENCY
0.00
0.20
0.40
0.60
0.80
1.00
260.00
270.00
280.00
290.00
300.00
310.00
320.00
330.00
DEG. KELVIN
Area: NEVL (Lake)
Lambda = 3.9 - 4.7 μm
Subareas

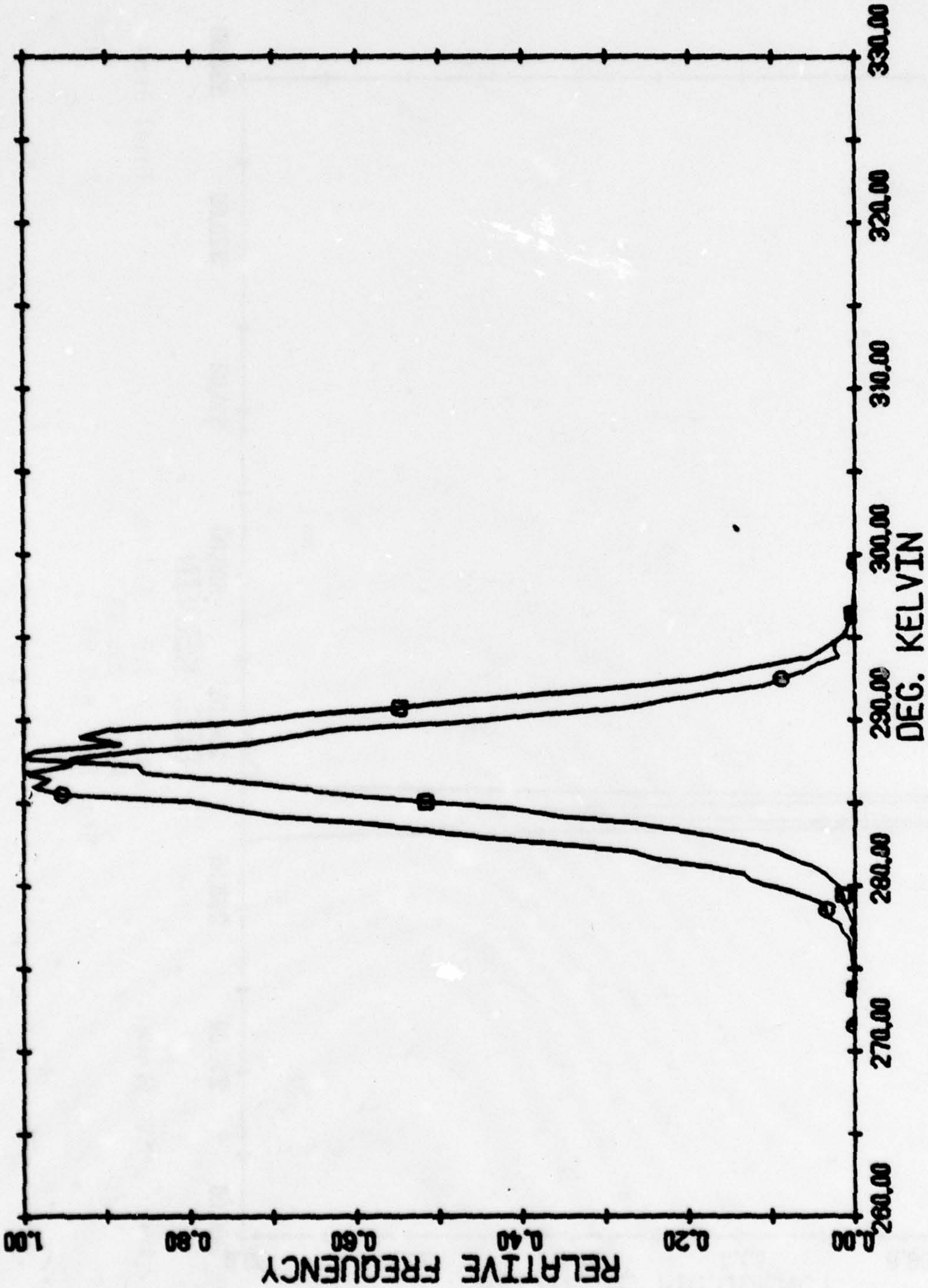

Area: NEVL (Lake) Lambda = 3.5 - 3.9 µm Subareas

ERIM

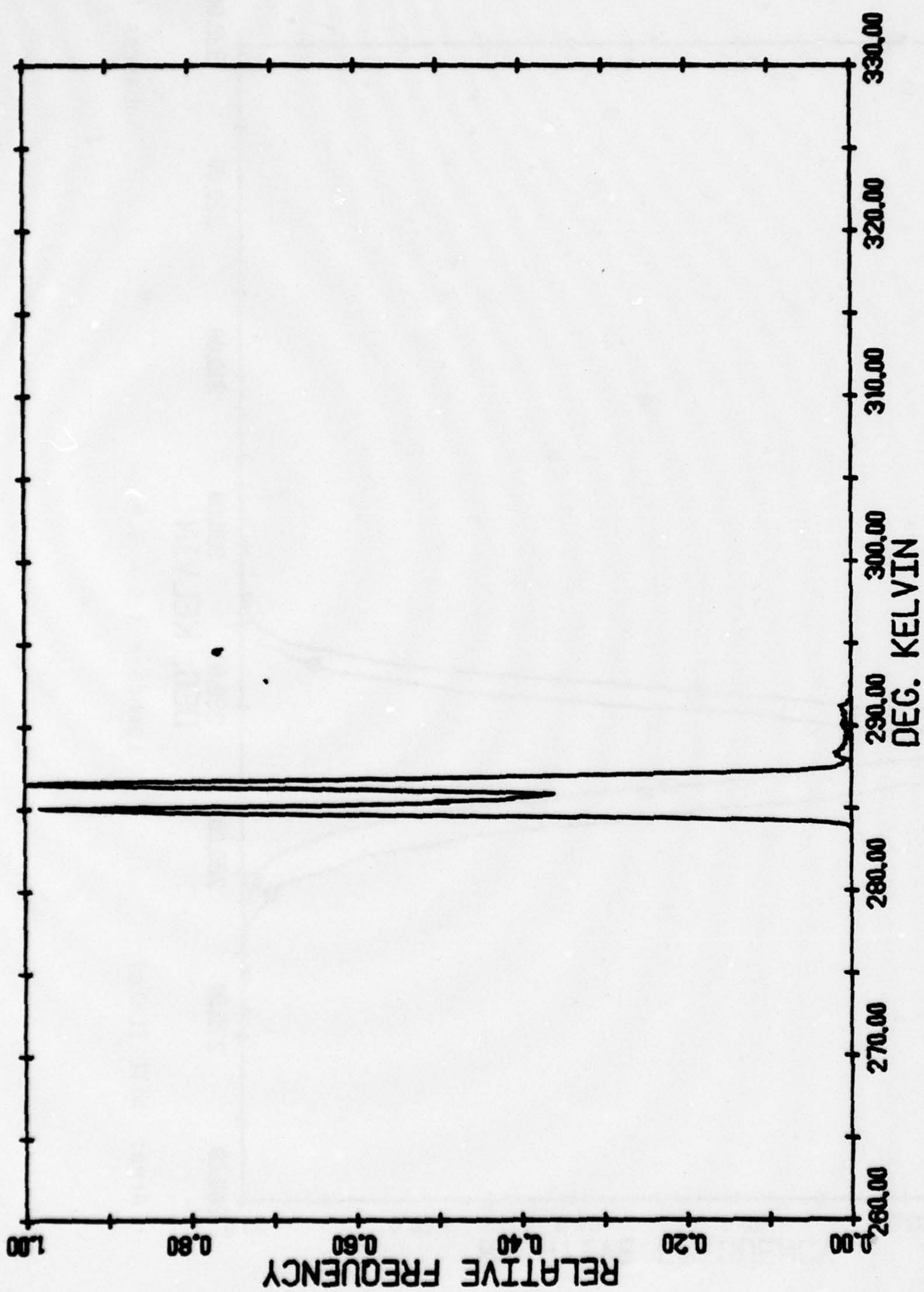

Area: NEVL (Lake)

Lambda = 3.9 - 4.7 μm
Mean = 285.83
Std. Dev. = 0.98

Total Area

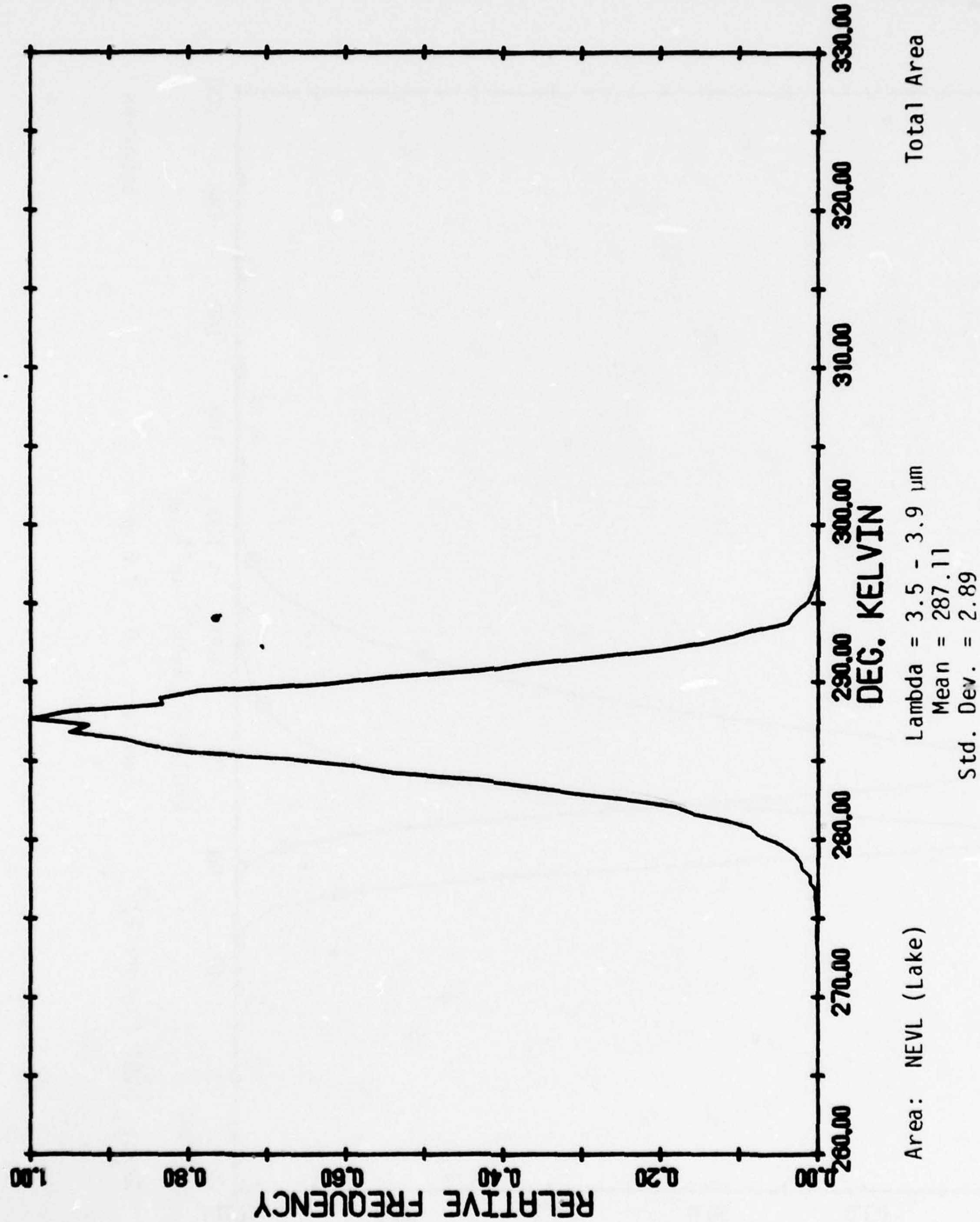

RELATIVE FREQUENCY
0.00
0.20
0.40
0.60
0.80
1.00
DEG. KELVIN
260.00
270.00
280.00
290.00
300.00
310.00
320.00
330.00
Area: NEVL (Lake)
Lambda = 3.5 - 3.9 µm
Mean = 287.11
Std. Dev. = 2.89
Total Area

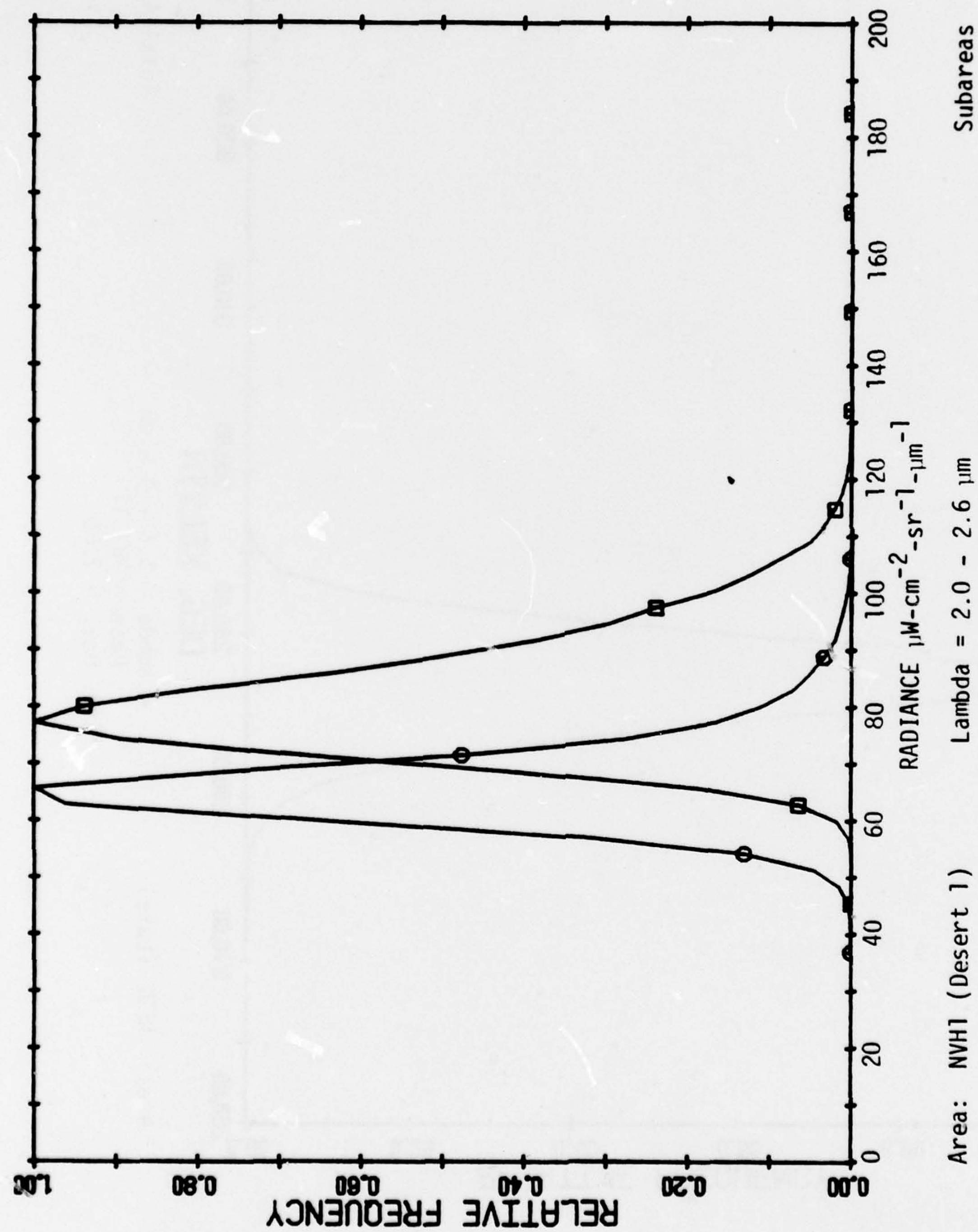
RELATIVE FREQUENCY
0.00
0.20
0.40
0.60
0.80
1.00
RADIANCE μW-cm^-2-sr^-1-μm^-1
0
20
40
60
80
100
120
140
160
180
200
Area: NVH1 (Desert 1)
Lambda = 2.0 - 2.6 μm
Subareas

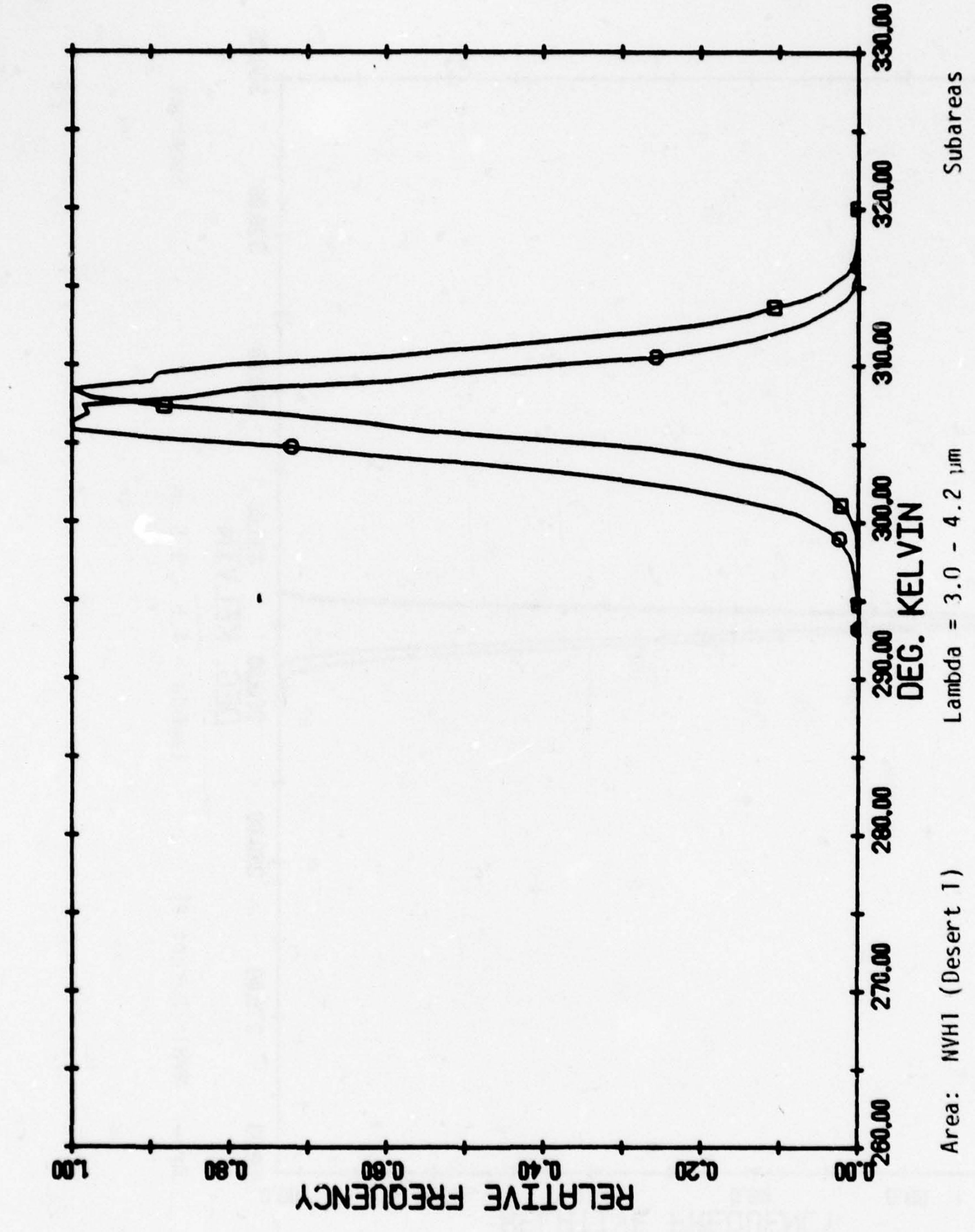
RELATIVE FREQUENCY
0.00
0.20
0.40
0.60
0.80
1.00
DEG. KELVIN
260.00
270.00
280.00
290.00
300.00
310.00
320.00
330.00
Area: NVH1 (Desert 1)
Lambda = 3.0 - 4.2 µm
Subareas

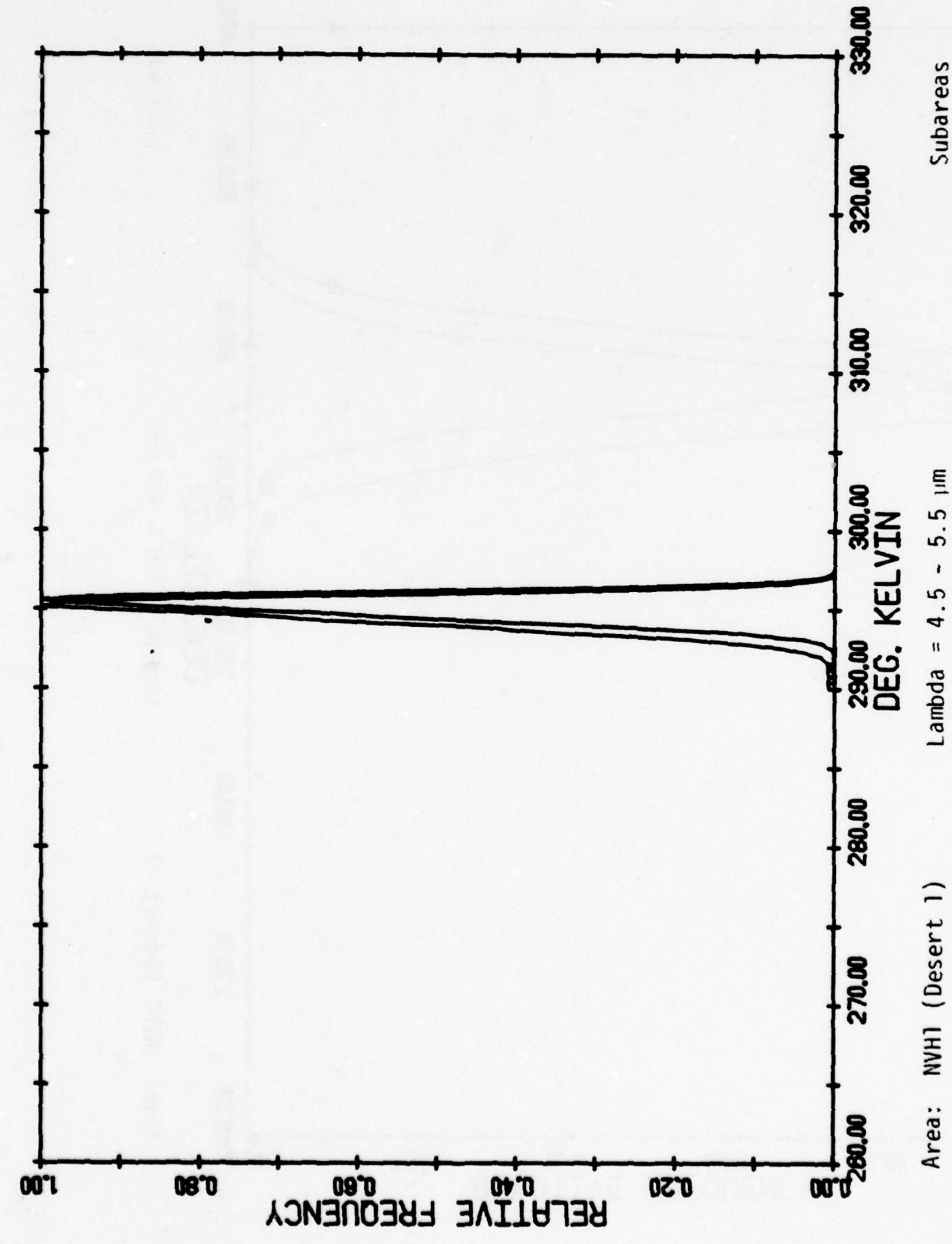
RELATIVE FREQUENCY
0.00
0.20
0.40
0.60
0.80
1.00
DEG. KELVIN
260.00
270.00
280.00
290.00
300.00
310.00
320.00
330.00
Area: NVH1 (Desert 1)
Lambda = 4.5 - 5.5 μm
Subareas

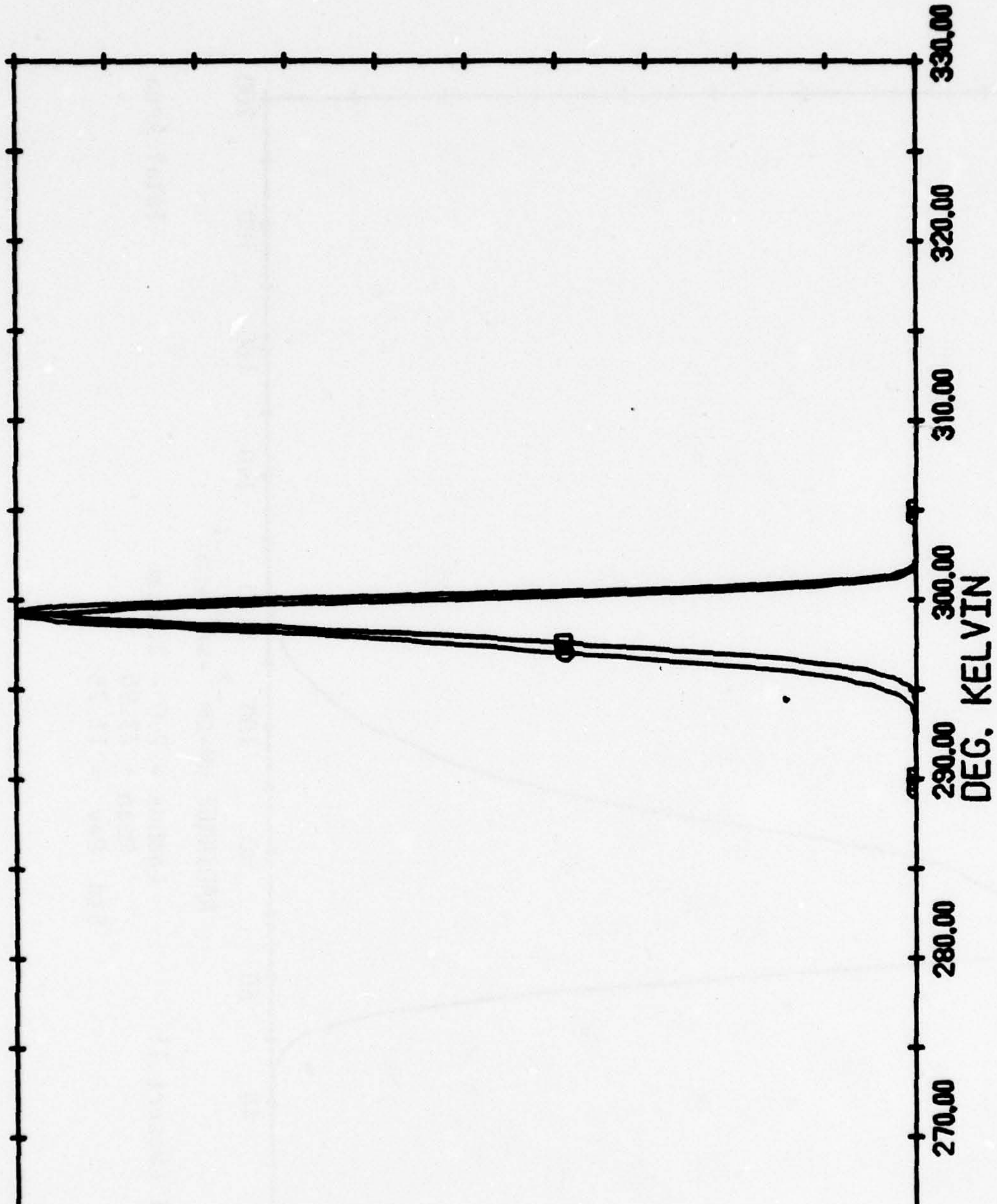

Area: NVH1 (Desert 1)

Lambda = 9.0 - 11.4 μm

Subareas

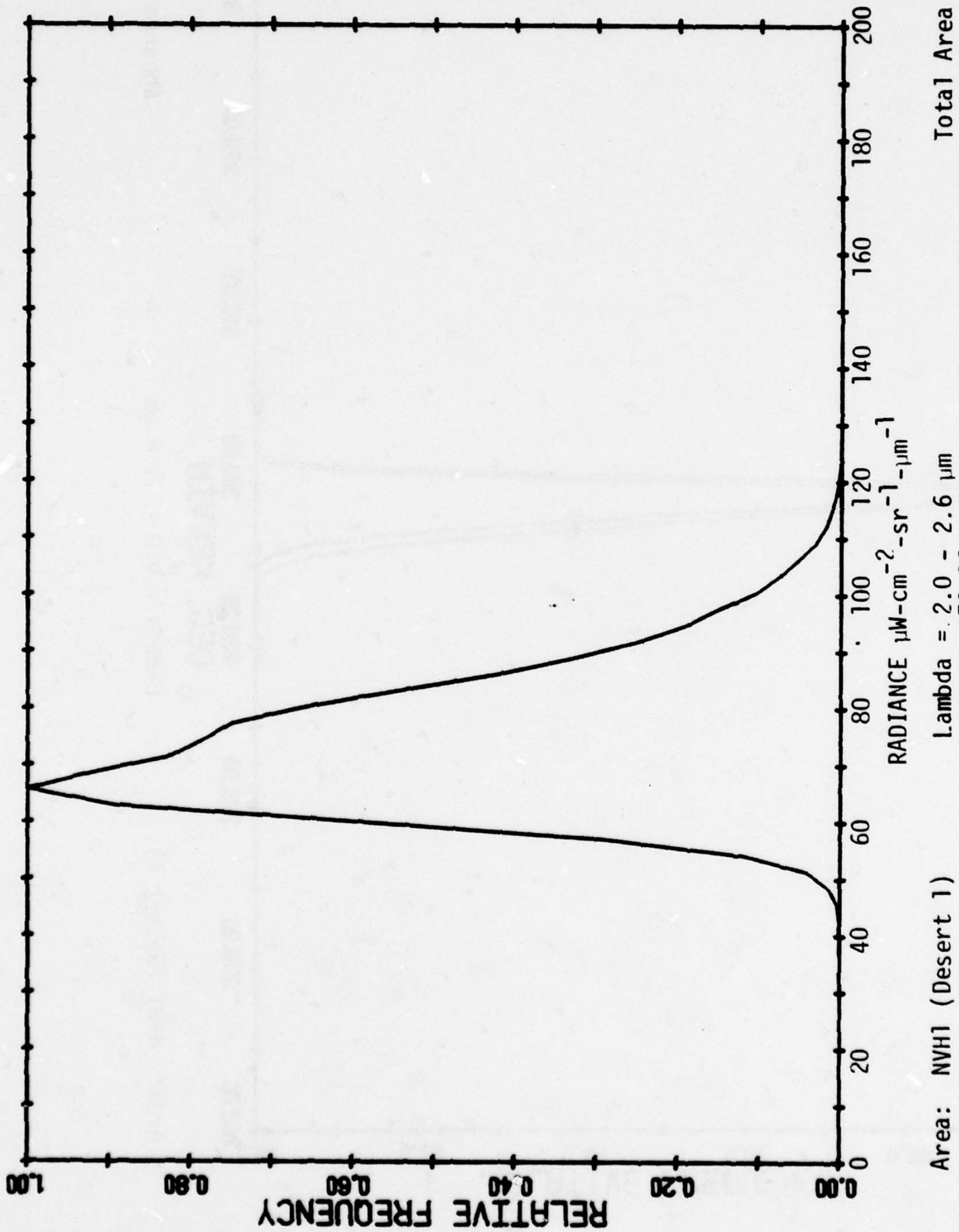
RELATIVE FREQUENCY
0.00
0.20
0.40
0.60
0.80
1.00
RADIANCE μW-cm-2-sr-1-μm-1
0
20
40
60
80
100
120
140
160
180
200
Area: NVH1 (Desert 1)
Lambda = 2.0 - 2.6 μm
Mean = 73.96
Std. Dev. = 11.75
Total Area

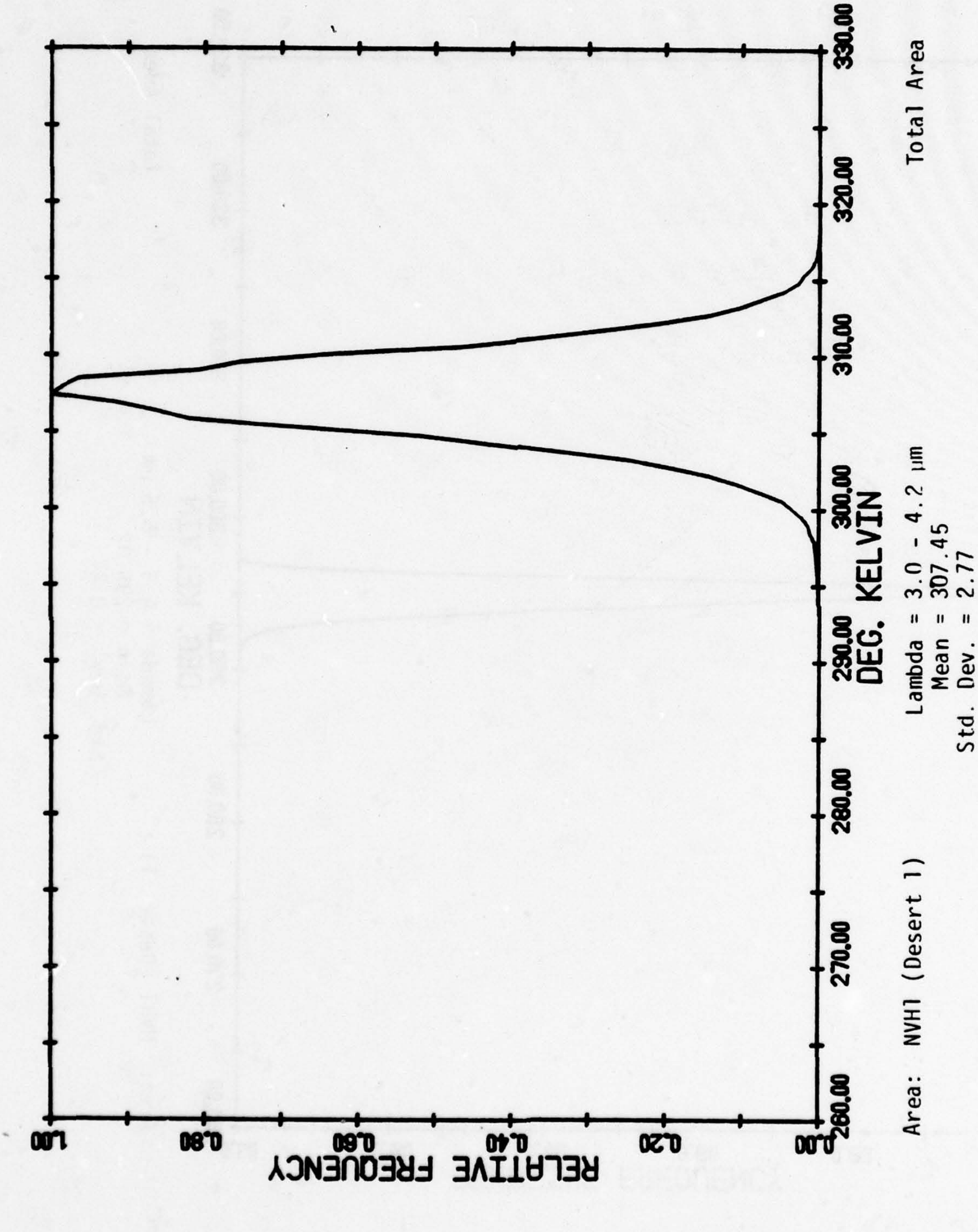

RELATIVE FREQUENCY
0.00
0.20
0.40
0.60
0.80
1.00
DEG. KELVIN
260.00
270.00
280.00
290.00
300.00
310.00
320.00
330.00
Area: NVH1 (Desert 1)
Lambda = 3.0 - 4.2 μm
Mean = 307.45
Std. Dev. = 2.77
Total Area

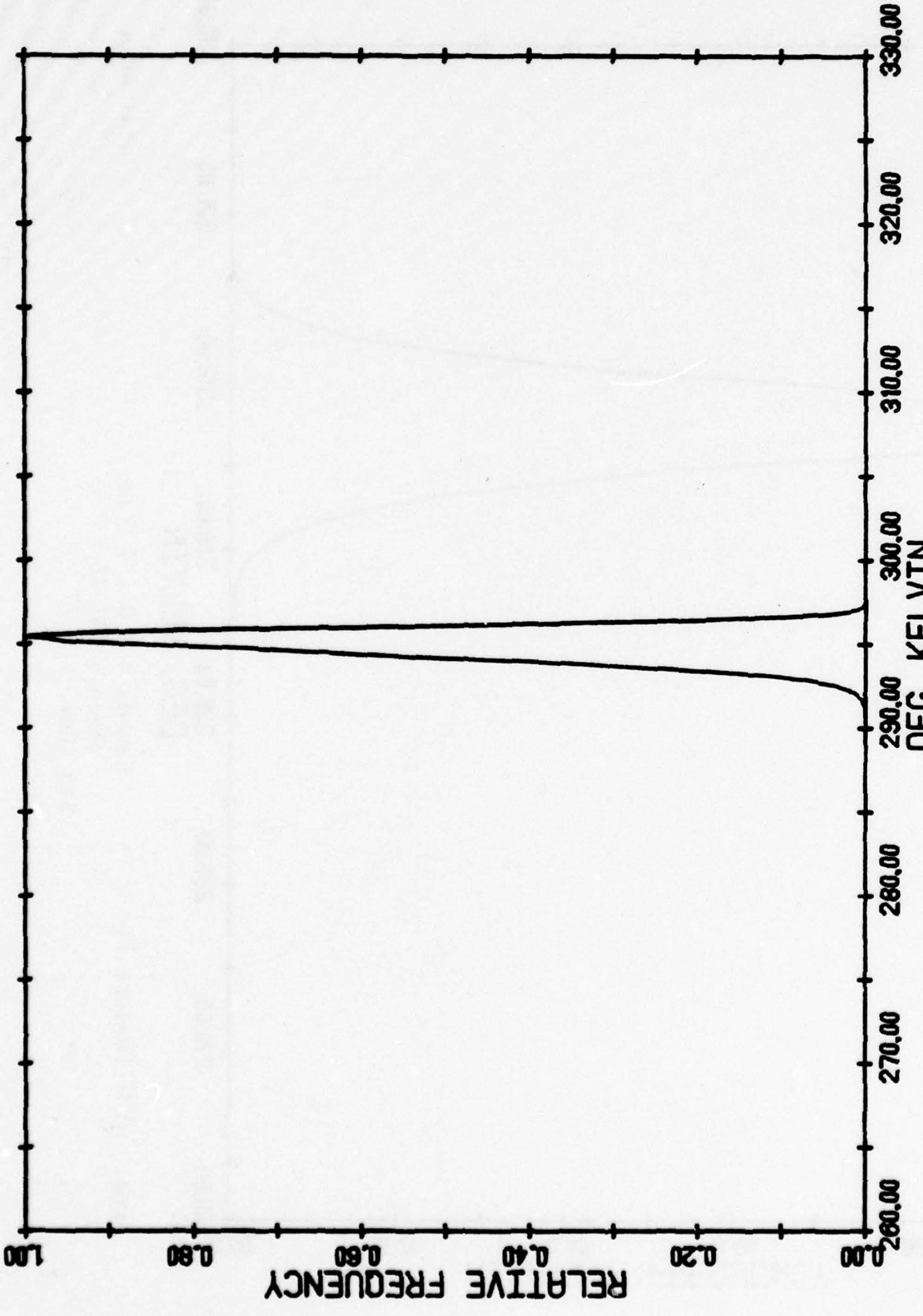

Area: NVH1 (Desert 1)

Lambda = 4.5 - 5.5 μm
Mean = 295.02
Std. Dev. = 0.87

Total Area

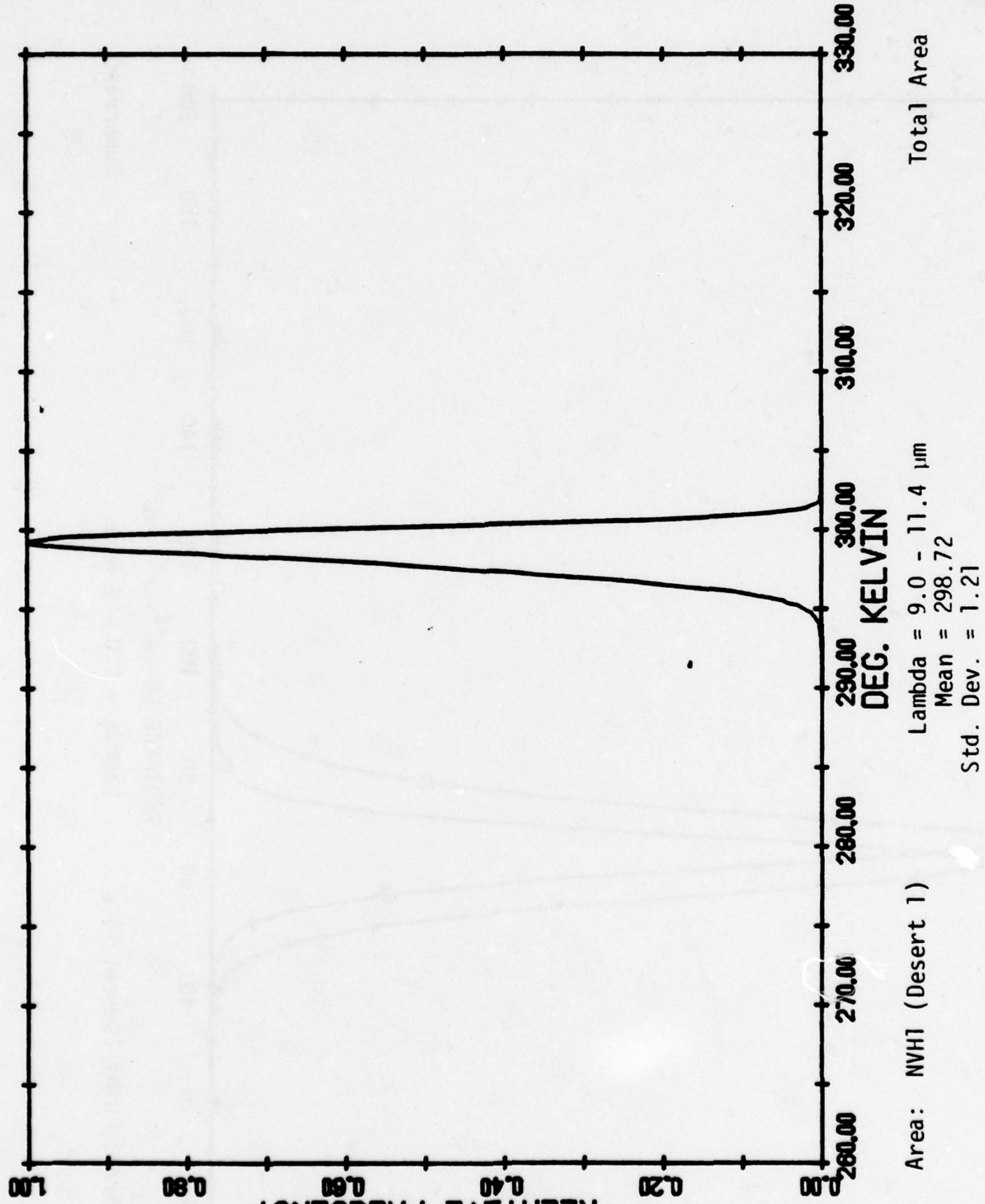
RELATIVE FREQUENCY
0.00
0.20
0.40
0.60
0.80
1.00
DEG. KELVIN
260.00
270.00
280.00
290.00
300.00
310.00
320.00
330.00
Area: NVHI (Desert 1) Total Area
Lambda = 9.0 - 11.4 μm
Mean = 298.72
Std. Dev. = 1.21

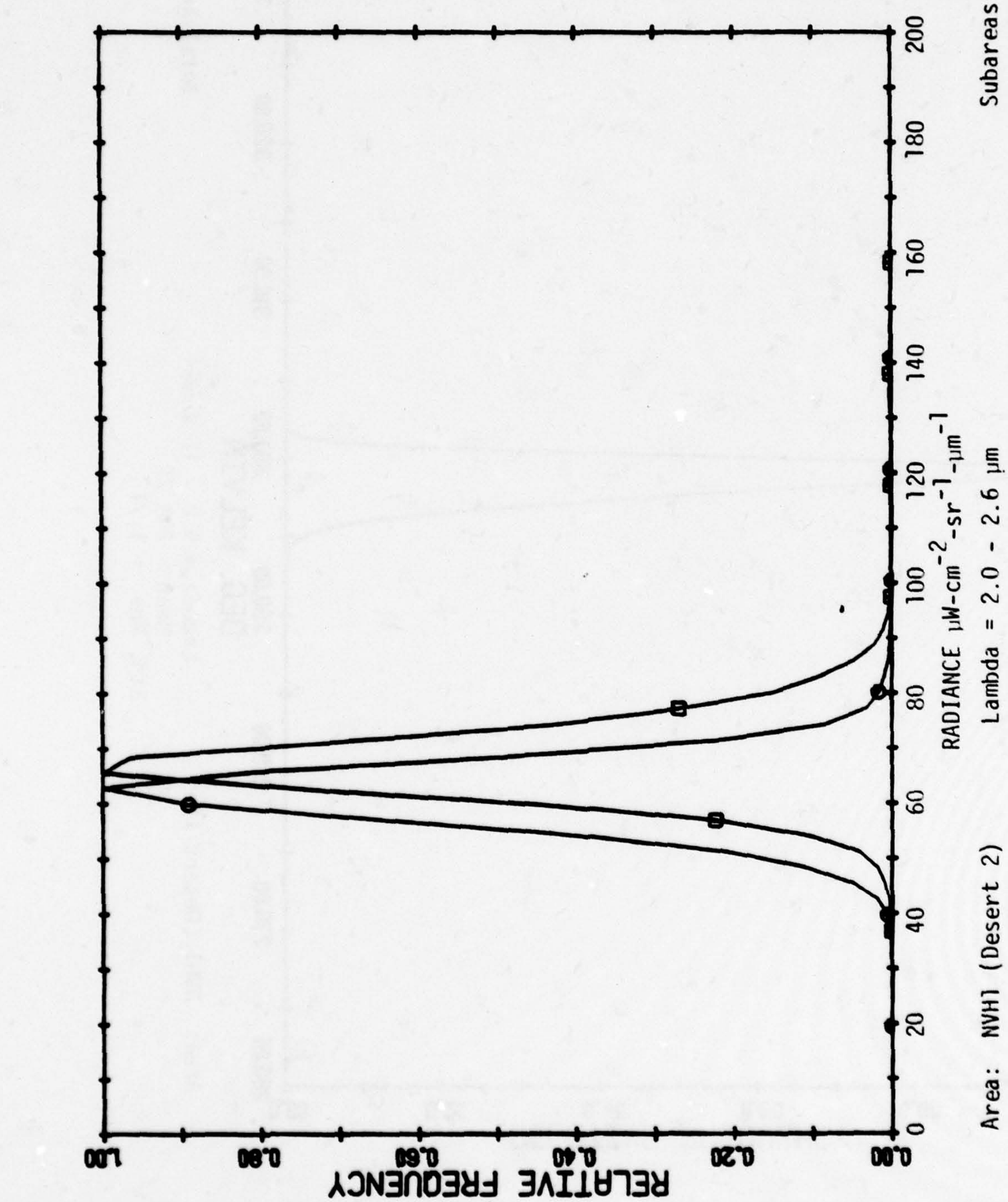

RELATIVE FREQUENCY
0.00
0.20
0.40
0.60
0.80
1.00
0
20
40
60
80
100
120
140
160
180
200
RADIANCE μW-cm^-2-sr^-1-μm^-1
Area: NVH1 (Desert 2)
Lambda = 2.0 - 2.6 μm
Subareas

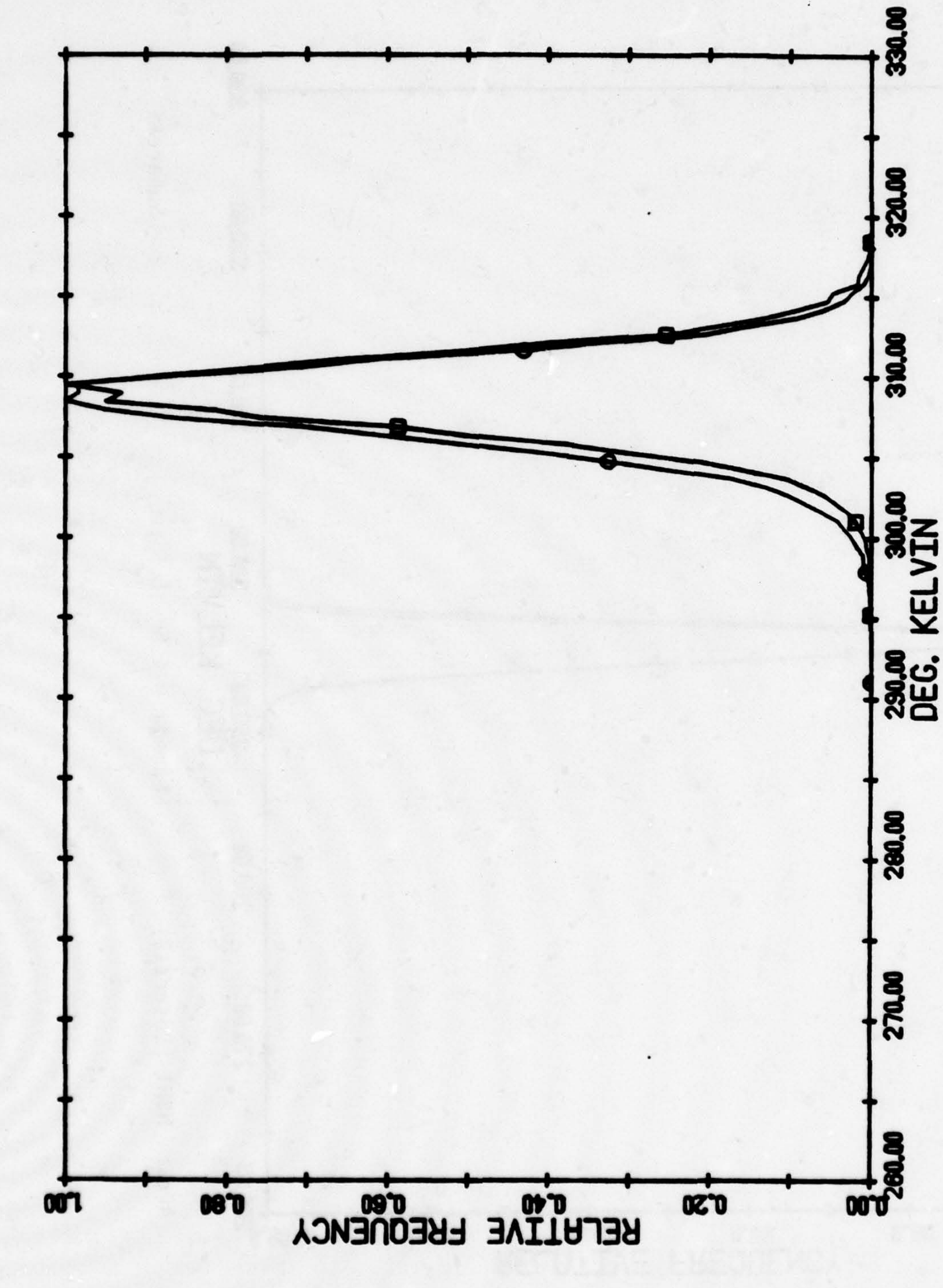

Area: NVH1 (Desert 2)

Lambda = 3.0 - 4.2 µm

Subareas

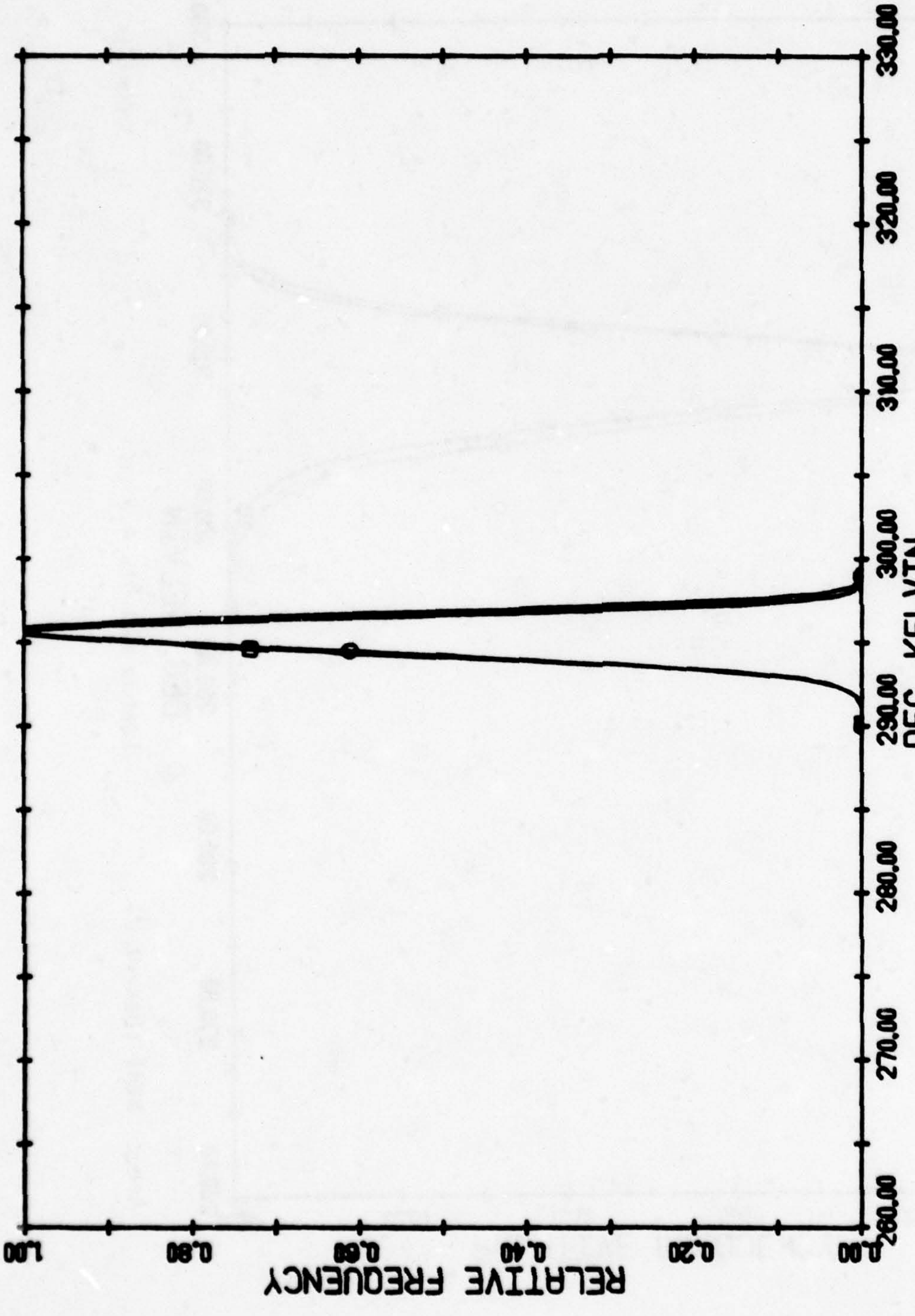

Area: NVH1 (Desert 2) Lambda = 4.5 - 5.5 μm Subareas

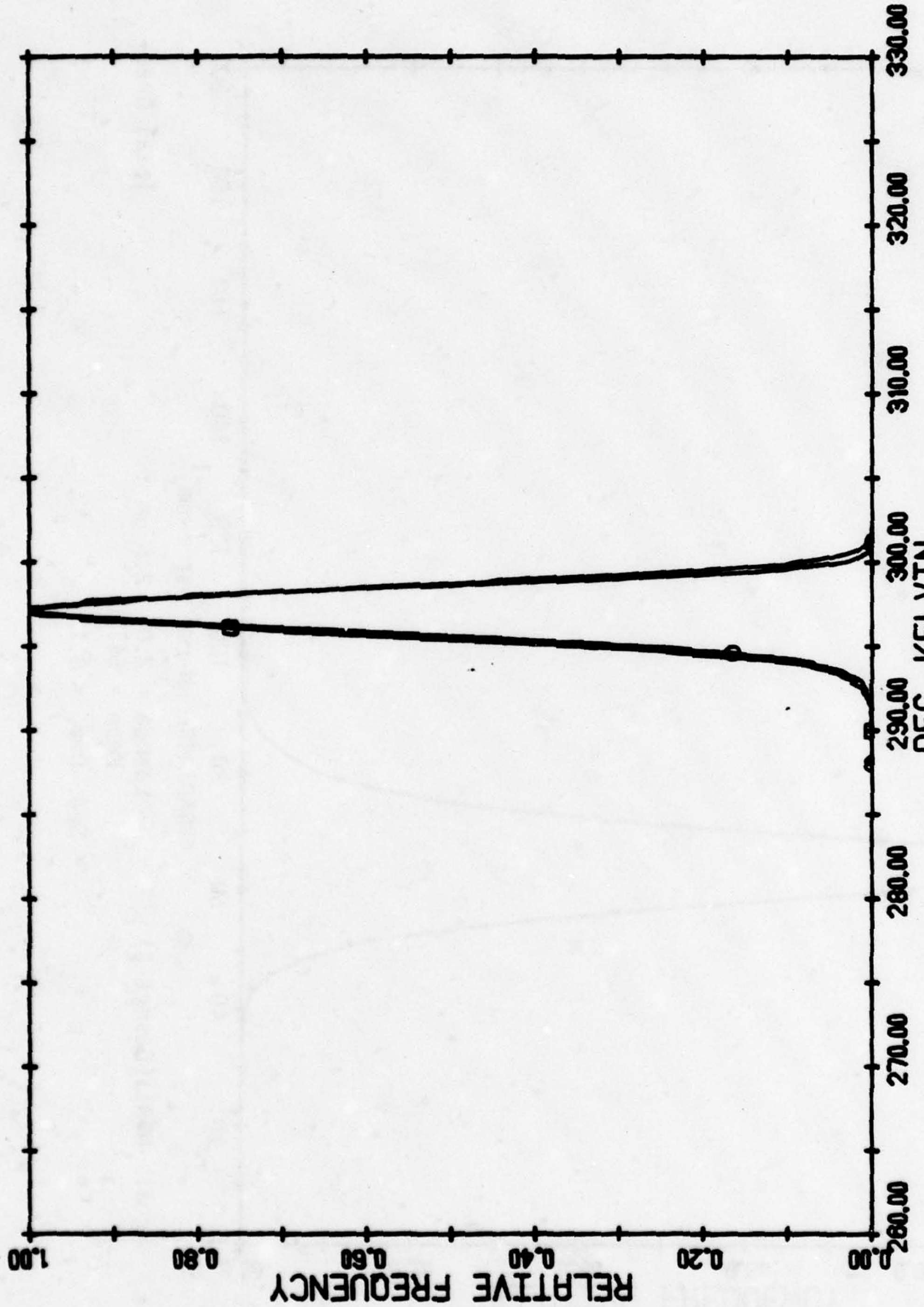

Area: NVH1 (Desert 2)   Lambda = 9.0 - 11.4 µm   Subareas

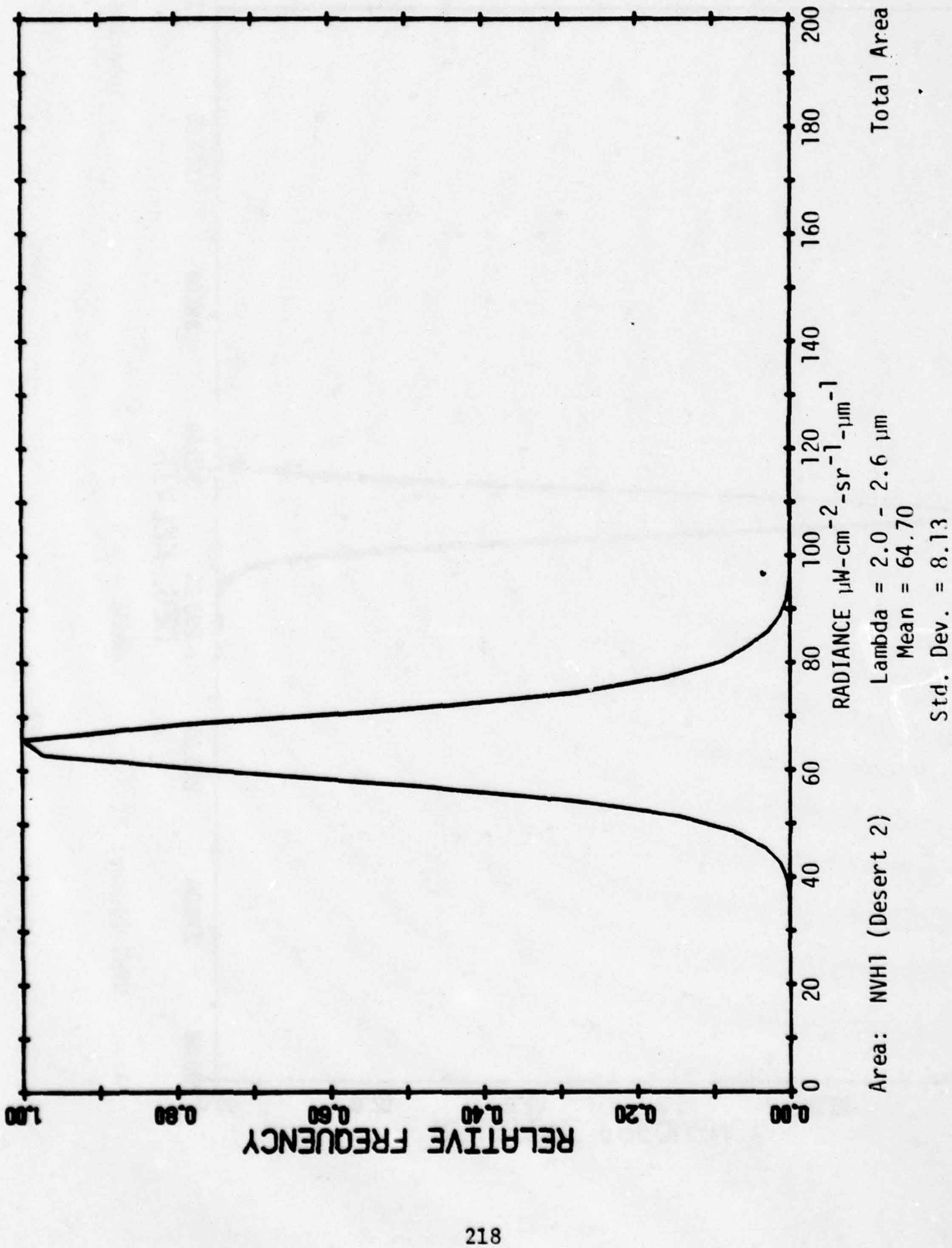
RELATIVE FREQUENCY
0.00
0.20
0.40
0.60
0.80
1.00
0
20
40
60
80
100
120
140
160
180
200
RADIANCE μW-cm^{-2}-sr^{-1}-μm^{-1}
Area: NVH1 (Desert 2)
Lambda = 2.0 - 2.6 μm
Mean = 64.70
Std. Dev. = 8.13
Total Area

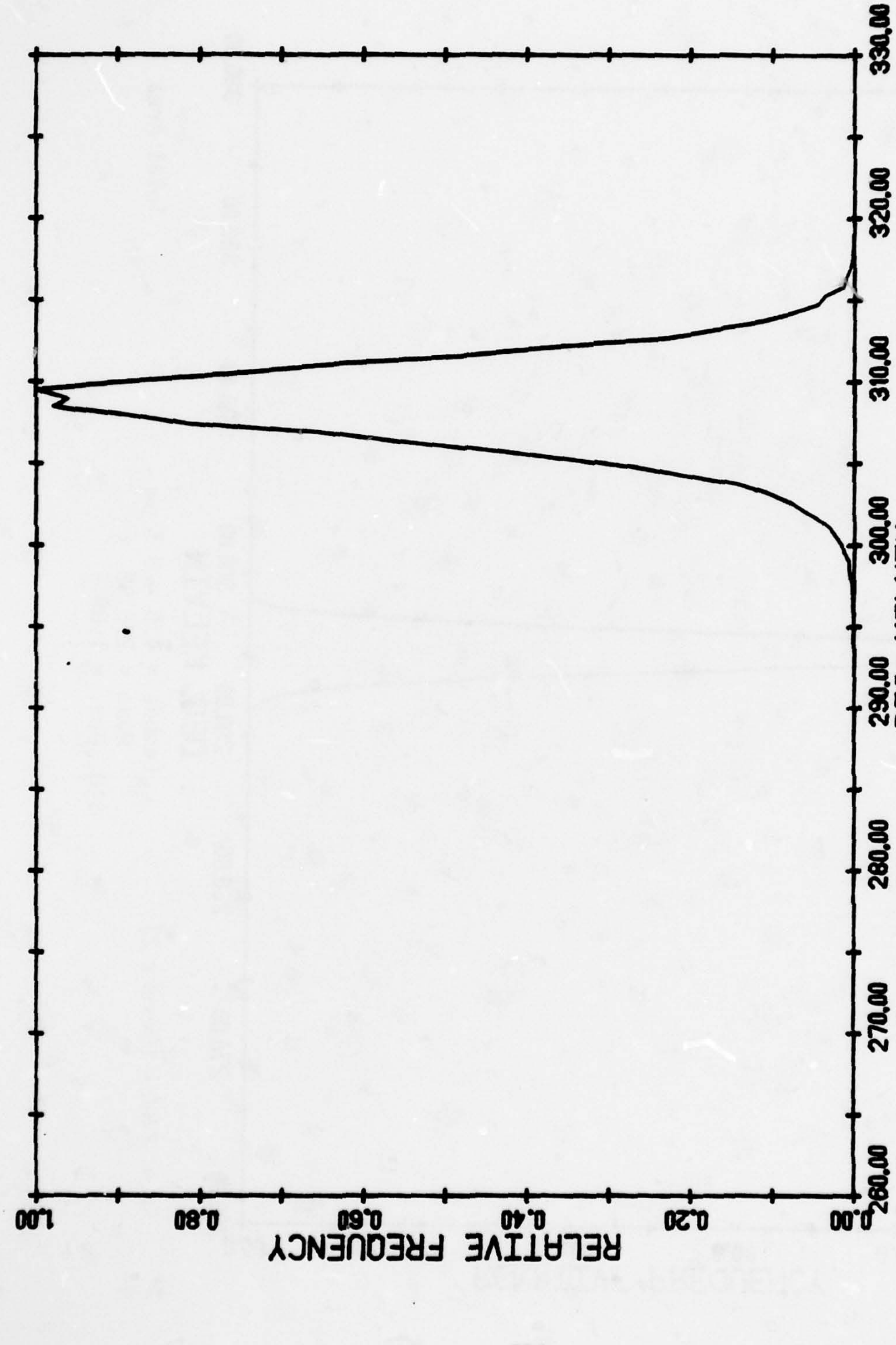

Area: NVH1 (Desert 2)

Lambda = 3.0 - 4.2 μm
Mean = 308.60
Std. Dev. = 2.65

Total Area

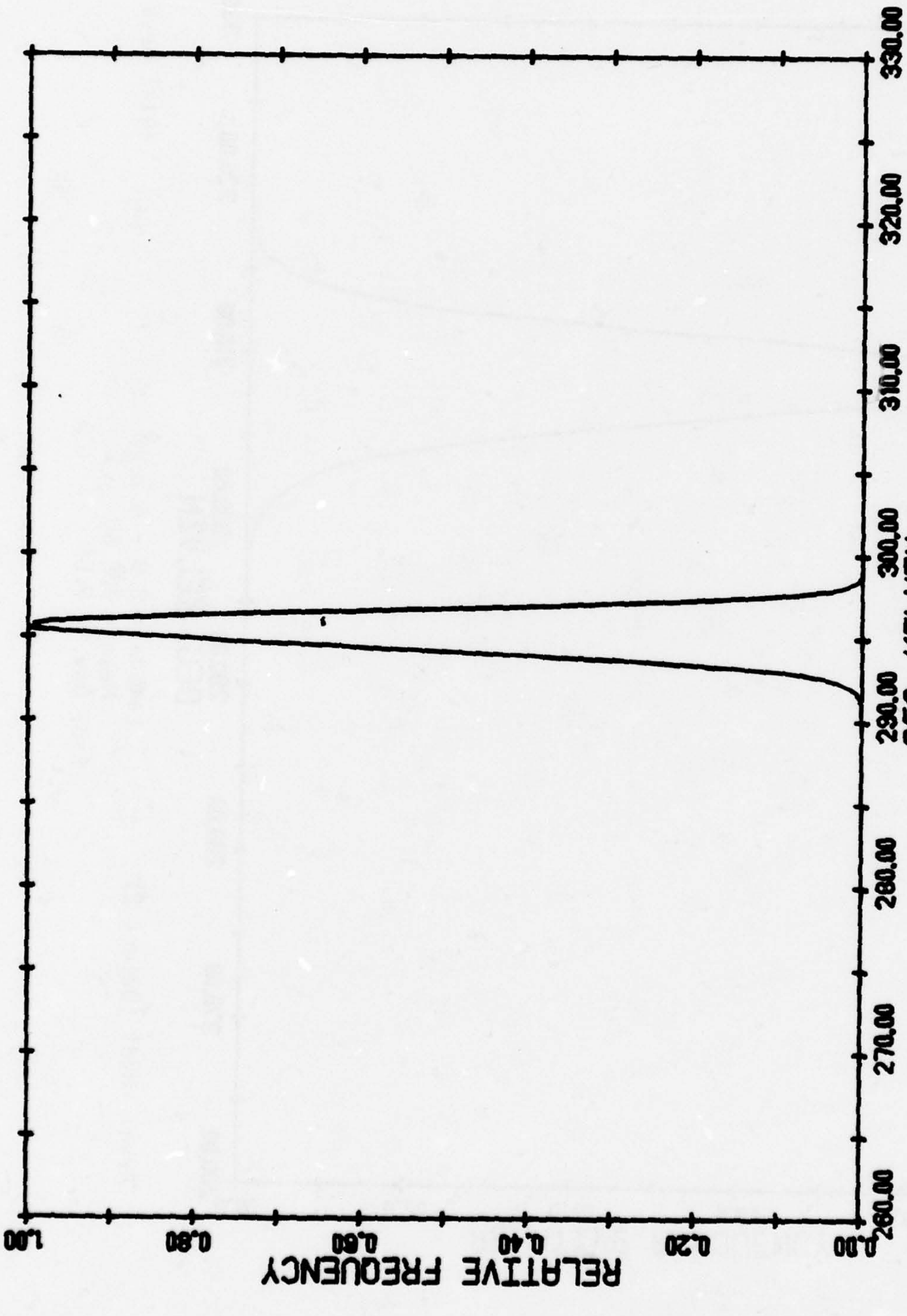

Total Area

Lambda = 4.5 - 5.5 μm
Mean = 295.38
Std. Dev. = 1.08

Area: NVH1 (Desert 2)

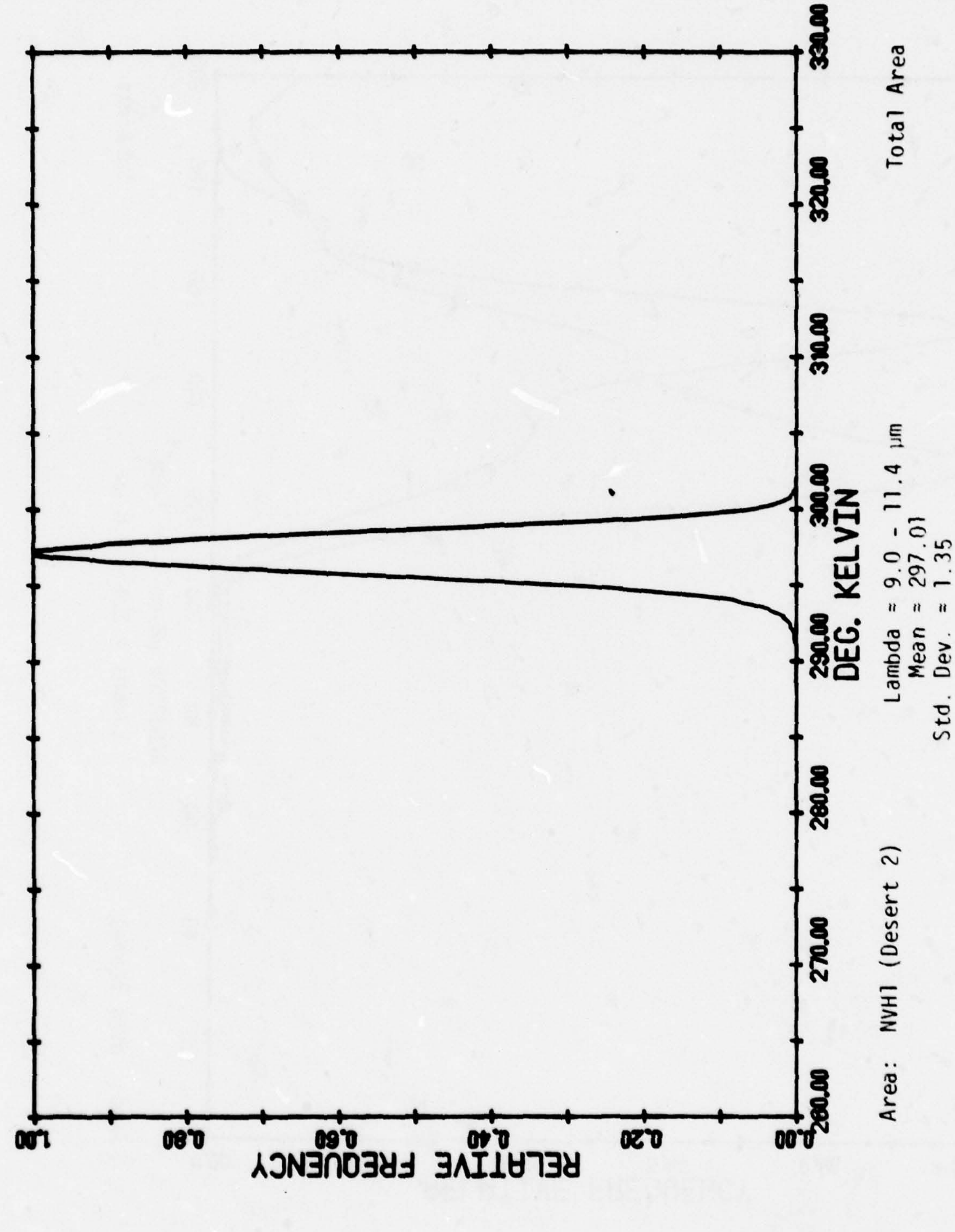
Total Area
Lambda = 9.0 - 11.4 μm
Mean = 297.01
Std. Dev. = 1.35
Area: NVH1 (Desert 2)
DEG. KELVIN
RELATIVE FREQUENCY
260.00
270.00
280.00
290.00
300.00
310.00
320.00
330.00
0.00
0.20
0.40
0.60
0.80
1.00

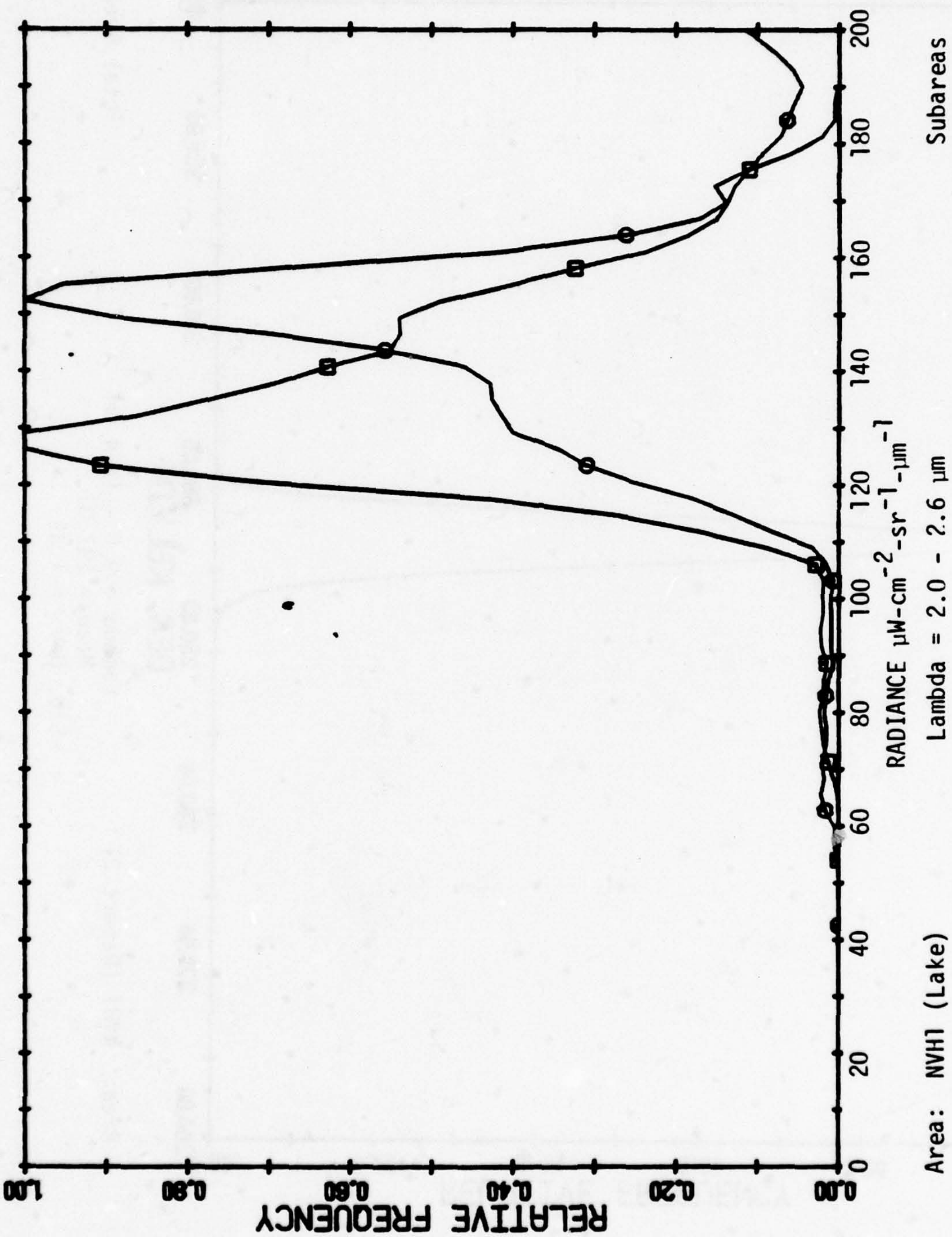
RELATIVE FREQUENCY
0.00
0.20
0.40
0.60
0.80
1.00
0
20
40
60
80
100
120
140
160
180
200
RADIANCE μW-cm^{-2}-sr^{-1}-μm^{-1}
Area: NVH1 (Lake)
Lambda = 2.0 - 2.6 μm
Subareas

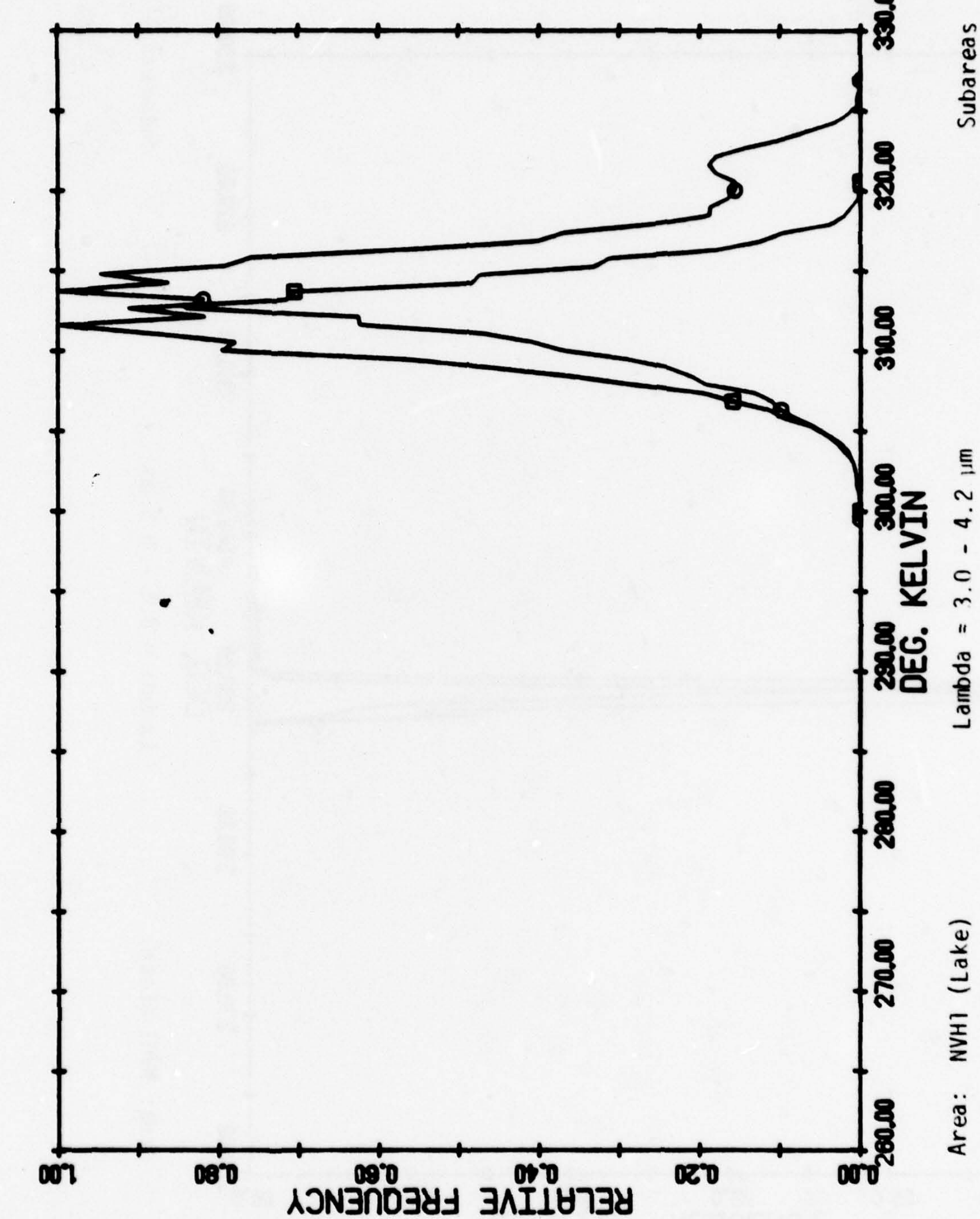

RELATIVE FREQUENCY
0.00
0.20
0.40
0.60
0.80
1.00
DEG. KELVIN
260.00
270.00
280.00
290.00
300.00
310.00
320.00
330.00
Area: NVH1 (Lake)
Lambda = 3.0 - 4.2 μm
Subareas

ΣERIM

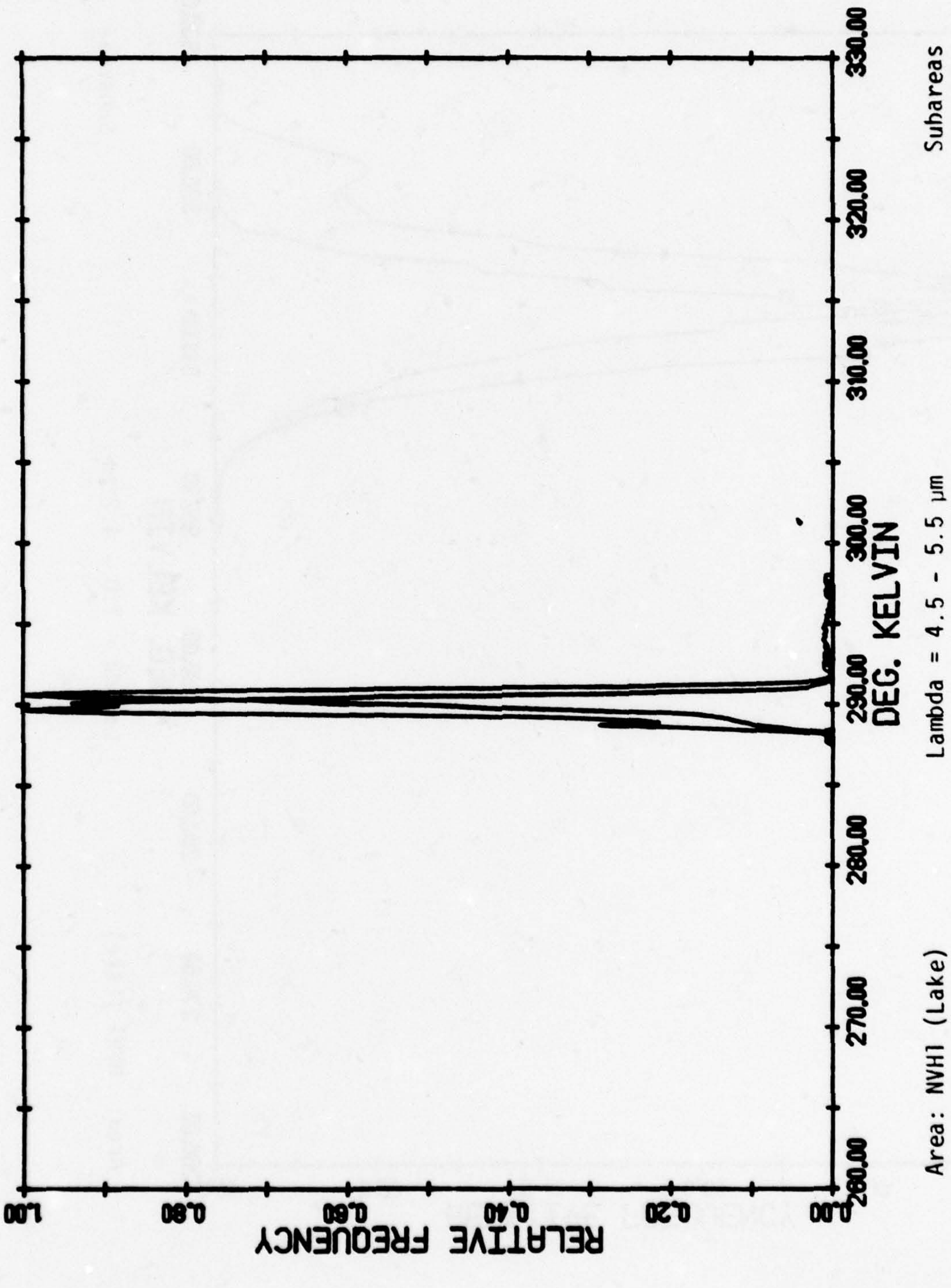
RELATIVE FREQUENCY
0.00
0.20
0.40
0.60
0.80
1.00
DEG. KELVIN
260.00
270.00
280.00
290.00
300.00
310.00
320.00
330.00
Area: NVH1 (Lake)
Lambda = 4.5 - 5.5 μm
Subareas

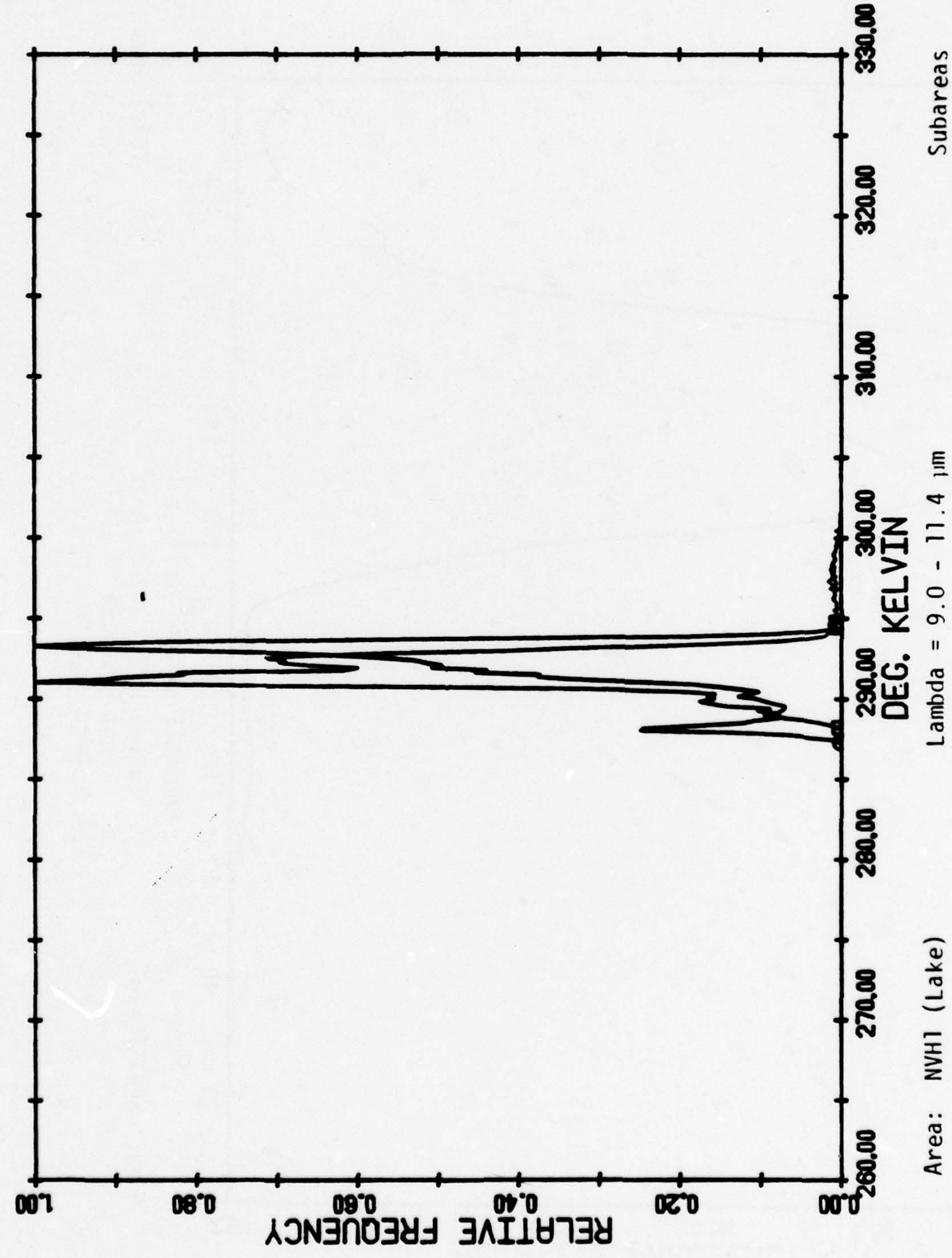
RELATIVE FREQUENCY
0.00
0.20
0.40
0.60
0.80
1.00
DEG. KELVIN
260.00
270.00
280.00
290.00
300.00
310.00
320.00
330.00
Area: NVH1 (Lake)
Lambda = 9.0 - 11.4 μm
Subareas

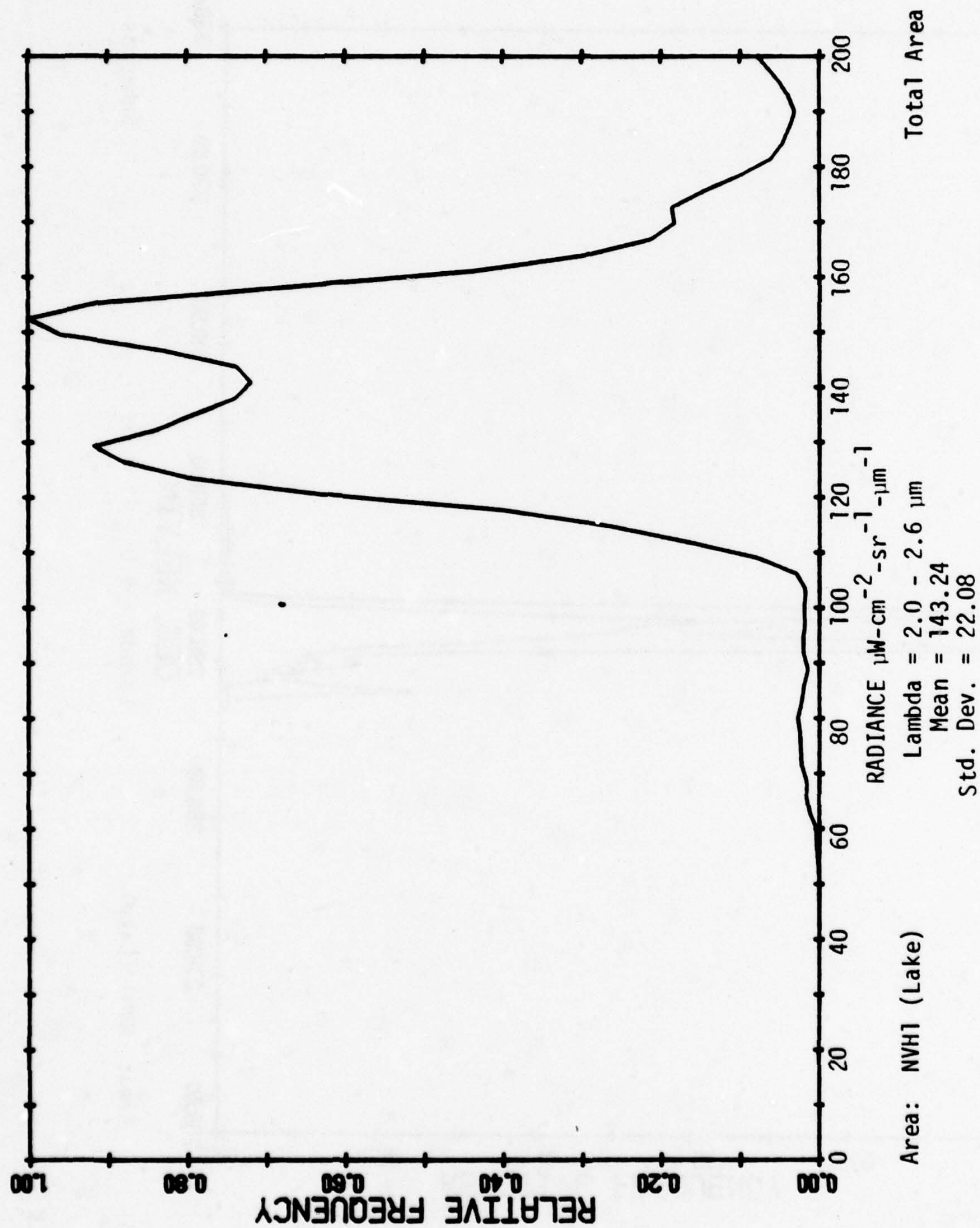
RELATIVE FREQUENCY
0.00
0.20
0.40
0.60
0.80
1.00
0
20
40
60
80
100
120
140
160
180
200
RADIANCE µW-cm^-2-sr^-1-µm^-1
Area: NWH1 (Lake)
Total Area
Lambda = 2.0 - 2.6 µm
Mean = 143.24
Std. Dev. = 22.08

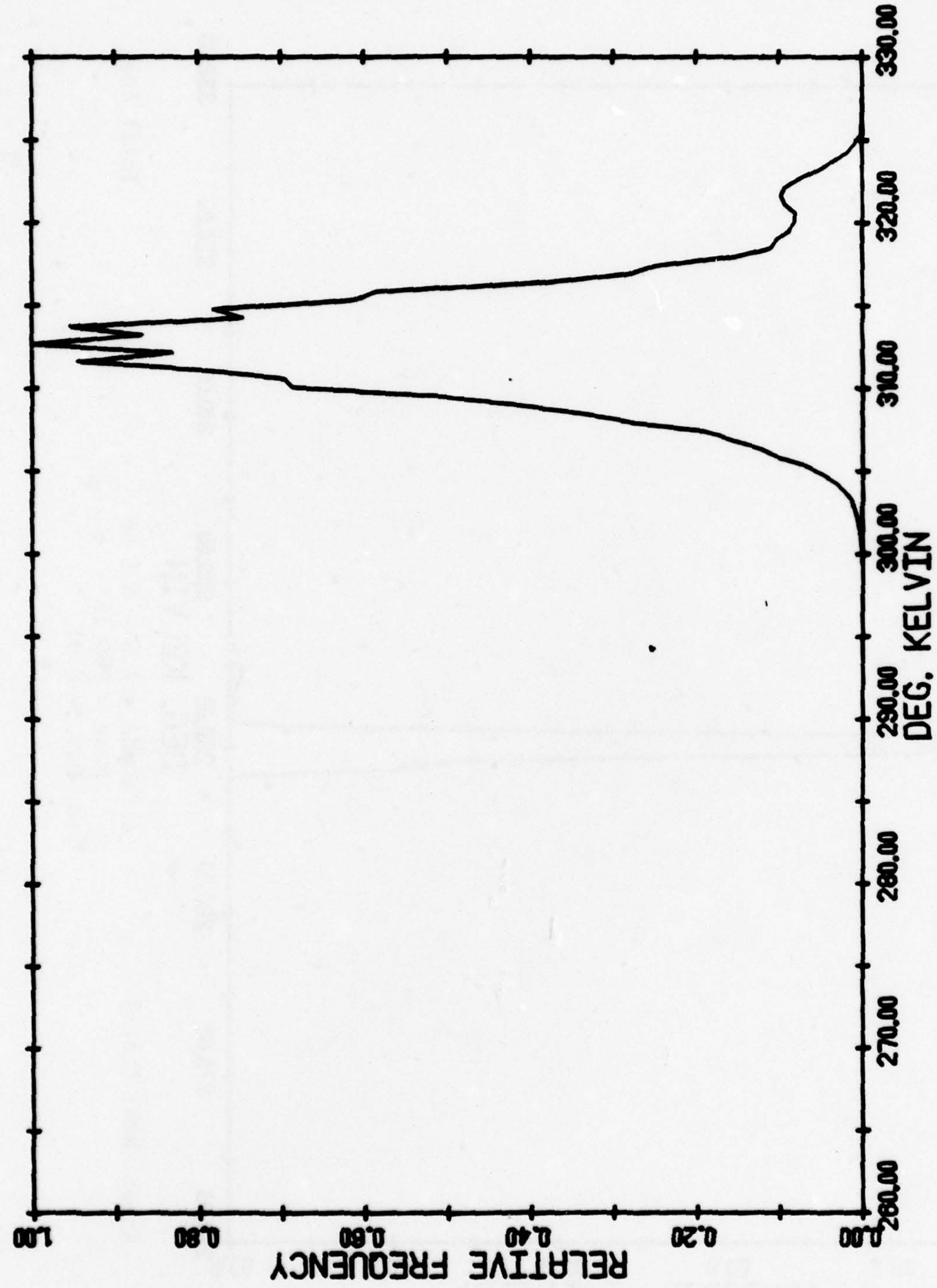

Area: NVH1 (Lake) Total Area

Lambda = 3.0 - 4.2 μm
Mean = 312.90
Std. Dev. = 3.52

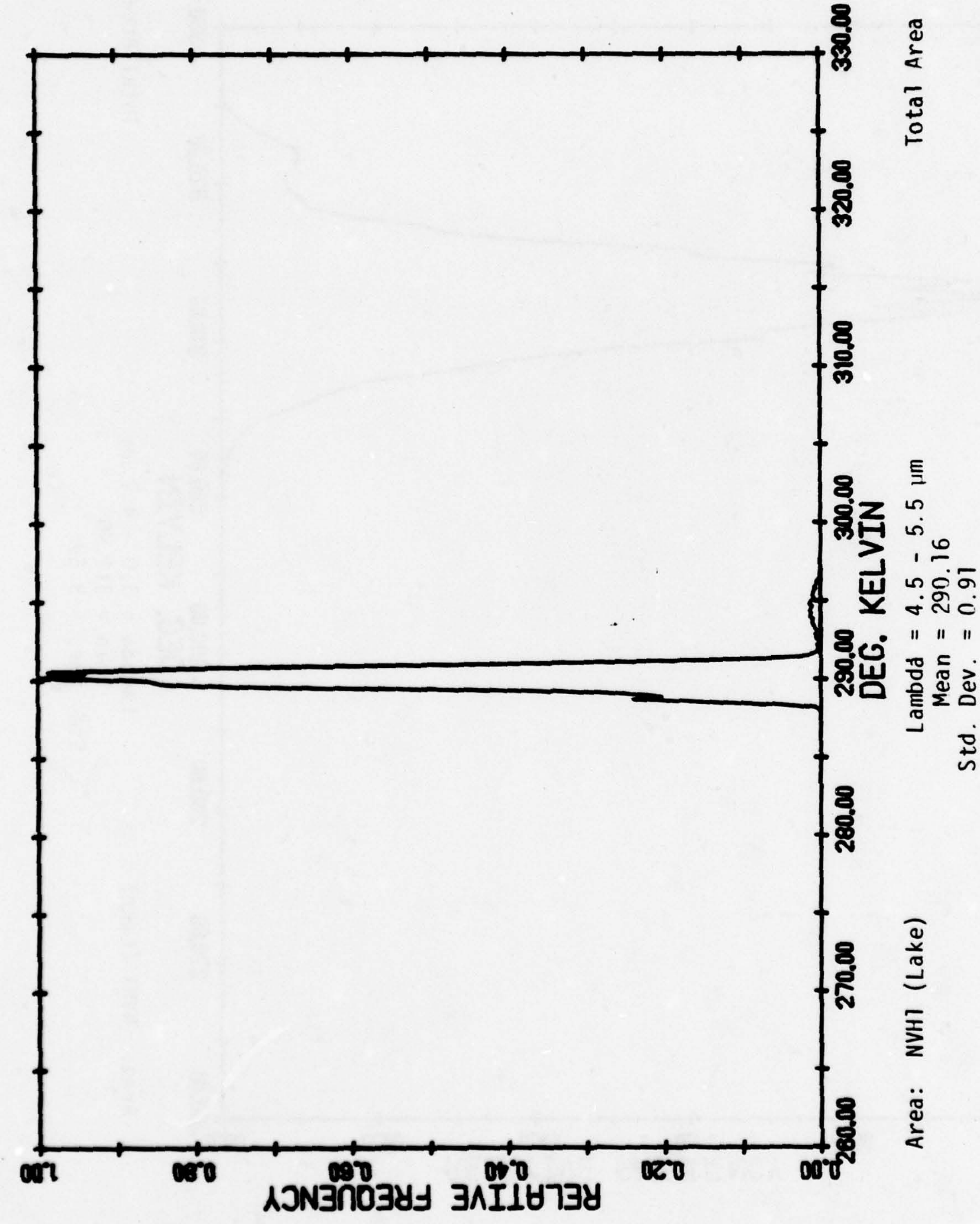
RELATIVE FREQUENCY
0.00
0.20
0.40
0.60
0.80
1.00
DEG. KELVIN
260.00
270.00
280.00
290.00
300.00
310.00
320.00
330.00
Area: NVH1 (Lake)
Lambda = 4.5 - 5.5 µm
Mean = 290.16
Std. Dev. = 0.91
Total Area

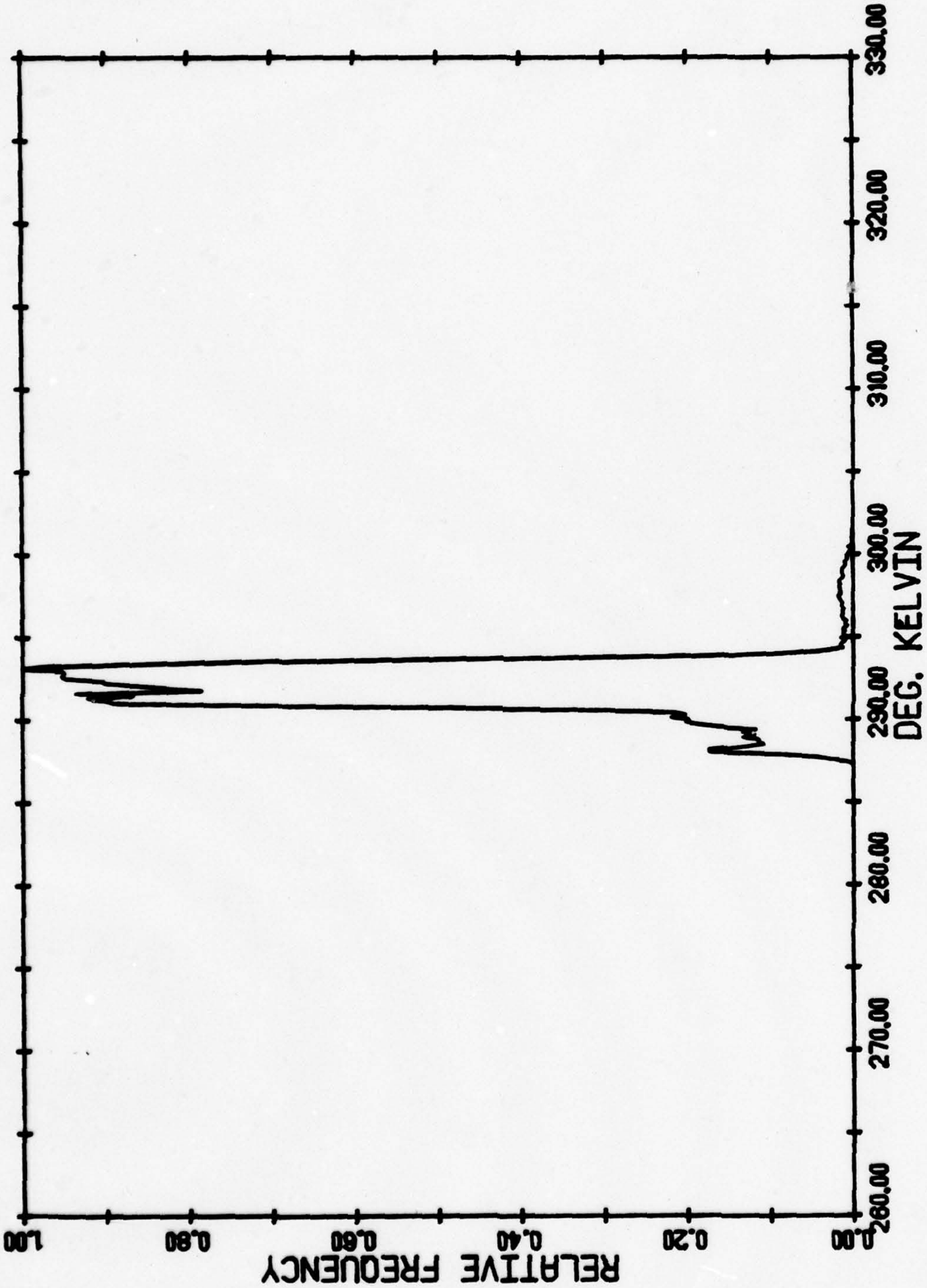

Area: NVH1 (Lake)

Lambda = 9.0 - 11.4 μm
Mean = 291.94
Std. Dev. = 1.57

Total Area

APPENDIX B

POWER SPECTRA

This appendix shows the one-dimensional power spectra for the imagery analyzed in the body of the report for the runs shown in Table 1, in which the essential parameters associated with the different runs are shown.

The cross-track power spectra were obtained by averaging the one-dimensional power spectrum measured for all of the lines covering the areas described in the body of the report. The in-track power spectra were obtained by averaging the one-dimensional power spectrum of seventeen lines taken along the length of the image and equally spaced across it.

In Reference 2, it was noted that certain artifacts appearing in the imagery were apparently due to electrical pick-up on-board the aircraft. The same feature which appears as a discontinuity in the spectrum is present also in some of these spectra. An attempt will be made to eliminate it from future measurements.

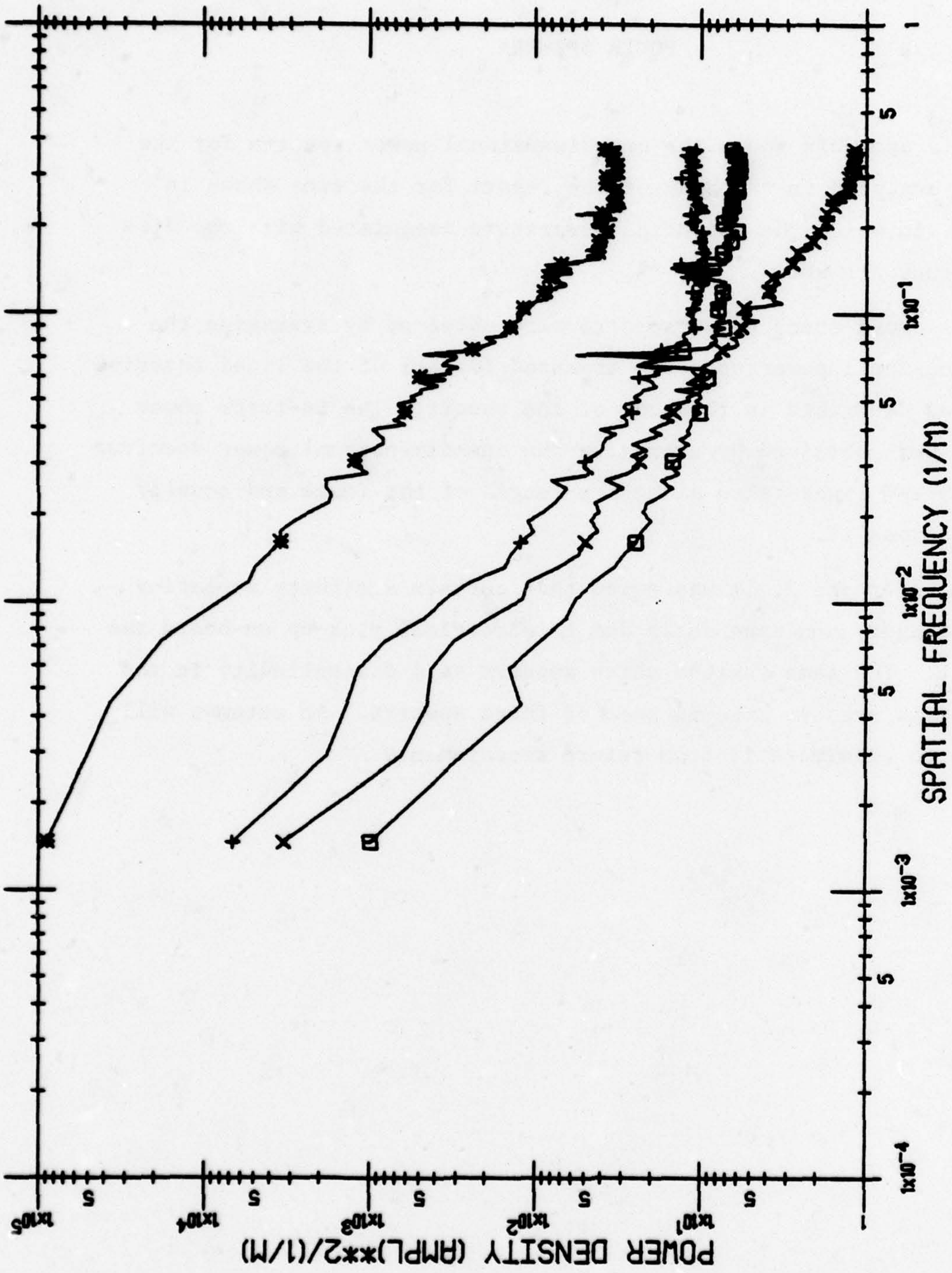

Area: NEVI CROSSTRACK Lambda = 2.0-2.6 (*), 3.0-4.2 (+), 4.5-5.5 (x), 5.1-5.7 (□)

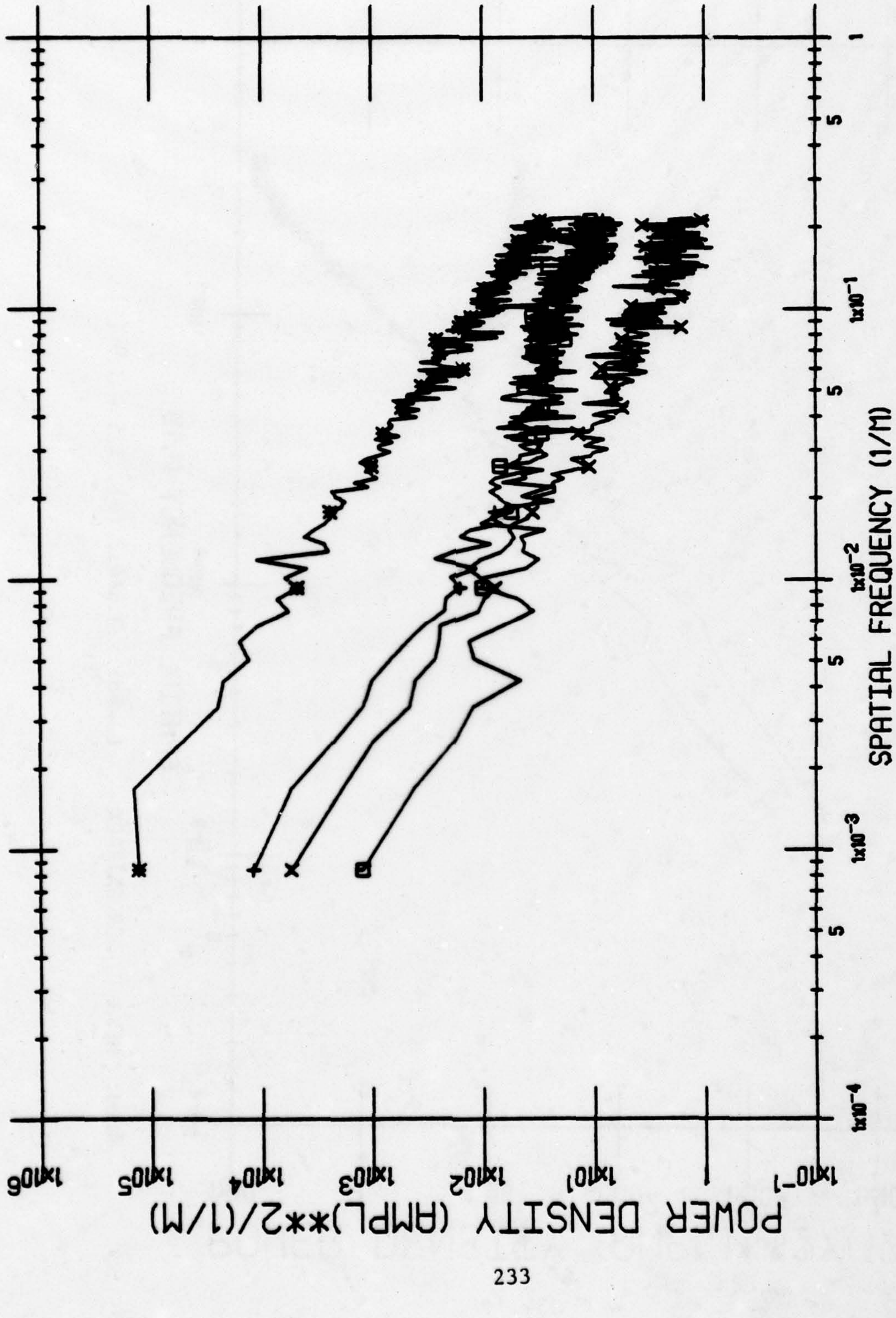

Area: NEVI INTRACK Lambda = 2.0-2.6 (*), 3.0-4.2 (+), 4.5-5.5 (x), 5.1-5.7 (⊡)

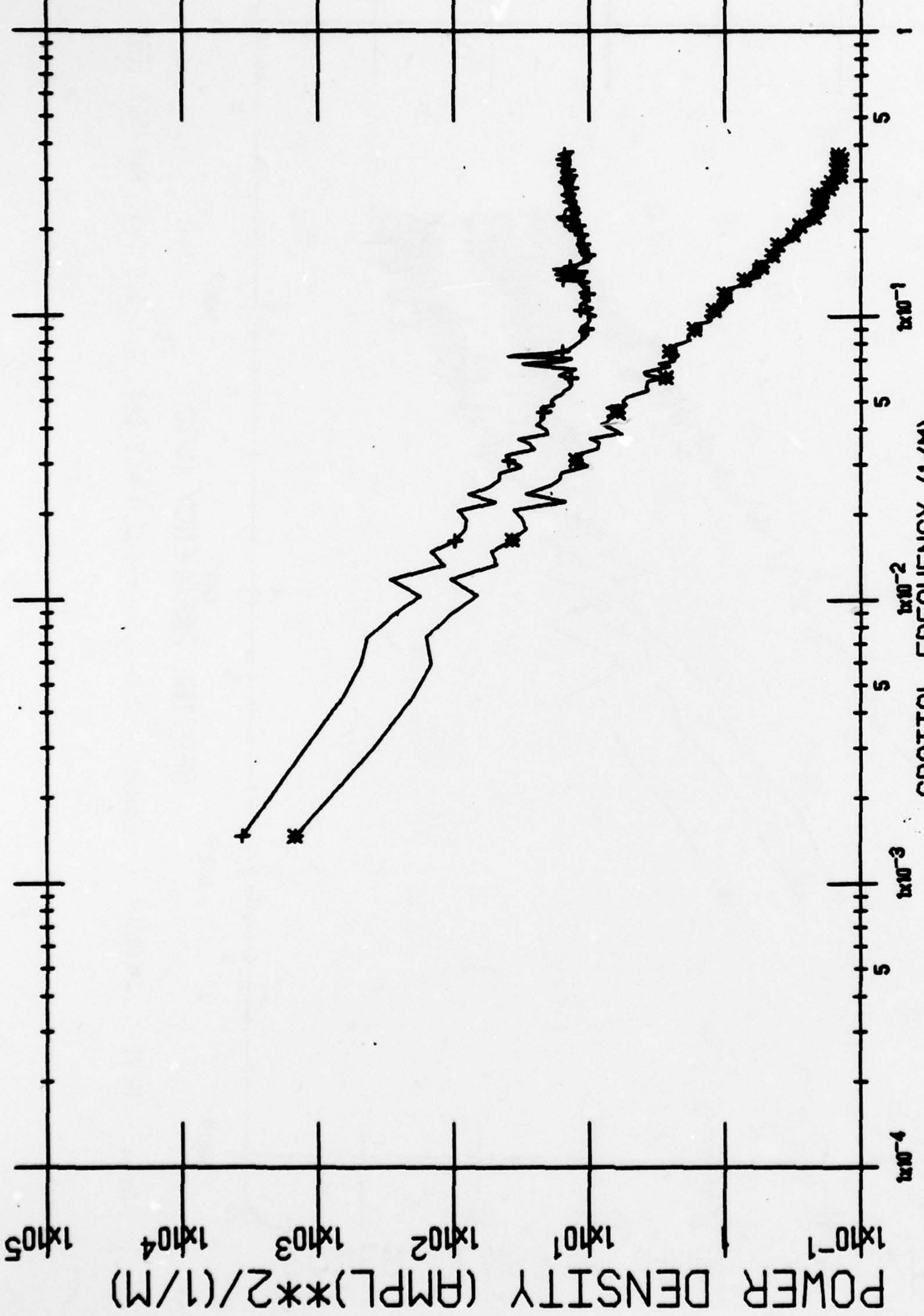

Area: NEVJ CROSSTRACK Lambda = 3.9-4.7 (*), 3.5 - 3.9 (+)

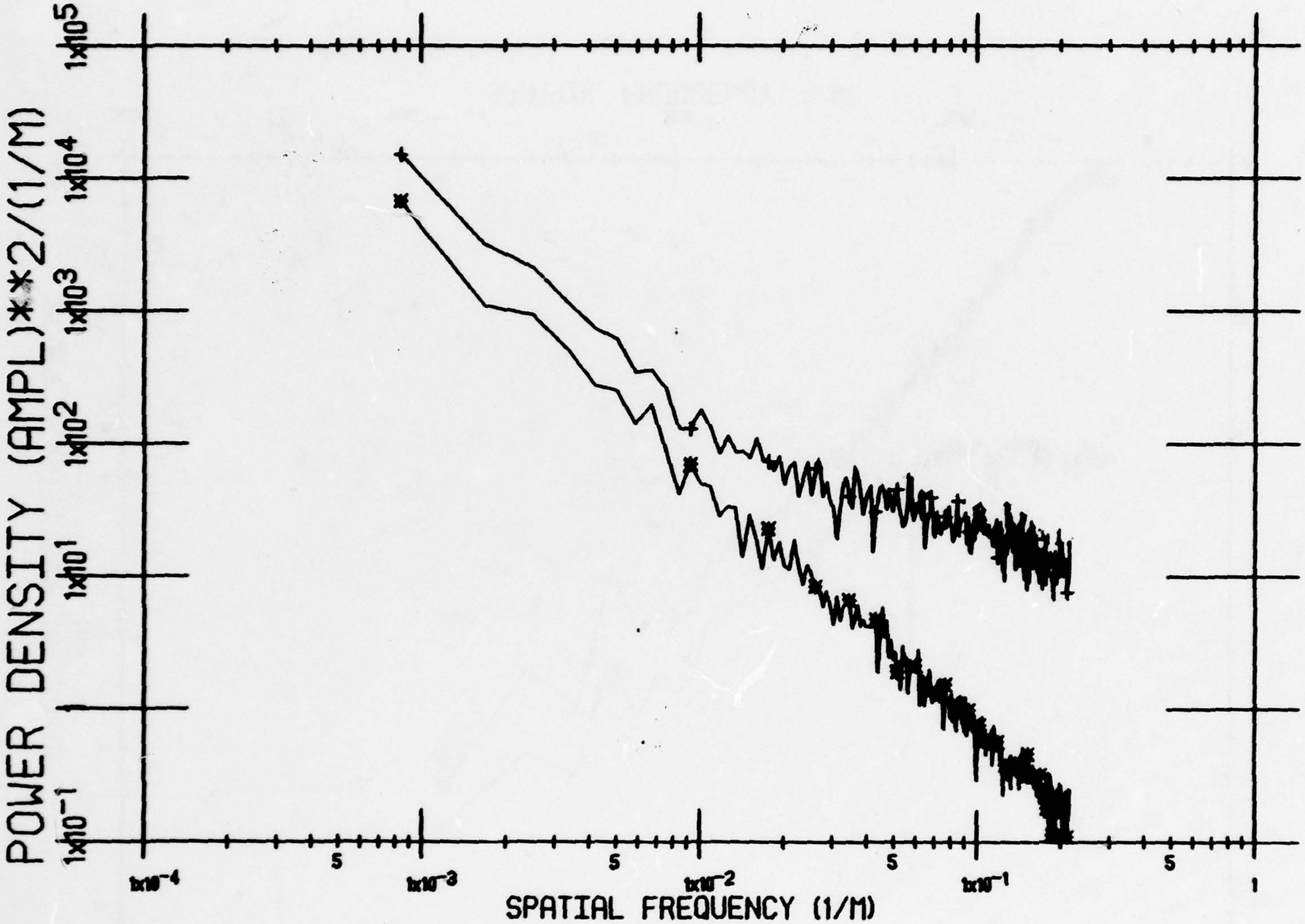

Area: NEVJ INTRACK Lambda = 3.9-4.7 (*), 3.5-3.9 (+)

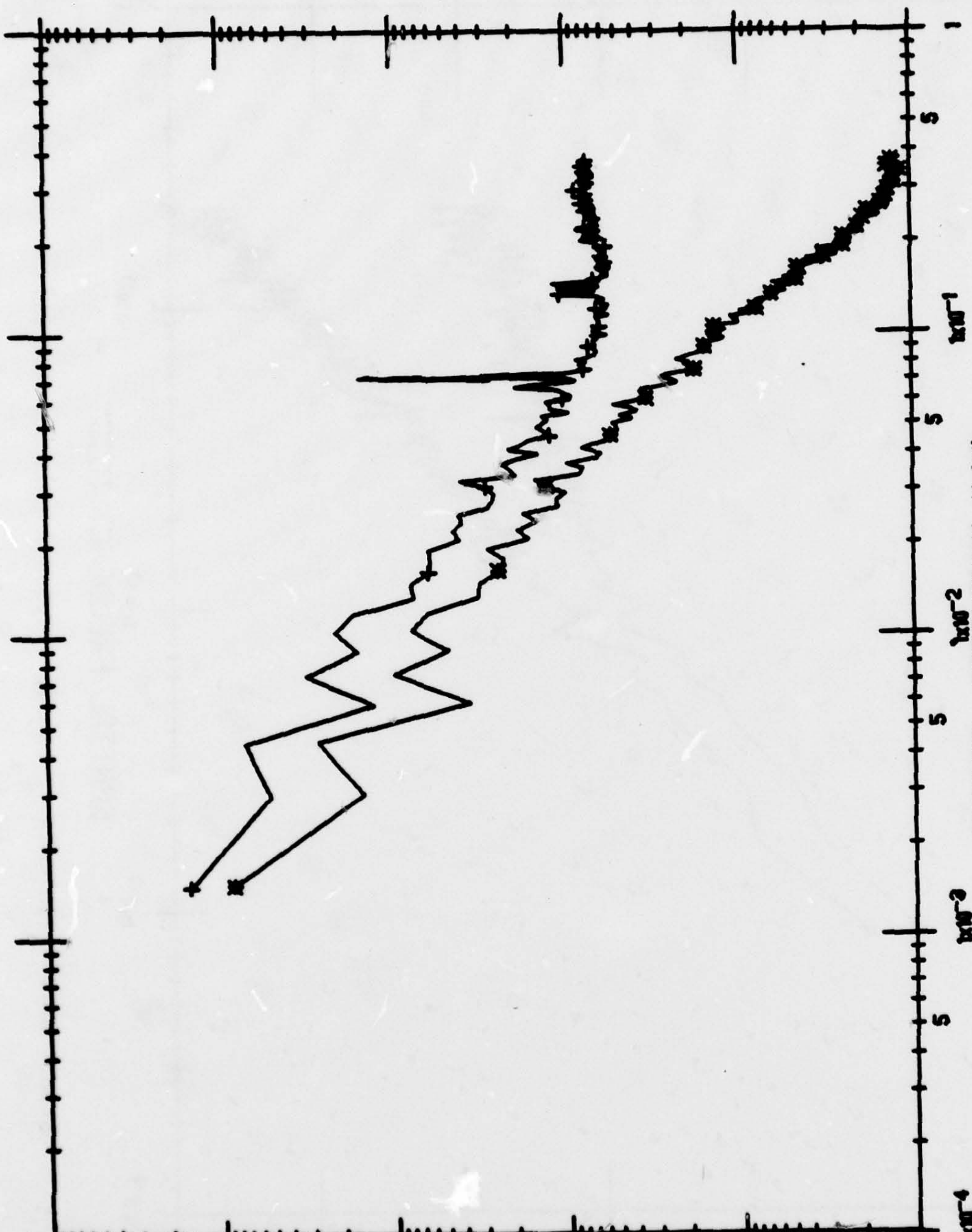

Area: NEVK   CROSSTRACK   Lambda = 3.9-4.7 (*), 3.5-3.9 (+)

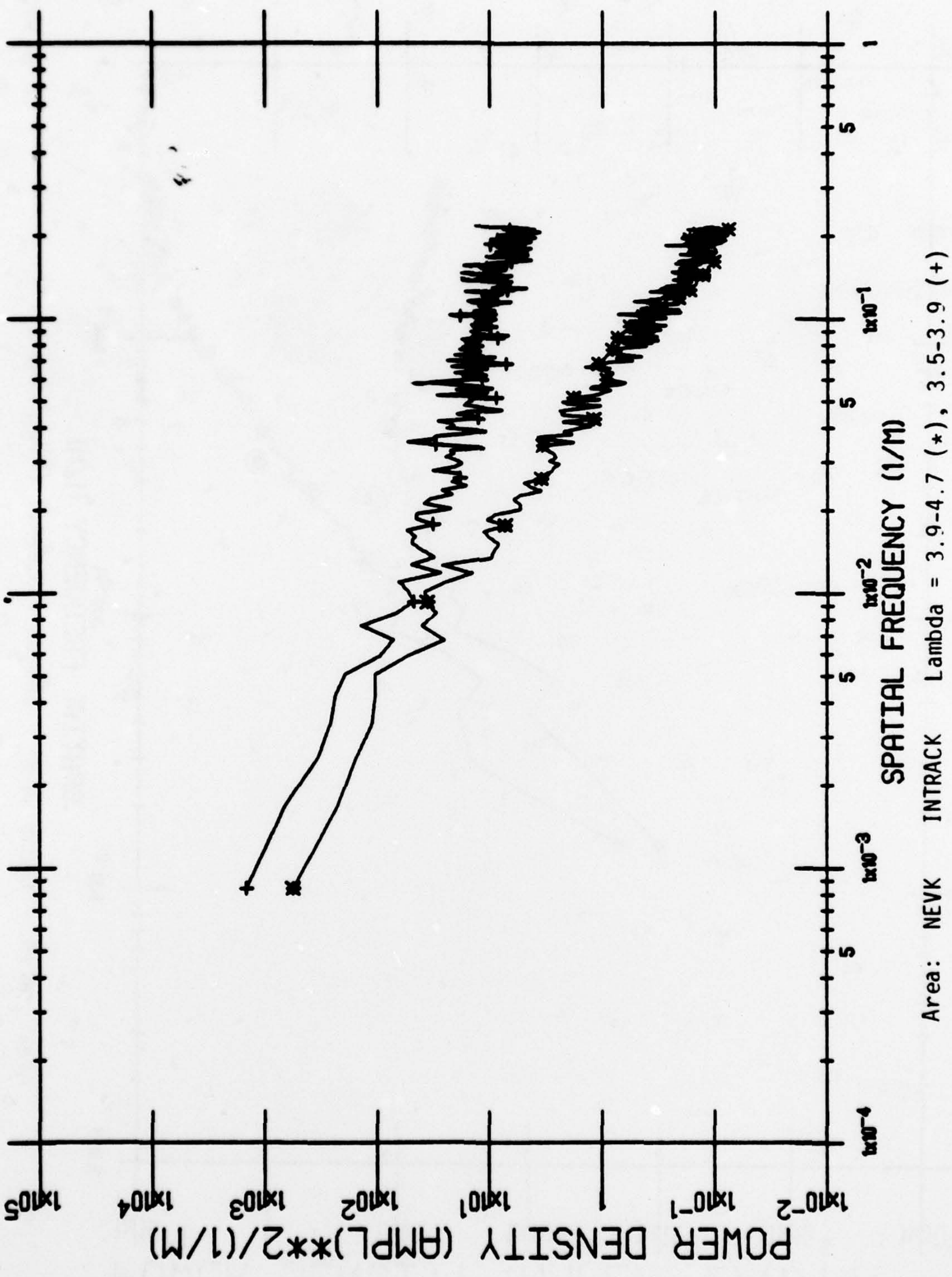

POWER DENSITY (AMPL)**2/(1/M)
1x10^5
1x10^4
1x10^3
1x10^2
1x10^1
1
1x10^-1
1x10^-2
SPATIAL FREQUENCY (1/M)
1x10^-4
5
1x10^-3
5
1x10^-2
5
1x10^-1
5
1
Area: NEVK INTRACK Lambda = 3.9-4.7 (*), 3.5-3.9 (+)

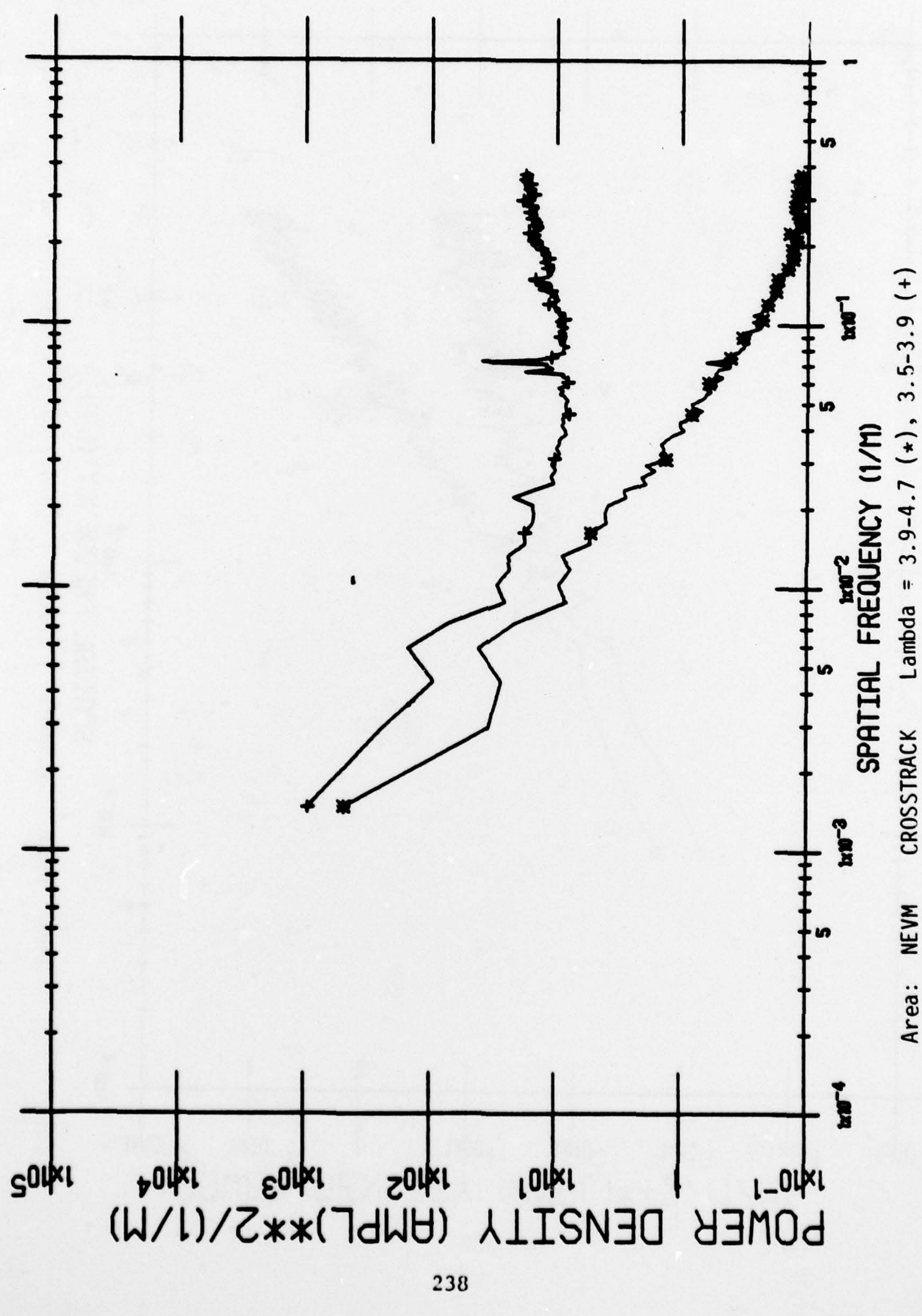
POWER DENSITY (AMPL)**2/(1/M)
1x10^-1
1
1x10^1
1x10^2
1x10^3
1x10^4
1x10^5
SPATIAL FREQUENCY (1/M)
1x10^-4
5
1x10^-3
5
1x10^-2
5
1x10^-1
5
1
Area: NEVM CROSSTRACK Lambda = 3.9-4.7 (*), 3.5-3.9 (+)

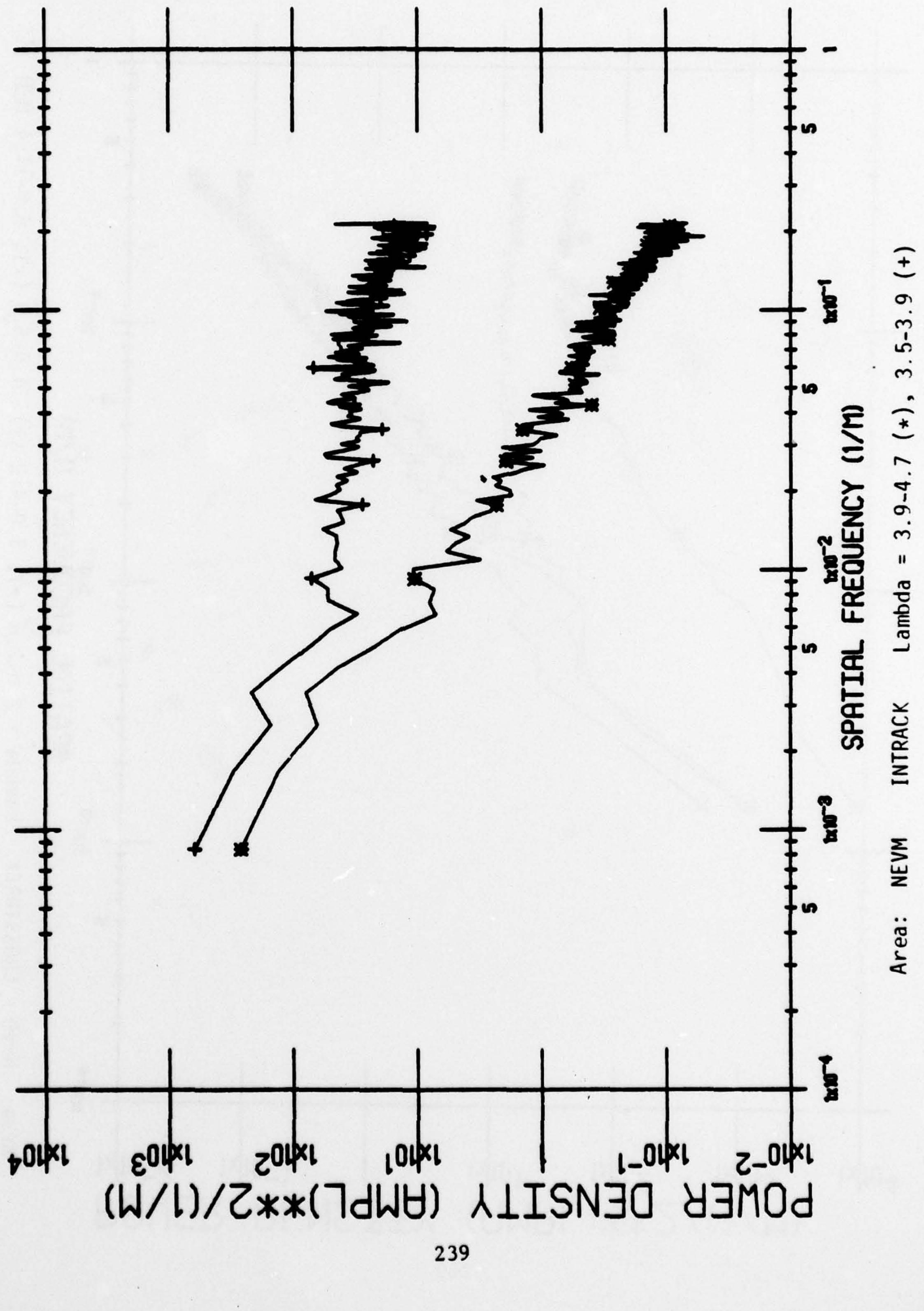
POWER DENSITY (AMPL)**2/(1/M)
1x10^4
1x10^3
1x10^2
1x10^1
1
1x10^-1
1x10^-2
1x10^-4
5
1x10^-3
5
1x10^-2
5
1x10^-1
5
1
SPATIAL FREQUENCY (1/M)
Area: NEVM INTRACK Lambda = 3.9-4.7 (*), 3.5-3.9 (+)

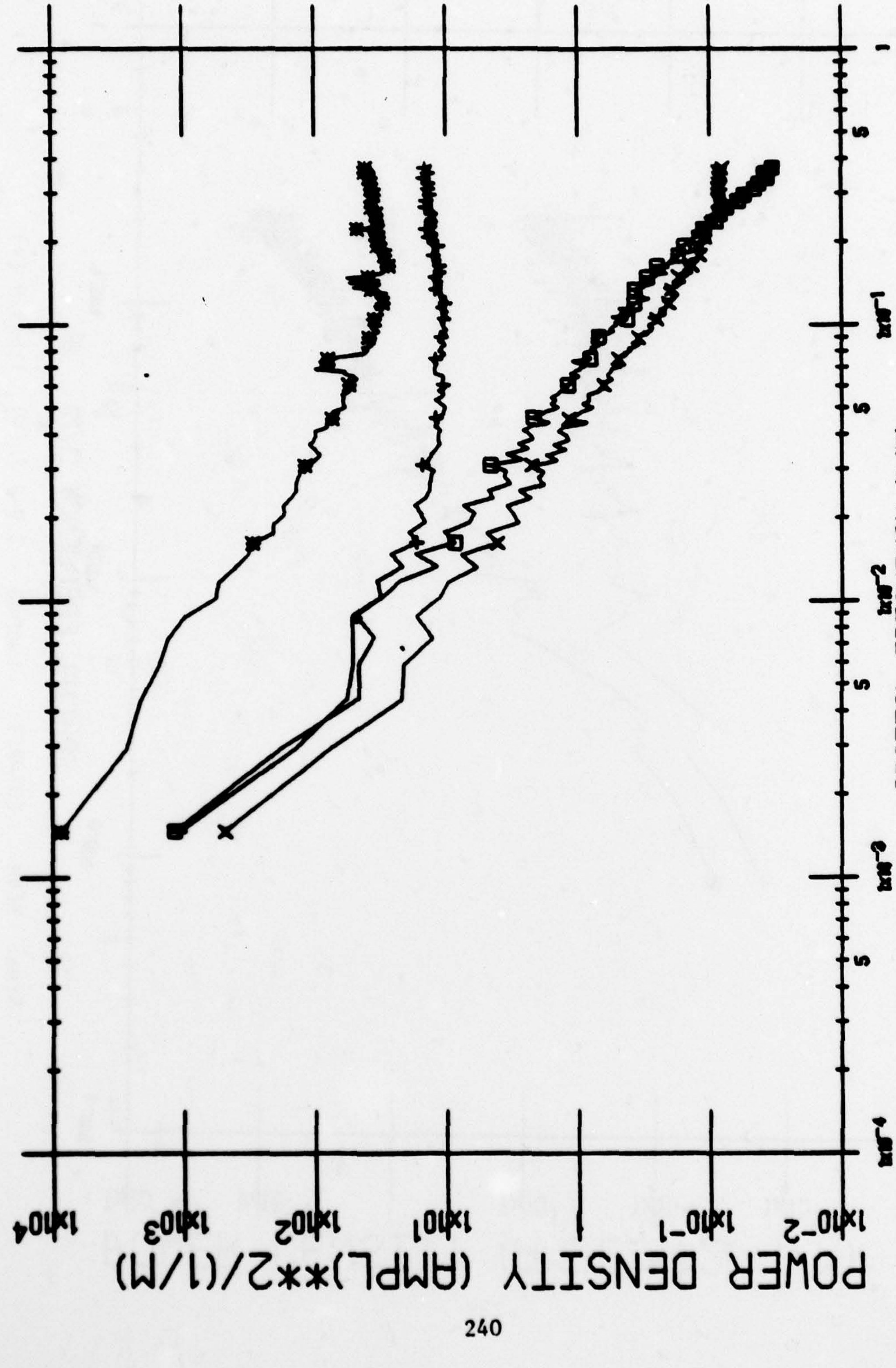

Area: NEVN CROSSTRACK Lambda = 2.0-2.6 (*), 3.0-4.2 (+), 4.5-5.9 (x), 9.0-11.4 (⊡)

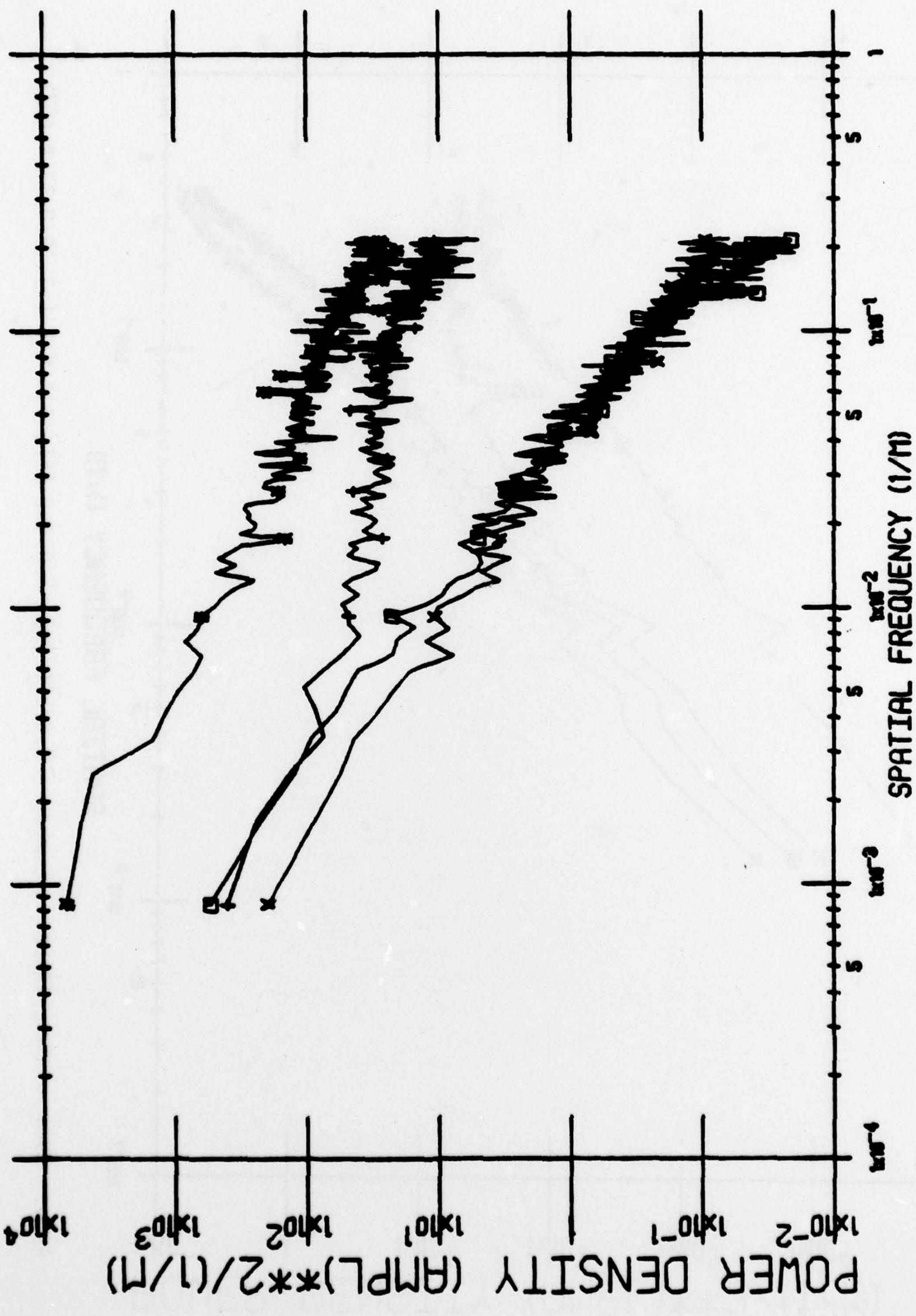

Area: NEVN INTRACK Lambda = 2.0-2.6 (*), 3.0-4.2 (+), 4.5-5.5 (x), 9.0-11.4 (⊡)

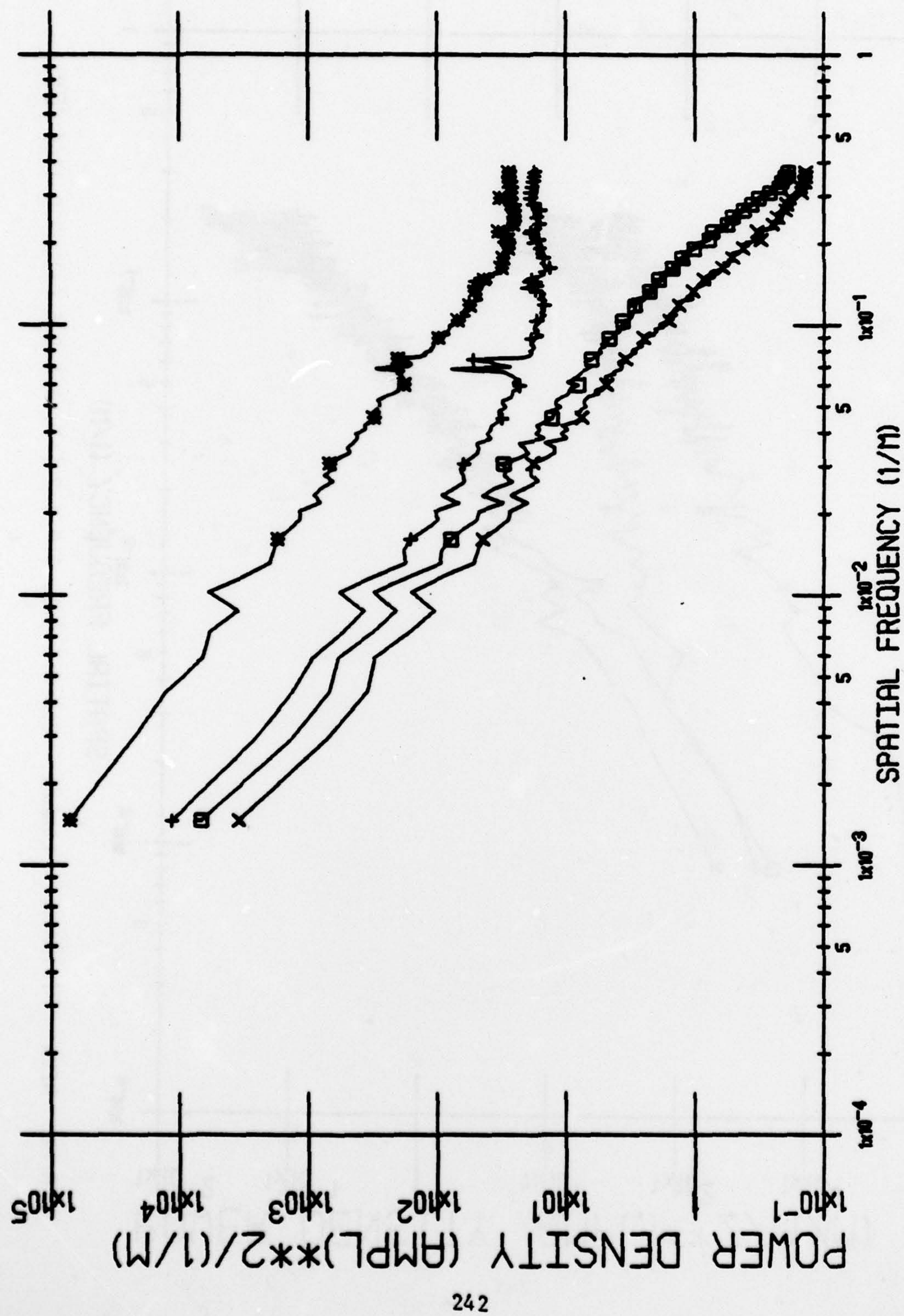

Area: NVG1 CROSSTRACK Lambda = 2.0-2.6 (*), 3.0-4.2 (+), 4.5-5.5 (x), 9.0-11.4 (⊡)

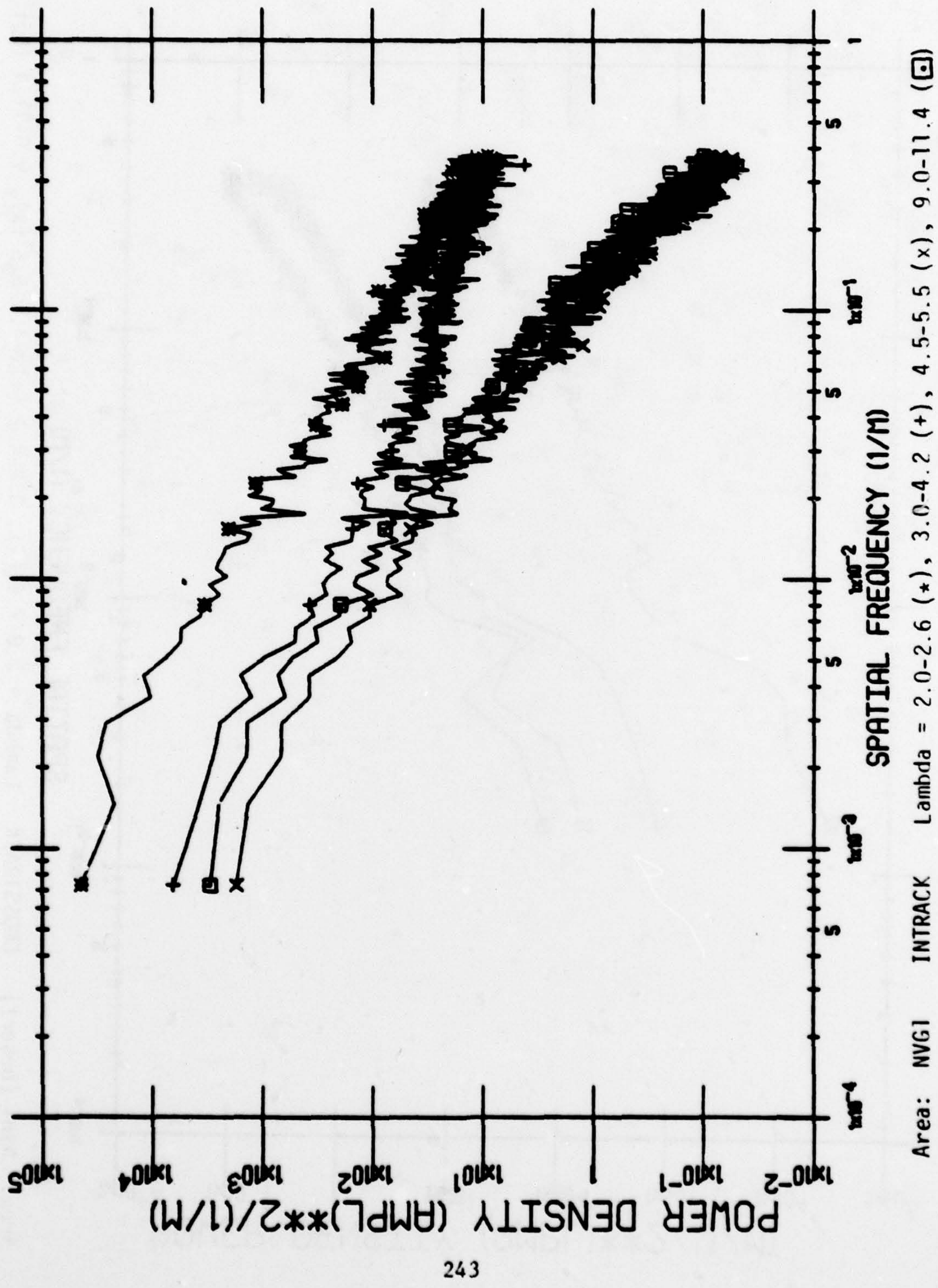
POWER DENSITY (AMPL)**2/(1/M)
1x10^5
1x10^4
1x10^3
1x10^2
1x10^1
1
1x10^-1
1x10^-2
1x10^-4
5
1x10^-3
5
1x10^-2
5
1x10^-1
5
1
SPATIAL FREQUENCY (1/M)
Area: NVG1 INTRACK Lambda = 2.0-2.6 (*), 3.0-4.2 (+), 4.5-5.5 (x), 9.0-11.4 (⊡)

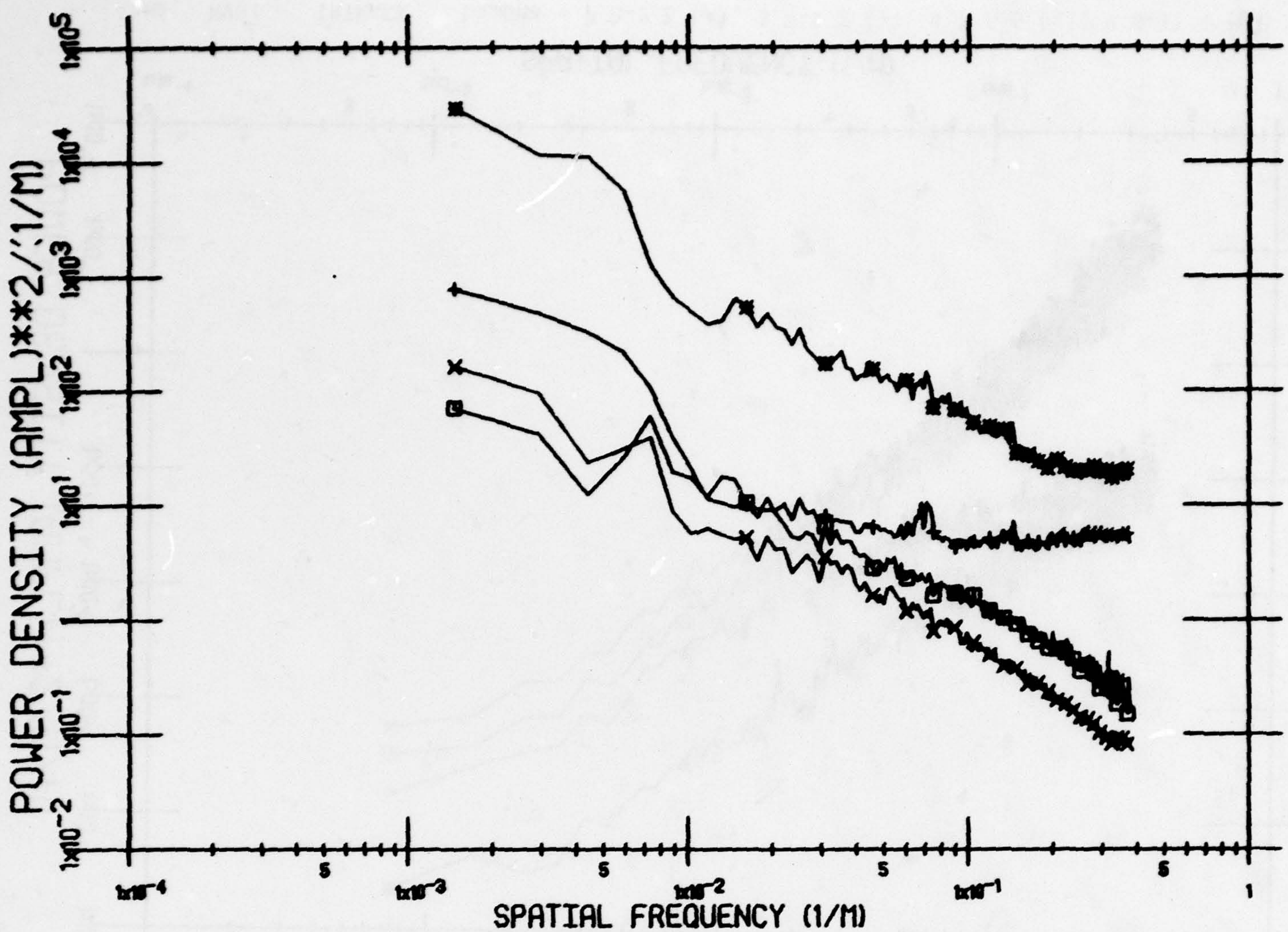

Area: NVH1 (Desert) CROSSTRACK Lambda = 2.0-2.6 (*), 3.0-4.2 (+), 4.5-5.5 (x), 9.0-11.4 (⊡)

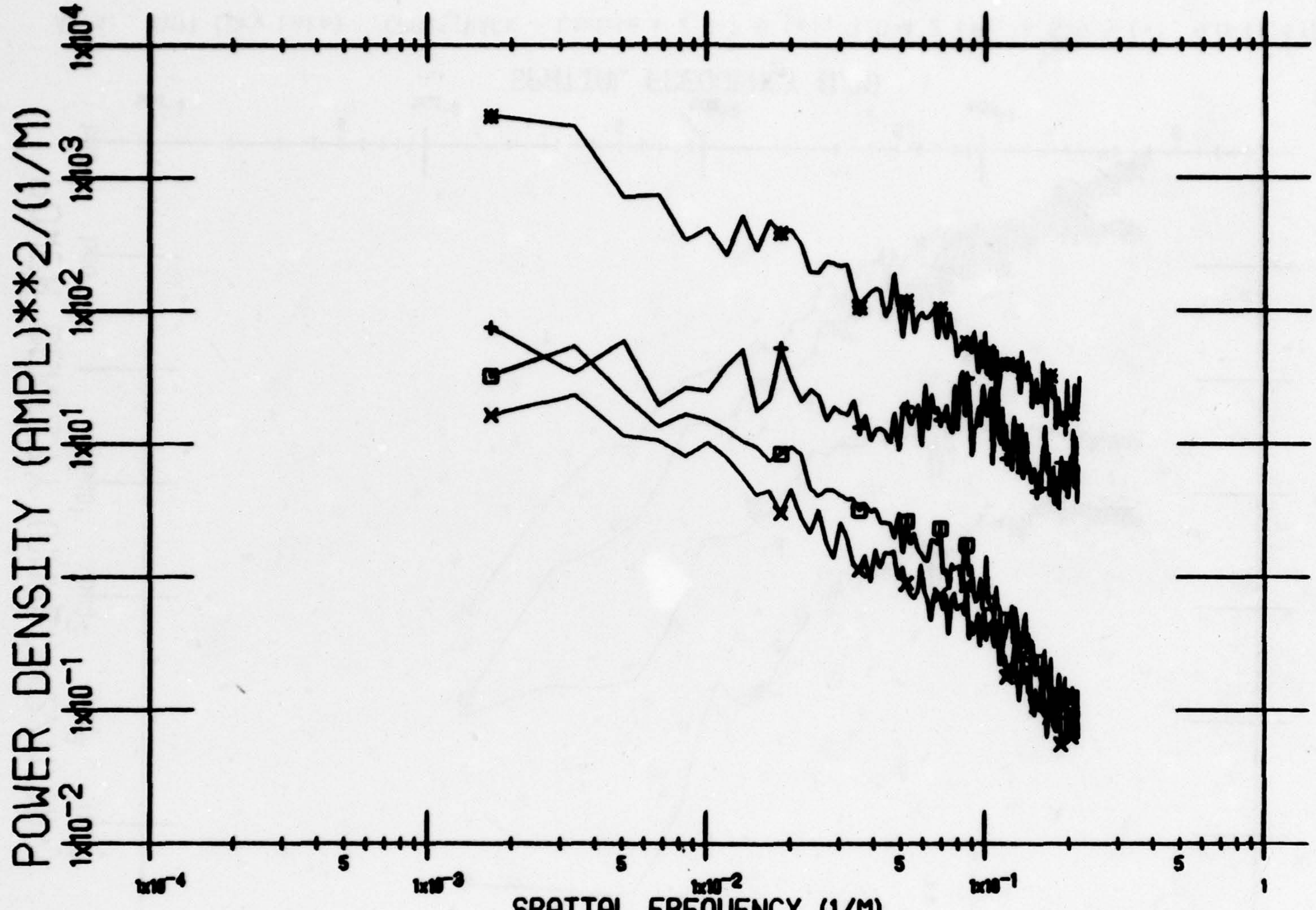

Area: NVH1 (Desert) INTRACK Lambda = 2.0-2.6 (*), 3.0-4.2 (+), 4.5-5.5 (x), 9.0-11.4 (⊡)

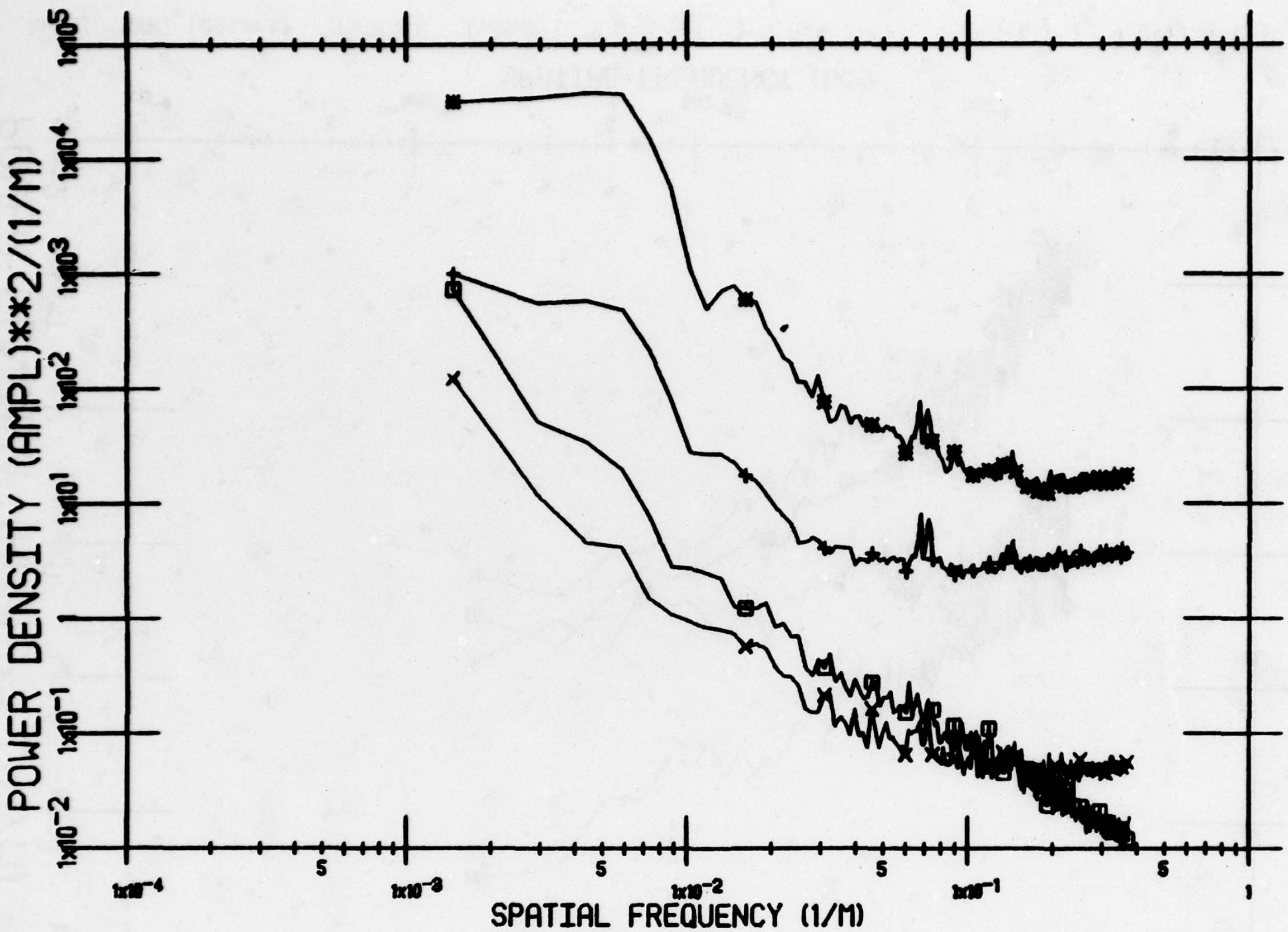

Area: NVH1 (Dry Lake) CROSSTRACK Lambda = 2.0-2.6 (*), 3.0-4.2 (+), 4.5-5.5 (x), 9.0-11.4 (⊡)

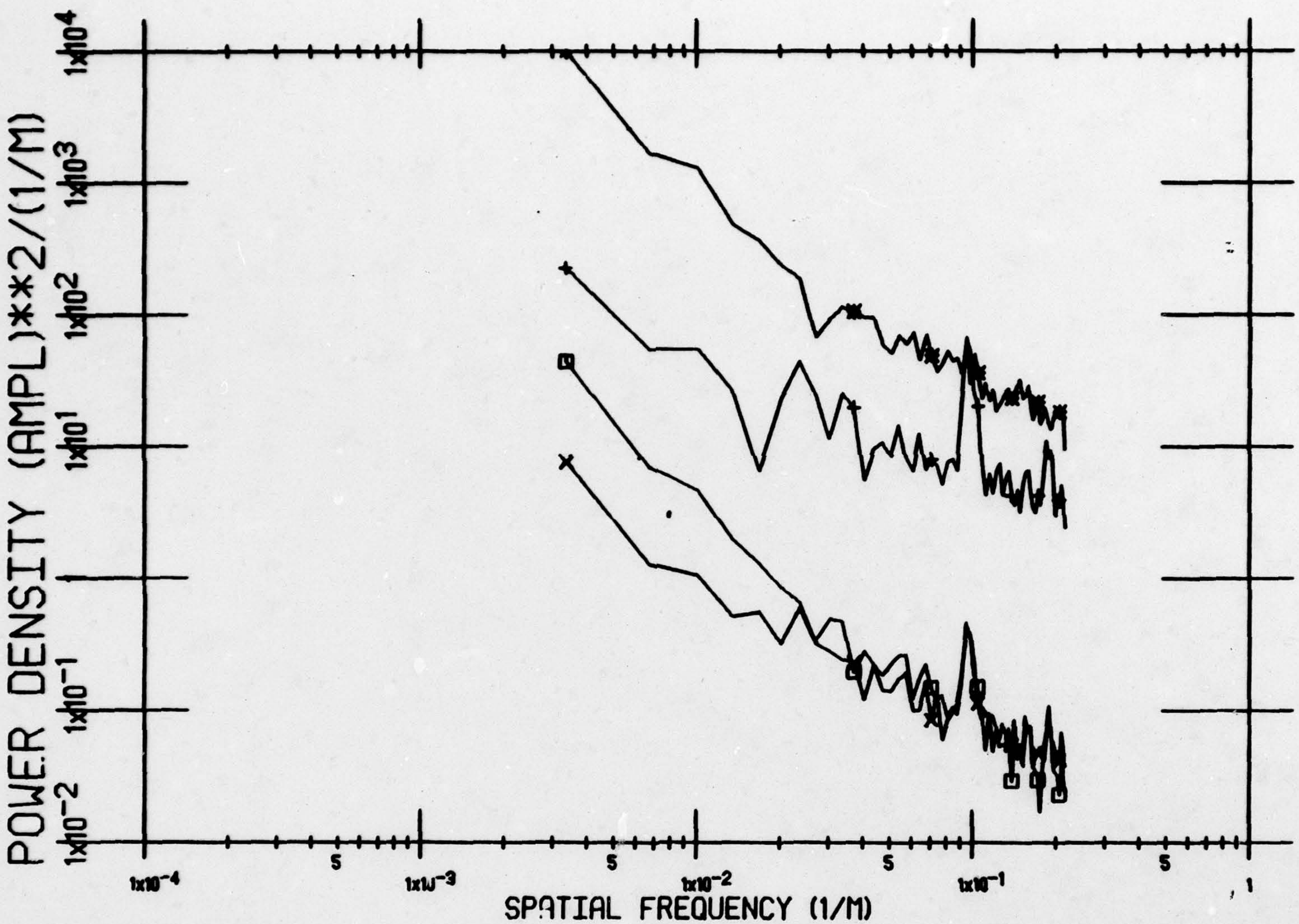

Area: NVH1 (Dry Lake) INTRACK Lambda = 2.0-2.6 (*), 3.0-4.2 (+), 4.5-5.5 (x), 9.0-11.4 (⊡)